CORE CHARACTERIZATION DURING STEADY- AND UNSTEADY-STATE FLOW EXPERIMENTS

By

Jeffrey Craig Smith, B.S. Petroleum Engineering

THESIS
Presented to the Faculty of the Graduate School of
The University of Texas at Austin
in Partial Fulfillment
of the Requirements
for the Degree of
MASTER OF SCIENCE IN PETROLEUM ENGINEERING

THE UNIVERSITY OF TEXAS AT AUSTIN

August 1987

ACKNOWLEDGMENT

I thank my supervising professor, Dr. Gary A. Pope, for his guidance and support during the course of this study. I am also grateful to Dr. Kamy Sepehrnoori for serving on my graduate committee.

My deepest appreciation is extended to Jeffrey D. Meyers and Dr. William G. Anderson, both of Conoco's Production Research Department, for their guidance and hard work in producing this manuscript.

The financial support of Conoco Oil Company is gratefully acknowledged. This research was done in Conoco's Production Research and Development laboratories while I was an "intern" student there.

Special appreciation is expressed to my parents for their love and support and to Denise Sanders for her understanding, encouragement, and patience.

August 1987

ABSTRACT

Two-phase steady- and unsteady-state relative permeability and dispersion experiments have been conducted in naturally water-wet and treated neutrally wet Berea sandstone cores. Partitioning and nonpartitioning tracers were used. An existing capacitance-dispersion model was used to fit the tracer breakthrough curves for the steady-state experiments. Saturation, dispersivity, and flowing fractions were determined. Wettability alteration was seen to have an effect on these parameters. Dispersivities and flowing fractions varied more in the neutrally wet core. A capacitance-dispersion computer model was developed to predict the behavior of tracers during waterfloods. This model was used to fit the unsteady-state tracer data. Residual saturations, dispersivity, and flowing fractions were determined. Resistivity values for both cores were measured using a four-point electrode system.

TABLE OF CONTENTS

TABLE OF CONTENTS (CONTINUED)

TABLE OF CONTENTS (CONTINUED)

TABLE OF CONTENTS (CONTINUED)

LIST OF TABLES

LIST OF TABLES (CONTINUED)

LIST OF FIGURES

LIST OF FIGURES (CONTINUED)

LIST OF FIGURES (CONTINUED)

LIST OF FIGURES (CONTINUED)

LIST OF FIGURES (CONTINUED)

LIST OF FIGURES (CONTINUED)

LIST OF FIGURES (CONTINUED)

LIST OF FIGURES (CONTINUED)

LIST OF FIGURES (CONTINUED)

LIST OF FIGURES (CONTINUED)

CHAPTER 1

INTRODUCTION

This report contains the theoretical background and experiments on core characterization with tracers. What we hope to gain from this research are tracer methods that can be applied to steady- and/or unsteady-state relative permeability measurements.

Our objectives are to:

1. Develop and test an apparatus for using tracers in steady- and unsteady-state flow.

2. Determine the suitability of plugs for relative permeability measurements and help explain variability.

3. Characterize core using partitioning and nonpartitioning tracers in steady-state flow using water-wet and neutrally wet Berea cores. This includes measuring parameters, such as dispersivity, which are used in predicting miscible floods.

4. Determine if tracers can be used to determine saturations during steady-state measurements and at endpoints of unsteady-state measurements.

5. Develop a computer model to predict the behavior of tracers during waterfloods.

6. Determine what information tracer measurements can provide to aid in calculating relative permeabilities from unsteady-state waterfloods. This includes testing a method proposed by Deans (1978) which, if valid, would allow an independent saturation determination.

SATURATION DETERMINATION

There are two main methods of measuring relative permeability: steady- and unsteady-state. Accurate results can generally be obtained with either method. In both methods, one of the most difficult problems is accurately determining the water and oil saturations. As we will discuss below, we examined the use of tracers to provide a simple, reliable method of saturation determination for both steady- and unsteady-state methods.

Steady-State Measurements

In the steady-state method, the relative permeabilities are measured at a series of discrete steps, starting with 100 percent oil flowing and ending with 100 percent water flowing. At each step, water and oil are injected simultaneously at known, constant flow rates while the pressure drop across the core is measured. Steady-state is reached when the pressure drop is constant and the inflow of both oil and water equals their outflow from the core. The relative permeability can then be calculated from the pressure drop, saturations, core dimensions, and flow rates.

The major problem with the steady-state method is determining the oil and water saturations in the core. At present, there are several relatively common methods, each of which has some advantages and disadvantages. The two most commonly used are the gravimetric method and the X-ray absorption method. In the

gravimetric method, the average saturations in the core are determined by removing the sample from the holder at each step and weighing it. This method may cause gas to enter into the core, which will then be difficult to remove. In addition, the frequent handling may cause the loss of sand grains from the core, with subsequent loss of accuracy. The advantages are that it is cheap, requires no special precautions, and can give good results when the proper precautions are taken.

Today, the X-ray absorption method is probably the most common method used in commercial core laboratories. It provides a saturation distribution along the core, so any inhomogeneities can be detected. In this method, a strong X-ray absorber is added to either the oil or water, the core is scanned with an X-ray beam, and the X-ray absorption data along the core measured. The X-ray absorption data is also measured when the core is dry and when it is 100 percent saturated with the fluid containing the absorber. The three curves are then compared to subtract out the effects of variations in the rock, allowing the determination of the saturation distribution along the core (Boyer, Morgan, and Muskat, 1947; Morgan, McDowell, and Doty, 1950: Geffen and Gladfelter, 1952; Laird and Putnam, 1951; Oak and Ehrlich, 1985). Typical tracers are 12.5 volume percent iodobenzene in the oil, or 126 g/L sodium iodide in the brine (Schneider and Owens, 1970). For example, if the absorbing tracer is in the brine, the X-ray absorption will be relatively high for saturations near the residual oil saturation (ROS) then decrease as the brine saturation is lowered to the irreducible water saturation (IWS). The disadvantages of the X-ray method are (1) it is expensive because of the equipment and shielding required and (2) the effect on wettability of the high concentration of X-ray absorber is unknown.

In addition to the X-ray and gravimetric methods, a large number of additional methods have been developed, most of which have been used to measure the saturation profile along the core. These methods are briefly described in Table 1-1 taken from Anderson and Whitebay (1987). These methods have been very helpful in relative permeability research, particularly three-phase measurements and in fundamental research on EOR recovery mechanisms. However, they are not often used for routine steady-state relative permeability measurements since they suffer from one or more of the following problems:

1. Nonmetallic core holder required.

2. Limited size or shape of the core.

3. Limited resolution.

4. Very elaborate equipment requirements, so the method is only suitable for fundamental research.

5. The method is designed for research on three-phase relative permeability and will only determine one saturation when oil, water, and gas are present simultaneously. A second method must be used to determine the remaining two saturations.

In this report, we have examined the use of partitioning and nonpartitioning tracers to determine saturations during steady-state water/oil relative permeability measurements. The use of these tracers for saturation determination was proposed by Delshad et al. (1985) but not tested by comparison with other methods. The advantage of tracers over the X-ray absorption method is that the equipment is relatively simple with no elaborate shielding requirements. The advantage over the gravimetric method is reduced handling of the core, eliminating the introduction of trapped gas. An additional advantage of the tracer measurement is that other parameters useful in miscible displacements are measured, such as dispersivity.

Unsteady-State Measurements

The steady-state method is generally accepted as the industry standard. However, it is very slow, requiring one to two weeks to make measurements on a single core. Because of this, an unsteady-state method has been developed, which generally gives comparable results. The method is much faster and cheaper,

generally requiring several hours per core. During the unsteady-state relative permeability measurements, water is injected into a core initially at IWS while the pressure drop and fluid production are measured. Buckley-Leverett (1942) flow through the core is assumed, so there is a sharp displacement front followed by a zone of two-phase flow. Initially, only oil is produced from the core. After the displacement front reaches the end of the core, both water and oil are produced. At the end of the run, the core is essentially at ROS, with only trace amounts of oil production. To measure relative permeability hysteresis, measurements can also be made by oilflooding a core initially at ROS.

The pressure drop and oil and water production data are used to calculate the relative permeabilities using the Johnson-Bossler-Naumann (JBN) method (1959) which is based on earlier work by Welge (1952) for determining relative permeability ratios. The method assumes Buckley-Leverett flow through a homogeneous, uniform core with negligible inlet and outlet effects. The procedure is relatively complicated, but programs to perform the calculations are generally available. Alternatively, an equivalent graphical procedure developed by Jones and Roszelle (1978) can be used if only a few relative permeabilities are calculated.

There are two areas where tracers can help determine saturations for unsteady-state measurements: (1) average saturations at the endpoints before and after the floods (IWS and ROS) and (2) endface saturations at selected points during a flood. The problem of determining saturations at the endpoints before and after flooding is identical to determining saturations during steady-state relative permeability measurements. Currently, the saturation in a native-state core is measured by extraction after all of the floods are completed. Saturations before and after earlier floods are determined by using material balance to work back from the final saturation. Tracers can be used to directly measure the saturations at these intermediate points. For example, tracers could be used in the following set of floods, which simulates a waterflood, followed by an oilflood (oil bank), then a miscible flood:

1. Inject tracer to determine the initial saturation.

2. Waterflood to measure imbibition relative permeability.

3. Inject tracer, determine saturation.

4. Oilflood and measure drainage relative permeability.

5. Inject tracer, determine saturation.

6. Flood the plug with carbon dioxide.

7. Waterflood the plug to displace the CO_2.

8. Extract the plug to determine the final saturation.

In addition to using tracers to measure saturations at the endpoints, the use of tracers to measure saturations during the floods was also investigated. In the JBN method, the saturations at the end of the core must be calculated. This is a fairly complicated procedure which involves differentiating the experimental production data and making a number of assumptions. Deans (1978) proposed a method that uses partitioning tracers to determine when the endface saturation reaches certain known values, see Appendix K. If valid, the use of this method would allow an independent calculation of saturation, providing an independent check of the saturations calculated by the JBN method.

TABLE 1-1

ADDITIONAL METHODS OF SATURATION DETERMINATION FOR STEADY-STATE RELATIVE PERMEABILITY MEASUREMENTS (ANDERSON AND WHITEBAY, 1987)

Method	Comments
1. Electrical Resistivity (Leverett and Lewis, 1941; Geffen et al., 1951; Levine, 1954)	Determines average brine saturation. Suitable only for strongly water-wet cores, since the resistivity measurements are also dependent on wettability and saturation history.
2. Recycling System (Braun and Blackwell, 1981)	Average saturation. Very sensitive to small leaks.
3. Gamma Ray Absorption (Reid, 1958; Saraf and Fatt, 1967; Nicholls and Heaviside, 1985)	Determines the saturation profile along the core. Similar to the X-ray absorption method.
4. Gamma-Emitting Tracers (Josendal et al., 1952; Russel et al., 1947; Bailey et al., 1981)	Determines the saturation profile along the core. The saturations are determined from gamma rays emitted from tracers in the oil or water. Shielding requirements are relatively elaborate.
5. Computer-Aided Tomography, CAT Scan (Wang et al., 1984a,b; Wellington and Vinegar, 1985)	Provides detailed information about the distribution of oil, water, and gas at any cross section along the core. Currently used only for fundamental research.

TABLE 1-1 (CONTINUED)

ADDITIONAL METHODS OF SATURATION DETERMINATION FOR STEADY-STATE RELATIVE PERMEABILITY MEASUREMENTS (ANDERSON AND WHITEBAY, 1987)

Method	Comments
6. Nuclear Magnetic Resonance (NMR) (Saraf and Fatt, 1967; Dreher and Sydansk, 1976; Baldwin and Yamanashi, 1986)	Provides detailed information about the fluid distribution at any cross section along the core. Currently a proposed method that needs further work. Signals may also be dependent on core wettability.
7. Partitioning Tracers (Delshad et al., 1985)	Average saturation of the core.
8. Very High Frequency (VHF) Electrical Measurements (Davis, 1980)	The water and oil saturations are determined by measuring the dielectric constant in the VHF (above 100 MHz). A nonmetallic core holder is required.
9. Microwave Attenuation (Parsons, 1975; Baker, 1975; Gladfelter and Gupta, 1978; Wasan et al., 1979; Aggarwal and Johnston, 1983)	Brine saturation is determined by measuring absorption of microwaves. The core, oil, and gas are almost transparent to the microwaves. This method requires elaborate equipment and a nonmetallic core holder. It is limited to flat, thin sheets of the porous material.
10. Capacitance Probe (Baker, 1973)	Saturations were qualitatively measured using a small capacitor sliding in a thin glass tube inserted in an unconsolidated sandpack. The probe was sensitive to the

TABLE 1-1 (CONTINUED)

ADDITIONAL METHODS OF SATURATION DETERMINATION FOR STEADY-STATE RELATIVE PERMEABILITY MEASUREMENTS (ANDERSON AND WHITEBAY, 1987)

Method	Comments
	composite dielectric constant of the core and liquids. Unfortunately, the probe is very fragile and will only penetrate a short distance into the sandpack.
11. High Magnetic Susceptibility Materials (Whalen, 1954)	20 percent by weight of the brine is cobaltous chloride, which has a high paramagnetic susceptibility. The tracer might alter the interfacial properties.
12. Neutron Diffraction (Brunner and Mardock, 1946; Snell, 1959, 1962)	The gas versus liquid saturation is determined by measuring the thermal neutrons produced when fast neutrons are moderated by the hydrogen atoms in oil and water. An additional method must be used to distinguish between oil and water.
13. Gamma-Neutron Interaction (Bailey, Rowland, and Robinson, 1981)	Heavy water, D_2O, is added to the brine. The core is bombarded with gamma rays, which produce neutrons when they are absorbed by the deuterium. The water saturation is proportional to the neutron flux.

TABLE 1-1 (CONTINUED)

ADDITIONAL METHODS OF SATURATION DETERMINATION

FOR STEADY-STATE RELATIVE PERMEABILITY MEASUREMENTS

(ANDERSON AND WHITEBAY, 1987)

Method	Comments
14. Determination of Three-Phase Saturations by Vacuum Distillation (Caudle, Slobod, and Brownscombe, 1951)	In this very tedious procedure, the saturation of the core is determined by vacuum distillation at each combination of flow rates. Obviously, the native wettability of the core is not maintained.

CHAPTER 2

SINGLE-PHASE FLOW DISPLACEMENTS

When one fluid displaces another in a miscible displacement, a transition zone develops between the two fluids. This can easily be detected if tracer is added to the injected fluid. As injection continues, the tracer spreads and mixes with the displaced fluid. A tracer concentration gradient develops, ranging from zero downstream to the injected concentration upstream. When a small slug labeled with tracer is injected, a bell-shaped pulse is formed. As the pulse travels through the porous medium, the width of the pulse increases, while the maximum concentration decreases. This spreading of the tracer is known as dispersion.

Dispersion results primarily from the complex nature of the flow paths in the media, although there are a variety of mechanisms that can cause mixing and spreading of the injected tracer, including (Greenkorn, 1981):

1. Molecular Diffusion — Dispersion can result from molecular diffusion if time scales are sufficiently long, but is usually not important when compared to other causes of mixing.

2. Small Scale Heterogeneities — Since flow channels in a porous medium are tortuous, local velocities in the direction of flow will be uneven. Thus fluid elements starting a given distance from each other will become separated as they move through the medium.

3. Incomplete Connectivity of Flow Paths—Once a fluid element has entered a particular flow path, not all of the pores in the medium are accessible to that element, causing dispersion.

4. Taylor-Aris (1953) Dispersion—Nonuniform flow velocities in individual pores can be caused by the adherence of the fluid to the wall. This causes fluid particles at different distances from the pore wall to move at different velocities relative to each other.

5. Dead-End Pores—Dead-end pores cause mixing because, as the tracer front passes the pore, molecular diffusion into the pore will occur. If the tracer was injected as a finite slug, tracer from the dead-end pore will diffuse back into the flow stream after the slug has passed.

In general, mixing in a porous media occurs both longitudinally, in the direction of flow, and transversely, perpendicular to flow. In this report, we will be only concerned with longitudinal dispersion, since the experiments will involve one-dimensional, flow-through plugs, with no tracer spreading in the transverse direction.

DISPERSION COEFFICIENT

A thorough review of dispersion was given by Perkins and Johnston (1963). The equations that summarize their key results are:

$$K_l = \frac{D}{F_R \phi} + \alpha_l v^{\beta_l} \tag{2-1}$$

$$K_t = \frac{D}{F_R \phi} + \alpha_t v^{\beta_t} \tag{2-2}$$

where

K_l, K_t = longitudinal and transverse dispersion coefficients

D = molecular diffusion coefficient

F_R = formation electrical resistivity factor

ϕ = porosity

α_l, α_t = longitudinal and transverse dispersivity

v = frontal velocity, $q/A\phi$

β_l, β_t = longitudinal and transverse dispersion parameters

Thus it is implied that dispersion is the sum of a diffusion term and a mechanical mixing term that is proportional to the frontal velocity v (Baker, 1977; Delshad, M., 1981; Gupta, 1972; Shuler, 1978). At very low flow rates, the diffusion term dominates and dispersion is equal to Fick's diffusion coefficient D reduced by the factor $F_R\phi$ due to the tortuosity of the porous material. For longitudinal dispersion, the second term dominates when frontal advance rates are on the order of 0.5 to 1 foot per day or higher (Blackwell, 1962; Brigham et al., 1961; Lake and Hirasaki. 1981; Spence and Watkins, 1980; Shuler, 1978). The exponent β varies between 1.0 and 1.4 with a reasonable value for sandstone considered to be 1.2 (Baker, 1977; Brigham et al., 1961; Lake and Hirasaki. 1981; Spence and Watkins, 1980). Procedures for estimating the dispersion coefficient from tracer experiments are given in Appendix D.

The longitudinal and transverse dispersivities are not equal, with the ratio α_l/α_t being on the order of 30 depending on the porous material (Perkins and Johnston, 1963; Blackwell, 1962). In this report we will only be interested in longitudinal dispersion since it can be used more easily to characterize core with tracers.

ONE-DIMENSIONAL CONVECTION-DIFFUSION EQUATION

The simplest equation to describe the dispersion of tracer in core is the one-dimensional convection-diffusion equation. Consider a tracer i that is ideal and noninteracting which flows through an ideal, homogeneous. linear porous medium. The material balance equation for the case of single-phase flow with dispersion is described by the well-known convection-diffusion (C-D) equation:

$$\frac{\partial C_i}{\partial t} + \frac{q}{A\phi}\frac{\partial C_i}{\partial x} = \frac{\partial}{\partial x}\left(K_l \frac{\partial C_i}{\partial x}\right) \tag{2-3}$$

The longitudinal dispersion coefficient K_l can be assumed constant since the fluid velocity ($v = q/A\phi$) is constant, see Equation (2-1) (Delshad, 1981; Delshad, 1984). Equation (2-3) can be nondimensionalized with the following variables:

1. Dimensionless time (cumulative pore volume produced at any time)

$$t_D = \frac{qt}{AL\phi} = \frac{V_T - V_E}{V_P} \tag{2-4}$$

where V_T is the total volume injected and V_E is the volume of fluid between the outlet of the core and the sample collector and between the tracer reservoir and the core inlet.

2. Dimensionless distance

$$x_D = \frac{x}{L} \tag{2-5}$$

3. Dimensionless tracer concentration

$$C_D = \frac{C_i}{C_i^o} \tag{2-6}$$

where C_i^o is the injected tracer concentration.

4. Peclet Number, the ratio of convective to dispersive transport

$$N_{Pe} = \frac{vL}{K_l} \tag{2-7}$$

Using Equations (2-4) to (2-7), Equation (2-3) can be written in dimensionless form:

$$\frac{\partial C_D}{\partial t_D} + \frac{\partial C_D}{\partial x_D} = \frac{1}{N_{Pe}} \frac{\partial^2}{\partial x_D^2} C_D \tag{2-8}$$

Analytical Solutions

We will first examine analytical solutions applicable to concentrations in the core. As we will discuss in more detail below, the concentration profile in the core can differ from the effluent profile, particularly when the mixing zone is comparable to the length of the core. There are two general solutions of interest: step injection and slug injection.

Step Injection

During the step injection of tracer, the tracer concentration in the injected fluid is raised from a value of zero to its maximum, where $C_D = 1$. The first example we will consider is an infinite porous media, with a step change in tracer concentration at the origin at $t = 0$. As time increases, the fluid movement carries tracer in the positive x direction. At the same time, dispersion forces smear out the initial step gradient. The initial and boundary conditions for an infinite porous media, with $N_{Pe} > 14$, are (Brigham, 1974):

$$\begin{aligned} C_D &= 1 \qquad t_D = 0, \; -\infty \le x_D \le 0 \\ C_D &= 0 \qquad t_D = 0, \; 0 \le x_D \le +\infty \\ C_D &= 1 \qquad t_D > 0, \; x_D = 0 \\ \frac{\partial C_D}{\partial x_D} &= 0, \; t > 0, \; x = \pm \infty \end{aligned} \tag{2-9}$$

Brigham (1974) has shown that the choice of boundary conditions makes little difference except for systems with a small Peclet Number ($N_{Pe} = vL/K_l < 14$) or a transition (mixing) zone that is large compared with the length of the system.

The solution for the tracer concentration in the infinite porous media is:

$$C_D = \frac{1}{2}\left[1 - \text{erf}\left(\frac{x_D - t_D}{\sqrt{\frac{4t_D}{N_{Pe}}}}\right)\right] \tag{2-10}$$

At the endpoint of a finite core, $x = L$, $x_D = 1$, and Equation (2-10) become:

$$C_D = \frac{1}{2}\left[1 - \text{erf}\left(\frac{1 - t_D}{\sqrt{\frac{4t_D}{N_{Pe}}}}\right)\right] \tag{2-11}$$

In the solution above, the finite length core was modeled as an infinite porous media. A somewhat more realistic closed-form, analytic solution can be obtained by modeling the core as a semi-infinite porous media, extending from zero to infinity. At $x = 0$, the tracer concentration is fixed to the maximum value for positive time. The boundary conditions for the semi-infinite porous media are:

$$C_D = 0 \qquad t_D = 0,\ x_D \geq 0$$

$$C_D = 0 \qquad t_D \geq 0,\ x_D \sim +\infty \tag{2-12}$$

$$C_D = 1 \qquad t_D > 0,\ x_D = 0$$

The solution is (Naiki, 1979)

$$C_D = \frac{1}{2}\ \text{erfc}\left(\frac{x_D - t_D}{\sqrt{\frac{4t_D}{N_{Pe}}}}\right) + \frac{e^{N_{Pe}}}{2}\ \text{erfc}\left(\frac{x_D + t_D}{\sqrt{\frac{4t_D}{N_{Pe}}}}\right) \tag{2-13}$$

where erfc is the complementary error function. At the end of the core, $x_D = 1$, and the solution is:

$$C_D = \frac{1}{2}\ \text{erfc}\left(\frac{1 - t_D}{\sqrt{\frac{4t_D}{N_{Pe}}}}\right) + \frac{e^{N_{Pe}}}{2}\ \text{erfc}\left(\frac{1 + t_D}{\sqrt{\frac{4t_D}{N_{Pe}}}}\right) \tag{2-14}$$

Slug Injection

In our experiments, a finite slug of tracer is injected into the core. At $t_D = 0$, the tracer concentration at the inlet is increased to its maximum value for a time t_{DS}, then brought back to zero for $t_D > t_{DS}$. The boundary conditions are:

$$\begin{aligned} C_D &= 0 \qquad && t_D = 0,\ x_D > 0 \\ C_D &= 1 \qquad && 0 < t_D < t_{DS},\ x_D = 0 \\ C_D &= 0 \qquad && t_D > t_{DS},\ x_D = 0 \\ C_D &= 0 \qquad && x_D \sim +\infty \end{aligned} \tag{2-15}$$

The injection of a finite slug can be visualized as the injection of two step changes in tracer concentration: first, a step increase to the maximum concentration; second, a step decrease back to zero. The solution is obtained by superposing two solutions to Equation (2-14), with the second delayed after the first. The solution at $x_D = 1$ is:

$$\begin{aligned} C_D = \frac{1}{2}\ \mathrm{erfc}\left(\frac{1 - t_D}{\sqrt{\frac{4t_D}{N_{Pe}}}}\right) + \frac{e^{N_{Pe}}}{2}\ \mathrm{erfc}\left(\frac{1 + t_D}{\sqrt{\frac{4t_D}{N_{Pe}}}}\right) \\ - \frac{1}{2}\ \mathrm{erfc}\left(\frac{1 - (t_D - t_{DS})}{\sqrt{\frac{4(t_D - t_{DS})}{N_{Pe}}}}\right) - \frac{e^{N_{Pe}}}{2}\ \mathrm{erfc}\left(\frac{1 + (t_D - t_{DS})}{\sqrt{\frac{4(t_D - t_{DS})}{N_{Pe}}}}\right) \end{aligned} \tag{2-16}$$

Short Cores

An approximation was made in the above solutions for the step change (Equation (2-14)) and finite slug (Equation (2-16)). The concentrations are given for a fixed time in a semi-infinite porous media. The midpoint of the mixing zone moves with the tracer velocity v_T, and the tracer concentration profile in the core is symmetric about the midpoint. However, the concentration profile in a core cannot easily be observed at a fixed time. Instead, the tracer concentration in the fluid effluent from the core is measured. Since the transition zone continues to grow while it is being produced, a plot of effluent tracer concentration versus pore volumes injected is slightly asymmetric for this reason. This asymmetry occurs because the tracer produced near the end of the slug has undergone mixing in the core for a longer time than the tracer produced at the beginning of the slug.

Brigham (1974) pointed out that the asymmetry is greatest for short cores, where the mixing zone length is similar to or greater than the core length. Brigham (1974) has shown how the boundary conditions and analytical solutions of the convection-diffusion equation can be modified to solve for the tracer concentration in the effluent. These solutions will not be discussed here. Our tracer experiments will be matched with a finite difference computer model, which uses similar boundary conditions and solves for the effluent tracer concentration.

CAPACITANCE-DISPERSION (COATS-SMITH) MODEL

As discussed above, the effects of core length cause a slight asymmetry to the effluent tracer curve. However, in actual displacement experiments, the effluent concentration profile is often more asymmetric than can be explained by this mechanism. The tracer is recovered more slowly at the trailing edge of the

transition zone than is predicted by Equations (2-13) and (2-15). This is caused by diffusion of the tracer from dead-end pores into the flow stream after the slug has passed, as discussed previously. Dead-end pores also cause early breakthrough because the porosity actually available to flow is less than that used to calculate the velocity. The increased length of the breakthrough curve is caused by diffusion into and out of the pores, even though dead-end pores do not contribute to flow.

A capacitance-dispersion model to account for this asymmetry has been developed by Coats and Smith (1964). Their model divides each phase into a flowing fraction and a dendritic or dead-end fraction. A dispersion coefficient K describes mixing in the flowing fraction, while a single mass transfer coefficient M models the communication between the flowing and dendritic fractions. The model has two equations, an overall tracer material balance:

$$F \frac{\partial C_D^f}{\partial t_D} + (1 - F) \frac{\partial C_D^d}{\partial t_D} + \frac{\partial C_D^f}{\partial x_D} - \frac{1}{N_{Pe}} \frac{\partial^2 C_D^f}{\partial x_D^2} = 0 \qquad (2\text{-}17)$$

and an equation for the mass transfer between the flowing and dendritic saturations:

$$(1 - F) \frac{\partial C_D^d}{\partial t_D} = a (C_D^f - C_D^d) \qquad (2\text{-}18)$$

where C_D^f is the concentration of tracer in the flowing stream, F the flowing fraction, C_D^d the concentration of tracer in the stagnant volume, (1 − F) the stagnant fraction, M the mass transfer coefficient, and

$$a = \frac{\phi ML}{v} \qquad (2\text{-}19)$$

The parameters a, F, and K are determined by history-matching the effluent concentration data.

When tracer is injected into the core, the tracer concentration at the leading edge is lowered by mass transfer of tracer to the dead-end pores. After the highest tracer concentration has passed by a given point, the tracer in the dead-end pores mixes back into the flowing fluid. The mass transfer of tracers to the dead-end pores gives an asymmetric profile and a long tail in the tracer concentration. Coats and Smith (1964) solved Equations (2-17) and (2-18) by Laplace transform and found that for data with early asymmetrical production, a better fit was obtained with this model than with the C-D equation. When no dead-end pore volume is present, the model reduces to the C-D equation. Variations of the basic Coats-Smith model are also used in two-phase tracer experiments. These models will be discussed in Chapters 5 and 6.

CHAPTER 3

MODEL FOR TRACER FLOW DURING AN UNSTEADY-STATE WATERFLOOD

This chapter develops the unsteady-state capacitance-dispersion model for tracer concentrations during a constant rate waterflood. Both partitioning and nonpartitioning tracers can be modeled. The oil and water are divided into dendritic and flowing fractions, with mass transfer of tracer allowed between each of the dendritic and flowing fractions.

The variables and parameters in the model are summarized in Figure 3-1. Variables are functions of position and time, while the parameters are numbers which are constant for any given simulation. The subscript i is used to refer to tracer i, while j and k refer to the liquid phase (1 = oil, 2 = water). The 14 variables are:

S_1, S_2 Oil and water saturations

S_1^f, S_1^d Flowing and dendritic saturations of oil

S_2^f, S_2^d Flowing and dendritic saturations of water

C_{i1}^f, C_{i1}^d Tracer concentrations of tracer i in the flowing and dendritic oil saturations

C_{i2}^f, C_{i2}^d Tracer concentrations of tracer i in the flowing and dendritic water saturations

k_{r1}, k_{r2} Oil and water relative permeabilities

f_1, f_2 Oil and water fractional flow

The parameters are:

A Area

ϕ Porosity

q Water injection flow rate

C^o_{i2} Tracer concentration in the injected water slug

M_{ij} Mass transfer coefficients

K_{ij} Dispersion coefficients. Dispersivity α_{ij} is input in the computer model, $K_{ij} = \alpha_{ij} v_j$

The equations are derived below and summarized in Table 3-1.

EQUATIONS FOR TRACER CONCENTRATION DURING AN UNSTEADY-STATE WATERFLOOD

1. Tracer Material Balance

The tracer material balance is obtained by balancing the flux and accumulation of tracer i in a control volume. The total flux of tracer i at any point x along the core is:

$$\text{Total Flux} = \sum_{j=1}^{2} \left\{ f_j \, q \, C_{ij}^f - A\phi \, S_j^f \, K_{ij} \frac{\partial}{\partial x} C_{ij}^f \right\} \qquad (3\text{-}1)$$

where the following convention is used for the subscripts:

i = component (individual tracer) = 1, 2, 3, . . .

j, k = phase (1 = oil, 2 = water)

Consider a control volume with a length of Δx. The tracer in the control volume is obtained by summing over the flowing and dendritic fractions of the oil and water.

$$\text{Tracer in C. V.} = A\phi\Delta x \sum_{j=1}^{2} (S_j^f C_{ij}^f + S_j^d C_{ij}^d) \qquad (3\text{-}2)$$

The tracer material balance equation is derived by setting the difference in the flux of the tracer at x and x + Δx equal to the accumulation of tracer in the control volume:

$$\{\text{Total Flux}|_x - \text{Total Flux}|_{x-\Delta x}\} \, \Delta t = \{\text{Tracer in C. V.}|_{t-\Delta t} - \text{Tracer in C. V.}|_t\} \quad . \qquad (3\text{-}3)$$

Substituting Equations (3-1) and (3-2) into Equation (3-3), dividing by $\Delta t \Delta x$, and grouping similar terms, the material balance equation becomes:

$$\sum_{j=1}^{2} \left\{ \frac{(f_j\, q\, C_{ij}^f \big|_{x-\Delta x} - f_j\, q\, C_{ij}^f \big|_x)}{\Delta x} - \frac{A\phi \left\{ S_j^f K_{ij} \frac{\partial}{\partial x} C_{ij}^f \Big|_{x+\Delta x} - S_j^f K_{ij} \frac{\partial}{\partial x} C_{ij}^f \Big|_x \right\}}{\Delta x} \right\} =$$

$$\sum_{j=1}^{2} \left\{ \frac{- A\phi \left[\{ S_j^f C_{ij}^f \big|_{t-\Delta t} - S_j^f C_{ij}^f \big|_t \} + \{ S_j^d C_{ij}^d \big|_{t-\Delta t} - S_j^d C_{ij}^d \big|_t \} \right]}{\Delta t} \right\} \qquad (3\text{-}4)$$

where we have summed over the number of phases. In the limit, Equation (3-4) becomes:

$$\sum_{j=1}^{2} \frac{\partial}{\partial x} (f_j\, q\, C_{ij}^f) - \sum_{j=1}^{2} A\phi \frac{\partial}{\partial x} \left(S_j^f K_{ij} \frac{\partial}{\partial x} C_{ij}^f \right) =$$

$$\sum_{j=1}^{2} - A\phi \frac{\partial}{\partial t} [S_j^f C_{ij}^f + S_j^d C_{ij}^d] \qquad (3\text{-}5)$$

Performing the summation on both sides of Equation (3-5) and rearranging, the material balance equation becomes:

$$A\phi \frac{\partial}{\partial t} (S_1^f C_{i1}^f + S_1^d C_{i1}^d + S_2^f C_{i2}^f + S_2^d C_{i2}^d) + \frac{\partial}{\partial x} (f_1\, q\, C_{i1}^f + f_2\, q\, C_{i2}^f) =$$

$$A\phi \frac{\partial}{\partial x} \left(S_1^f K_{i1} \frac{\partial}{\partial x} C_{i1}^f + S_2^f K_{i2} \frac{\partial}{\partial x} C_{i2}^f \right) \qquad (3\text{-}6)$$

Next, introduce the dispersivity α_{ij}:

$$K_{ij} = \alpha_{ij} v_j = \alpha_{ij} \left\{ \frac{q\, f_j}{A\phi S_j^f} \right\} \qquad (3\text{-}7)$$

where v_j is the velocity of the flowing fraction of phase j.

Substituting into Equation (3-6) gives:

$$A\phi \frac{\partial}{\partial t}\left(S_1^f C_{i1}^f + S_1^d C_{i1}^d + S_2^f C_{i2}^f + S_2^d C_{i2}^d\right) + \frac{\partial}{\partial x}\left(f_1 q C_{i1}^f + f_2 q C_{i2}^f\right) =$$

$$q \frac{\partial}{\partial x}\left(f_1 \alpha_{i1} \frac{\partial}{\partial x} C_{i1}^f\right) + q \frac{\partial}{\partial x}\left(f_2 \alpha_{i2} \frac{\partial}{\partial x} C_{i2}^f\right) \qquad (3\text{-}8)$$

The next three equations are concerned with the mass transfer of the tracer between the flowing and dendritic saturations. See Figure 3-2. We have assumed that tracer mass transfer can occur between the flowing oil and water and between the flowing and dendritic saturations of both oil and water but not between dendritic oil and water.

2. Partitioning Coefficient

When the tracer is partitioning, it is assumed that the tracer concentrations in the flowing water and oil are in equilibrium. For tracer i partitioning between the j and k phases, the partitioning coefficient P_{ijk} is:

$$P_{ijk} = \frac{C_{ij}^f}{C_{ik}^f} \qquad (3\text{-}9)$$

then

$$C_{ij}^f = P_{ijk} C_{ik}^f \qquad (3\text{-}10)$$

Choosing j = 1 and k = 2, Equation (3-10) becomes:

$$C_{i1}^f = P_{i12} C_{i2}^f \qquad (3\text{-}11)$$

For a nonpartitioning tracer, $P_{i12} = 0$.

3, 4. Rate Equations for Mass Transfer Between the Flowing and Dendritic Fractions

Diffusion of the tracer from the flowing to the dendritic phases is given by a first-order rate equation:

$$\frac{\partial}{\partial t}(S_1^d C_{i1}^d) = M_{i1}(C_{i1}^f - C_{i1}^d) \tag{3-12}$$

$$\frac{\partial}{\partial t}(S_2^d C_{i2}^d) = M_{i2}(C_{i2}^f - C_{i2}^d) \tag{3-13}$$

where M_{ij} is the mass transfer coefficients for each phase.

5, 6. Relationship Between Flowing and Total Saturations

The relationship between the flowing and total saturations is taken from steady-state measurements.

$$S_1^f = \text{function}_1(S_1) \tag{3-14}$$

$$S_2^f = \text{function}_2(S_2) \tag{3-15}$$

7. Saturation Material Balance

From continuity considerations, the equation for the flow of water through the core is (Craig, 1971; Marle, 1981) (1 = oil, 2 = water):

$$\frac{\partial}{\partial t} S_2 + \frac{q}{A\phi} \frac{\partial}{\partial x} f_2 = 0 \tag{3-16}$$

where q is the constant rate at which water is injected into the core during the waterflood.

8, 9, 10. Saturation Constraints

The saturation in each phase is divided into the flowing and dendritic saturations:

$$S_1 = S_1^d + S_1^f \tag{3-17}$$

$$S_2 = S_2^d + S_2^f \tag{3-18}$$

The saturations must add up to 1:

$$(S_1^d + S_1^f) + (S_2^d + S_2^f) = 1 \tag{3-19}$$

or

$$S_1 + S_2 = 1 \tag{3-20}$$

11. Fractional Flow Versus Water Saturation

Neglecting capillary pressure effects and assuming horizontal flow, the fractional flow equation is (Craig, 1971):

$$f_2 = \frac{1}{1 + \frac{(\mu_2 k_{r1})}{(\mu_1 k_{r2})}} \tag{3-21}$$

where μ_1 and μ_2 are the oil and water viscosities, and k_{r1} and k_{r2} are the oil and water relative permeabilities.

12. Fractional Flow Constraint

The fractional flow of oil and water must add up to 1:

$$f_1 + f_2 = 1 \tag{3-22}$$

13, 14. Relative Permeability Relationships

The oil-and-water-relative-permeability-versus-water-saturation relationships are determined from steady-state relative permeability measurements or from mathematical relationships:

$$k_{r1} = \text{function}_3\,(S_2) \tag{3-23}$$

$$k_{r2} = \text{function}_4\,(S_2) \tag{3-24}$$

Initial and Boundary Conditions

The core is initially at IWS and contains no tracer:

$$S_2 = (S_2)_{IWS} \qquad x \geq 0,\ t = 0 \tag{3-25}$$

$$C^f_{i1} = C^d_{i1} = C^f_{i2} = C^d_{i2} = 0 \qquad x \geq 0,\ t = 0 \tag{3-26}$$

Start water injection at $t = 0$, and inject a slug of tracer for time t_s with a concentration of C^0_{i2}:

$$f_2 = 1.0 \qquad x = 0,\ 0 < t \tag{3-27}$$

$$C^f_{i2} = C^0_{i2} \qquad x = 0,\ 0 < t \leq t_s \tag{3-28a}$$

$$C^f_{i2} = 0 \qquad x = 0,\ t > t_s \tag{3-28b}$$

$$\frac{\partial}{\partial x} C^f_{i2} = 0 \qquad x = L,\ 0 < t \tag{3-28c}$$

NONDIMENSIONAL EQUATIONS

The equations for the unsteady-state model are put into dimensionless form prior to deriving the finite difference equations. The equations that must be nondimensionalized are the tracer material balance equation (Equation (3-8)), the partitioning equation (Equation (3-11)), the mass transfer rate equations (Equations (3-12) and (3-13)), the saturation material balance (Equation (3-16)), and the initial and boundary conditions (Equations (3-25) to (3-28)). The remaining equations for the saturations and fractional flow are already dimensionless. The following variables and parameters are used to nondimensionalize the equations:

1. Dimensionless Time (Cumulative Pore Volumes Injected)

$$t_D = \frac{\int_0^t q\,dt}{AL\phi} = \frac{q\,t}{AL\phi} = \frac{v\,t}{L} \tag{3-29}$$

where the total flow rate, q, is constant and v is:

$$v = \frac{q}{A\phi} \tag{3-30}$$

2. Dimensionless Distance

$$x_D = x/L \tag{3-31}$$

3. Dimensionless Concentrations

$$C^f_{D_{ij}} = \frac{C^f_{ij}}{C^0_{i2}} \qquad j = 1 \text{ and } 2 \tag{3-32}$$

$$C^d_{D_{ij}} = \frac{C^d_{ij}}{C^0_{i2}} \qquad j = 1 \text{ and } 2 \qquad (3\text{-}33)$$

where C^0_{i2} is the original tracer concentration in the injected slug.

4. Damkohler Number, $M_{D_{ij}}$, the Ratio of Mass Transfer to Convection

$$M_{D_{ij}} = \frac{M_{ij}\, L}{v} \qquad (3\text{-}34)$$

5. Dimensionless Dispersivity

$$\alpha_{D_{ij}} = \frac{K_{ij}}{v_j\, L} = \frac{\alpha_{ij}}{L} \qquad (3\text{-}35)$$

In nondimensionalizing the equations, we will use an average nondimensional dispersivity, $\bar{\alpha}_D$,

$$\bar{\alpha}_D = f_1\, \alpha_{D_{i1}}\, P_{i12} + f_2\, \alpha_{D_{i2}} \qquad (3\text{-}36)$$

or written using α_{ij}:

$$\bar{\alpha}_D = \frac{[f_1\, \alpha_{i1}\, P_{i12} + f_2\, \alpha_{i2}]}{L} \qquad (3\text{-}37)$$

α_{i1} and α_{i2} are input as constants, and $\bar{\alpha}_D$ varies during the simulations.

Tracer Material Balance

Substituting in Equation (3-11) for the partitioning coefficient, the tracer material balance equation (Equation (3-8)) becomes:

$$A\phi \frac{\partial}{\partial t}\left[C_{i2}^{f}\left(S_1^{f} P_{i12} + S_2^{f}\right) + S_1^{d} C_{i1}^{d} + S_2^{d} C_{i2}^{d}\right] + q \frac{\partial}{\partial x}\left[C_{i2}^{f}\left(f_1 P_{i12} + f_2\right)\right] =$$

$$q \frac{\partial}{\partial x}\left[\left(f_1 \alpha_{i1} P_{i12} + f_2 \alpha_{i2}\right) \frac{\partial}{\partial x} C_{i2}^{f}\right] \qquad (3\text{-}38)$$

Substituting in Equations (3-29) to (3-34) to nondimensionalize the equation and rearranging:

$$\frac{q C_{i2}^{0}}{L} \frac{\partial}{\partial\left(\frac{q t}{A\phi L}\right)}\left[\frac{C_{i2}^{f}}{C_{i2}^{0}}\left(S_1^{f} P_{i12} + S_2^{f}\right) + S_1^{d} \frac{C_{i1}^{d}}{C_{i2}^{0}} + S_2^{d} \frac{C_{i2}^{d}}{C_{i2}^{0}}\right] +$$

$$\frac{q C_{i2}^{0}}{L} \frac{\partial}{\partial(x/L)}\left[\frac{C_{i2}^{f}}{C_{i2}^{0}}\left(f_1 P_{i12} + f_2\right)\right] =$$

$$\frac{q C_{i2}^{0}}{L} \frac{\partial}{\partial(x/L)}\left[\frac{\left(f_1 \alpha_{i1} P_{i12} + f_2 \alpha_{i2}\right)}{L} \frac{\partial}{\partial(x/L)} \frac{C_{i2}^{f}}{C_{i2}^{0}}\right] \qquad (3\text{-}39)$$

Simplifying and using Equation (3-37) for $\bar{\alpha}_D$ gives the dimensionless form of the tracer material balance equation:

$$\frac{\partial}{\partial t_D}\left[C_{D_{i2}}^{f}\left(S_1^{f} P_{i12} + S_2^{f}\right)\right] + \frac{\partial}{\partial t_D}\left(C_{D_{i1}}^{d} S_1^{d}\right) + \frac{\partial}{\partial t_D}\left(C_{D_{i2}}^{d} S_2^{d}\right) +$$

$$\frac{\partial}{\partial x_D}\left[C_{D_{i2}}^{f}\left(f_1 P_{i12} + f_2\right)\right] = \frac{\partial}{\partial x_D}\left[\bar{\alpha}_D \frac{\partial}{\partial x_D} C_{D_{i2}}^{f}\right] \qquad (3\text{-}40)$$

Partitioning Coefficient

Substituting Equations (3-32) and (3-33) into Equation (3-11) for the partitioning coefficient gives:

$$C^f_{D_{i1}} = P_{i12}\, C^f_{D_{i2}} \tag{3-41}$$

Rate Equations for Mass Transfer Between the Flowing and Dendritic Fractions

The rate equations for the mass transfer are:

$$\frac{\partial}{\partial t}\left(S^d_1\, C^d_{i1}\right) = M_{i1}\left(C^f_{i1} - C^d_{i1}\right) \tag{3-12}$$

$$\frac{\partial}{\partial t}\left(S^d_2\, C^d_{i2}\right) = M_{i2}\left(C^f_{i2} - C^d_{i2}\right) \tag{3-13}$$

Substituting Equations (3-29) to (3-34) into Equation (3-12) gives:

$$\frac{C^0_{i2}}{L/v}\,\frac{\partial}{\partial(vt/L)}\left[\frac{S^d_1\, C^d_{i1}}{C^0_{i2}}\right] = \frac{C^0_{i2}}{L/v}\left[\frac{M_{i1}\, L}{v}\right]\left[\frac{C^f_{i1} - C^d_{i1}}{C^0_{i2}}\right] \tag{3-42}$$

which can be simplified to:

$$\frac{\partial}{\partial t_D}\left(C^d_{D_{i1}}\, S^d_1\right) = M_{D_{i1}}\left(C^f_{D_{i1}} - C^d_{D_{i1}}\right) \tag{3-43}$$

Similarly, Equation (3-13) becomes:

$$\frac{\partial}{\partial t_D}\left(C^d_{D_{i2}}\, S^g_2\right) = M_{D_{i2}}\left(C^f_{D_{i2}} - C^d_{D_{i2}}\right) \tag{3-44}$$

Saturation Material Balance

The saturation material balance equation is:

$$\frac{\partial}{\partial t} S_2 + \frac{q}{A\phi}\frac{\partial}{\partial x} f_2 = 0 \tag{3-16}$$

Substituting Equations (3-29) and (3-31) into (3-16),

$$\frac{q}{AL\phi}\frac{\partial}{\partial\left(\frac{q\,t}{AL\phi}\right)} S_2 + \frac{q}{AL\phi}\frac{\partial}{\partial(x/L)} f_2 = 0 \tag{3-45}$$

which simplifies to:

$$\frac{\partial}{\partial t_D} S_2 + \frac{\partial}{\partial x_D} f_2 = 0 \tag{3-46}$$

Initial and Boundary Conditions

Core initially at IWS; contains no tracer:

$$S_2 = (S_2)_{IWS} \qquad x \geq 0,\ t = 0 \qquad (3\text{-}25)$$

$$C^f_{i1} = C^d_{i1} = C^f_{i2} = C^d_{i2} = 0 \qquad x \geq 0,\ t = 0 \qquad (3\text{-}26)$$

Making these dimensionless:

$$S_2 = (S_2)_{IWS} \qquad x_D \geq 0,\ t_D = 0 \qquad (3\text{-}47)$$

$$C^f_{D_{i1}} = C^d_{D_{i1}} = C^f_{D_{i2}} = C^d_{D_{i2}} = 0 \qquad x_D \geq 0,\ t_D = 0 \qquad (3\text{-}48)$$

Boundary conditions—start water injection at $t = 0$ and inject a slug of tracer for time t_s:

$$f_2 = 1.0 \qquad x = 0,\ 0 < t \qquad (3\text{-}27)$$

$$C^f_{i2} = C^0_{i2} \qquad x = 0,\ 0 < t \leq t_s \qquad (3\text{-}28a)$$

$$C^f_{i2} = 0 \qquad x = 0,\ t > t_s \qquad (3\text{-}28b)$$

$$\frac{\partial}{\partial_x} C^f_{i2} = 0 \qquad x = L,\ 0 < t \qquad (3\text{-}28c)$$

In nondimensional form, the slug of tracer is injected for time t_{Ds}:

$$f_2 = 0 \qquad x_D = 0,\ 0 < t_D \qquad (3\text{-}49)$$

$$C^f_{D_{i2}} = 1 \qquad x_D = 0,\ 0 < t_D \leq t_{Ds} \qquad (3\text{-}50a)$$

$$C^f_{D_{i2}} = 0 \qquad x_D = 0,\ t_D > t_{Ds} \qquad (3\text{-}50b)$$

$$\frac{\partial}{\partial x_D} C^f_{D_{i2}} = 0 \qquad x_D = 1,\ 0 < t_D \qquad (3\text{-}50c)$$

The nondimensionalized equations derived above, along with the additional, already-dimensionless equations in the model, are summarized in Table 3-1.

TABLE 3-1

DIMENSIONLESS EQUATIONS FOR TRACER

CONCENTRATION IN UNSTEADY-STATE FLOW

Note: Let 1 = oil, 2 = water

1. Tracer Material Balance:

$$\frac{\partial}{\partial t_D}\left[C^f_{D_{i2}}\left(S^f_1 P_{i12} + S^f_2\right)\right] + \frac{\partial}{\partial t_D}\left(C^d_{D_{i1}} S^d_1\right) + \frac{\partial}{\partial t_D}\left(C^d_{D_{i2}} S^d_2\right) +$$

$$\frac{\partial}{\partial x_D}\left[C^f_{D_{i2}}\left(f_1 P_{i12} + f_2\right)\right] = \frac{\partial}{\partial x_D}\left[\bar{\alpha}_D \frac{\partial}{\partial x_D} C^f_{D_{i2}}\right] \qquad (3\text{-}40)$$

2. Partitioning Coefficient

$$C^f_{D_{i1}} = P_{i12}\, C^f_{D_{i2}} \qquad (3\text{-}41)$$

3, 4. Rate Equations for Mass Transfer Between the Flowing and Dendritic Fractions

$$\frac{\partial}{\partial t_D}\left(C^d_{D_{i1}} S^d_1\right) = M_{D_{i1}}\left(C^f_{D_{i1}} - C^d_{D_{i1}}\right) \qquad (3\text{-}43)$$

$$\frac{\partial}{\partial t_D}\left(C^d_{D_{i2}} S^d_2\right) = M_{D_{i2}}\left(C^f_{D_{i2}} - C^d_{D_{i2}}\right) \qquad (3\text{-}44)$$

5, 6. Relationship Between Flowing and Dendritic Fractions

$$S^f_1 = \text{function}_1\left(S_1\right) \qquad (3\text{-}14)$$

TABLE 3-1 (CONTINUED)

DIMENSIONLESS EQUATIONS FOR TRACER CONCENTRATION IN UNSTEADY-STATE FLOW

$$S_2^f = \text{function}_2\,(S_2) \tag{3-15}$$

7. Saturation Material Balance

$$\frac{\partial}{\partial t_D} S_2 + \frac{\partial}{\partial x_D} f_2 = 0 \tag{3-46}$$

8, 9, 10. Saturation Constraints

$$S_1 = S_1^d + S_1^f \tag{3-17}$$

$$S_2 = S_2^d + S_2^f \tag{3-18}$$

$$(S_1^d + S_1^f) + (S_2^d + S_2^f) = 1 \tag{3-19}$$

or

$$S_1 + S_2 = 1 \tag{3-20}$$

11. Fractional Flow Versus Water Saturation

$$f_2 = \frac{1}{1 + \frac{(\mu_2\, k_{r1})}{(\mu_1\, k_{r2})}} \tag{3-21}$$

TABLE 3-1 (CONTINUED)

DIMENSIONLESS EQUATIONS FOR TRACER CONCENTRATION IN UNSTEADY-STATE FLOW

12. Fractional Flow Constraint

$$f_1 + f_2 = 1 \tag{3-22}$$

13, 14. Relative Permeability Relations

$$k_{r1} = \text{function}_3\,(S_2) \tag{3-23}$$

$$k_{r2} = \text{function}_4\,(S_2) \tag{3-24}$$

15. Average Dimensionless Dispersivity

$$\bar{\alpha}_D = \frac{[f_1\,\alpha_{i1}\,P_{i12} + f_2\,\alpha_{i2}]}{L} \tag{3-37}$$

Initial and Boundary Conditions

Core initially at IWS; contains no tracer:

$$S_2 = (S_2)_{IWS} \qquad x_D \geq 0,\ t_D = 0 \tag{3-47}$$

$$C^f_{D_{i1}} = C^d_{D_{i1}} = C^f_{D_{i2}} = C^d_{D_{i2}} = 0 \qquad x_D \geq 0,\ t_D = 0 \qquad (3\text{-}48)$$

Start water injection at $t = 0$ and inject a slug of tracer for time t_{Ds}

$$f_2 = 0 \qquad x_D = 0,\ 0 < t_D \qquad (3\text{-}49)$$

$$C^f_{D_{i2}} = 1 \qquad x_D = 0,\ 0 < t_D \leq t_{Ds} \qquad (3\text{-}50a)$$

$$C^f_{D_{i2}} = 0 \qquad x_D = 0,\ t_D > t_{Ds} \qquad (3\text{-}50b)$$

$$\frac{\partial}{\partial x_D} C^f_{D_{i2}} = 0 \qquad x_D = 1,\ 0 < t_D \qquad (3\text{-}50c)$$

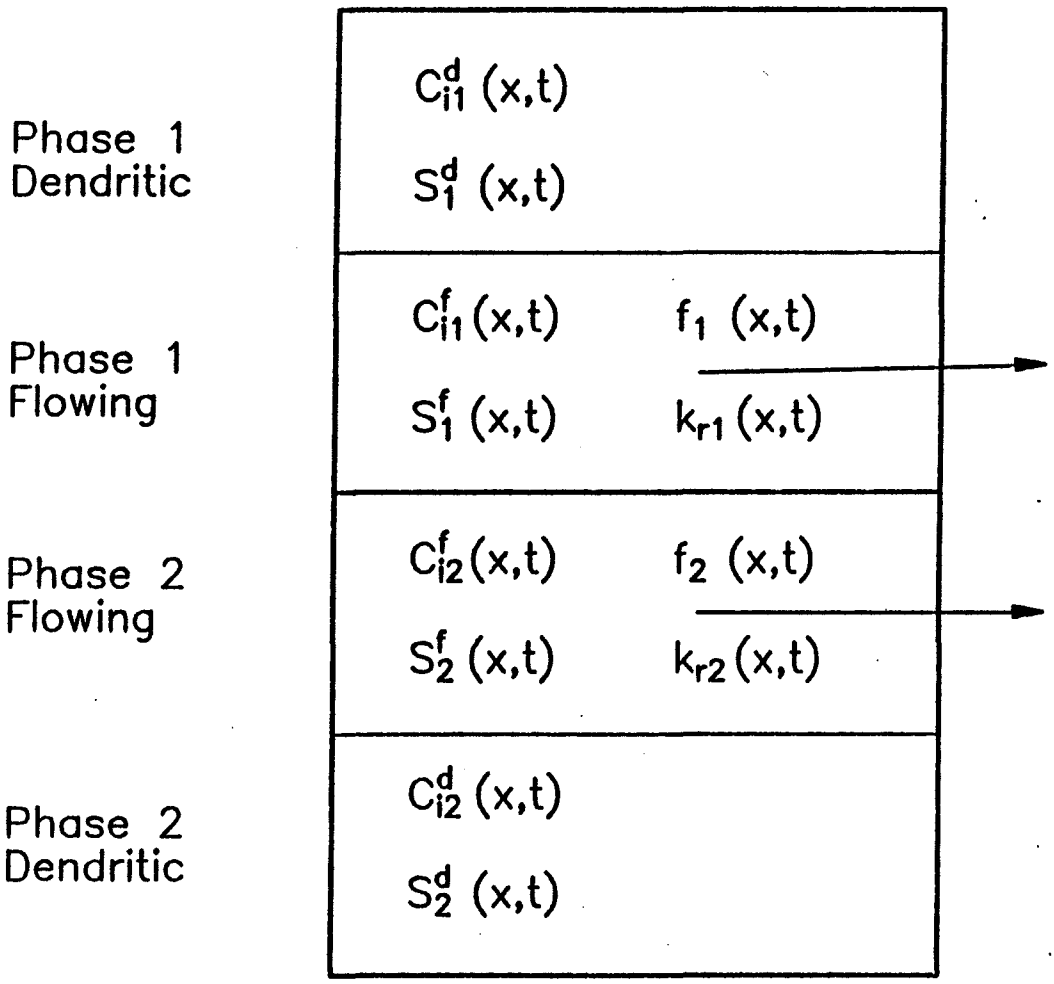

Parameters

A	φ	q
C_{i2}^{0}	P_{i12}	
M_{ij}	K_{ij}	

Figure 3-1 Diagram showing the variables and parameters in the unsteady-state capacitance model.

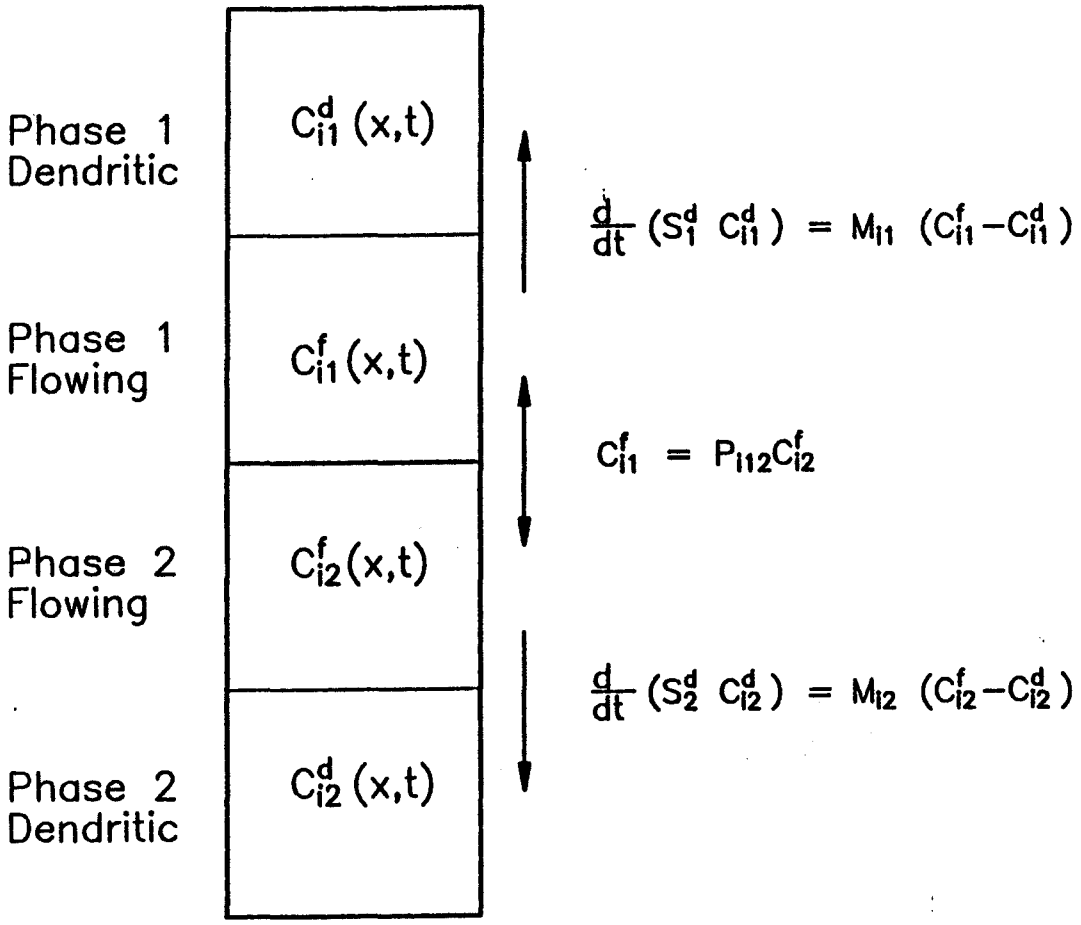

Mass Transfer of Tracer i

Figure 3-2 Diagram showing assumed tracer mass transfer and partitioning behavior in the unsteady-state model.

CHAPTER 4

CAPACITANCE-DISPERSION MODEL FOR STEADY, TWO-PHASE FLOW

A capacitance-dispersion model for steady, two- or three-phase flow which includes partitioning has been developed by Mojdeh Delshad (1986). The following equations describe the capacitance-dispersion model for the case of steady, two-phase flow. Because of the steady-flow assumption, the model is a simplified version of the unsteady-state model developed in the previous chapter.

In the steady-flow experiments, water and oil are injected at constant rates until equilibrium is reached. A slug of tracer is then injected, and the model calculates the tracer concentrations along the core as a function of distance, x, and time, t. The variables and parameters in the model are summarized in Figure 4-1. Phase 1 is the oil, and Phase 2 is the water. The variables are functions of position and time, while the parameters are numbers which are constant for any given simulation. The oil and water flowing fractions are constant, and it is assumed that the flowing and dendritic saturations in the core are also constant. The only variables are the concentrations of tracer in the dendritic and flowing fractions of the water and oil:

C_{i1}^{f}, C_{i1}^{d} Tracer concentrations of tracer i in the flowing and dendritic oil saturations

C_{i2}^{f}, C_{i2}^{d} Tracer concentrations of tracer i in the flowing and dendritic water saturations

To model a steady-state experiment, values of the parameters below are used to predict the tracer effluent from the core. Some of the parameters are measured, while the remainder are adjustable parameters that are varied until good agreement is obtained between the predicted and experimental data. The parameters known from the experiment are:

A	Cross-sectional area
ϕ	Porosity
q	Total injected flow rate of water and oil
f_1, f_2	Oil and water fractional flow
P_{i12}	The tracer partitioning coefficient between oil and water
C_{i2}^0	The tracer concentration in the injected water

The adjustable parameters are:

M_{ij}	Mass transfer coefficients
K_{ij}	Dispersion coefficients. Dispersivity α_{ij} is input in the computer model, $K_{ij} = \alpha_{ij} v_j$, where v_j is the frontal velocity of Phase J
S_1, S_2	Oil and water saturations
S_1^f, S_1^d	Flowing and dendritic saturations of oil

S_2^f, S_2^d Flowing and dendritic saturations of water

Not all of the parameters are independent. For example, the fractional flows of oil and water must add up to 1. The constraints are derived below for the model.

EQUATIONS FOR TRACER CONCENTRATION DURING STEADY-STATE, TWO-PHASE FLOW

The equations for the tracer concentrations and the parameter constraints are derived below and summarized in Table 4-7. The equations are put into dimensionless form with Equations (3-29) to (3-35). There are four unknowns in the model: C_{i1}^f, C_{i1}^d, C_{i2}^f, and C_{i2}^d. The first three model equations for the tracer concentrations are concerned with the mass transfer of the tracer between the flowing and dendritic saturations. See Figure 4-2. As in the unsteady-state case, we have assumed that tracer mass transfer can only occur between the flowing oil and water, flowing and dendritic oil, and flowing and dendritic water.

1. Partitioning Coefficient

When the tracer is partitioning, it is assumed that the tracer concentrations in the flowing water and oil are instantaneously in equilibrium. For tracer i partitioning between oil and water, the partitioning coefficient P_{ijk} is:

$$C_{i1}^f = P_{i12} C_{i2}^f \tag{3-11}$$

For a nonpartitioning tracer, P_{i12} is 0. Substituting Equations (3-32) and (3-33) into Equation (3-11) gives:

$$C^f_{D_{i1}} = P_{i12}\, C^f_{D_{i2}} \tag{4-1}$$

2, 3. Rate Equations for Mass Transfer Between the Flowing and Dendritic Fractions

The first-order rate equations for diffusion of tracer from the flowing to dendritic phases are:

$$\frac{\partial}{\partial t}(S^d_1\, C^d_{i1}) = M_{i1}\,(C^f_{i1} - C^d_{i1}) \tag{3-12}$$

$$\frac{\partial}{\partial t}(S^d_2\, C^d_{i2}) = M_{i2}\,(C^f_{i2} - C^d_{i2}) \tag{3-13}$$

For steady-flow conditions, the saturations are constant and the equations simplify:

$$S^d_1 \frac{\partial}{\partial t}(C^d_{i1}) = M_{i1}\,(C^f_{i1} - C^d_{i1}) \tag{4-2}$$

$$S^d_2 \frac{\partial}{\partial t}(C^d_{i2}) = M_{i2}\,(C^f_{i2} - C^d_{i2}) \tag{4-3}$$

Putting into dimensionless form:

$$S^d_1 \frac{\partial}{\partial t_D}(C^d_{D_{i1}}) = M_{D_{i1}}\,(C^f_{D_{i1}} - C^d_{D_{i1}}) \tag{4-4}$$

$$S^d_2 \frac{\partial}{\partial t_D}(C^d_{D_{i2}}) = M_{D_{i2}}\,(C^f_{D_{i2}} - C^d_{D_{i2}}) \tag{4-5}$$

4. Tracer Material Balance

The fourth equation for the tracer concentrations is the overall tracer material balance equation. The unsteady-state equation was derived in the previous chapter:

$$A\phi \frac{\partial}{\partial t}\left(C^f_{i2}\,(S^f_1\,P_{i12} + S^f_2) + S^d_1\,C^d_{i1} + S^d_2\,C^d_{i2}\right) + q\,\frac{\partial}{\partial x}\left[C^f_{i2}\,(f_1 P_{i12} + f_2)\right] =$$

$$q\,\frac{\partial}{\partial x}\left((f_1\,\alpha_{i1}\,P_{i12} + f_2\,\alpha_{i2})\,\frac{\partial}{\partial x}\,C^f_{i2}\right) \qquad (3\text{-}38)$$

where we have already substituted in Equation (3-11) for the partitioning coefficient. Simplifying the equation for steady-flow conditions:

$$A\phi\,(S^f_1\,P_{i12} + S^f_2)\,\frac{\partial}{\partial t}\,C^f_{i2} + A\phi\,S^d_1\,\frac{\partial}{\partial t}\,C^d_{i1} + A\phi\,S^d_2\,\frac{\partial}{\partial t}\,C^d_{i2} + q\,(f_1 P_{i12} + f_2)\,\frac{\partial}{\partial x}\,C^f_{i2} =$$

$$q\,(f_1\,\alpha_{i1}\,P_{i12} + f_2\,\alpha_{i2})\,\frac{\partial^2}{\partial x^2}\,C^f_{i2} \qquad (4\text{-}6)$$

Using Equations (3-29) to (3-35) gives the dimensionless form of the equation:

$$(S^f_1\,P_{i12} + S^f_2)\,\frac{\partial}{\partial t_D}\,C^f_{D_{i2}} + S^d_1\,\frac{\partial}{\partial t_D}\,C^d_{D_{i1}} + S^d_2\,\frac{\partial}{\partial t_D}\,C^d_{D_{i2}} + (f_1 P_{i12} + f_2)\,\frac{\partial}{\partial x_D}\,C^f_{D_{i2}} =$$

$$(f_1\,\alpha_{i1}\,P_{i12} + f_2\,\alpha_{i2})\,\frac{\partial^2}{\partial x_D{}^2}\,C^f_{D_{i2}} \qquad (4\text{-}7)$$

For computational convenience, Delshad introduced the following parameters which are constant for a given fractional flow:

Averaged nondimensional dispersivity, $\bar{\alpha}_D$:

$$\bar{\alpha}_D = f_1\,\alpha_{D_{i1}}\,P_{i12} + f_2\,\alpha_{D_{i2}} \qquad (4\text{-}8)$$

For the steady-state case, $\bar{\alpha}_D$ is constant.

Averaged saturation, $\bar{S}$:

$$\bar{S} = S_1^f P_{i12} + S_2^f \tag{4-9}$$

Averaged fractional flow, $\bar{f}$:

$$\bar{f} = f_1 P_{i12} + f_2 \tag{4-10}$$

Substituting Equations (4-8) to (4-10) into Equation (4-7) gives the tracer material balance equation:

$$\bar{S} \frac{\partial}{\partial t_D} C_{D_{i2}}^f + S_1^d \frac{\partial}{\partial t_D} C_{D_{i1}}^d + S_2^d \frac{\partial}{\partial t_D} C_{D_{i2}}^d + \bar{f} \frac{\partial}{\partial x_D} C_{D_{i2}}^f = \bar{\alpha} \frac{\partial^2}{\partial x_D{}^2} C_{D_{i2}}^f \tag{4-11}$$

PARAMETER CONSTRAINTS

Saturation Constraints

The saturation in each phase is divided into the flowing and dendritic saturations (Equations (3-17) and (3-18)):

$$S_1 = S_1^d + S_1^f \tag{4-12}$$

$$S_2 = S_2^d + S_2^f \tag{4-13}$$

The saturations must add up to 1 (Equations (3-19) and (3-20)):

$$(S_1^d + S_1^f) + (S_2^d + S_2^f) = 1 \tag{4-14}$$

or

$$S_1 + S_2 = 1 \tag{4-15}$$

Fractional Flow Constraint

The fractional flow of oil and water must also add up to 1 (Equation (3-22)):

$$f_1 + f_2 = 1 \tag{4-16}$$

Initial and Boundary Conditions

Core initially contains no tracer

$$C^f_{i1} = C^d_{i1} = C^f_{i2} = C^d_{i2} = 0 \qquad x \geq 0,\ t = 0 \tag{4-17}$$

In dimensionless form

$$C^f_{D_{i1}} = C^d_{D_{i1}} = C^f_{D_{i2}} = C^d_{D_{i2}} = 0 \qquad x_D \geq 0,\ t_D = 0 \tag{4-18}$$

Boundary conditions: start water injection at t - 0, and inject a slug of tracer for time t_s

$$C^f_{i2} = C^0_{i2} \qquad x = 0,\ 0 < t \leq t_s \tag{4-19a}$$

For a partitioning tracer

$$C^f_{i1} = P_{i12}\, C^0_{i2} \qquad x = 0,\ 0 < t \leq t_s \qquad (4\text{-}19b)$$

For a nonpartitioning tracer (different values of i for Phase 1 and Phase 2)

$$C^f_{i1} = C^0_{i1} \qquad (4\text{-}19c)$$

After slug injection

$$C^f_{i2} = C^f_{i1} = 0 \qquad x = 0,\ t > t_s \qquad (4\text{-}19d)$$

At the outlet

$$\frac{\partial}{\partial x} C^f_{i2} = \frac{\partial}{\partial x} C^f_{i1} = 0 \qquad x = L,\ 0 < t \qquad (4\text{-}20)$$

In nondimensional form, the slug of tracer is injected for time t_{Ds}

$$C^f_{D_{i2}} = 1 \qquad x_D = 0,\ 0 < t_D \leq t_{Ds} \qquad (4\text{-}21a)$$

For a partitioning tracer

$$C^f_{D_{i1}} = P_{i12} \qquad x_D = 0,\ 0 < t_D \leq t_{Ds} \qquad (4\text{-}21b)$$

For a nonpartitioning tracer

$$C^f_{D_{i1}} = 1 \qquad x_D = 0,\ 0 < t_D \leq t_{Ds} \qquad (4\text{-}21c)$$

$$C^f_{D_{i2}} = C^f_{D_{i1}} = 0 \qquad x_D = 0,\ t > t_{Ds} \qquad (4\text{-}21d)$$

$$\frac{\partial}{\partial x_D} C^f_{D_{i2}} = \frac{\partial}{\partial x_D} C^f_{D_{i1}} = 0 \qquad x_D = 1,\ 0 < t_D \qquad (4\text{-}22)$$

The nondimensionalized equations derived above are summarized in Table 4-1. To solve these equations, they must be put into finite difference form. This is shown in Appendix C, while Appendix D contains the listing of the computer program.

TABLE 4-1

DIMENSIONLESS EQUATIONS

FOR TRACER CONCENTRATION IN STEADY-STATE FLOW

Note: Let 1 = oil, 2 = water

1. Partitioning Coefficient

$$C^f_{D_{i1}} = P_{i12}\, C^f_{D_{i2}} \qquad (4\text{-}1)$$

2. 3. Rate Equations for Mass Transfer Between the Flowing and Dendritic Fractions

$$S^d_1 \frac{\partial}{\partial t_D} (C^d_{D_{i1}}) = M_{D_{i1}} (C^f_{D_{i1}} - C^d_{D_{i1}}) \qquad (4\text{-}4)$$

$$S^d_2 \frac{\partial}{\partial t_D} (C^d_{D_{i2}}) = M_{D_{i2}} (C^f_{D_{i2}} - C^d_{D_{i2}}) \qquad (4\text{-}5)$$

TABLE 4-1 (CONTINUED)

DIMENSIONLESS EQUATIONS

FOR TRACER CONCENTRATION IN STEADY-STATE FLOW

4. Tracer Material Balance

$$\bar{S}\frac{\partial}{\partial t_D}C^f_{D_{i2}} + S^d_1\frac{\partial}{\partial t_D}C^d_{D_{i1}} + S^d_2\frac{\partial}{\partial t_D}C^d_{D_{i2}} + \bar{f}\frac{\partial}{\partial x_D}C^f_{D_{i2}} = \bar{\alpha}\frac{\partial^2}{\partial x_D{}^2}C^f_{D_{i2}} \qquad (4\text{-}11)$$

PARAMETERS

$$\bar{\alpha}_D = f_1\,\alpha_{D_{i1}}\,P_{i12} + f_2\,\alpha_{D_{i2}} \qquad (4\text{-}8)$$

$$\bar{S} = S^f_1\,P_{i12} + S^f_2 \qquad (4\text{-}9)$$

$$\bar{f} = f_1\,P_{i12} + f_2 \qquad (4\text{-}10)$$

PARAMETER CONSTRAINTS

Saturation

$$S_1 = S^d_1 + S^f_1 \qquad (4\text{-}12)$$

$$S_2 = S^d_2 + S^f_2 \qquad (4\text{-}13)$$

$$(S^d_1 + S^f_1) + (S^d_2 + S^f_2) = 1 \qquad (4\text{-}14)$$

or

$$S_1 + S_2 = 1 \tag{4-15}$$

Fractional Flow Constraint

$$f_1 + f_2 = 1 \tag{4-16}$$

Initial and Boundary Conditions

Core initially contains no tracer:

$$C^f_{D_{i1}} = C^d_{D_{i1}} = C^f_{D_{i2}} = C^d_{D_{i2}} = 0 \qquad x_D \geq 0,\ t_D = 0 \tag{4-18}$$

Boundary conditions: start water injection at $t_D = 0$, and inject a slug of tracer for time t_{Ds}:

$$C^f_{D_{i2}} = 1 \qquad x_D = 0,\ 0 < t_D \leq t_{Ds} \tag{4-21a}$$

$$C^f_{D_{i1}} = P_{i12} \qquad x_D = 0,\ 0 < t_D \leq t_{Ds} \tag{4-21b}$$

$$C^f_{D_{i1}} = 1 \qquad x_D = 0,\ 0 < t_D \leq t_{Ds} \tag{4-21c}$$

$$C^f_{D_{i2}} = C^f_{D_{i1}} = 0 \qquad x_D = 0,\ t > t_{Ds} \tag{4-21d}$$

$$\frac{\partial}{\partial x_D} C^f_{D_{i2}} = \frac{\partial}{\partial x_D} C^f_{D_{i1}} = 0 \qquad x_D = 1,\ 0 < t_D \tag{4-22}$$

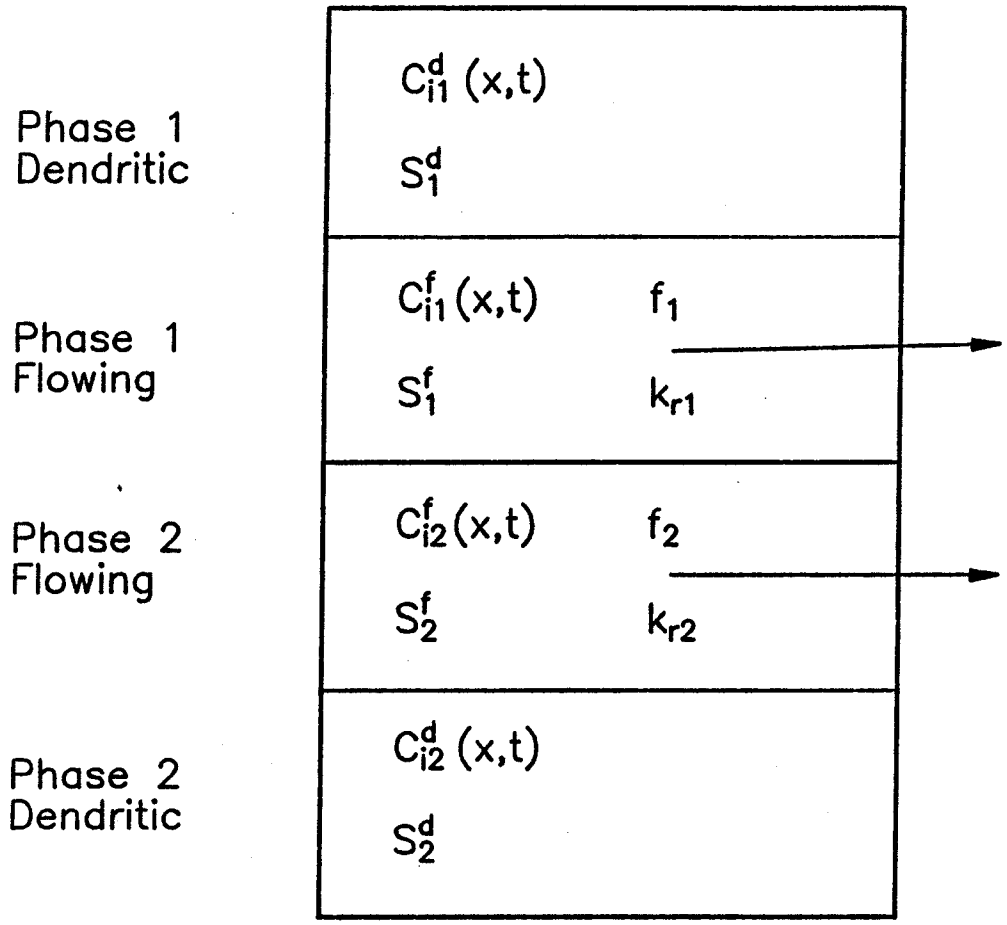

Parameters

A	φ	q
C_{i2}^{0}	P_{i12}	
M_{ij}	K_{ij}	

Figure 4-1 Diagram showing the variables and parameters in the steady-state capacitance model.

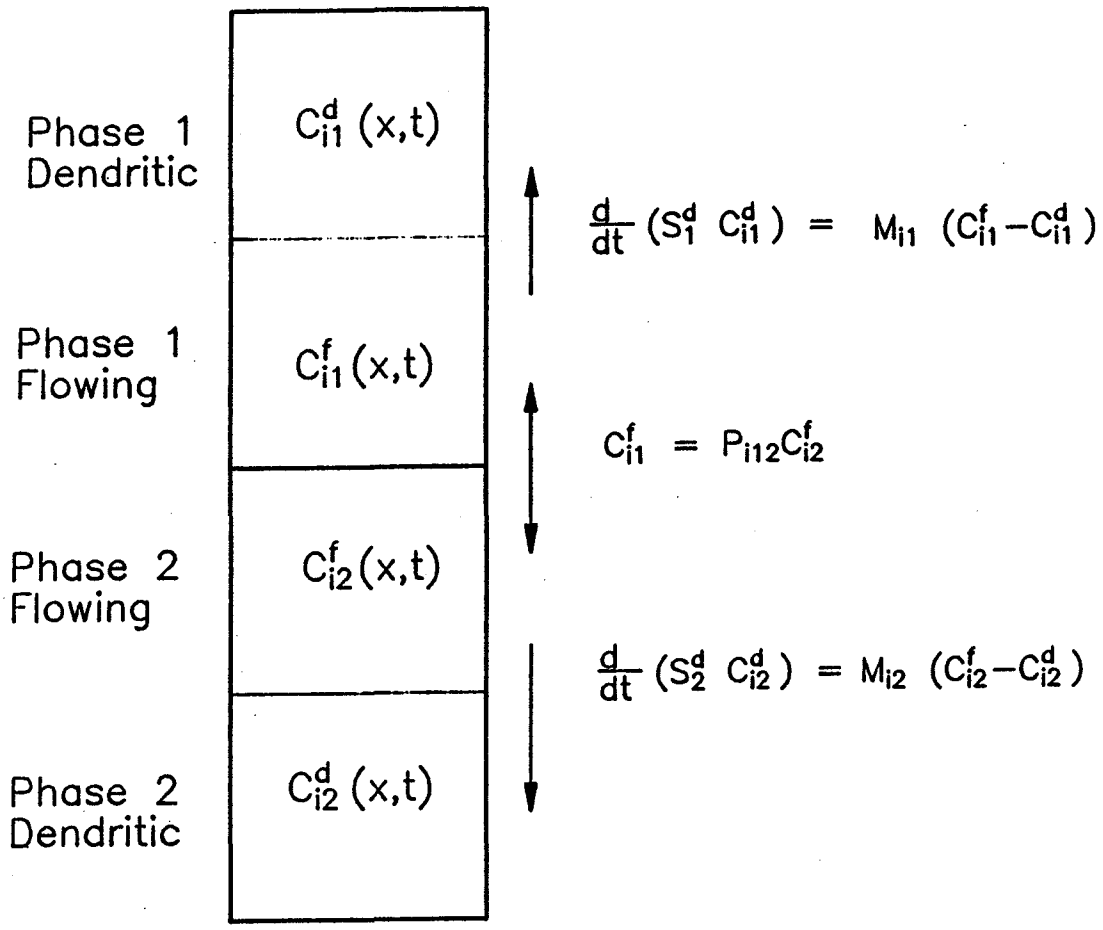

Figure 4-2 Diagram showing assumed tracer mass transfer and partitioning behavior in the steady-state model.

CHAPTER 5

EXPERIMENTAL PROCEDURES

A water-wet and a neutrally wet Berea core were tested. Prior to the experiments, the cores were mounted in epoxy, the wettability of the neutrally wet core was established, the wettability of both cores was measured, and the cores were saturated with brine.

Three sets of experiments were then conducted for each Berea core:

1. Single-phase tracer tests
2. Steady-flow, two-phase tracer tests
3. Unsteady-state waterfloods with a tracer slug

The single-phase tracer tests measured the dispersion of tracer in 100 percent brine-saturated core at different velocities. These tests were performed for three reasons: (1) test the experimental system before starting the more complicated two-phase tests, (2) determine the dependence of dispersion on velocity, and (3) obtain a qualitative idea of core heterogeneity.

A series of steady-flow, two-phase tracer tests were conducted at several different fractional flows of oil and water, starting at the irreducible water saturation (IWS), with 100 percent oil flowing. At each fractional flow, oil and water were injected into the core until steady state was reached, then the pressure drop across the core was measured to determine the relative permeability. While maintaining steady-state flow conditions, a slug containing partitioning and nonpartitioning tracers was injected into the core and the concentration of

the different tracers in the effluent measured. A series of tracer measurements were made by increasing the fractional flow of water (and water saturation) and simultaneously decreasing the fractional flow of oil (and oil saturation). The final steady-state measurement had 100 percent water flowing at the residual oil saturation (ROS).

There were two reasons for the steady-flow tracer measurements. First, they were used to estimate saturations with the steady-state capacitance-dispersion model. These estimated saturations were compared with saturations determined by material balance to determine if partitioning tracers could accurately determine saturations. Second, the steady-state data were used as input to the unsteady-state capacitance-dispersion model. The model output using the steady-state data was compared with the unsteady-state tracer experiments.

The final set of experiments were unsteady-state waterfloods. The core was flooded with oil to drive it to IWS, then an unsteady-state, constant rate waterflood was started. A slug of tracers was injected at the start of the waterflood, followed by unlabeled brine. Pressure drop, oil and water production, and tracer concentration in the effluent were all measured. Tracer effluent data was compared with model predictions based on the steady-state data.

CORE PREPARATION

The first preparation step was mounting 2- by 2- by 24-inch Berea cores in epoxy. The mounted core, shown in Figure 5-1, has two pressure taps located 6 inches from each end and 12 inches apart. These pressure taps were used to measure pressure drop during steady-flow measurements. Pressure drop could also be measured across the entire core, as was done during the unsteady-state measurements. Four electrodes were attached to the core for electrical resistivity measurements: two silver screens located beneath the

headers and two wires wrapped around the core as shown in Figure 5-1. Details on the mounting procedure can be found in Appendix F.

One variable examined in these experiments was wettability. A water-wet and a neutrally wet core were tested. The water-wet Berea core was not treated prior to the experiments, while the neutrally wet Berea core was prepared with organochlorosilanes. A detailed procedure is given in Appendix E. The wettability of both cores was determined using the combined USBM-Amott method on adjacent, identically treated plugs. See Appendix E.

The results are shown in Table 5-1. The untreated plugs are strongly water-wet, with an average USBM wettability index of 1.06 and an average $D_{by\text{-}water}$ of 0.89. The organochlorosilane-treated plugs show greater variability in the wettability measurements. Some of the USBM wettability indices are negative. The volume of water imbibition is smaller than for untreated Berea, and one of the plugs imbibed oil. The organochlorosilane-treated long core probably has a wettability somewhere between mildly water-wet and neutrally wet.

TABLE 5-1

USBM AND AMOTT WETTABILITY MEASUREMENTS

Untreated, Water-Wet Plugs

Plug No.	USBM Index	Amott	
		$D_{by\text{-}water}$	$D_{by\text{-}oil}$
DIR-W4	1.0	0.92	0.0
DIR-W5	1.1	0.91	0.0
DIR-W6	1.1	0.83	0.0

TABLE 5-1 (CONTINUED)

USBM AND AMOTT WETTABILITY MEASUREMENTS

Organochlorosilane-Treated Plugs

Plug No.	USBM Index	Amott $D_{by\text{-}water}$	Amott $D_{by\text{-}oil}$
DIR-O1	0.46	0.39	0.02
DIR-O1	0.30	0.41	0.0
DIR-O5	−0.29	0.26	0.0
DIR-O6	−0.14	0.21	0.0

After the neutrally wet core was treated, both cores were saturated with brine and the porosity determined. The cores were evacuated, and brine was metered in, providing a liquid pore volume. The pore volume was also determined gravimetrically by the increase in weight of the brine-saturated core. The complete procedure is given in Table 5-2.

TABLE 5-2

SATURATION AND POROSITY DETERMINATION

1. Connect two-way valves to all of the pressure taps on the dry, epoxy-coated core.

2. Connect a vacuum pump to one valve and close all of the others. Evacuate the core under vacuum of 30 millitorr for 24 hours.

TABLE 5-2 (CONTINUED)

SATURATION AND POROSITY DETERMINATION

3. Weigh the evacuated core.

4. To saturate the core, connect a burette filled with brine to the end of the core opposite the vacuum pump. Allow brine to flow into the core under the pressure differential created by vacuum pump and the hydraulic head of the burette. Disconnect the vacuum pump when approximately 80 percent of the core has been saturated, and leave the burette connected for another 24 hours to completely saturate the core.

5. An approximate pore volume can be obtained from the volume of brine used to saturate the core, after subtracting out the small volume in the pressure taps and the lines connected to the valves.

6. Weigh the core after saturation. The difference between the weight of the dry and saturated core divided by the brine density is a verification of the pore volume.

7. Calculate the porosity by dividing the pore volume by the bulk volume of the core, which was obtained by caliper measurements.

SINGLE-PHASE TRACER TESTS

The first set of experiments were single-phase tracer tests in 100 percent brine-saturated cores. As stated previously, these experiments were designed to (1) test the system, (2) determine the dependence of dispersion on velocity, and (3) obtain a rough idea of core heterogeneity. The experimental setup shown in Figure 5-2 was used for the single-phase tracer tests and also for the unsteady-state, two-phase flow tests. A detailed procedure for the single-phase tracer tests is given in Table 5-3.

TABLE 5-3

STEADY, SINGLE-PHASE BRINE FLOW PROCEDURES

PREFLOOD

1. Fill short sections of tubing leading from bottle of labeled brine to the three-way valve (see Figure 5-2). Set the labeled bottle on top of a digital balance.

2. Set pump at desired flow rate. Set sample collector for desired test tube collection time.

3. Start pump, flowing unlabeled brine to the waste container. Once the pump reaches the correct flow rate, open inlet and outlet valves to the core. Open three-way valve to the core.

4. Turn on sample collector.

5. Open the pressure tap valves to the core.

TABLE 5-3 (CONTINUED)

STEADY, SINGLE-PHASE BRINE FLOW PROCEDURES

6. Start data acquisition on the HP-1000 computer.

TRACER INJECTION

When steady-state conditions are reached, the following steps are taken for tracer injection:

1. Zero the digital balance.

2. Open the three-way valve to the labeled brine, start the stopwatch, and note the time.

3. Move the sample collector ahead to a new rack of test tubes in the automated fraction collector.

4. After the balance shows that the desired amount of labeled brine has been injected, switch the three-way valve back to the unlabeled brine.

5. Read the balance and note the time on the stopwatch.

6. Continue injecting brine at a constant rate and collect the produced brine in the fraction collector. Throughout the entire run, stopper the test tubes as soon after collection as possible to prevent evaporation of the isobutyl alcohol, IBA (if it is being used).

TABLE 5-3 (CONTINUED)

STEADY, SINGLE-PHASE BRINE FLOW PROCEDURES

POSTFLOOD

The following steps are taken after the run:

1. Open the three-way valve to the waste container.

2. Stop the stopwatch; note time.

3. Turn off pump.

4. Close core valves.

5. Turn off sample collector.

6. Stop data acquisition on the HP-1000.

To start a tracer experiment, unlabeled brine was injected at a constant rate into the Berea core using one of the pumps in a Hewlett-Packard HP-1082B Dual Liquid Chromatograph pump. Pressure was monitored with a Rosemount Alphaline Pressure Transducer (dual scale, 0-100 psi, 0-17 psi) powered by a Hewlett-Packard 6218B Power Supply. The transducer was calibrated for 0-17 psi. The details of the connection to the pressure transducer are shown in Figure 5-3. To prevent brine from corroding the transducer, the tubing next to the pressure transducer was filled with BLANDOL[4], a refined mineral oil.

Once steady-state conditions were reached, a three-way valve was opened to the brine containing tracer, and a slug of brine labeled with chloride-36 was injected into the core. The volume of the slug was monitored with a Sauter RC-4021 digital balance. Once the desired volume of tracer was injected, the three-way valve was opened to the unlabeled brine and injection continued. The effluent from the core was collected in test tubes using an Isco Retriever III Fraction Collector. After the experiment was finished, the test tubes were analyzed for chloride-36 by the Radiochemistry Group, Analytical Sevices. A discussion of the fluids, tracers, and the analysis procedures for all of the experiments is given below.

Tracer measurements were repeated at several different flow rates to determine the relationship between flow rate and dispersion. In addition to tracer measurements, brine permeability and electrical resistivity of the 100 percent brine-saturated core were also measured. The brine permeability was determined by injecting brine at a constant rate while measuring the pressure drop across the center 12 inches of the core, then calculating with Darcy's Law:

$$k_2 = \frac{q\,\mu_2\,L}{A\,\Delta P} \qquad (5\text{-}1)$$

Pressure drop was measured over the center 12 inches of the core in the steady-state, single-phase and two-phase experiments to avoid the outlet capillary end effect in the two-phase measurements. Electrical resistivity was measured using the four-electrode method and a Hewlett-Packard HP-4262A LCR meter. The procedure used is discussed in Appendix G.

STEADY-FLOW, TWO-PHASE TRACER TESTS

After the single-phase experiments, steady-flow, two-phase relative permeability and tracer measurements were made. These experiments had two purposes: (1) compare saturations calculated by the two-phase,

steady-flow computer model with saturations estimated from material balance, and (2) collect data that was used in the unsteady-state model to predict the unsteady-state experiments. The experimental apparatus for the steady-state experiments is shown in Figure 5-4. The modification from the single-phase apparatus is the addition of labeled and unlabeled decane injected with the second pump of the HP-1082B Liquid Chromatograph (LC) pumps. Brine and decane were pumped directly from the LC pumps, thus avoiding the need for transfer cylinders. Fluids were mixed in the flow line approximately 6 inches before entering the core.

Prior to the steady-state experiments, the core was driven with decane to its irreducible water saturation. The volume of produced fluids was used to keep track of the saturations. A series of steady-flow, two-phase tracer and relative permeability measurements were made at different fractional flows of water and oil, starting with 100 percent oil flowing at IWS and ending with 100 percent water flowing at ROS. These relative permeabilities were measured with the water saturation increasing (imbibition relative permeabilities in a water-wet core), since the water saturation also increases in the unsteady-state relative permeability measurements. Saturations were determined both from material balance and by using the two-phase capacitance-dispersion model developed in Chapter 4.

At the start of the measurements at each fractional flow of water, water and oil were injected at the desired fractional flows until steady-state conditions were reached. The criteria for steady-state were:

1. Constant flow rates.
2. Constant phase fractional flows.
3. Constant pressure drop across the 1-foot center section of the core.

Once steady state was reached, electrical resistivity and effective and relative permeabilities were measured. The procedures used to measure electrical resistivity are given in Appendix G. Effective permeability is defined as the permeability to each flowing phase in the presence of other flowing or stationary phase. It is calculated using:

$$k_j = \frac{q f_j \mu_j L}{A \Delta P} \tag{5-2}$$

where the pressure drop was measured across the center 12 inches of the core. For relative permeability calculations, the effective permeabilities are normalized with the absolute permeability at 100 percent brine saturation:

$$k_{rj} = \frac{k_j}{k_w} \tag{5-3}$$

The steady-state tracer measurements were begun once the relative permeability and electrical resistivity measurements were completed. The detailed procedure is given in Table 5-4. To start a tracer measurement, unlabeled brine and decane were injected into the Berea core at a desired fractional flow rate. Once steady state was reached, three-way valves were opened to the labeled brine and decane, and slugs of each were injected. The volumes of the slugs were monitored with two Sauter RC-4021 digital balances. Once the desired volumes of tracers were injected, the three-way valves were opened to the unlabeled fluids and injection continued. As for single-phase tests, the effluent from the core was collected in test tubes using an Isco Retriever III Fraction Collector. The experiment continued until all of the labeled fluids were produced from the core.

TABLE 5-4

STEADY, TWO-PHASE FLOW PROCEDURES

PREFLOOD

The following steps are taken before tracer injection starts:

TABLE 5-4 (CONTINUED)

STEADY, TWO-PHASE FLOW PROCEDURES

1. To ensure accurate material balance, drain the tubing that leads from the effluent end of the core to the sample collector.

2. Fill the short sections of tubing leading from the bottles of labeled fluids to the three-way valve. (See Figure 5-4.) Set each of the labeled bottles on top of a digital balance.

3. Set the pumps at desired flow rates. Set the sample collector for the desired test tube collection time.

4. Start the pumps, flowing unlabeled fluids to the waste container. Once the pumps reach their correct flow rates, open the inlet and outlet valves to the core. Open the three-way valve to the core.

5. Turn on the sample collector.

6. Open the pressure tap valves to the core.

7. Start data aquisition on the HP-1000 computer.

TRACER INJECTION

When steady-state conditions are reached, the following steps are taken for the tracer injection:

1. Zero the digital balances.

2. Open the three-way valves to the labeled fluids, start the stopwatch, and note the time.

TABLE 5-4 (CONTINUED)

STEADY, TWO-PHASE FLOW PROCEDURES

3. Move the sample collector ahead to a new rack of test tubes.

4. After the balance shows that the desired amount of labeled fluids is injected, switch the three-way valves back to the unlabeled fluids.

5. Read the balances and note the time on the stopwatch.

6. Continue injecting the fluids at a constant rate and collect the produced fluids in the fraction collector. Throughout the entire run, stopper the test tubes as soon after collection as possible to prevent evaporation of the isobutyl alcohol (IBA) tracer.

POSTFLOOD

The following steps are taken after the run:

1. Open the three-way valve to the waste container.

2. Stop the stopwatch and note the time.

3. Turn off the pumps.

4. Close the core valves.

TABLE 5-4 (CONTINUED)

STEADY, TWO-PHASE FLOW PROCEDURES

5. Turn off the sample collector.

6. Stop data acquisition on the HP-1000.

Three tracers were used in the steady-state tests: (1) chloride-36, a nonpartitioning tracer in the brine; (2) tritiated decane, a nonpartitioning tracer in the decane; and (3) isobutyl alcohol (IBA), a tracer that partitions between the oil and water with a partitioning coefficient, P_{i12}, of 4.8. Once an experiment was finished. test tubes were analyzed for the three tracers. A discussion of the fluids, tracers, and analysis procedures is given below.

UNSTEADY-STATE EXPERIMENTS

The final set of experiments was the unsteady-state waterfloods, which used the apparatus shown in Figure 5-2. A detailed procedure is given in Table 5-5. For these experiments, pressure drop was measured across the entire core, rather than the center 12 inches, since this is the pressure drop used in the JBN method of calculating relative permeability. Prior to each unsteady-state waterflood experiment, decane was injected at 20 mL/min until IWS was reached. A constant rate waterflood was then started using brine labeled with chloride-36, IBA, and Carbon-14 labeled IPA. Pressure drop and electrical resistivity were measured, and the effluent collected using the fraction collector. The injected volume of labeled brine was

measured with the digital balance. Once the desired slug size of labeled brine was injected, the constant rate water injection was switched to unlabeled brine and continued until all of the labeled brine was produced. The volume of oil and water produced as a function of time was determined from the test tubes in the fraction collector.

Three tracers were used in the unsteady-state tests: chloride-36, a nonpartitioning tracer in the brine, and two partitioning tracers: (1) isobutyl alcohol (IBA) with a partitioning coefficient, P_{i12}, of 4.8 and (2) carbon-14 labeled isopropyl alcohol (IPA) with a partitioning coefficient of 30. The analysis procedures for the tracers are given below.

TABLE 5-5

UNSTEADY-STATE EXPERIMENTAL PROCEDURES

PREFLOOD

The following steps are taken before starting water injection:

1. Drain the tubing leading from the effluent end of the core to the sample collector for material balance purposes.

2. Set the desired water flow rate on the pump. Set the sample collector for the desired test tube collection time.

3. Start the pump flowing labeled brine to the waste container. See Figure 5-2. This is done so that labeled brine will enter the core immediately when the waterflood is started.

TABLE 5-5 (CONTINUED)

UNSTEADY-STATE EXPERIMENTAL PROCEDURES

4. Open the pressure valves to the core. Open the inlet and outlet valves to the core.

WATERFLOOD AND TRACER INJECTION

The following steps are taken during the waterflood:

5. The waterflood is started with the following four steps being performed simultaneously:

   a. Open the three-way valve to the core.

   b. Zero the digital balance.

   c. Start the data acquisition program on the HP-1000 computer to measure pressure and electrical resistivity.

   d. Start the stopwatch and note the time.

6. Start the sample collector when the first drops come out of the tubing that connects the effluent end of the core to the collector.

7. When the desired amount of labeled brine has been injected according to the balance, switch the three-way valve to start injecting unlabeled brine. Read the balance and note the time on the stopwatch. When calculating the amount of labeled brine injected, the labeled brine in the tubing that leads to the core must be included.

TABLE 5-5 (CONTINUED)

UNSTEADY-STATE EXPERIMENTAL PROCEDURES

8. Continue injecting water at a constant rate and collect the produced fluids in the fraction collector. Stopper the test tubes as often as possible to prevent evaporation of IBA and IPA.

POSTFLOOD

The following steps are taken to end the run:

1. Open the three-way valve to the waste container.

2. Stop the stopwatch and note the time.

3. Turn off the pump.

4. Close the core valves.

5. Turn off the sample collector.

6. Stop data acquisition on the HP-1000.

FLUIDS AND TRACERS

Brine and n-decane were used in all experiments. The brine contained 1.1 weight percent NaCl, 25 ppm $CaCl_2$, and 500 ppm active glutaraldehyde (a biocide) by weight. The technical grade n-decane was obtained from Phillips Petroleum. All fluids were filtered through a 0.45-micron Millipore-type HA filter paper using a Millipore filter and a vacuum flask. Fluids were degassed before injection by applying a vacuum to the fluids while stirring with a magnetic stirrer. Physical properties of the fluids can be found in Table 5-6.

TABLE 5-6

PHYSICAL PROPERTIES OF BRINE

AND n-DECANE AT 75°F

	Density, g/cc	Viscosity, cp
n-Decane, Technical Grade	0.7273	0.866
Brine	1.0048	0.917

Partitioning and nonpartitioning tracers were used in the two-phase experiments, while only the nonpartitioning tracers could be used in the single-phase experiments. In order to obtain 4 different tracers that could be easily measured, both radioactive and nonradioactive tracers were used. Three different radioactive tracers were used:

1. Chloride-36 was added to the brine and used as a nonpartitioning tracer in all of the experiments.

2. Tritiated decane was used as a tracer in the steady-state, two-phase experiments.

3. Carbon-14 labeled isopropyl alcohol (IPA) was used as a partitioning tracer in the unsteady-state, two-phase experiments.

In addition to the radioactive tracers, isobutyl alcohol (IBA) was used as a chemical tracer in the steady- and unsteady-state, two-phase experiments. The procedures for measuring the radioactive and chemical tracers are given in Tables 5-7 and 5-8, respectively. Tracer concentrations were normalized with the initial concentrations using the program Rawdata; see Appendix H.

TABLE 5-7

RADIOACTIVE TRACER MEASUREMENTS

1. Plastic scintillation vials (20 mL) were numbered to correspond to the sampling order of the test tubes. Vials with caps were weighed empty.

2. Depending on the amount of fluid available in the test tube, 1- or 5-mL samples of brine or decane were taken and placed in the appropriately numbered vial. Three samples were taken of the labeled fluids that were injected into the core and used to normalize the data.

3. Vials were weighed again to determine the exact weight of the liquid sample.

TABLE 5-7 (CONTINUED)

RADIOACTIVE TRACER MEASUREMENTS

4. Fifteen ml of Aquasol, a commercial scintillation cocktail, was added to each vial. Vials were then shaken vigorously by hand.

5. Vials were place in a Packard Tricarb 4530 liquid scintillation spectrometer and counted for 20 minutes each. Disintegrations per minute per gram were calculated and reported. Standards (traceable to the National Bureau of Standards) were obtained from New England Nuclear Co. and used to generate calibration curves. Data were collected, stored, and analyzed with software written by Conoco's Radiochemistry group on a DEC PDP 11/73.

TABLE 5-8

ISOBUTYL ALCOHOL MEASUREMENTS

1. The 1-mL samples of brine or decane were taken and placed in small glass vials. Three samples were taken of the labeled fluids that were injected into the core and used to normalize the data.

2. Decane was analyzed for alcohol using a Varian 3700 gas chromatograph with a flame ionization detector (FID) equipped with a backflush valve.

3. Brine was analyzed for alcohol using an HP 5710 gas chromatograph with an FID.

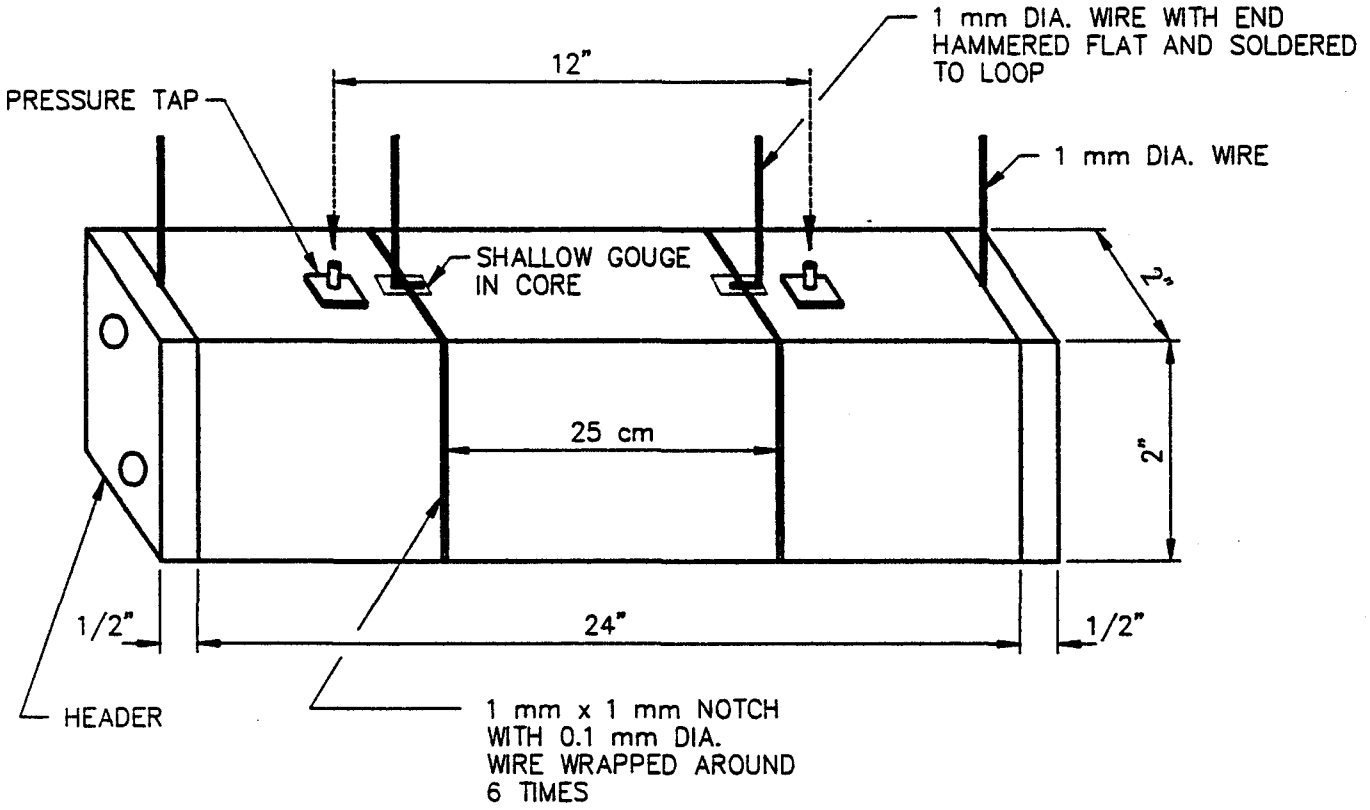

Figure 5-1 Diagram of core.

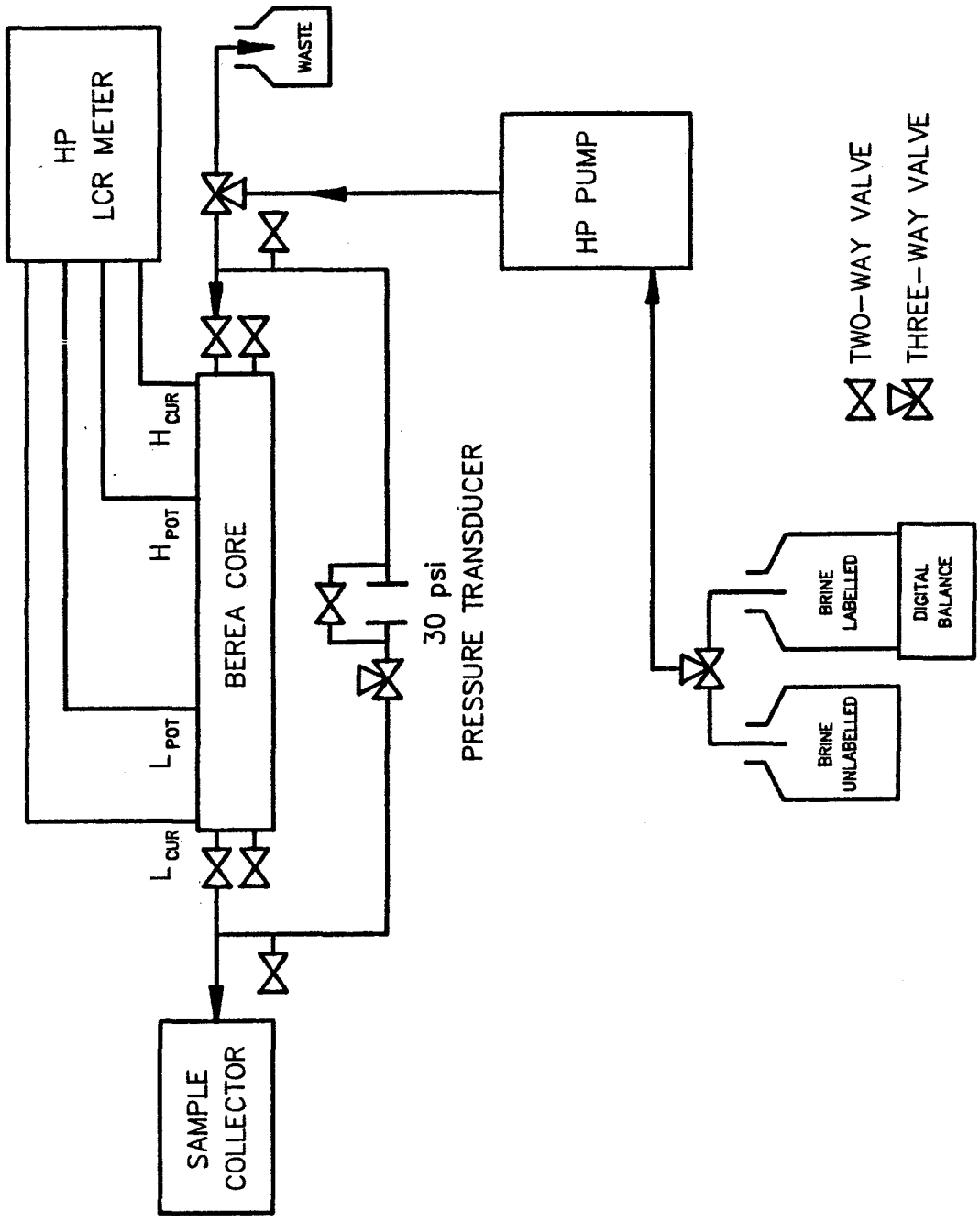

Figure 5-2 Diagram of apparatus used for unsteady-state experiments.

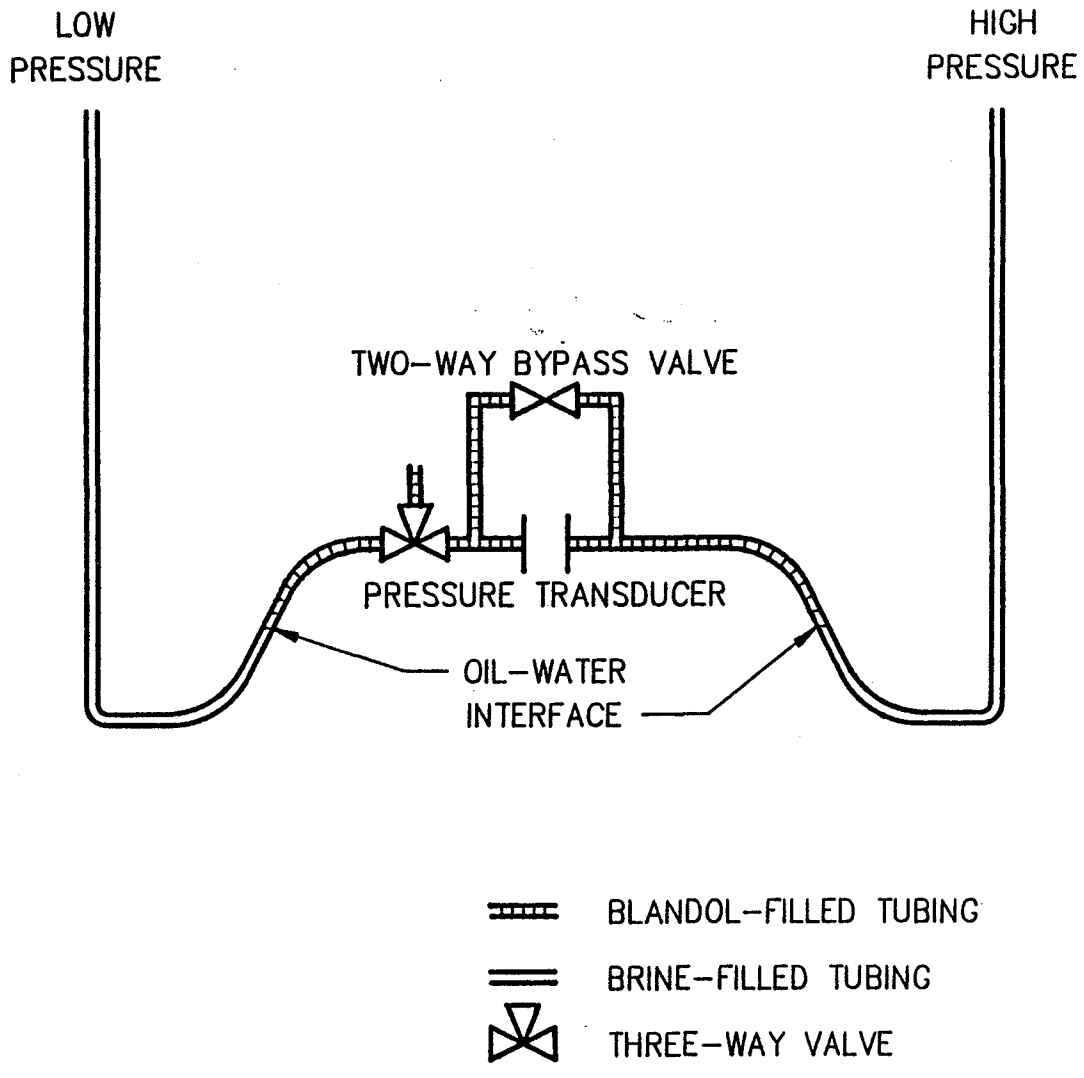

Figure 5-3 Diagram showing arrangement of pressure transducer.

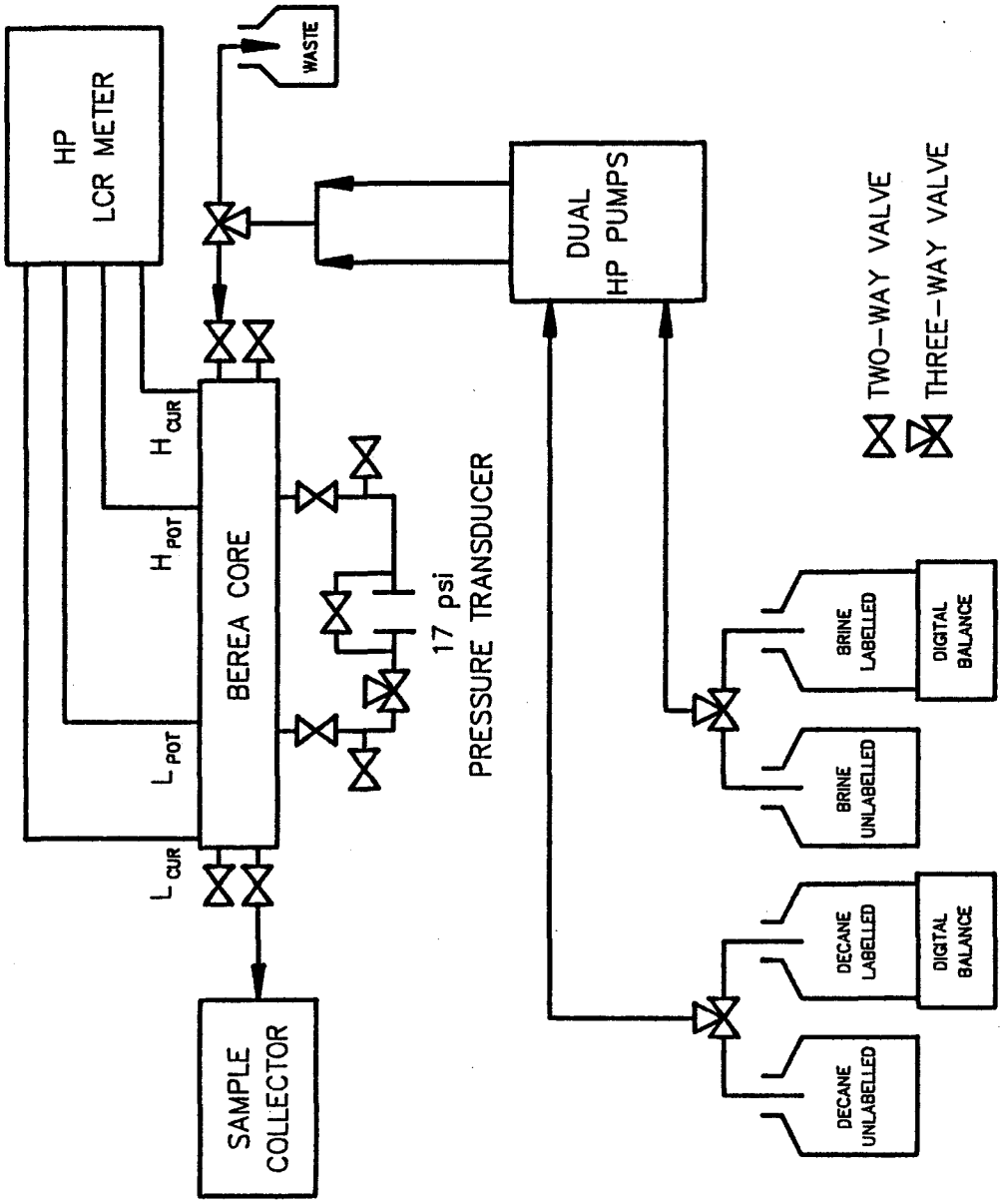

Figure 5-4 Diagram of apparatus used for steady-state experiments.

CHAPTER 6

SINGLE-PHASE EXPERIMENTAL RESULTS

In the first set of experiments, the Berea cores were 100 percent saturated with brine. The objectives of the single-phase experiments were:

1. Determine basic core properties such as liquid porosity and permeability.

2. Determine the homogeneity of the core.

3. Determine the dependence of the dispersion coefficient on velocity.

The single-phase experiments were performed at a room temperature of 27°C on two Berea sandstone cores cut approximately 2 feet long and 2 inches square. Table 6-1 shows the basic properties of each core. Since gravity segregation was not expected to occur, the cores were positioned horizontally.

TABLE 6-1

BEREA CORE PROPERTIES

	Water-Wet Core	Treated Core
Length (cm)	60.75	60.85
Cross-Sectional Area (cm^2)	24.90	25.95
Bulk Volume (cm^3)	1512.7	1579.1
Porosity	0.217	0.204
Absolute Brine Permeability (md)	662.0	512.0
Residual Brine Saturation	0.315	0.300
Residual Decane Saturation	0.345	0.259
Average USBM Wettability Index	1.06	0.08

EXPERIMENT W1: WATER-WET CORE

After the water-wet Berea core had been saturated with brine, three tracer injection experiments were performed at constant flow rates of 4.74, 0.977, and 0.585 mL/min. The absolute brine permeability was measured at steady-state. A slug of brine tagged with Cl-36 was then injected as a method of assessing the homogeneity of the porous medium as well as determining the dispersion coefficient for Cl-36 and its dependence on velocity. A detailed description of the procedure is given in Table 5-3.

The dispersion data is presented as normalized tracer concentration versus total pore volumes of brine injected in Figures 6-1 to 6-3. Values for dispersivity, mass transfer coefficient, flowing fraction, and other basic core properties are reported above the curves. The lines shown in Figures 6-1 to 6-3 are a best fit to the data using the capacitance dispersion model Capslug, which is discussed in Appendix I.

The symmetrical shape of the curves indicates that the core is homogeneous. For each of these experiments, a best fit of the experimental data was obtained with a flowing fraction of 0.96, indicating that a small portion of the brine was stagnant (dendritic). Some of this stagnant brine is due to dead-end pore structures in the sandstone and dead-spots such as corners and pressure taps. However, some of the calculated stagnant fluid may also come from experimental errors. There are several sources of experimental error, including (1) errors in subtracting the tubing volume from the volume of fluid injected; (2) errors in the tracer measurement, since each data point is actually the average concentration of the fluid collected in a test tube (about 9 mL); and (3) errors in the measured pore volume of the core. Each of these errors may cause an apparent shifting of the curve to the left or right. This would affect the value of the flowing fraction needed to fit the data.

EXPERIMENTS W2 AND W3: ORGANOCHLOROSILANE-TREATED CORE

The second Berea core was treated with organochlorosilanes to render it neutrally wet, see Appendix E. Steady-state measurements were made using the same procedures as Experiment W1. Measurements were made at 100 percent brine saturation on the core both before (W2) and after (W3) treatment with the organochlorosilanes. This enabled us to determine whether the dependence of the dispersion coefficient on velocity was altered by the treatment. The basic core properties after treatment are shown in Table 6-1.

Normalized tracer concentrations versus pore volumes of brine injected are presented in Figures 6-4 through 6-7. These curves are symmetrically shaped, indicating that the core was homogenous, both before and after treatment. The curves are a best fit of the data, using the program Capslug, see Appendix I.

Dispersion coefficient versus velocity for both cores is given in Table 6-2 and plotted in Figure 6-8. The velocity is computed from the injection rate:

$$v_w = \frac{q}{A\,\phi} \tag{6-1}$$

and the dispersion coefficient is calculated from the history-matched value of dispersivity:

$$k_w = \alpha_w\, v_w \tag{6-2}$$

Although only two velocities were used before and after treatment in the second core, Figure 6-8 shows that dependence of the dispersion coefficient on velocity was not altered significantly by the treatment. Equation (2-1) relates the dispersion coefficient and velocity:

$$K_l = \frac{D}{F_R\,\phi} + \alpha_l\, v^{\beta_l} \tag{2-1}$$

A least squares fit was used to determine β_l in the water-wet Berea core, while β_l in the neutrally wet core was determined by the slope of the line between the two data points. β_l was 1.24 for both cores when water-wet and decreased to 1.15 for the neutrally wet core after treatment. The slightly lower values of dispersion coefficient seen after the treatment may indicate that a small amount of silane remained in the core and reacted with water to form a gel. This would probably have occurred in the smallest pores, thus reducing the pore size distribution. Brine would then flow in the larger, less tortuous pore spaces, reducing dispersion. Since no reduction in pore space was observed after treatment, however, the volume of these small, blocked pores is not significant.

TABLE 6-2

DISPERSION COEFFICIENT, SINGLE-PHASE FLOW

	Injection Rate, mL/min	Velocity, cm/s	Dispersion Coefficient, cm^2/s	Slug Size Pore Volumes
Water-Wet Berea (W1)	4.74	1.46×10^{-2}	3.94×10^{-3}	0.490
	0.977	3.01×10^{-3}	5.72×10^{-4}	0.193
	0.585	1.80×10^{-3}	3.24×10^{-4}	0.211
Neutral-Wet Berea	4.91	1.55×10^{-2}	3.88×10^{-3}	0.199
Prior to Treatment (W2)	0.933	2.94×10^{-3}	5.00×10^{-4}	0.199
Neutral-Wet Berea (W3)	4.92	1.55×10^{-2}	2.79×10^{-3}	0.200
After Treatment	0.933	2.94×10^{-3}	4.41×10^{-4}	0.200

The β_I values of 1.24 and 1.15 are in the range expected for Berea sandstone and agree with other values published in the literature (Baker, 1977; Brigham et al., 1961; Delshad, 1981; Delshad, 1984; Perkins and Johnston, 1963; Spence and Watkins, 1980).

S1=1.000	S2=0.000	F1= .96	F2=1.00
AREA=24.90	L=60.75	POR= .217	
ALPHA1= .27	ALPHA2= 0.00	M1= .15E-03	M2= .0E+00
FF1=1.000	FF2=0.000	QT= 4.740	PART1= 0.00
NB= 100	NP=7000	PVINJ= 4.00	PVS= .490

C_i^o = 1024 dpm/ml

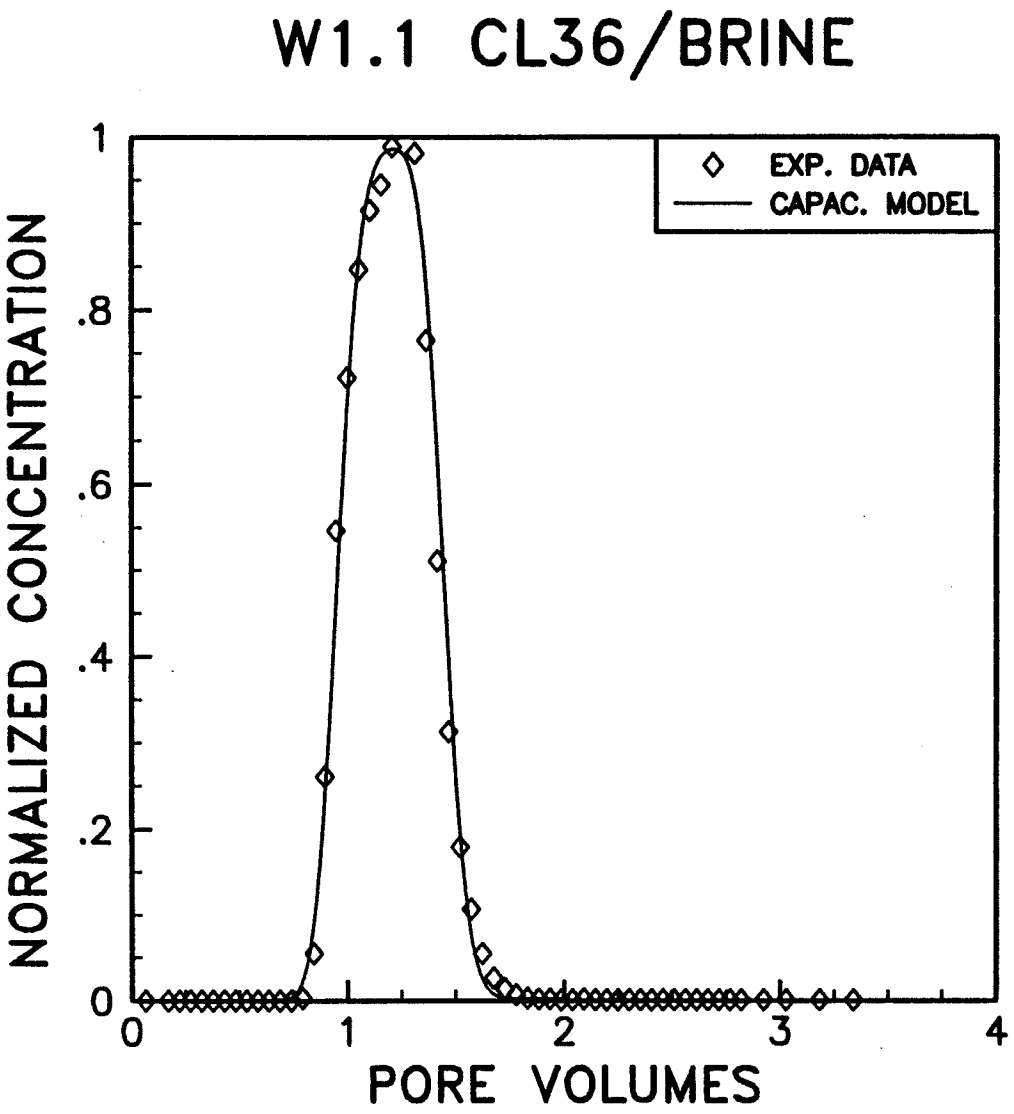

Figure 6-1 Tracer concentration versus pore volumes for water-wet Berea, single-phase brine flow. Tracer is chlorine-35, flow rate is 4.74 ml/min.

S1=1.000	S2=0.000	F1= .96	F2=1.00
AREA=24.90	L=60.75	POR= .217	
ALPHA1= .19	ALPHA2= 0.00	M1= .3E-03	M2= .0E+00
FF1=1.000	FF2=0.000	QT= .977	PART1= 0.00
NB= 100	NP=7000	PVINJ= 4.00	PVS= .193

C_i^o = 1009 dpm/ml

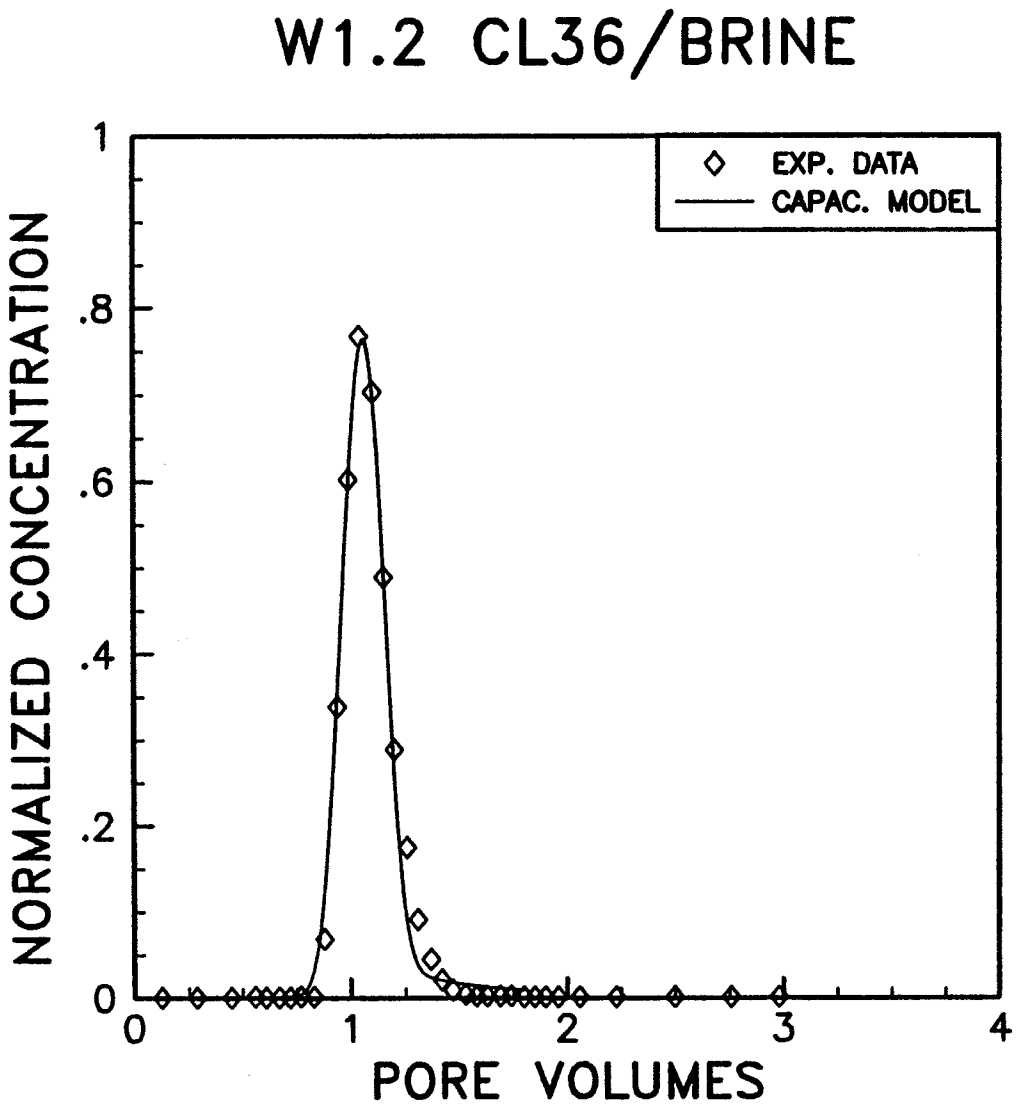

Figure 6-2 Tracer concentration versus pore volumes for water-wet Berea, single-phase brine flow. Tracer is chlorine-36, flow rate is 0.977 ml/min.

S1=1.000	S2=0.000	F1= .96	F2=1.00
AREA=24.90	L=60.75	POR= .217	
ALPHA1= .18	ALPHA2= 0.00	M1= .14E-03	M2= .0E+00
FF1=1.000	FF2=0.000	QT= .585	PART1= 0.00
NB= 100	NP=7000	PVINJ= 4.00	PVS= .211

C_i^o = 1031 dpm/ml

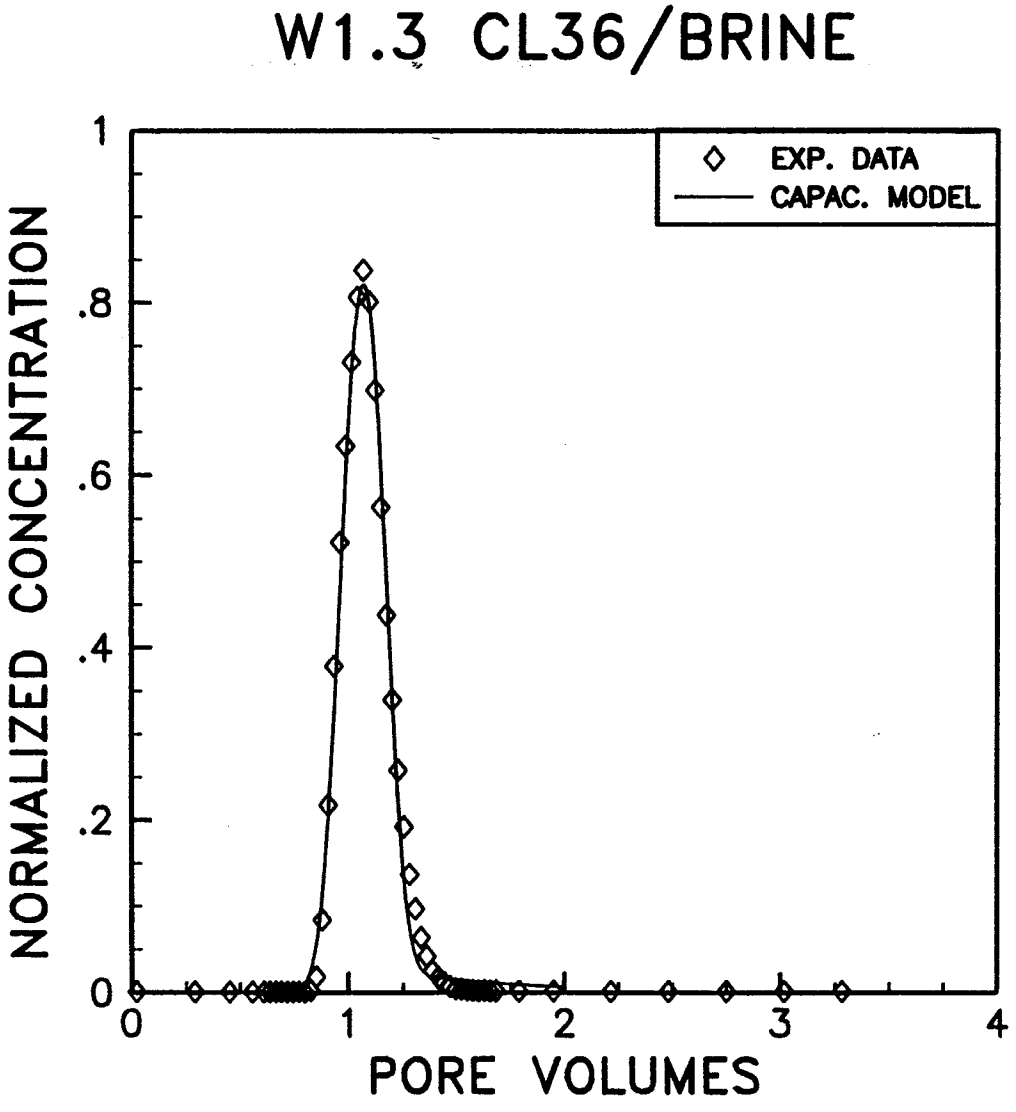

Figure 6-3 Tracer concentration versus pore volumes for water-wet Berea, single-phase brine flow. Tracer is chlorine-36, flow rate is 0.585 ml/min.

S1=1.000	S2=0.000	F1=1.00	F2=1.00
AREA=25.95	L=60.85	POR= .204	
ALPHA1= .25	ALPHA2= 0.00	M1= .00E+00	M2= .00E+00
FF1=1.000	FF2=0.000	QT= 4.910	PART1= 0.00
NB= 100	NP=7000	PVINJ= 4.00	PVS= .199

C_i^o = 1015 dpm/ml

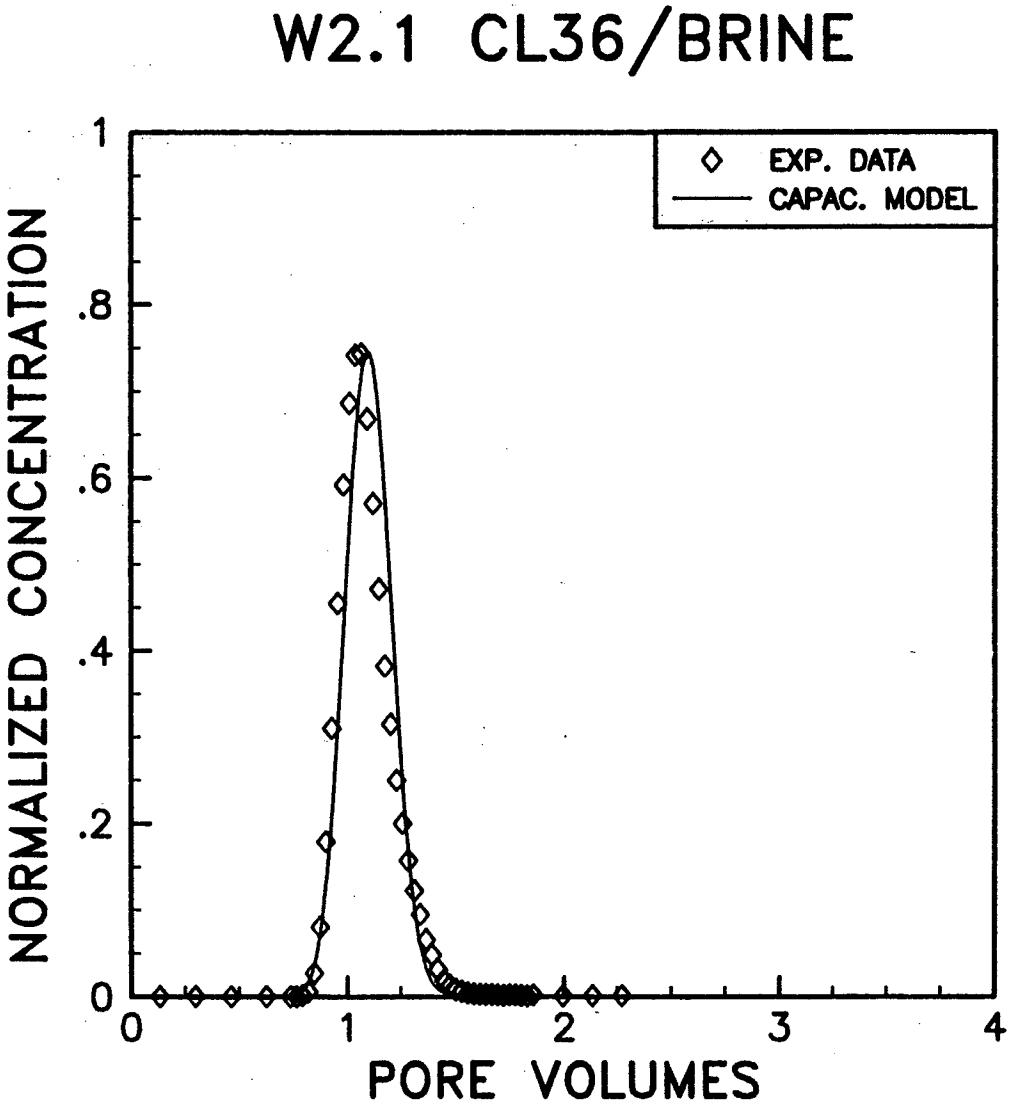

Figure 6-4 Tracer concentration versus pore volumes for treated core before treatment, single-phase brine flow. Tracer is chlorine-36, flow rate is 4.91 ml/min.

S1=1.000	S2=0.000	F1= .98	F2=1.00
AREA=25.95	L=60.85	POR= .204	
ALPHA1= .17	ALPHA2= 0.00	M1= .10E-02	M2= .00E+00
FF1=1.000	FF2=0.000	QT= .993	PART1= 0.00
NB= 100	NP=7000	PVINJ= 4.00	PVS= .199

C_i^o = 1015 dpm/ml

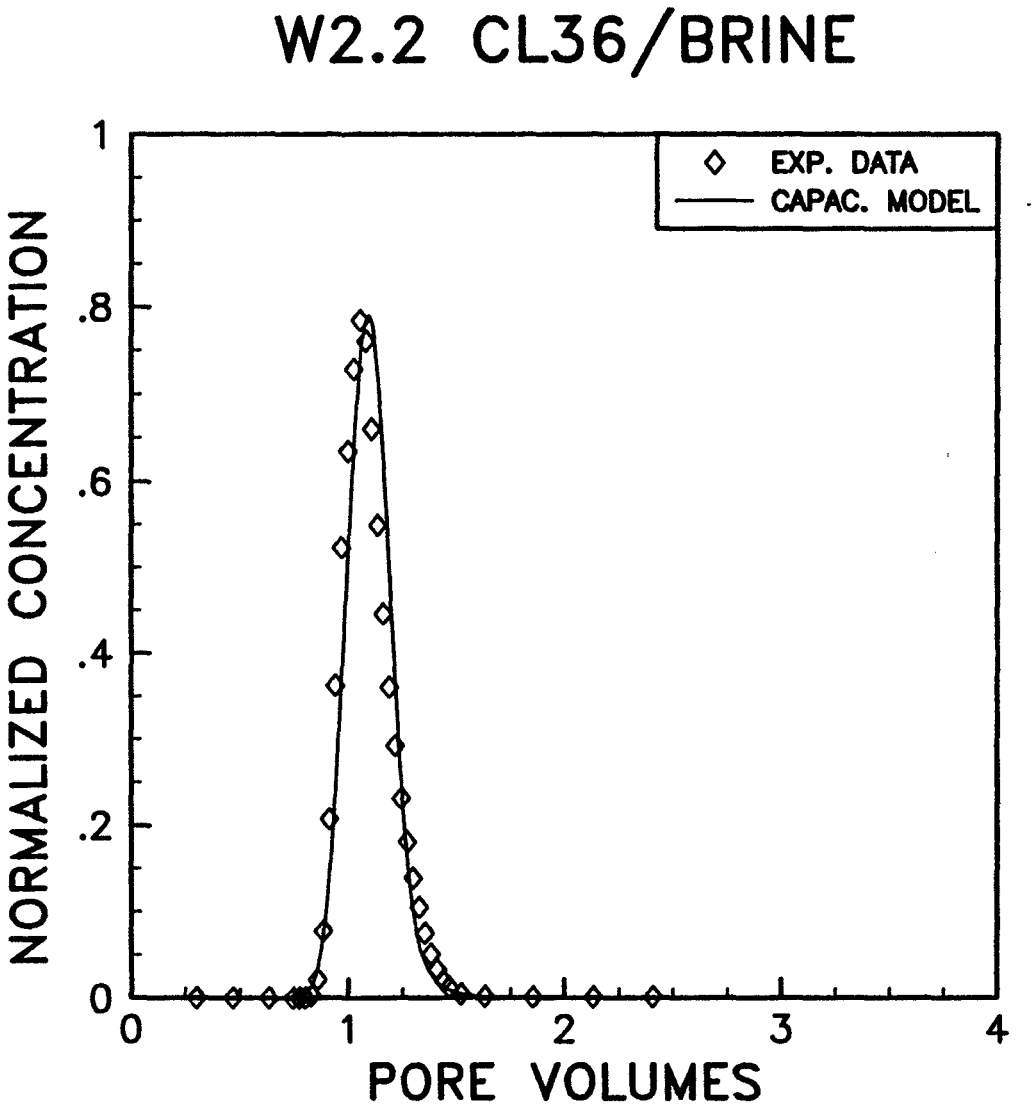

Figure 6-5 Tracer concentration versus pore volumes for treated core before treatment, single-phase brine flow. Tracer is chlorine-36, flow rate is 0.993 ml/min.

S1=1.000	S2=0.000	F1=1.00	F2=1.00
AREA=25.95	L=60.85	POR= .204	
ALPHA1= .18	ALPHA2= 0.00	M1= .00E+00	M2= .00E+00
FF1=1.000	FF2=0.000	QT= 4.920	PART1= 0.00
NB= 100	NP=7000	PVINJ= 4.00	PVS= .200

C_i^o = 1031 dpm/ml

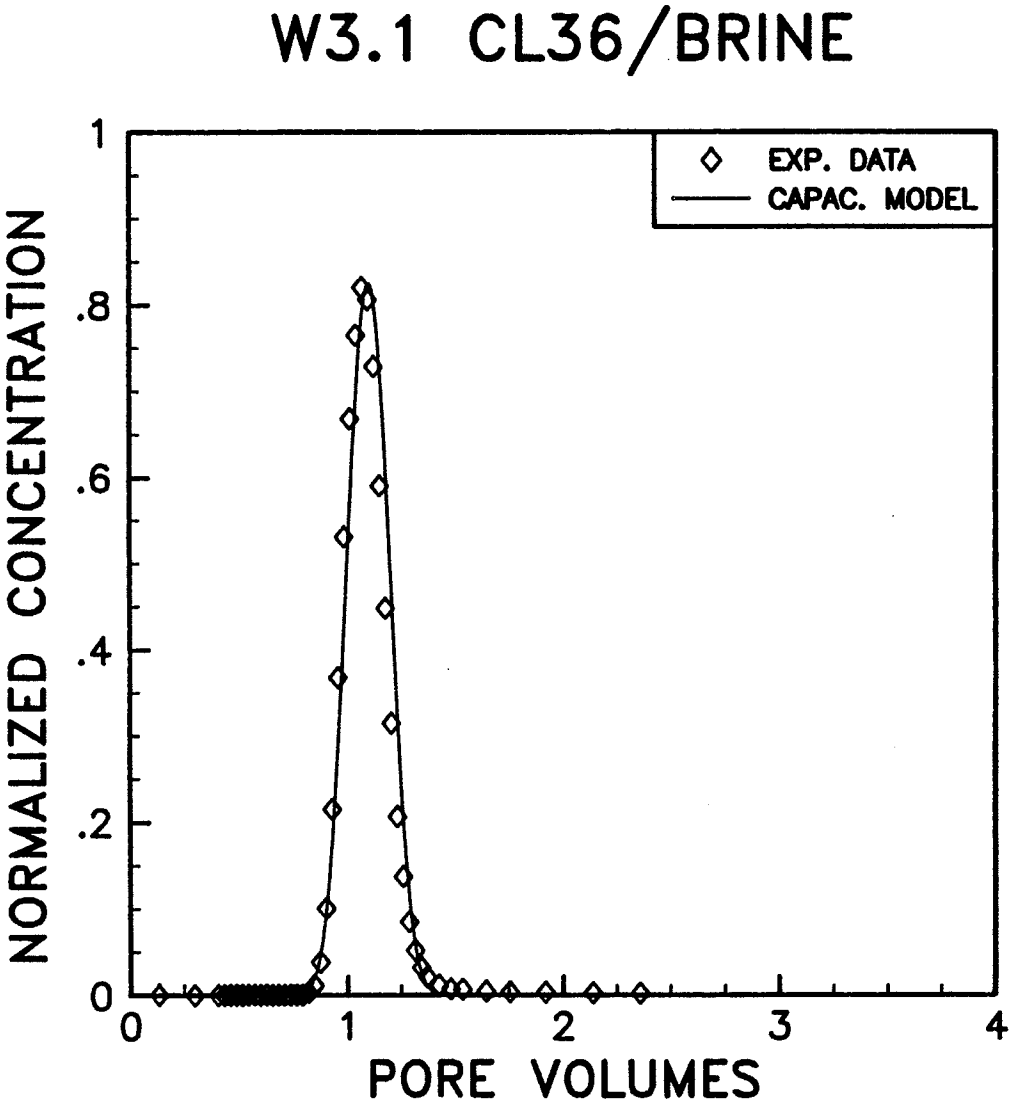

Figure 6-6 Tracer concentration versus pore volumes for treated core, single-phase brine flow. Tracer is chlorine-36, flow rate is 4.92 ml/min.

S1=1.000	S2=0.000	F1=1.00	F2=1.00
AREA=25.95	L=60.85	POR= .204	
ALPHA1= .15	ALPHA2= 0.00	M1= .00E+00	M2= .00E+00
FF1=1.000	FF2=0.000	QT= .993	PART1= 0.00
NB= 100	NP=7000	PVINJ= 4.00	PVS= .200

C_i^o = 1130 dpm/ml

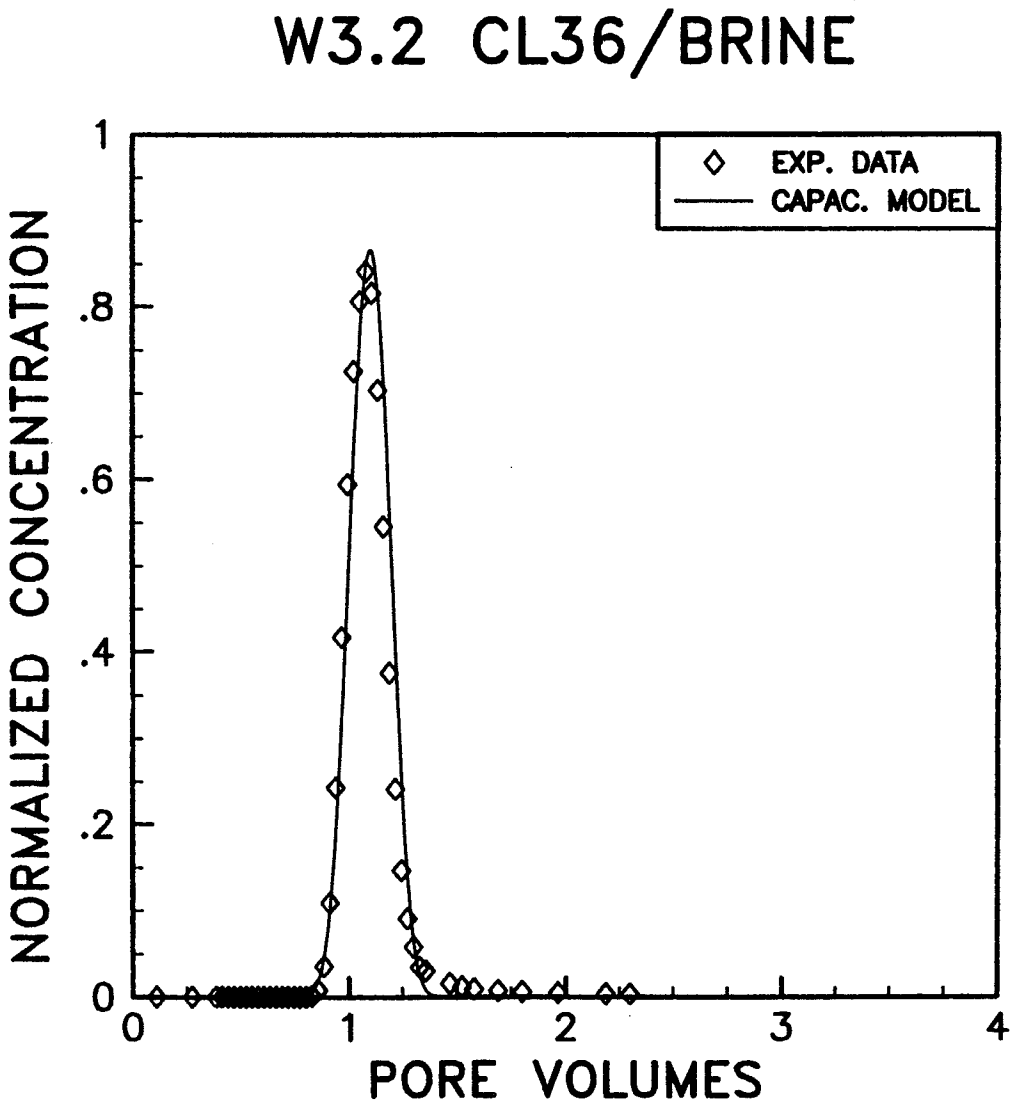

Figure 6-7 Tracer concentration versus pore volumes for treated core, single-phase brine flow. Tracer is chlorine-36, flow rate is 0.933 ml/min.

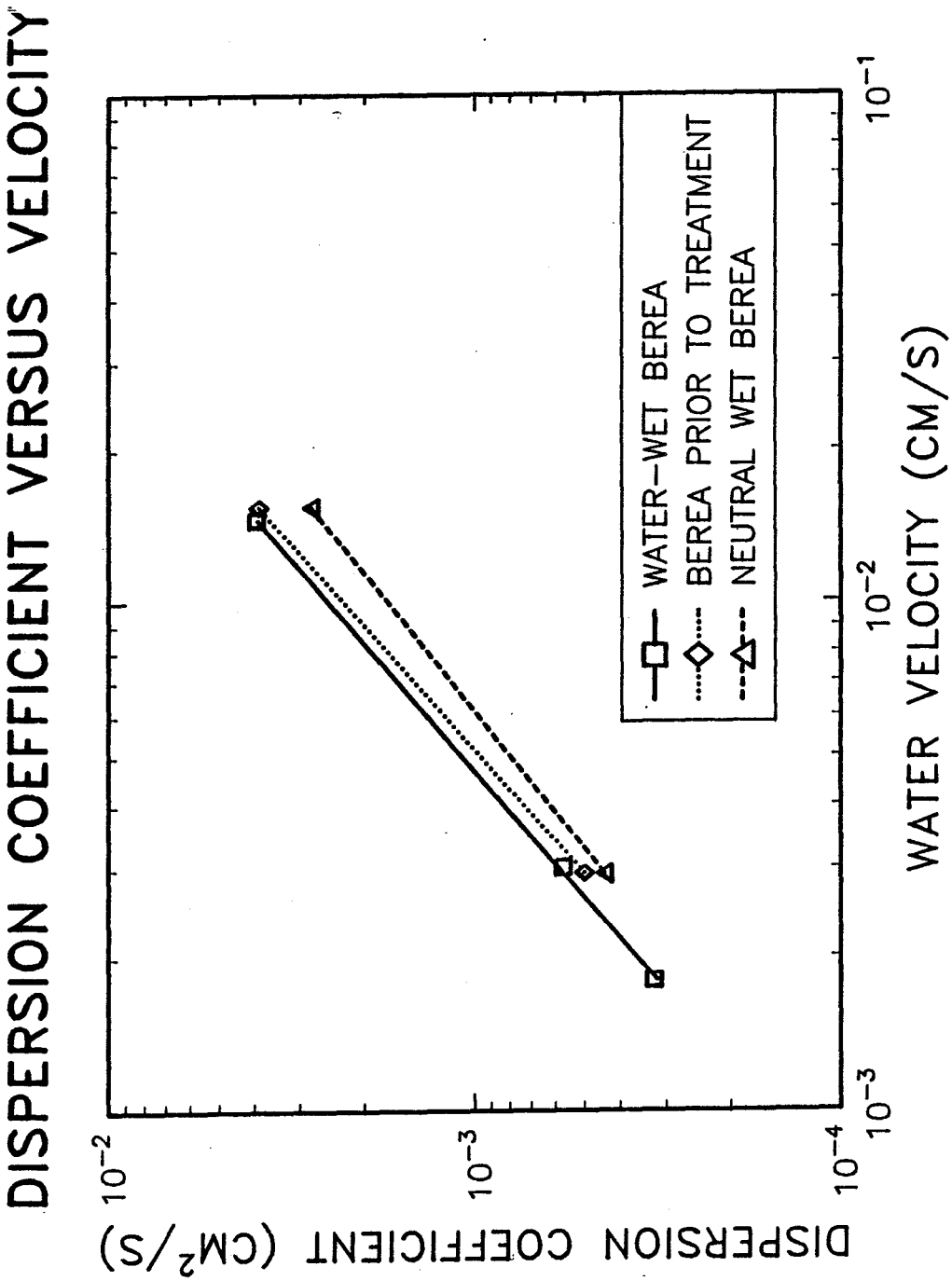

Figure 6-8 Dispersion coefficient versus water velocity for all three sets of single-phase experiments.

CHAPTER 7

TWO-PHASE, STEADY-FLOW EXPERIMENTAL RESULTS

After the single-phase experiments were completed, the core was driven to the irreducible water saturation (IWS). then a series of relative permeability and tracer experiments were made at increasing water fractional flow. The objectives of the two-phase, steady-flow experiments were:

1. Obtain imbibition (increasing brine saturation) steady-state relative permeability curves for brine and decane.

2. Determine saturations using partitioning and nonpartitioning tracers and compare with values obtained by material balance.

3. Compare the use of partitioning and nonpartitioning tracers for determining dispersivity, mass transfer coefficients, and capacitance behavior of each core.

4. Use the above information to model unsteady-flow (waterflood) experiments.

5. Determine the effects of wettability on each of the parameters mentioned above.

The two-phase experiments used the same two Berea cores as the single-phase experiments, see Table 7-1. The experiments were performed at a constant flow rate of approximately 1 mL/min. When steady-state flow conditions were reached, relative permeabilities and core resistivities were measured.

Slug displacement of chemical and radioactive tracers were also performed at steady state. The procedures and experimental apparatus are given in Table 5-4 and Figure 5-4, respectively. Brine labeled with Cl-36 and tritiated decane were the nonpartitioning tracers, while IBA was the partitioning tracer used.

Experiment WD1: Water-Wet Core

After the single-phase dispersion measurements were completed, 100 percent decane was injected at a flow rate of 20 mL/min, with a maximum pressure drop across the core of 35 psi. IWS was achieved after 77 pore volumes of decane had been injected.

Starting from IWS, ten steady-flow tracer and relative permeability measurements were run, beginning with a fractional flow of water of zero and ending at one. At each fractional flow rate, saturations were calculated by material balance after the system reached steady state. Fractional flows were calculated by averaging the test tube volumes at steady state. The pressure drop across the center 1-foot section of the core was measured and relative permeabilities to each phase were calculated. After these measurements were completed, a slug of labeled fluids was injected for dispersion analysis.

Table 7-1 gives the flow data for the experiments, including fractional flows, flow rates, saturations calculated by material balance, and relative permeabilities. Note that Experiments WD1.10 and WD1.11 are repeats of Experiments WD1.4 and WD1.6, respectively. This was necessary because the slug size used initially was not large enough to give good tracer data for both phases. This is also the reason for the missing tracer data in Experiments WD1.3 and WD1.7. After Experiment WD1.8 was completed, at residual oil saturation (ROS), the core was flooded with decane back to IWS. Experiments WD1.10 and WD1.11 were then run at the desired fractional flow rates.

Figure 7-1 shows the fractional flow curve for water, with saturation values estimated from both material balance and the capacitance model. This demonstrates good agreement between both estimates. Figure 7-2 gives the imbibition relative permeability curves. These curves are typical for a strongly water-wet sandstone (Anderson, 1986; Craig, 1971).

Normalized tracer concentration versus total pore volumes of fluids injected is shown in Figures 7-3 through 7-15 for the radioactive, nonpartitioning tracers. The data for IBA, which partitions between the oil and water, is discussed later in this chapter. The computer program Capslug, discussed in Appendix I, was used to history match the experimental effluent data. The parameters used in the model, saturation, flowing fraction, dispersivity, and mass transfer coefficient, were adjusted to obtain the best match for both the oil and water tracer data. The parameters that gave the best fit are shown in Table 7-2. They are compared with the neutrally wet data below. Material balance on tracers is given in Table 7-7.

Figures 7-3 through 7-15 show that the agreement between the experimental tracer data and the capacitance-dispersion model is generally quite good. However, when the fractional flow of a phase was low, 0.3 or less, good fits became more difficult to achieve. This is seen in Figures 7-8 and 7-12.

EXPERIMENT WD2: NEUTRALLY WET CORE

After the single-phase experiments were finished, the neutrally wet core was also driven to IWS with decane. Seven steady-state experiments were run with the water fractional flow increasing from zero to one. Table 7-3 gives material balance saturation, fractional flows, and permeabilities for each phase. Figure 7-16 shows the fractional flow curve for water with saturation values estimated from both material balance and the capacitance dispersion computer model, Appendix I. Again, good agreement is seen between the two estimates. Figure 7-17 gives the imbibition relative permeability curves. The residual oil

saturation for this core is less than that for the water-wet core. A review of the literature has shown that neutrally wet rocks have lower S_{or} values than either strongly oil-wet or water-wet rocks (Anderson, 1987).

Normalized tracer concentration versus total pore volumes of fluids injected is shown in Figures 7-18 through 7-29. As in the water-wet case, the capacitance-dispersion computer model, Appendix I, was used to obtain a history match to the nonpartitioning tracers in the oil and brine. The parameters that gave the best fit are shown in Table 7-4 for the nonpartitioning tracers. Material Balance on tracers is given in Table 7-7.

As with the water-wet core, curve fits of the tracer data are generally quite good for these experiments. Again, when the fractional flow of a phase was low, good fits became more difficult to achieve. This is seen in Figures 7-20, 7-22, 7-24, and 7-27. It is possible that a better fit would be achieved by considering more than one mass transfer coefficient. Stalkup (1970) suggested that the diffusion of a tracer flowing to dendritic fractions may actually be characterized by a spectrum of mass transfer coefficients. This is reasonable since the dendritic volumes would undoubtedly have varying degrees of accessibility to a diffusing tracer. The rate of mass transfer to easily accessible dendrites might be characterized by a relatively high mass transfer coefficient. Diffusion into and out of the least accessible dendrites would take longer, and the rate of mass transfer would be characterized by a much lower mass transfer coefficient. Stalkup considered a two-stagnant-volume model with one high and one low mass transfer coefficient. For data showing a large amount of capacitance (i.e., early tracer breakthrough and an asymmetrical concentration curve), this model produced a better fit than did the normal one-stagnant-volume model.

In Figures 7-19 and 7-21, the obvious discrepancy between the areas under the experimental and computed curves can be attributed to errors in the values used to normalize the tracer data. The discrepancy could also be attributed to errors in calculating the slug size or other analytical errors, although this is unlikely since slug size was calculated by two independent methods which were in agreement for all the experiments. Even with this discrepancy, the curve-fits in both figures are still quite good.

TABLE 7-1

IMBIBITION RELATIVE PERMEABILITIES OF

BRINE AND n-DECANE, WATER-WET BEREA CORE

Experiment No.	Water Fractional Flow	Water Saturation[1]	Total Flow Rate (mL/min)	Pressure Drop[2] (psi)	Effective Permeability (md)		Relative Permeability[3]	
					Water	Oil	Water	Oil
W1.2	1.0	1.0	0.99	0.410	662.0	0.0	1.0	0.0
WD1.1	0.0	0.315	5.06	1.929	0.0	678.9	0.0	1.03
WD1.2	0.0	0.315	1.014	0.375	0.0	699.5	0.0	1.06
WD1.3	0.073	0.543	1.029	1.33	15.46	186.0	0.023	0.281
WD1.4	0.129	0.577	1.021	1.89	19.06	122.0	0.029	0.184
WD1.5	0.297	0.601	1.014	3.61	22.86	51.1	0.035	0.077
WD1.6	0.852	0.639	0.994	7.14	32.47	5.35	0.049	0.008
WD1.7	0.934	0.644	0.996	7.42	34.35	2.31	0.052	0.003
WD1.8	1.0	0.655	0.9968	7.125	38.34	0.0	0.058	0.0

[1]Determined by material balance
[2]Across center 1-foot length of the core
[3]Relative permeabilities normalized to absolute permeability at 100 percent brine saturation

TABLE 7-2

DISPERSION DATA FOR BRINE AND n-DECANE,

NONPARTITIONING TRACERS, WATER-WET BEREA CORE

Experiment No.	Water Fractional Flow	Water Saturation[1]	Total Flow Rate (mL/min)	Phase Flowing Fraction		Effective Dispersivity (cm)		Mass Transfer Coefficient	
				Water	Oil	Water	Oil	Water	Oil
WD1.1	0.0	0.300	5.06	1.0	0.96	0.0	0.35	0.0	0.006
WD1.2	0.0	0.300	1.014	1.0	0.98	0.0	0.30	0.0	0.006
WD1.3	0.073	0.560	1.029	—	0.90	—	0.50	—	0.0013
WD1.4	0.129	0.600	1.021	—	0.87	—	0.70	—	0.0008
WD1.10	0.147	0.600	1.010	0.85	0.83	0.15	1.10	0.003	0.0008
WD1.5	0.297	0.601	1.014	0.85	0.78	0.15	0.65	0.001	0.0008
WD1.6	0.852	0.620	0.994	0.87	—	0.10	—	0.0015	—
WD1.11	0.855	0.600	0.995	0.89	0.17	0.15	10.0	0.0014	0.00015
WD1.7	0.934	0.630	0.996	0.88	—	0.10	—	0.0015	—
WD1.8	1.0	0.635	0.997	0.92	1.0	0.10	0.0	0.0015	0.0

[1]Determined by model fit

TABLE 7-3

IMBIBITION RELATIVE PERMEABILITIES OF

BRINE AND n-DECANE, NEUTRALLY WET BEREA CORE

Experiment No.	Water Fractional Flow	Water Saturation[1]	Total Flow Rate (mL/min)	Pressure Drop[2] (psi)	Effective Permeability (md)		Relative Permeability[3]	
					Water	Oil	Water	Oil
W3.2	1.0	1.0	0.993	0.510	512.0	0.0	1.0	0.0
WD2.1	0.0	0.300	1.015	0.659	0.0	382.0	0.0	0.746
WD2.2	0.0848	0.590	1.031	3.04	7.56	77.1	0.015	0.151
WD2.3	0.1511	0.638	1.020	3.57	11.4	60.2	0.022	0.118
WD2.4	0.3013	0.680	1.014	4.80	16.7	36.7	0.033	0.072
WD2.5	0.7023	0.707	0.998	7.91	23.3	9.33	0.046	0.018
WD2.6	0.8565	0.729	0.995	9.70	23.1	3.66	0.045	0.007
WD2.10	1.0	0.741	0.999	9.40	28.0	0.0	0.055	0.0

[1]Determined by material balance
[2]Across center 1-foot length of the core
[3]Relative permeabilities normalized to absolute permeability at 100 percent brine saturation

TABLE 7-4

DISPERSION DATA FOR BRINE AND n-DECANE,

NONPARTITIONING TRACERS, NEUTRALLY WET BEREA CORE

Experiment No.	Water Fractional Flow	Water Saturation[1]	Total Flow Rate (mL/min)	Phase Flowing Fraction		Effective Dispersivity (cm)		Mass Transfer Coefficient	
				Water	Oil	Water	Oil	Water	Oil
WD2.1	0.0	0.280	1.015	1.0	1.0	0.0	0.35	0.0	0.0
WD2.2	0.085	0.590	1.031	0.57	0.77	0.10	0.65	0.001	0.0013
WD2.3	0.151	0.665	1.020	0.63	0.75	0.50	1.50	0.0006	0.0015
WD2.4	0.301	0.710	1.014	0.70	0.60	0.50	5.50	0.001	0.0009
WD2.5	0.702	0.730	0.998	0.88	0.43	1.30	12.0	0.0003	0.00035
WD2.6	0.876	0.730	0.971	0.92	0.25	1.20	13.0	0.00005	0.0003
WD2.10	1.0	0.730	0.999	0.97	1.0	1.60	0.0	0.00001	0.0

[1]Determined by model fit

DISCUSSION OF MODEL PARAMETERS

This section discusses the variation of the model parameters: flowing (nondendritic) fraction, dispersivity, and mass transfer coefficients as the saturation and fractional flow were varied. Results from the water-wet and neutrally wet Berea cores are compared to show the effects of wettability.

As was discussed in the sections on modeling, at any given saturation, the water and oil saturations can be divided into flowing and dendritic fractions. For water, the flowing saturation is S_2^f, while the dendritic saturation is S_2^d. The ratio of the flowing water saturation to the total water saturation, S_2^f/S_2, is sometimes referred to as the flowing (nondendritic) fraction of water. The flowing fraction of water, S_2^f/S_2, can be plotted versus the water saturation or versus the water fractional flow, f_w. Recall that the water fractional flow, f_w, is the fraction of water (versus oil) that is injected into the core.

In Figure 7-30, the water flowing (nondendritic) fraction is plotted versus the water fractional flow for both the water-wet and neutrally wet cores. A linear relationship is seen for both cores, with the neutrally wet core showing a greater dependence on the fractional flow than the water-wet core. Figure 7-31 shows the flowing fraction of oil, S_1^f/S_1, versus the water fractional flow, f_w. In this case, the relationship is linear for the water-wet core and approximately linear for the neutrally wet core. Figures 7-30 and 7-31 confirm the validity of an assumption in the unsteady-state computer model: a linear dependence of flowing fraction on the fractional flow for each phase. See Appendix J.

Figures 7-32 and 7-33 show the water and oil flowing (nondendritic) fraction data plotted versus water saturation, respectively. The values used for saturation were the best fit values from the capacitance model. Figure 7-32 shows that as the water saturation increases, the fraction of dendritic water decreases, so that more and more of the water is flowing. Similarly, as the oil saturation increases, the oil dendritic fraction decreases, see Figure 7-33.

Dispersion data is presented in a similar manner. Figure 7-34 shows the water dispersivity versus water fractional flow for both cores. while Figure 7-35 shows oil dispersivity versus water fractional flow. The water and oil dispersivity versus water saturation are shown in Figures 7-36 and 7-37, respectively. The neutrally wet core shows a strong dependence of brine dispersivity on saturation (or fractional flow), while the water-wet core shows no such dependency. Other researchers (Delshad, 1981; Delshad, 1984) have also found that brine dispersivity is not dependent on saturation in a strongly water-wet core. However, the increase of brine dispersivity in the neutrally wet core as brine saturation increases is unexpected. Other researchers (Wang, 1986) found that the dispersivity decreases as the saturation increases.

Figures 7-36 and 7-37 show that the oil dispersivity is a function of saturation for both cores, but with a stronger dependence for the neutrally wet core. In both cases, the dispersivity increases as the oil saturation increases, as expected.

COMPARISON OF DISPERSIVITY DATA WITH WANG (1986)

Wang (1986) reported steady-state, two-phase water and oil dispersivity data. Two examples of wettability alteration were investigated. In the first case, a previously water-wet Berea core was made mixed-wet by aging the core with Loudon crude. In the other example, a mixed-wettability Loudon core was made more water-wet after Dean-Stark extraction with toluene.

Figure 7-38 shows a comparison of water and oil dispersivity data for the case of naturally water-wet Berea cores. The results are very similar: oil dispersivity increases significantly with increasing water saturation, while water dispersivity decreases slightly with increasing saturation.

Figure 7-39 shows a comparison of water and oil dispersivity data for the mixed- or neutrally wet Berea cores. The results for oil dispersivity are in agreement and show a significant increase as water saturation increases. However, the water dispersivity data do not agree and show opposite trends. The only similarity seen is that water dispersivity is relatively lower than oil dispersivity for both sets of data. The data reported here show an increase in water dispersivity as water saturation increases, while Wang's data show water dispersivity decreasing. This disagreement may be a result of the two different methods used to alter the wettability of the Berea cores.

COMPARISON OF FLOWING FRACTION DATA WITH OTHER REPORTS (NONPARTITIONING TRACERS)

This section compares the results of this work with those reported by Salter and Mohanty (1982) and Stalkup (1970). Salter and Mohanty performed tracer displacements during steady-state, two-phase flow using a strongly water-wet Berea sandstone core. Stalkup performed steady-state, two-phase flow experiments using strongly water-wet Boise, Berea, and Torpedo sandstone cores. Salter and Mohanty used tracers in both phases, while Stalkup displaced laboratory oils by propane and did not use a tracer in the brine phase.

Figures 7-68 and 7-69 show a comparison of water flowing fraction data versus water fractional flow and water saturation, respectively, for water-wet cores. Similar trends are observed in both figures. Salter and Mohanty reported data for water fractional flows much lower than reported in this work, so comparisons in this region are not possible.

Figures 7-70 and 7-71 show a comparison of oil flowing fraction data versus water fractional flow and water saturation, respectively, for water-wet cores. Figure 7-70 shows that the data of Salter and Mohanty and of Stalkup are not as linear as the data reported here, but the trends are still very similar.

PARTITIONING TRACER RESULTS

In addition to the nonpartitioning tracer results discussed above, measurements were also made during the steady-flow experiments with a partitioning tracer, isobutyl alcohol (IBA). Before each experiment, the IBA was added to the brine and decane and allowed to equilibrate between the two phases for at least two days. The partition coefficient for the IBA was determined by calculating an apparent coefficient for each test tube that was sampled, then averaging. This was done by dividing the total IBA concentration in the brine by the total concentration in the decane, then averaging. The average partition coefficient for the IBA was 4.8, in good agreement with the data reported in the literature (Delshad, 1984; Provoust, 1984). Attempts to measure the partition coefficient by placing a known amount of IBA in a test tube with brine and decane, allowing time for equilibration, and then taking samples gave inconsistent results.

Two problems affected the results of the dispersion data for the IBA: (1) slightly different injection times for the labeled brine and decane and (2) problems in normalizing the IBA data. The experimental apparatus for the steady-state, two-phase flow experiments is shown in Figure 5-4, while the experimental procedures are given in Table 5-4. Unfortunately, when both brine and decane were injected, our experimental procedure caused injection of the IBA-labeled brine and labeled decane to occur at slightly different times. After steady-state was reached, slugs of brine and oil containing IBA and the nonpartitioning tracers were injected. This was done by opening three-way valves to labeled brine and decane simultaneously. As a result, these slugs arrived at the core inlet at different times since the flow rates of brine and decane were not equal. The difference in arrival times was greater than expected due to the tubing length upstream of the core. Note that this was not a problem with the nonpartitioning tracers, since they have no mass transfer between the two phases. To correct this problem in future experiments, the travel time of each slug should be determined and valves opened at times that will cause the slugs to arrive simultaneously at the core inlet. Because of this problem, good fits of the experimental data could not be obtained using the saturation values obtained from fits of the nonpartitioning tracers.

A second problem occurred when normalizing the IBA data. Before every experiment, samples were taken from the labeled brine and decane and the initial IBA concentration in each phase was determined. When these values were used to normalize the tracer data, the tracer material balance (area under the curve) was usually incorrect. Therefore, the initial concentrations were adjusted up or down so that the tracer material balance and the value of the partition coefficient were satisfied.

EXPERIMENT WD1: WATER-WET CORE

Fractional flow of water versus water saturation is shown in Figure 7-40. Saturations are from both material balance and the capacitance model fit of the IBA data. Good agreement is seen between the two estimates.

Normalized tracer concentration versus pore volumes of fluid injection is shown in Figures 7-41 through 7-53. Table 7-5 lists the parameter values that gave the best fit of the experimental data. In general, the shapes of these curves are quite similar to the corresponding curves for the nonpartitioning tracers. In some cases, the IBA data is slightly more symmetrical than the nonpartitioning tracer data. The values reported for flowing fraction are often much higher than those of the nonpartitioning tracers. This occurs when the fractional flow of water is 0.3 or less. In several cases, the IBA data indicates a dendritic fraction of zero. Dispersivity values are constant, around 0.2, and do not vary with saturation. Material balance on tracers is given in Table 7-7.

EXPERIMENT WD2: NEUTRALLY WET CORE

Fractional flow of water versus water saturation is shown in Figure 7-54. Saturation values are from both material balance and the capacitance model fit of the IBA data. Good agreement is seen between the two

estimates. Normalized tracer concentration versus pore volumes of fluid injected is shown in Figures 7-55 through 7-66. Table 7-6 lists the parameter values that gave the best fit of the experimental data. Figure 7-67 shows a comparison of water saturation by partitioning and nonpartitioning tracers versus water saturation by material balance.

In these experiments, slug sizes were often much larger than those in the water-wet core. Also, the IBA concentration was approximately ten times lower. The concentration was lowered because the higher IBA concentration in the injected fluids caused a significant pressure increase along the water-wet core. The increase in slug size and the lowered concentration made good curve-fits much more difficult to obtain.

For Experiments WD2.2 through WD2.4, when the fractional flow of water was less than 0.3, the calculated phase flowing fractions were much higher than those determined from the nonpartitioning tracer data. In two of the experiments, no dendritic volume is indicated. This was also seen in Experiment WD1.1 where only oil is flowing. With two exceptions, the dispersivity values are constant, averaging about 1.5. This is an order of magnitude larger than the average dispersivity of the IBA data in the water-wet Berea core. Material balance in tracers is given in Table 7-7.

TABLE 7-5

DISPERSION DATA FOR BRINE AND n-DECANE,

PARTITIONING TRACER (IBA), WATER-WET BEREA CORE

Experiment No.	Water Fractional Flow	Water Saturation[1]	Total Flow Rate (mL/min)	Phase Flowing Fraction		Effective Dispersivity (cm)		Mass Transfer Coefficient	
				Water	Oil	Water	Oil	Water	Oil
WD1.1	0.0	0.32	5.06	—	0.96	—	0.20	—	0.006
WD1.2	0.0	0.32	1.014	1.0	0.98	0.0	0.20	—	0.006
WD1.3	0.073	0.56	1.029	1.0	1.0	0.10	0.10	—	—
WD1.4	0.129	0.60	1.021	1.0	1.0	0.15	0.15	—	—
WD1.5	0.297	0.62	1.014	1.0	1.0	0.10	0.10	—	—
WD1.6	0.852	0.62	0.994	0.90	0.20	0.30	1.00	0.001	0.001
WD1.7	0.934	0.63	0.996	0.88	0.20	0.20	1.00	0.001	0.001
WD1.8	1.0	0.635	0.997	0.92	—	0.10	—	0.001	—

[1]Determined by model fit

TABLE 7-6

DISPERSION DATA FOR BRINE AND n-DECANE,

PARTITIONING TRACER (IBA), NEUTRALLY WET BEREA CORE

Experiment No.	Water Fractional Flow	Water Saturation[1]	Total Flow Rate (mL/min)	Phase Flowing Fraction		Effective Dispersivity (cm)		Mass Transfer Coefficient	
				Water	Oil	Water	Oil	Water	Oil
WD2.1	0.0	0.32	1.015	—	1.0	—	0.15	—	0.0
WD2.2	0.085	0.59	1.031	1.0	1.0	2.0	2.0	0.0	0.0
WD2.3	0.151	0.665	1.020	1.0	1.0	8.0	8.0	0.0	0.0
WD2.4	0.301	0.71	1.014	0.9	0.9	1.5	1.5	8E-5	8E-5
WD2.5	0.702	0.73	0.998	0.88	0.43	1.4	1.4	4E-4	4E-4
WD2.6	0.876	0.73	0.971	0.92	0.25	1.2	1.2	3E-4	3E-4
WD2.10	1.0	0.73	0.999	0.97	—	1.8	—	8E-4	—

[1]Determined by model fit

TABLE 7-7
MATERIAL BALANCE ON TRACERS

Experiment No.	Tracer	Injected Concentration (dpm/ml)	Slug Size (ml)	Sum, Recovered Tracer (dpm/ml)	Test Tube Volume (ml)	Material Balance Recovered/ Injected
W1.1	C136	1024	161.00	18938	8.540	0.981
W1.2	C136	1009	63.24	7307	8.790	1.015
W1.3	C136	1031	69.31	8147	8.780	1.001
WD1.1	H3	761	65.83	4734	9.115	0.861
WD1.2	H3	769	65.70	4709	9.125	0.850
WD1.3	H3	737	61.13	3132	9.065	0.630
WD1.4	H3	767	57.17	4500	8.448	0.867
WD1.10	H3	1074	55.85	6553	8.327	0.910
WD1.10	C136	1130	31.07	22927	1.431	0.934
WD1.5	H3	835	46.01	5033	6.770	0.887
WD1.5	C136	1028	19.44	6772	2.860	0.969
Wd1.6	C136	1015	58.86	7455	8.037	1.003
WD1.11	H3	996	19.76	11168	1.386	0.786
WD1.11	C136	1103	55.86	7511	8.170	0.996
WD1.7	C136	1020	61.14	6639	9.114	0.970
WD1.8	C136	1026	65.72	6988	9.469	0.981
W2.1	C136	1015	64.30	7346	8.843	0.995
W2.2	C136	1015	64.21	7364	8.940	0.010
W3.1	C136	1031	64.58	7298	8.860	0.971
W3.2	C136	1130	64.53	8008	8.940	0.982
WD2.1	H3	866	64.53	5441	9.134	0.889
WD2.2	H3	924	177.59	16080	9.059	0.888
WD2.2	C136	1124	16.45	19987	0.839	0.907
WD2.3	H3	934	240.59	24301	8.309	0.899
WD2.3	C136	1127	42.46	29200	1.479	0.903
WD2.4	H3	915	48.84	5915	6.804	0.900
WD2.4	C136	1141	21.07	7945	2.934	0.970
WD2.5	H3	735	19.16	4099	2.853	0.811

TABLE 7-7 (Continued)
MATERIAL BALANCE ON TRACERS

Experiment No.	Tracer	Injected Concentration (dpm/ml)	Slug Size (ml)	Sum, Recovered Tracer (dpm/ml)	Test Tube Volume (ml)	Material Balance Recovered/ Injected
WD2.5	C136	1141	45.19	7449	6.731	0.972
WD2.6	H3	784	19.76	12250	1.156	0.914
WD2.6	C136	1136	139.60	19418	8.164	1.000
WD2.10	C136	1084	67.45	7543	9.590	0.989
US1C136	C136	1149	65.70	8443	9.050	1.012
US1C14	C14	941	65.70	6943	9.050	1.016
US2C136	C136	1150	65.49	11816	6.020	0.944
US2C14	C14	949	65.49	9526	6.020	0.923

TABLE 7-7
MATERIAL BALANCE ON TRACERS

Experiment No.	Tracer	Injected Concentration (measured) (ppm)	Injected Concentration (calculated) (ppm)	Slug Size (ml)	Sum, Recovered Tracer (ppm)	Test Tube Volume (ml)	Material Balance Recovered/ Injected (measured)	Material Balance Recovered/ Injected (calculated)
WD1.1	IBA/DEC	4622	3300	65.83	23776	9.115	0.712	0.998
WD1.2	IBA/DEC	3079	2700	65.70	18494	9.125	0.834	0.951
WD1.3	IBA/DEC	2882	3200	61.13	22351	9.065	1.247	1.031
WD1.3	IBA/DEC	10661	16500	4.81	113591	0.713		
WD1.4	IBA/DEC	4796	3000	57.17	21237	8.448	0.862	1.021
WD1.4	IBA/BRN	10563	16000	8.45	107100	1.249		
WD1.5	IBA/DEC	3641	2100	46.01	14529	6.770	0.920	1.051
WD1.5	IBA/BRN	11898	13000	19.44	93963	2.860		
WD1.6	IBA/DEC	3241	2100	10.26	15059	1.402	1.243	0.991
WD1.6	IBA/BRN	11686	15000	58.86	108855	8.037		
WD1.7	IBA/DEC	3027	2000	4.35	12903	0.648	0.939	0.997
WD1.7	IBA/BRN	11826	11200	61.14	74906	9.114		
WD1.8	IBA/BRN	11231	11231	65.72	79085	1.015	1.015	1.015
WD2.1	IBA/DEC	2725	2725	64.53	19795	9.134	1.028	1.028

TABLE 7-7 (Continued)
MATERIAL BALANCE ON TRACERS

Experiment No.	Tracer	Injected Concentration (measured) (ppm)	Injected Concentration (calculated) (ppm)	Slug Size (ml)	Sum, Recovered Tracer (ppm)	Test Tube Volume (ml)	Material Balance Recovered/ Injected (measured)	Material Balance Recovered/ Injected (calculated)
WD2.2	IBA/DEC	741	570	177.59	11017	9.059		
							0.824	0.998
WD2.2	IBA/BRN	1936	2050	16.45	41539	0.839		
WD2.3	IBA/DEC	742	590	240.59	16963	8.309		
							0.832	1.000
WD2.3	IBA/BRN	2581	2300	42.46	66768	1.479		
WD2.4	IBA/DEC	792	660	48.85	4629	6.804		
							0.874	1,005
WD2.4	IBA/BRN	2568	2300	21.07	16910	2.934		
WD2.5	IBA/DEC	790	700	19.16	4621	2.853		
							0.942	1.013
WD2.5	IBA/BRN	2413	2260	45.19	15426	6.731		
WD2.6	IBA/DEC	763	780	19.76	13213	1.156		
							0.970	0.969
WD2.6	IBA/BRN	2474	2474	139.60	40960	8.164		
WD2.10	IBA/BRN	2638	2638	67.45	17993	9.590	0.970	0.970
US1IBA	IBA/BRN	776	-	65.70	5624	9.050	0.998	-
US2IBA	IBA/BRN	807	-	65.49	9048	6.020	1.031	-

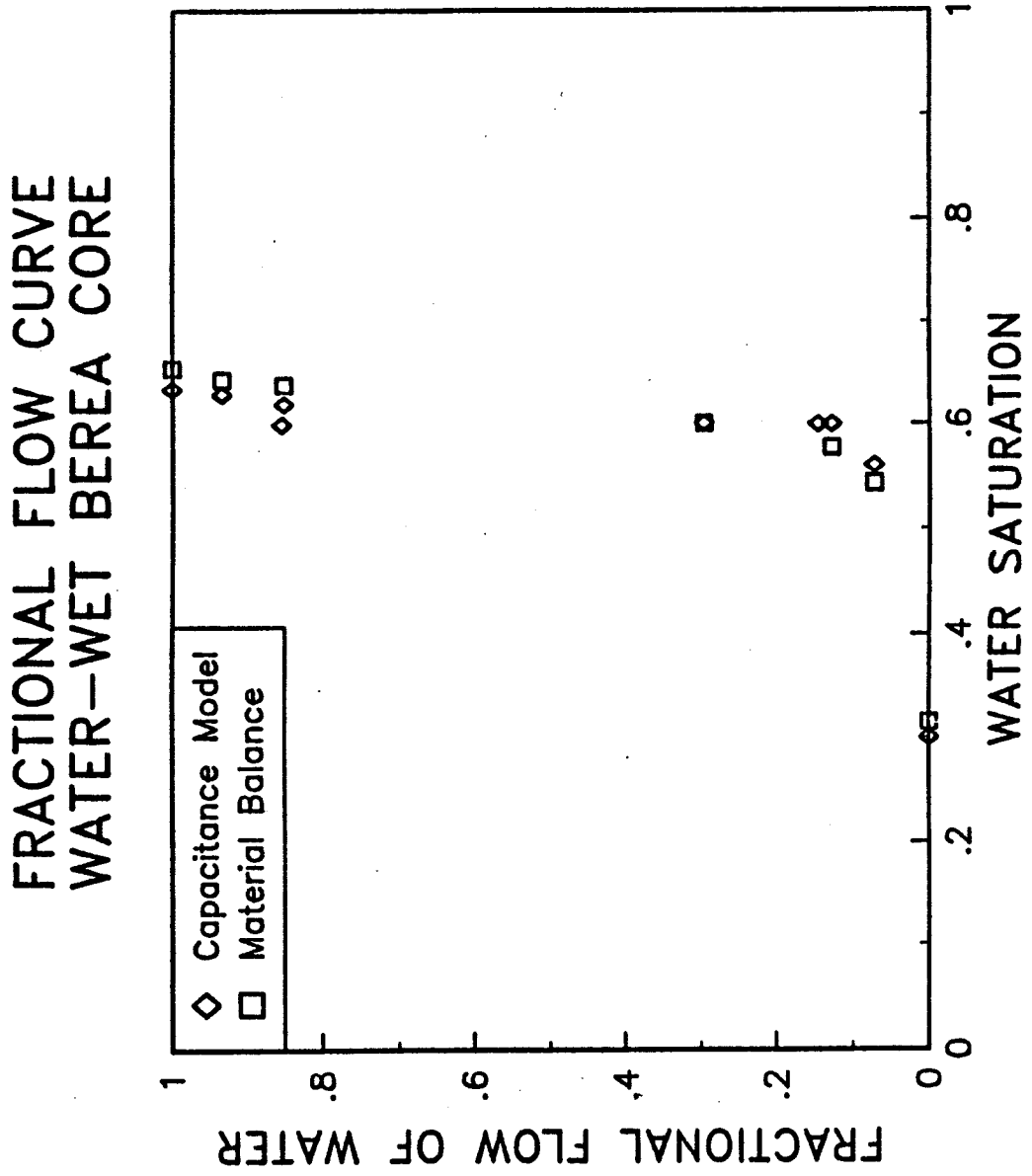

Figure 7-1 Water fractional flow curve for water-wet Berea core. Comparison of non-partitioning tracers and material balance.

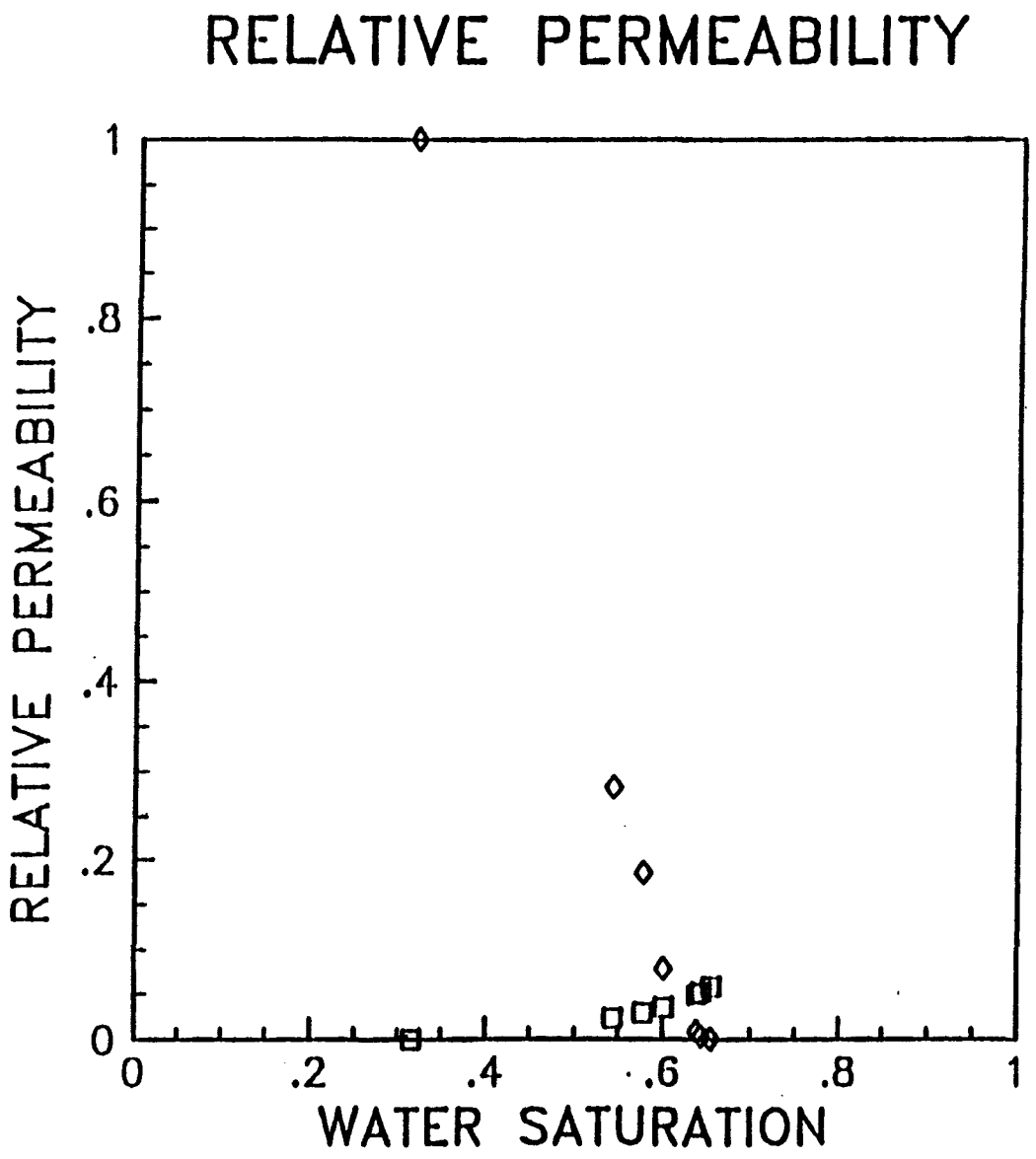

Figure 7-2 Relative permeability curve for water-wet Berea core. Saturation by material balance.

S1= .700	S2= .300	F1= .96	F2=1.00
AREA=24.90	L=60.75	POR= .217	
ALPHA1= .35	ALPHA2= 0.00	M1= .6E-02	M2= .0E+00
FF1=1.000	FF2=0.000	QT= 5.060	PART1= 0.00
NB= 100	NP=7000	PVINJ= 4.00	PVS= .200

C_i^o = 761 dpm/ml

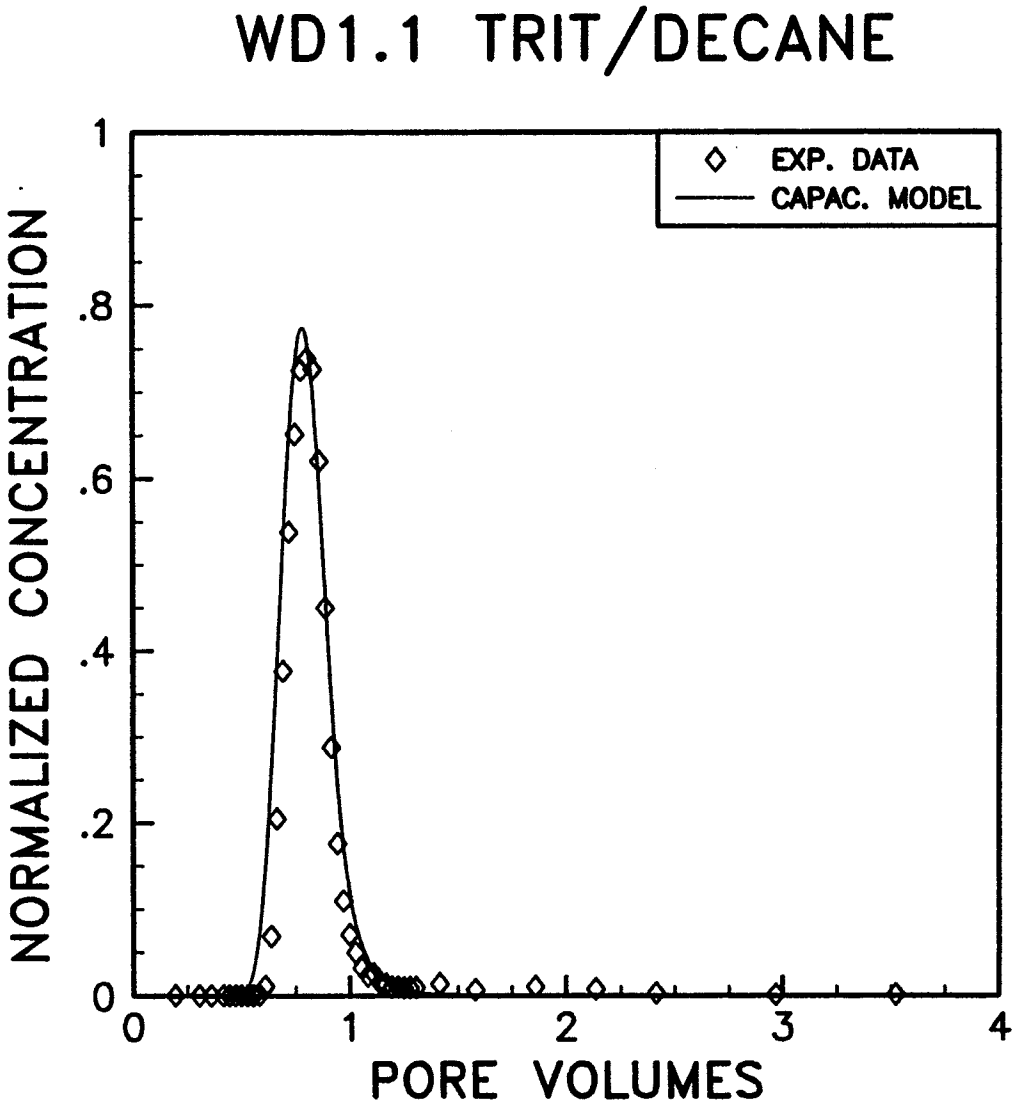

Figure 7-3 Tracer concentration versus pore volumes for water-wet Berea. Water saturation of 30%, water fractional flow of 0.0, flow rate of 5.06 ml/min, tritiated decane.

S1= .700	S2= .300	F1= .98	F2=1.00
AREA=24.90	L=60.75	POR= .217	
ALPHA1= .30	ALPHA2= 0.00	M1= .6E-02	M2= .0E+00
FF1=1.000	FF2=0.000	QT= 1.014	PART1= 0.00
NB= 100	NP=7000	PVINJ= 4.00	PVS= .200

C_i^o = 769 dpm/ml

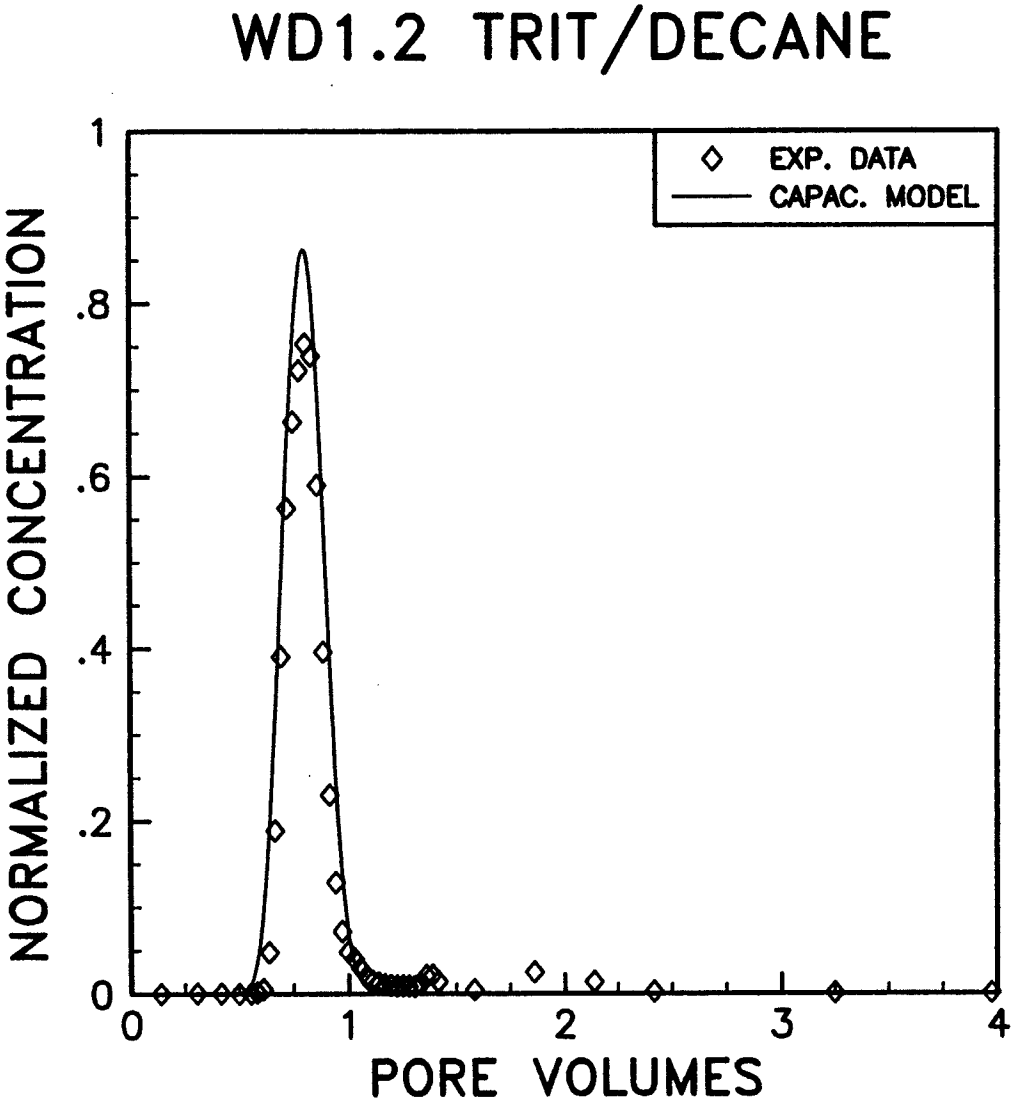

Figure 7-4 Tracer concentration versus pore volumes for water-wet Berea. Water saturation of 30%, water fractional flow of 0.0, flow rate of 1.014 ml/min, tritiated decane.

S1= .440	S2= .560	F1= .90	F2=1.00
AREA=24.90	L=60.75	POR= .217	
ALPHA1= .50	ALPHA2= 0.00	M1= .13E-02	M2= .0E+00
FF1= .927	FF2= .073	QT= 1.029	PART1= 0.00
NB= 50	NP=5000	PVINJ= 4.00	PVS= .201

C_i^o = 737 dpm/ml

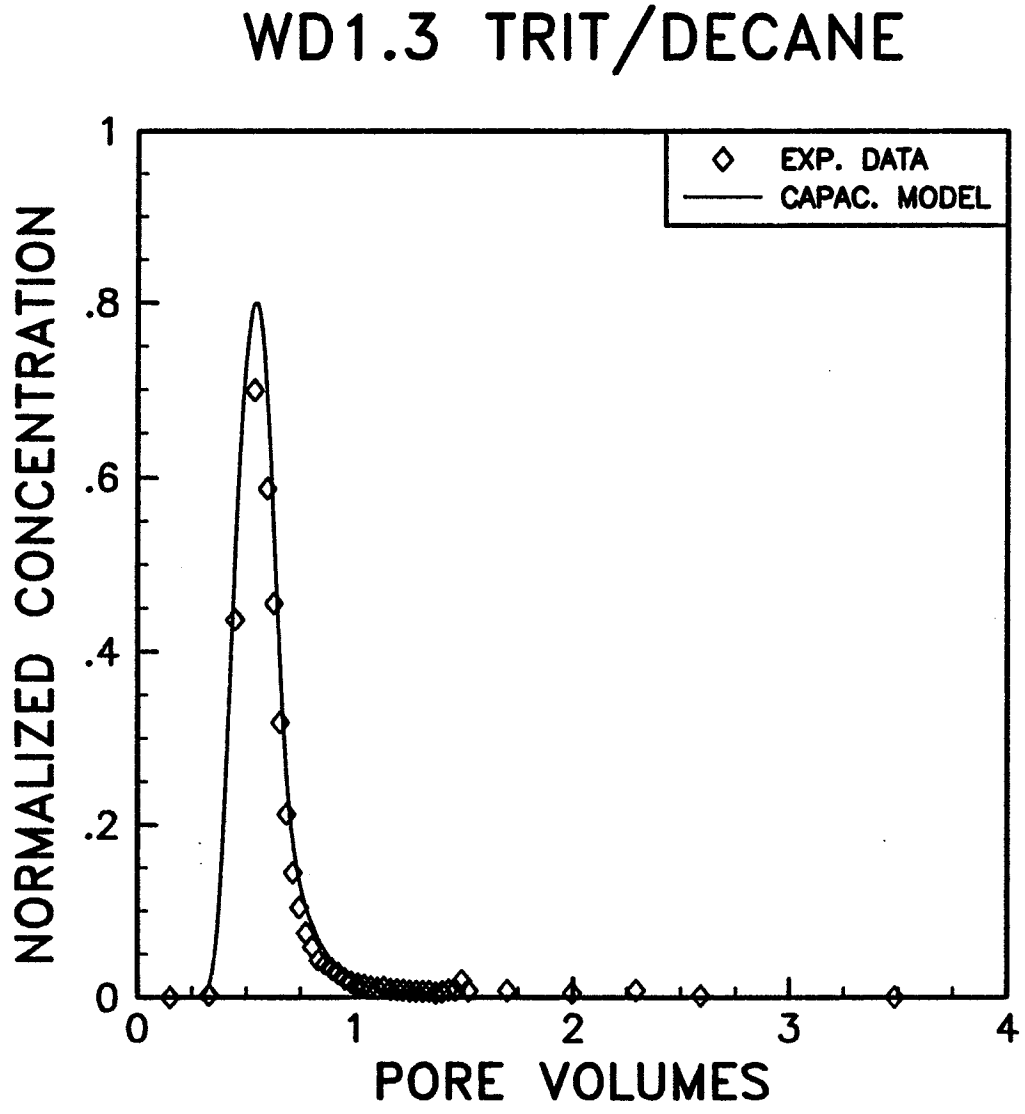

Figure 7-5 Tracer concentration versus pore volumes for water-wet Berea. Water saturation of 56%, water fractional flow of 0.073, tritiated decane.

S1= .400	S2= .600	F1= .87	F2=1.00
AREA=24.90	L=60.75	POR= .217	
ALPHA1= .70	ALPHA2= 0.00	M1= .8E-03	M2= .0E+00
FF1= .871	FF2= .129	QT= 1.021	PART1= 0.00
NB= 50	NP=5000	PVINJ= 4.00	PVS= .200

C_i^o = 767 dpm/ml

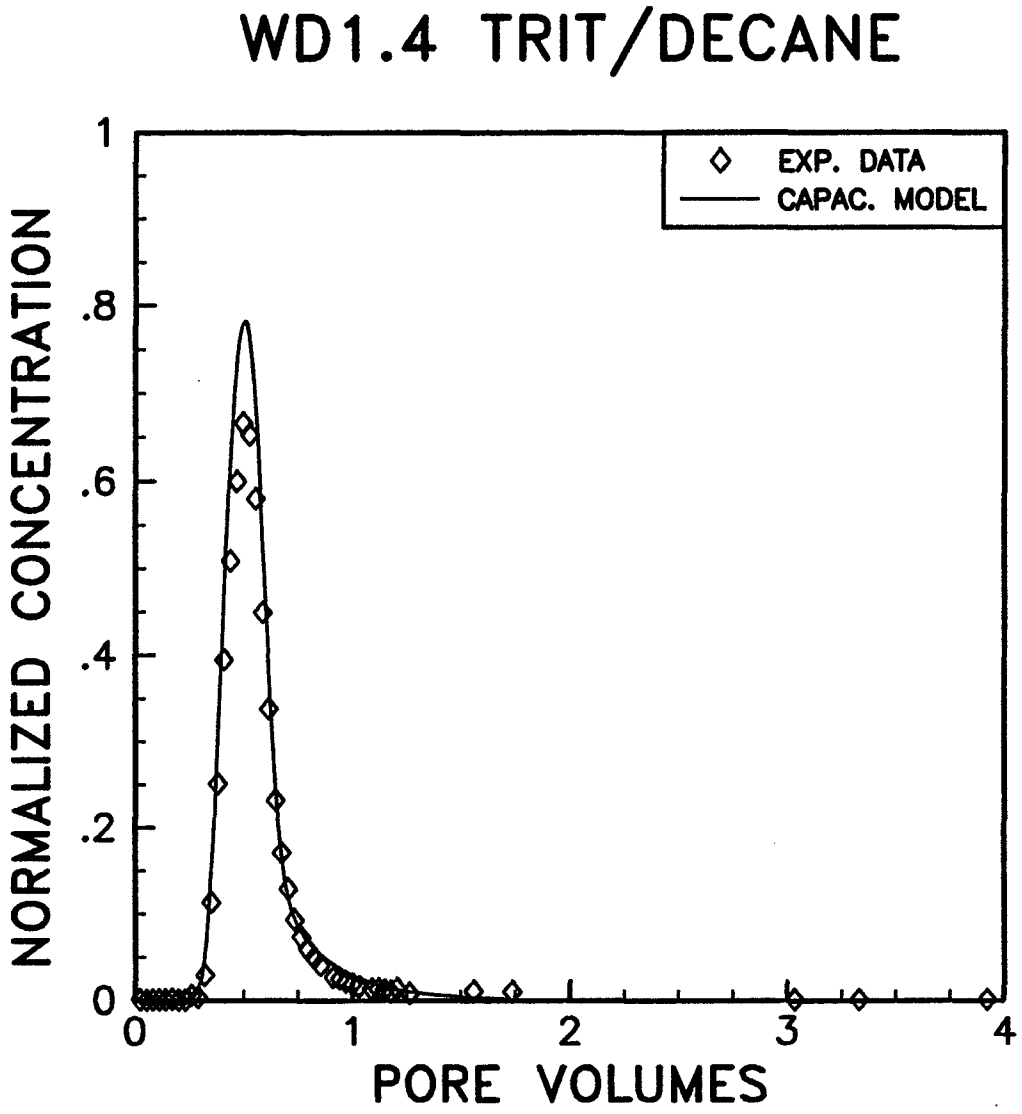

Figure 7-6 Tracer concentration versus pore volumes for water-wet Berea. Water saturation of 60%, water fractional flow of 0.129, tritiated decane.

S1= .400	S2= .600	F1= .83	F2=1.00
AREA=24.90	L=60.75	POR= .217	
ALPHA1= 1.10	ALPHA2= 0.00	M1= .80E-03	M2= .00E+00
FF1= .859	FF2= .141	QT= 1.010	PART1= 0.00
NB= 50	NP=5000	PVINJ= 4.00	PVS= .198

C_i^o = 1074 dpm/ml

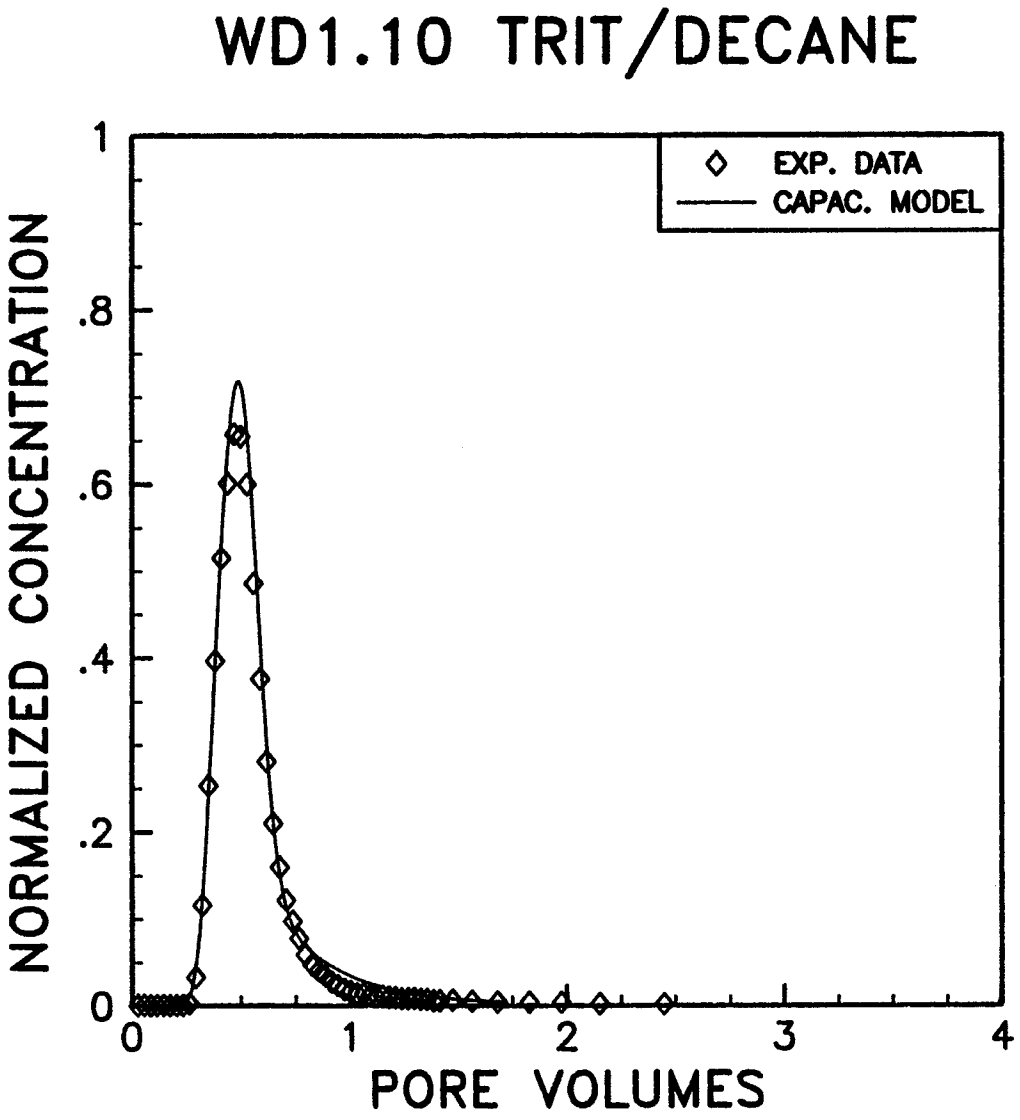

Figure 7-7 Tracer concentration versus pore volumes for water-wet Berea. Water saturation of 60%, water fractional flow of 0.141, tritiated decane.

S1= .600	S2= .400	F1= .85	F2=1.00
AREA=24.90	L=60.75	POR= .217	
ALPHA1= .15	ALPHA2= 0.00	M1= .30E-03	M2= .00E+00
FF1= .147	FF2= .853	QT= 1.016	PART1= 0.00
NB= 100	NP=7000	PVINJ=10.00	PVS= .678

C_i^o = 1130 dpm/ml

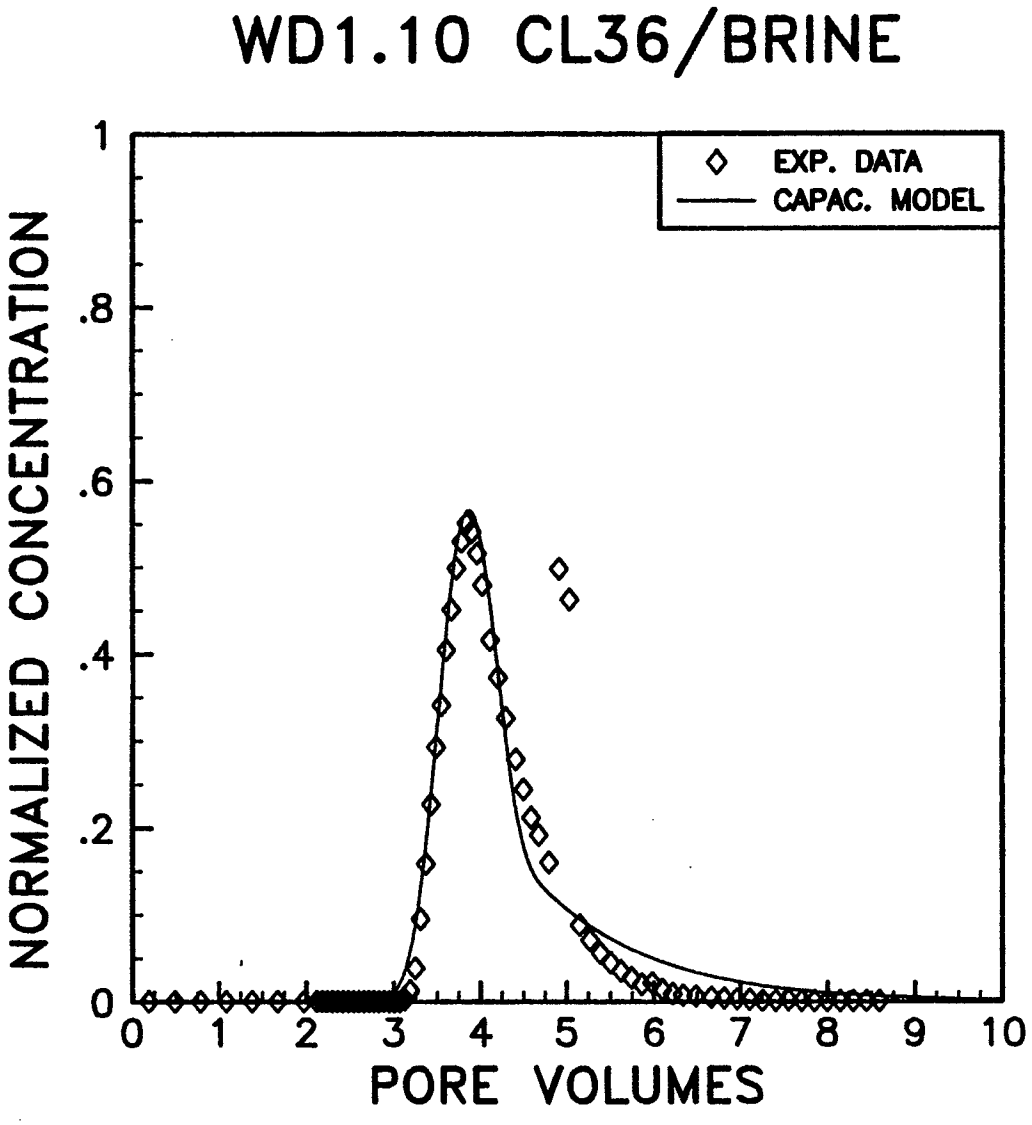

Figure 7-8 Tracer concentration versus pore volumes for water-wet Berea. Water saturation of 60%, water fractional flow of 0.141, chlorine-36.

S1= .399	S2= .601	F1= .78	F2=1.00
AREA=24.90	L=60.75	POR= .217	
ALPHA1= .65	ALPHA2= 0.00	M1= .8E-03	M2= .0E+00
FF1= .703	FF2= .297	QT= 1.014	PART1= 0.00
NB= 50	NP=5000	PVINJ= 4.00	PVS= .199

C_i^o = 835 dpm/ml

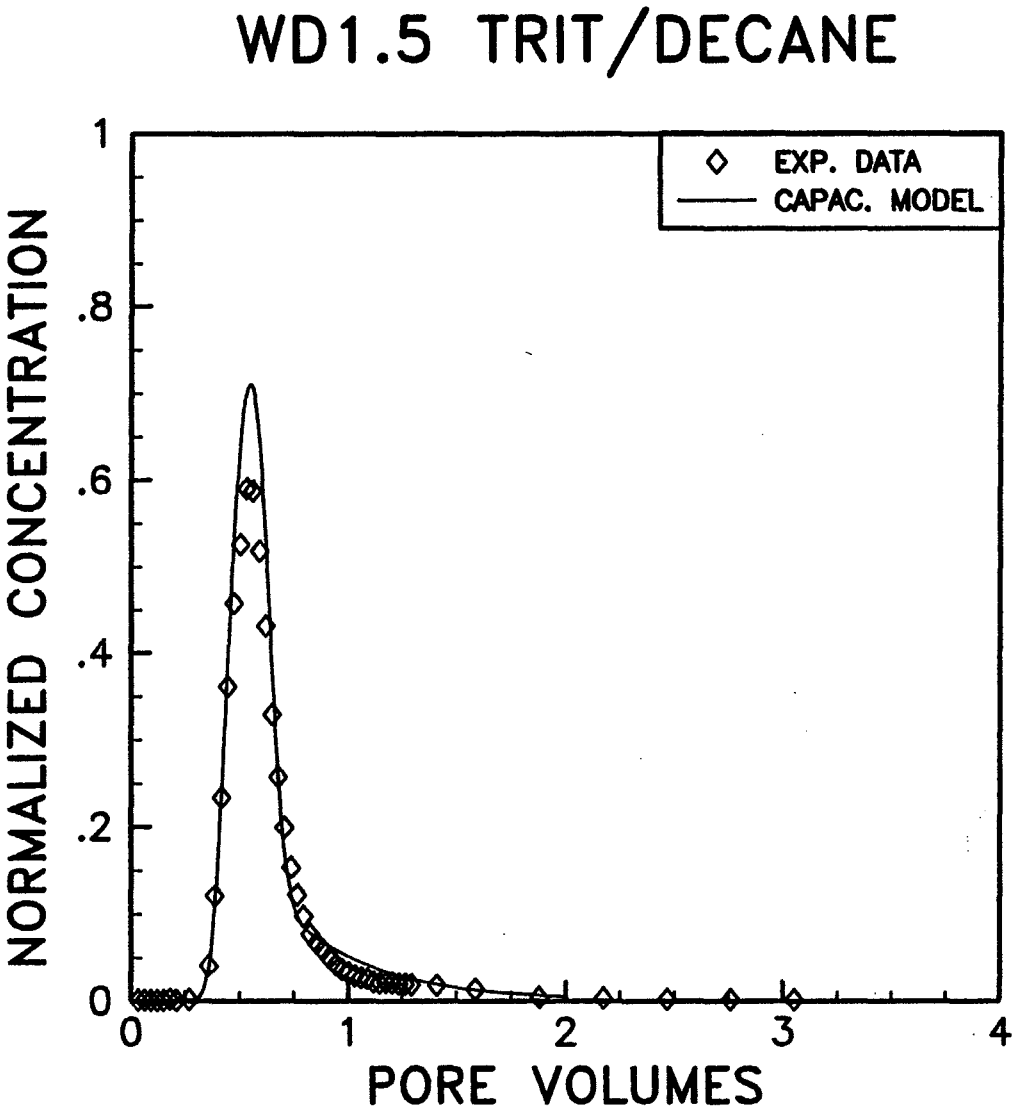

Figure 7-9 Tracer concentration versus pore volumes for water-wet Berea. Water saturation of 60.1%, water fractional flow of 0.297, tritiated decane.

S1= .601	S2= .399	F1= .85	F2=1.00
AREA=24.90	L=60.75	POR= .217	
ALPHA1= .15	ALPHA2= 0.00	M1= .1E-02	M2= .0E+00
FF1= .297	FF2= .703	QT= 1.014	PART1= 0.00
NB= 100	NP=7000	PVINJ= 4.00	PVS= .199

C_i^o = 1028 dpm/ml

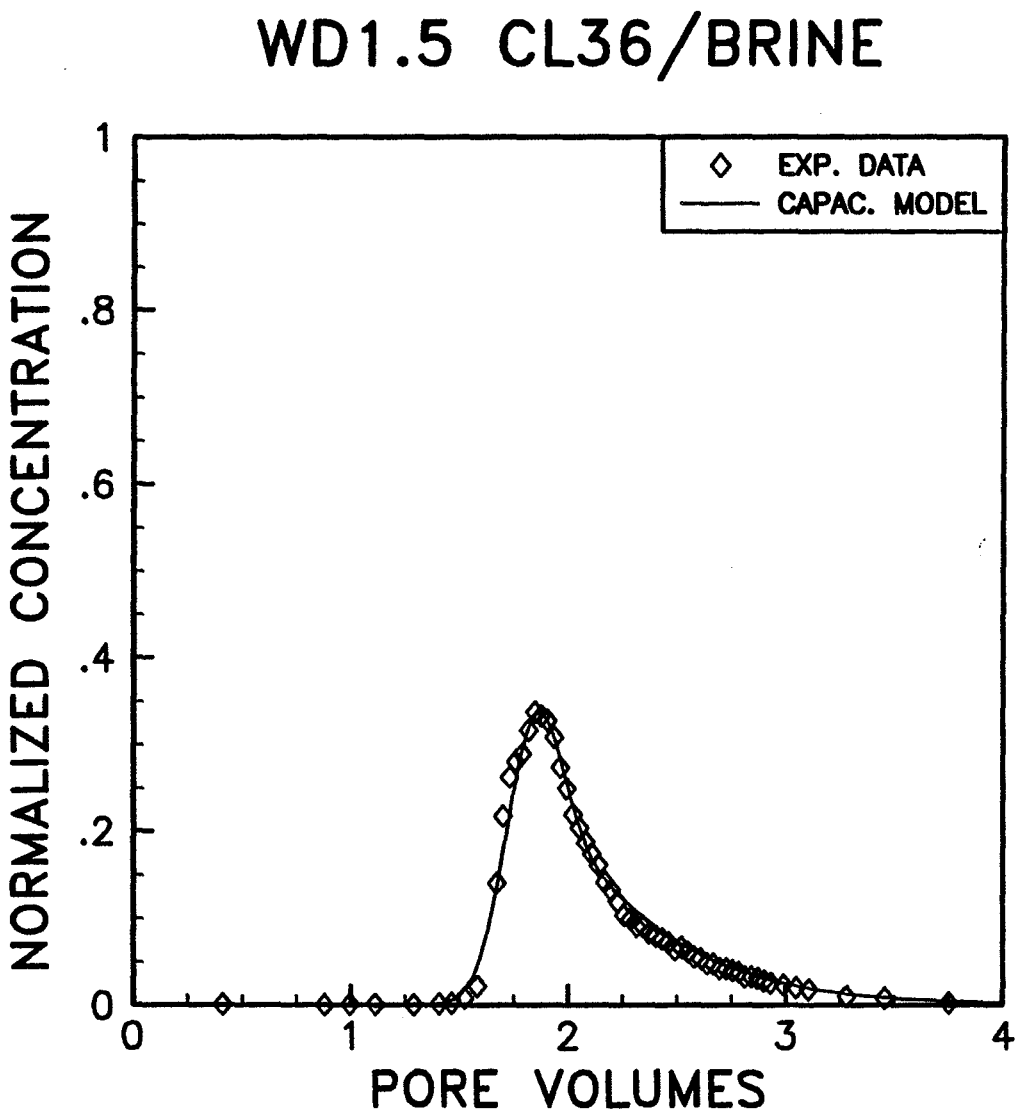

Figure 7-10 Tracer concentration versus pore volumes for water-wet Berea. Water saturation of 60.1%, water fractional flow of 0.297, chlorine-36.

S1= .620	S2= .380	F1= .87	F2=1.00
AREA=24.90	L=60.75	POR= .217	
ALPHA1= .10	ALPHA2= 0.00	M1= .15E-02	M2= .0E+00
FF1= .852	FF2= .148	QT= .994	PART1= 0.00
NB= 100	NP=7000	PVINJ= 4.00	PVS= .210

C_i^o = 1015 dpm/ml

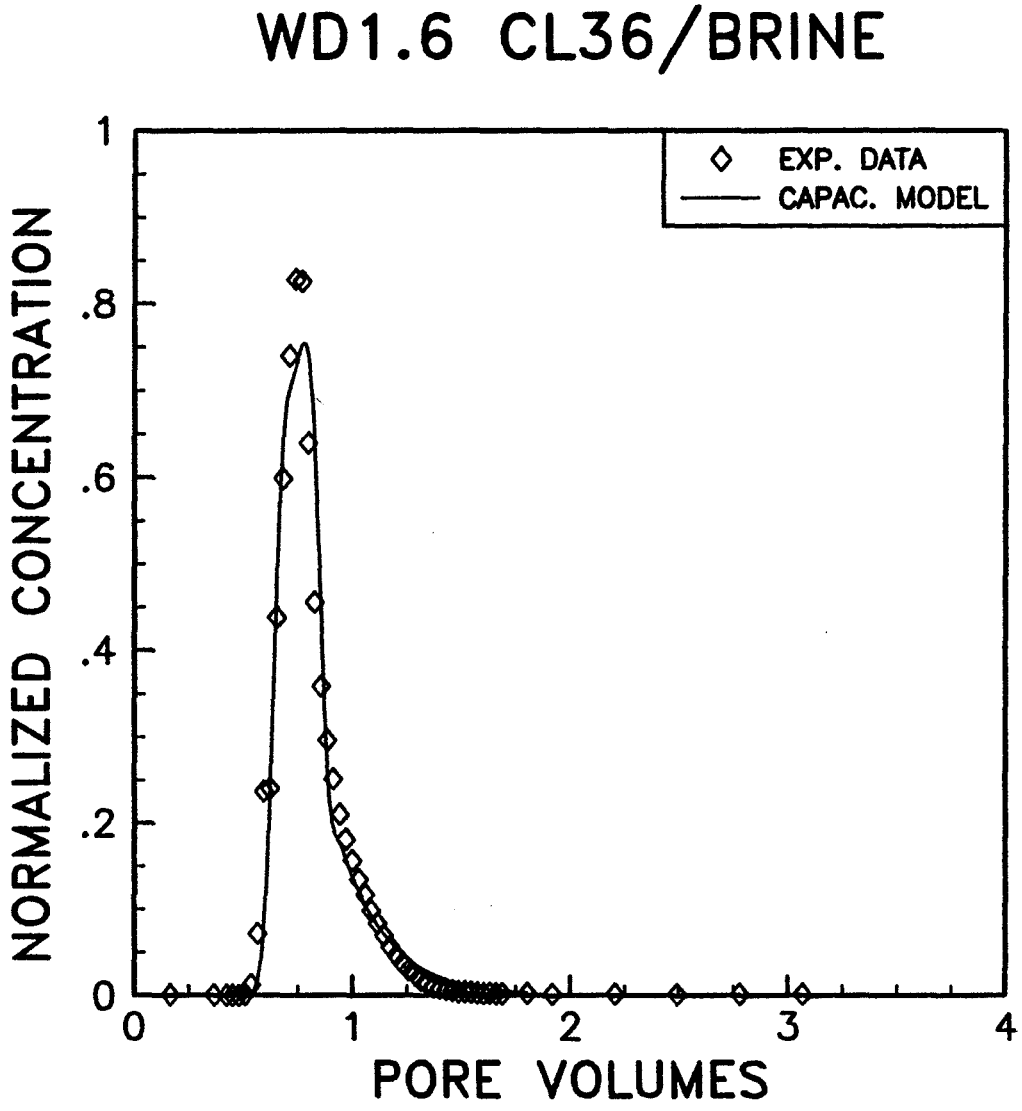

Figure 7-11 Tracer concentration versus pore volumes for water-wet Berea. Water saturation of 62%, water fractional flow of 0.852, chlorine-36.

S1= .400	S2= .600	F1= .17	F2=1.00
AREA=24.90	L=60.75	POR= .217	
ALPHA1=10.00	ALPHA2= 0.00	M1= .15E-03	M2= .00E+00
FF1= .145	FF2= .855	QT= .995	PART1= 0.00
NB= 100	NP=7000	PVINJ= 4.00	PVS= .406

C_i^o = 996 dpm/ml

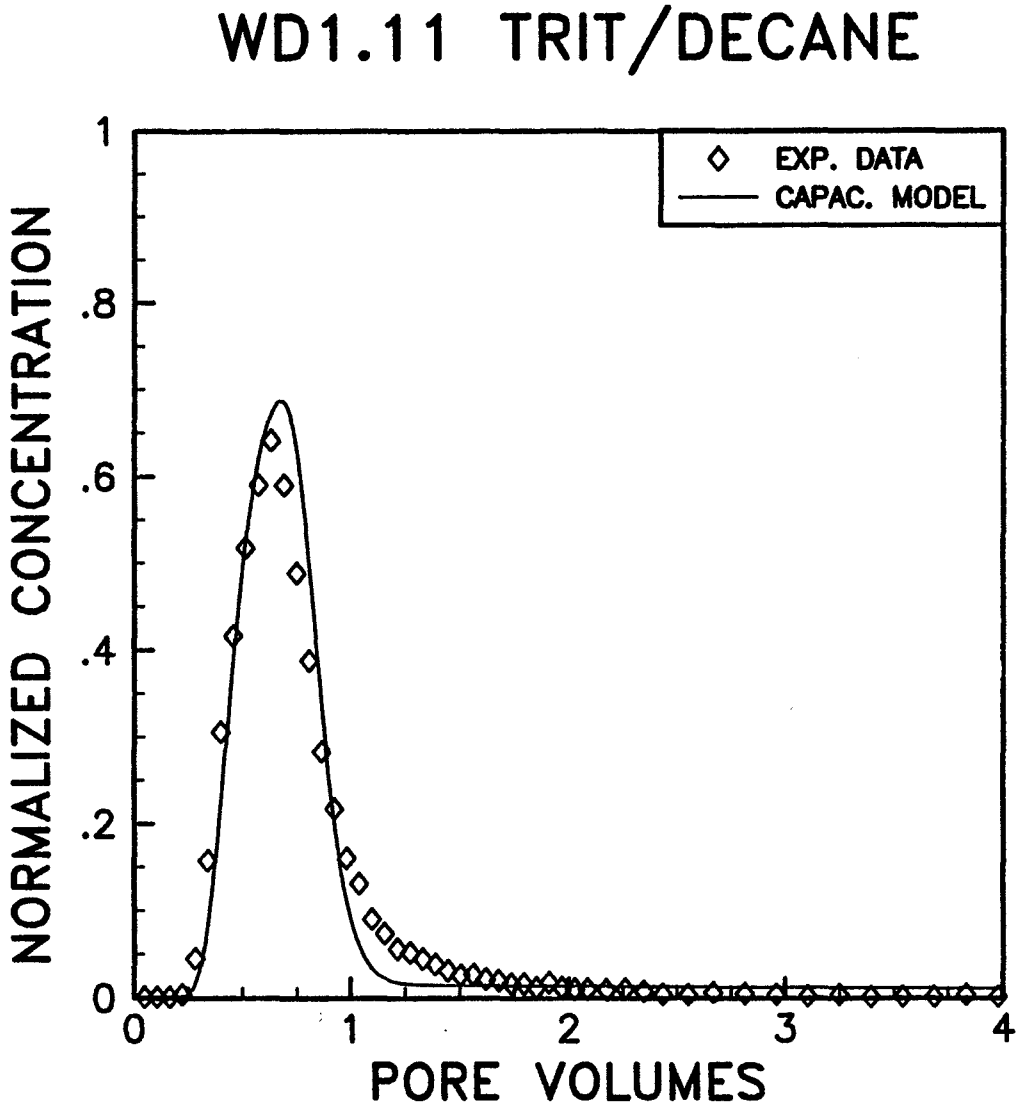

Figure 7-12 Tracer concentration versus pore volumes for water-wet Berea. Water saturation of 60%, water fractional flow of 0.855, tritiated decane.

S1= .600	S2= .400	F1= .89	F2=1.00
AREA=24.90	L=60.75	POR= .217	
ALPHA1= .15	ALPHA2= 0.00	M1= .14E-02	M2= .00E+00
FF1= .855	FF2= .145	QT= .995	PART1= 0.00
NB= 100	NP=7000	PVINJ= 4.00	PVS= .199

C_i^o = 1103 dpm/ml

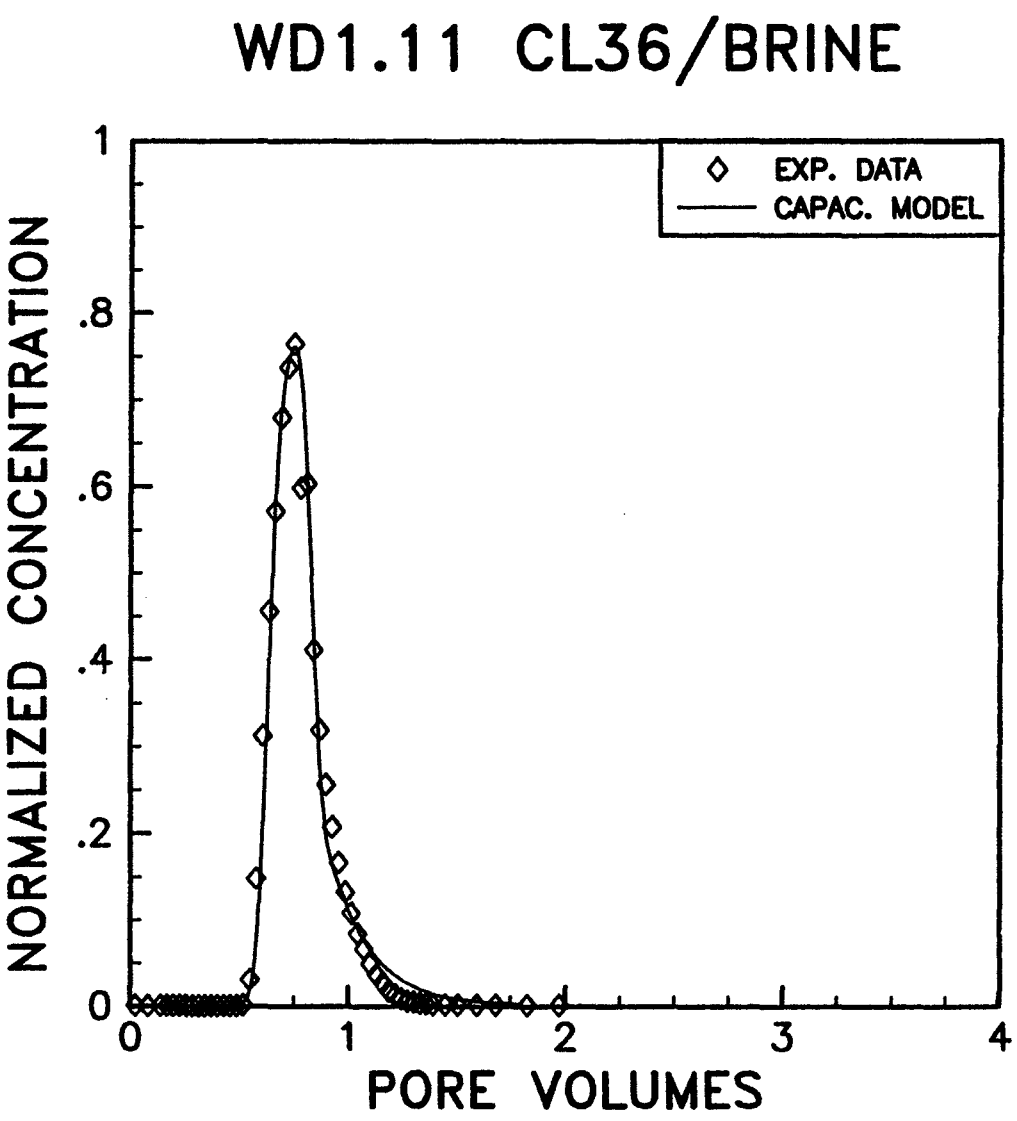

Figure 7-13 Tracer concentration versus pore volumes for water-wet Berea. Water saturation of 60%, water fractional flow of 0.855, chlorine-36.

S1= .630	S2= .370	F1= .88	F2=1.00
AREA=24.90	L=60.75	POR= .217	
ALPHA1= .10	ALPHA2= 0.00	M1= .15E-02	M2= .00E+00
FF1= .934	FF2= .066	QT= .996	PART1= 0.00
NB= 100	NP=9000	PVINJ= 4.00	PVS= .199

C_i^o = 1020 dpm/ml

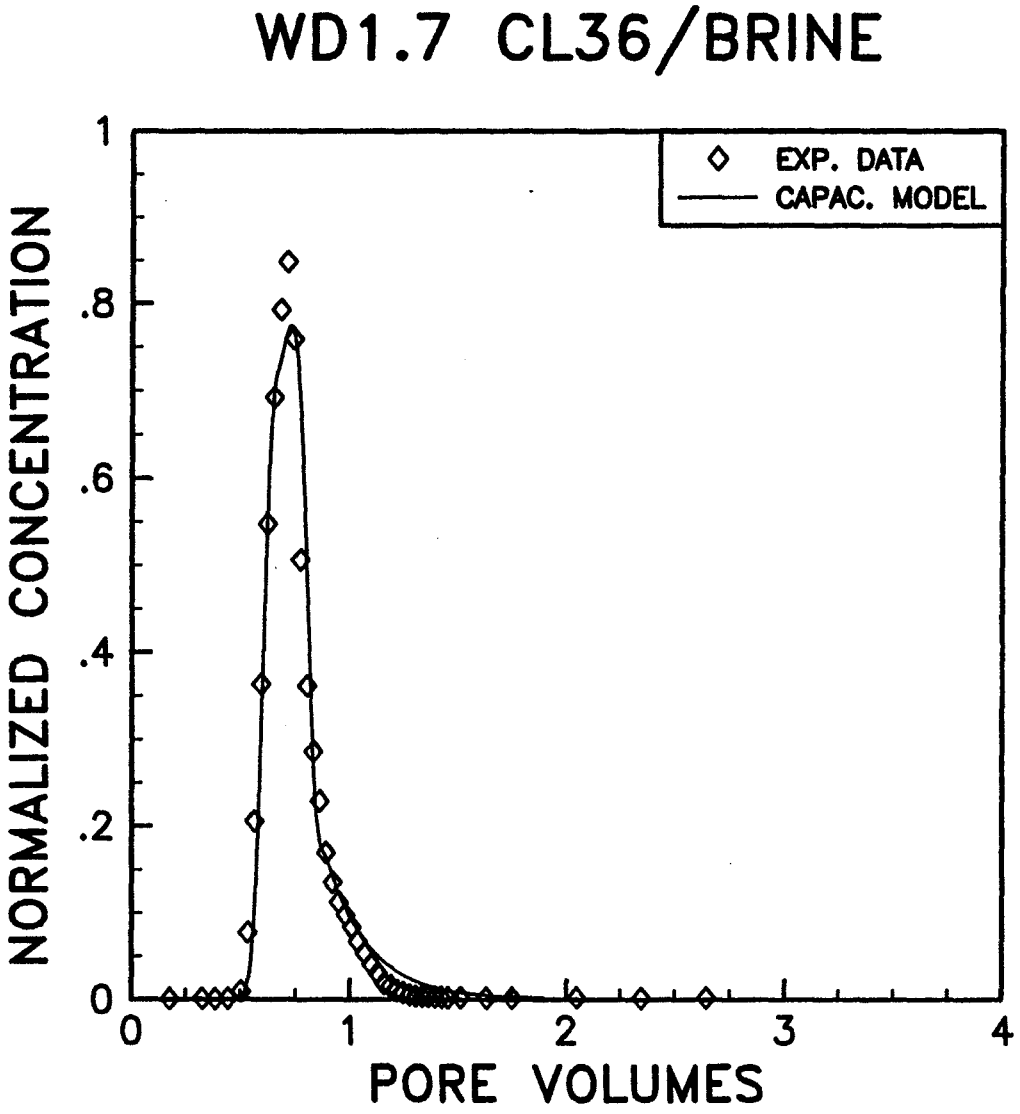

Figure 7-14 Tracer concentration versus pore volumes for water-wet Berea. Water saturation of 63%, water fractional flow of 0.934, chlorine-36.

S1= .635	S2= .365	F1= .92	F2=1.00
AREA=24.90	L=60.75	POR= .217	
ALPHA1= .10	ALPHA2= 0.00	M1= .15E-02	M2= .00E+00
FF1=1.000	FF2=0.000	QT= .997	PART1= 0.00
NB= 100	NP=7000	PVINJ= 4.00	PVS= .200

C_i^o = 1026 dpm/ml

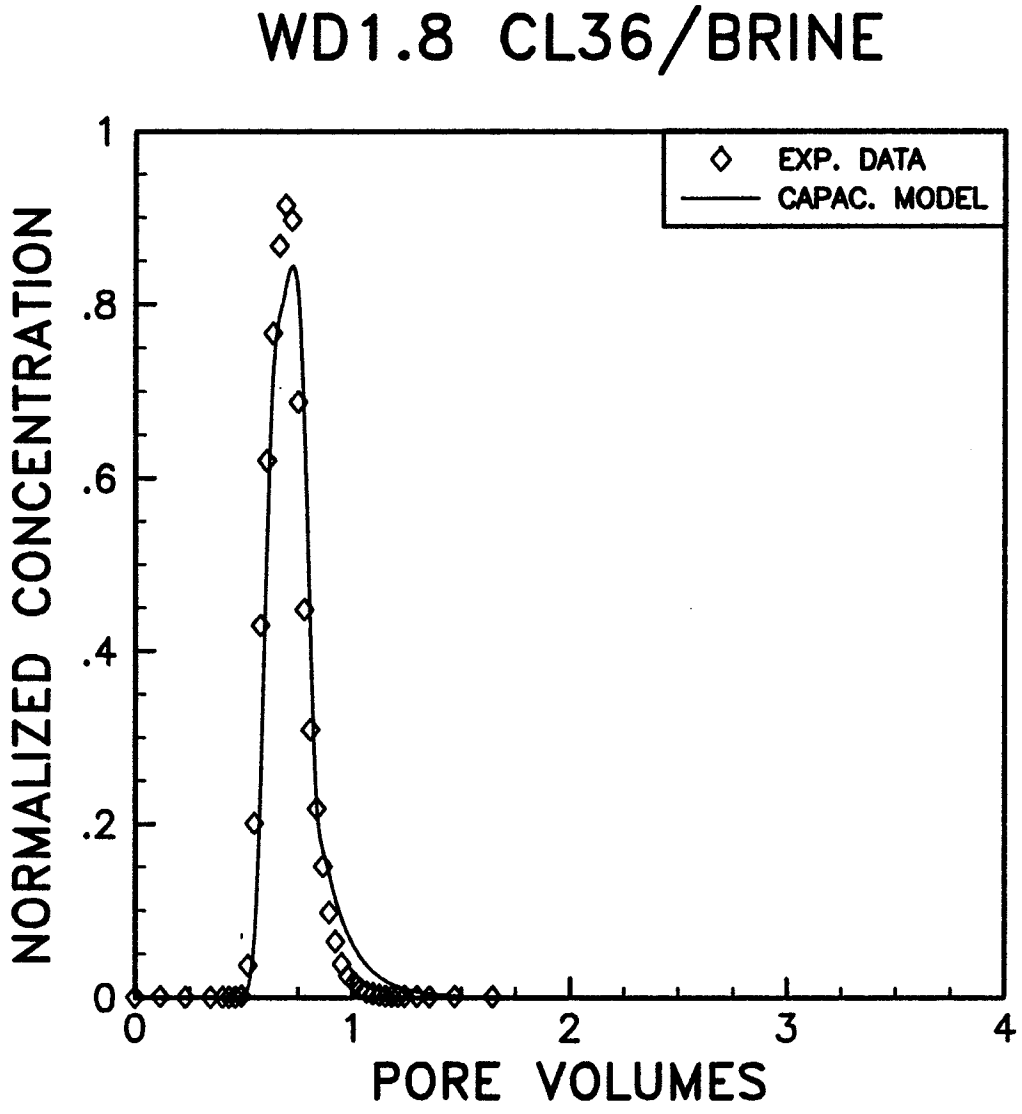

Figure 7-15 Tracer concentration versus pore volumes for water-wet Berea. Water saturation of 63.5%, water fractional flow of 1.0, chlorine-36.

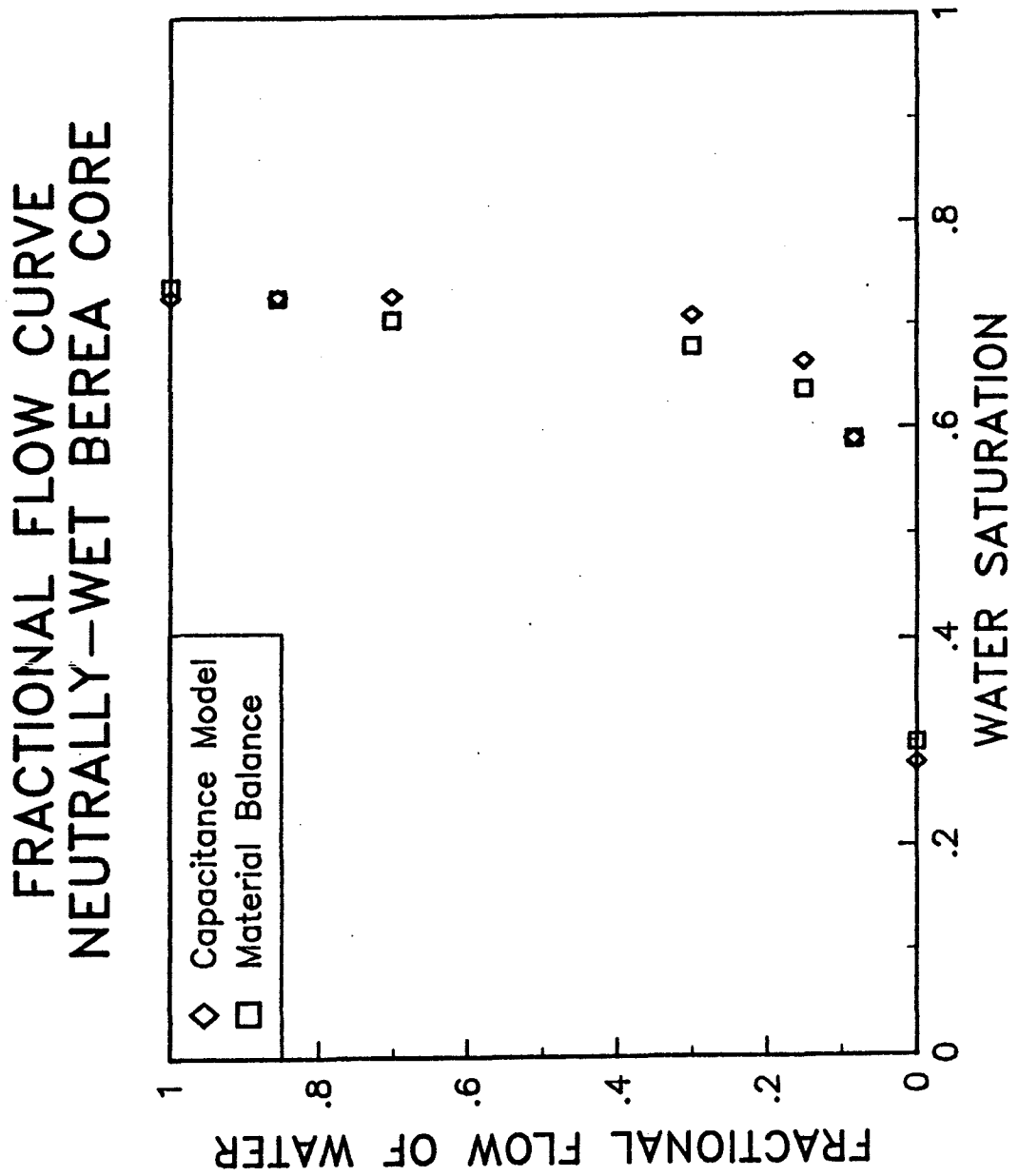

Figure 7-16 Water fractional flow curve for treated Berea core. Comparison of non-partitioning tracers and material balance.

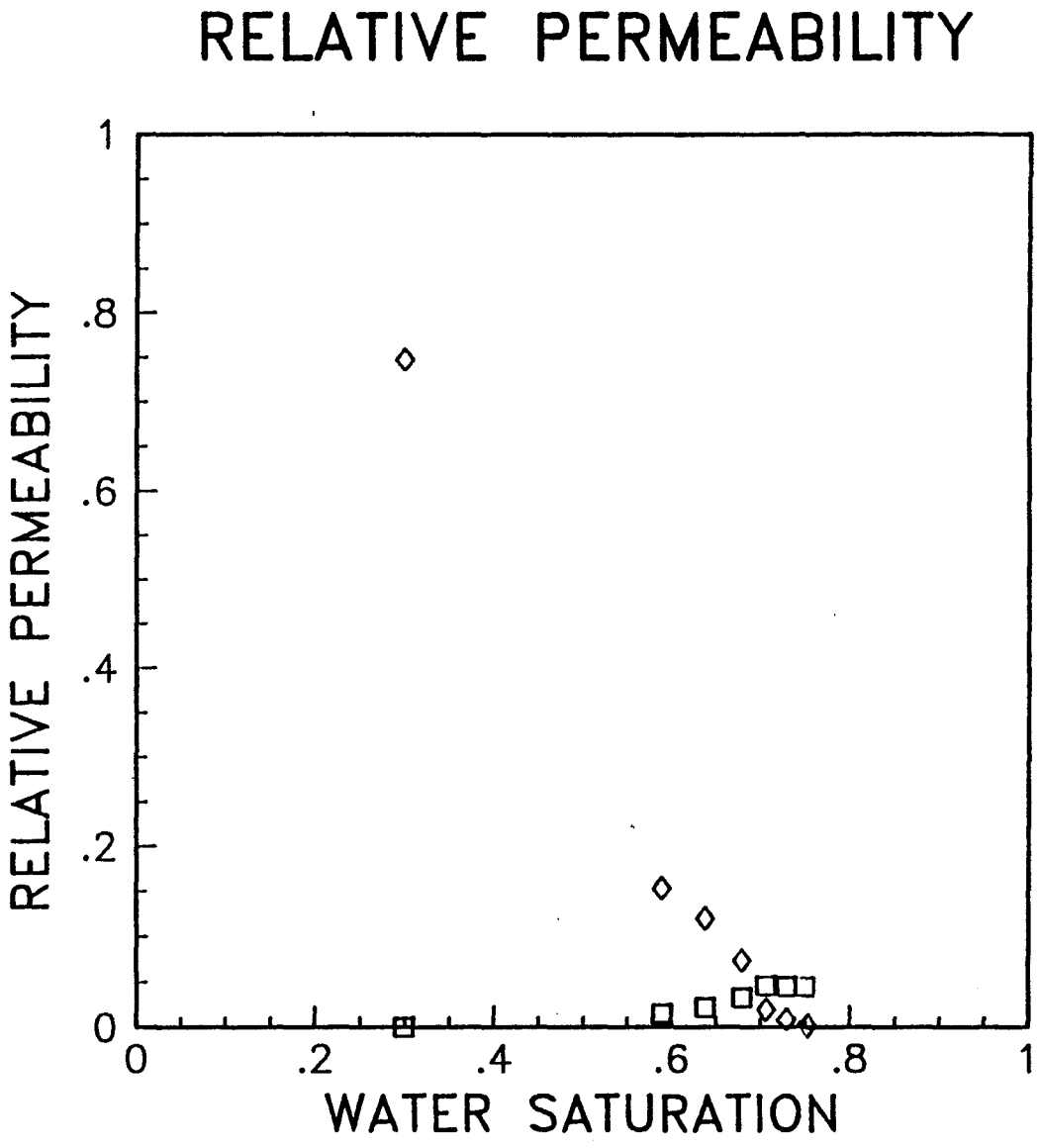

Figure 7-17 Relative permeability curve for treated Berea curve. Saturation by material balance.

S1= .720	S2= .280	F1=1.00	F2=1.00
AREA=25.95	L=60.85	POR= .204	
ALPHA1= .35	ALPHA2= 0.00	M1= .0E+00	M2= .0E+00
FF1=1.000	FF2=0.000	QT= 1.015	PART1= 0.00
NB= 50	NP=5000	PVINJ= 4.00	PVS= .200

C_i^o = 866 dpm/ml

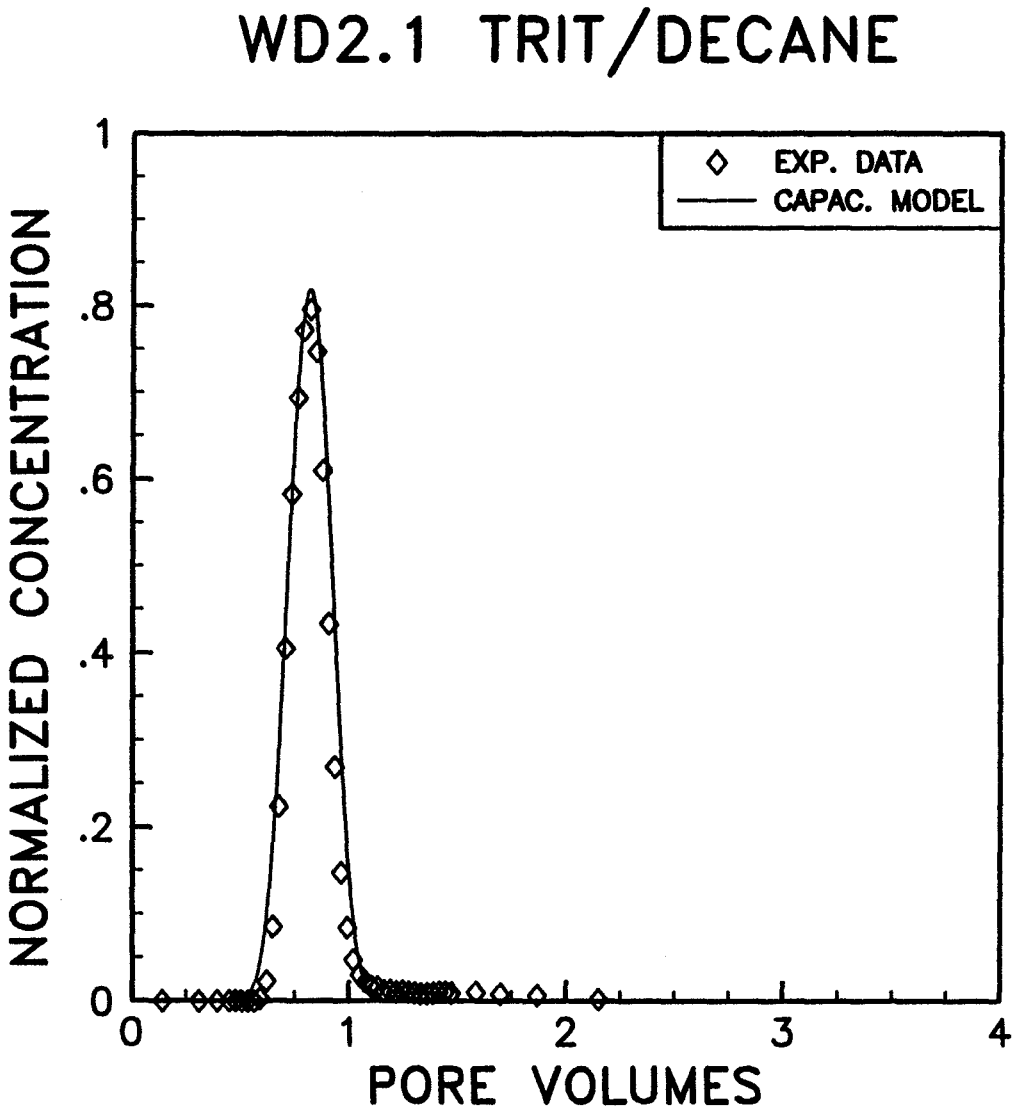

Figure 7-18 Tracer concentration versus pore volumes for treated core. Water saturation of 28%, water fractional flow of 0.0, tritiated decane.

S1= .410	S2= .590	F1= .77	F2=1.00
AREA=25.95	L=60.85	POR= .204	
ALPHA1= .65	ALPHA2= 0.00	M1= .13E-02	M2= .00E+00
FF1= .915	FF2= .085	QT= 1.031	PART1= 0.00
NB= 50	NP=5000	PVINJ= 4.00	PVS= .602

C_i^o = 924 dpm/ml

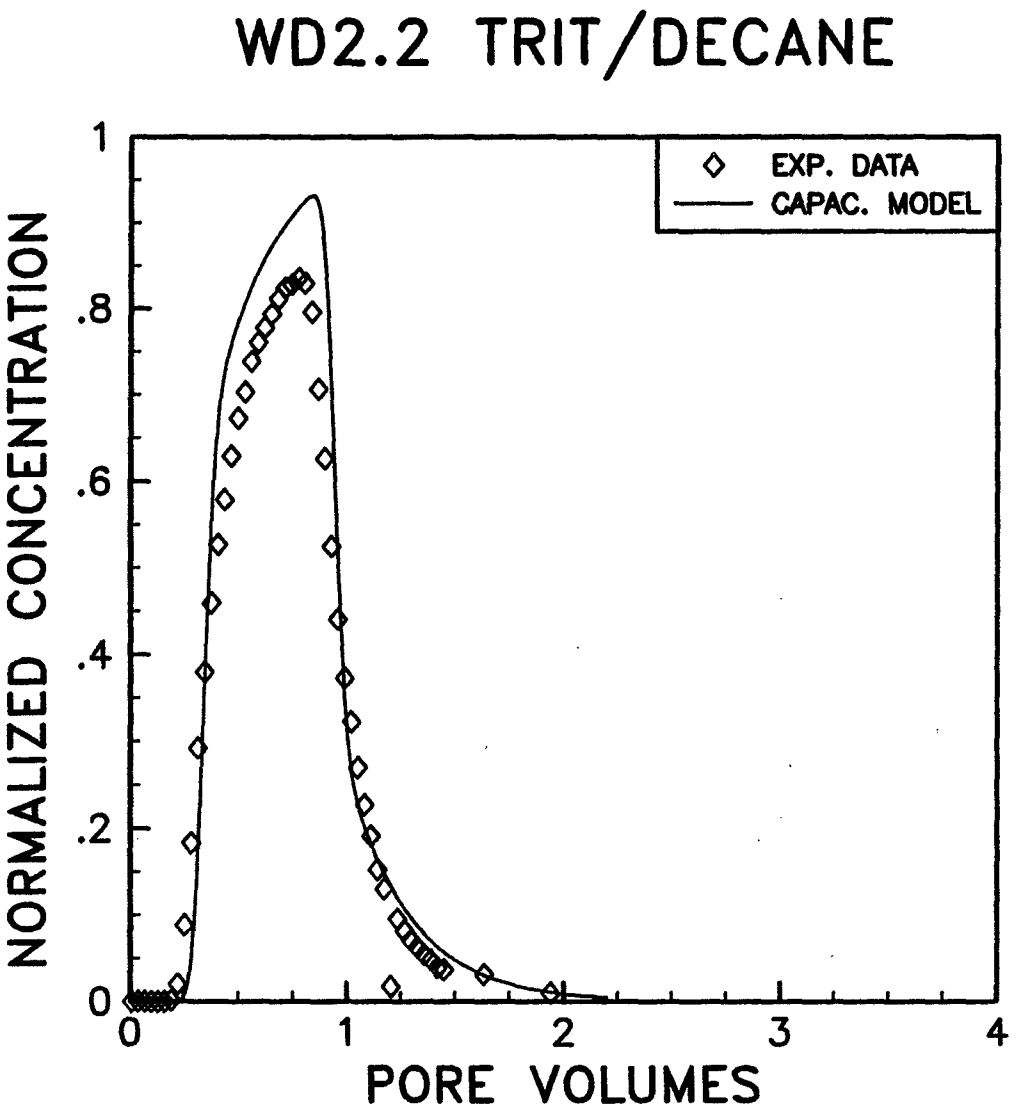

Figure 7-19 Tracer concentration versus pore volumes for treated core. Water saturation of 59%, water fractional flow of 0.085, tritiated decane.

S1= .590	S2= .410	F1= .57	F2=1.00
AREA=25.95	L=60.85	POR= .204	
ALPHA1= .10	ALPHA2= 0.00	M1= .1E-02	M2= .0E+00
FF1= .085	FF2= .915	QT= 1.031	PART1= 0.00
NB= 100	NP=7000	PVINJ=12.00	PVS= .602

C_i^o = 1124 dpm/ml

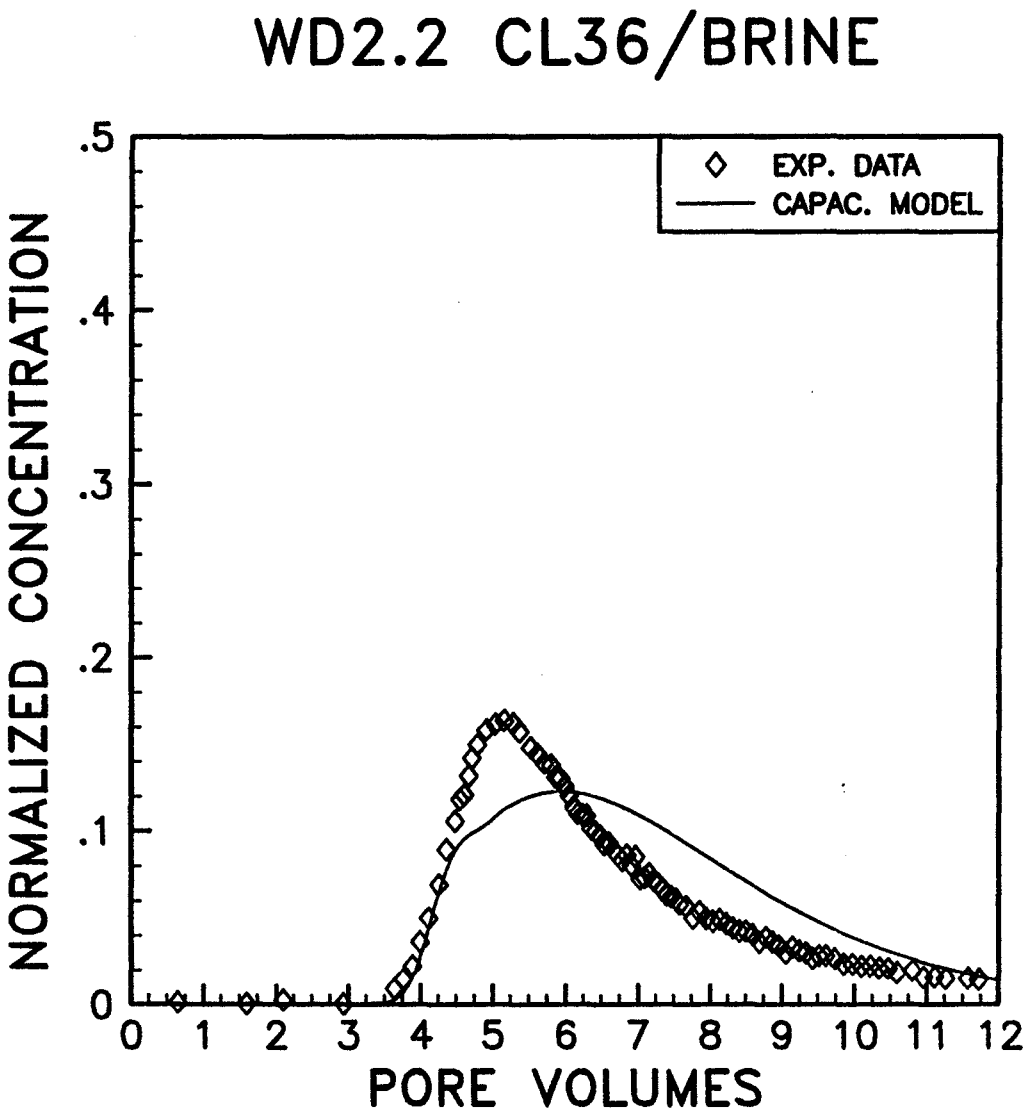

Figure 7-20 Tracer concentration versus pore volumes for treated core. Water saturation of 59%, water fractional flow of 0.085, chlorine-36.

S1= .335	S2= .665	F1= .75	F2=1.00
AREA=25.95	L=60.85	POR= .204	
ALPHA1= 1.50	ALPHA2= 0.00	M1= .15E-02	M2= .0E+00
FF1= .849	FF2= .151	QT= 1.020	PART1= 0.00
NB= 50	NP=5000	PVINJ= 4.00	PVS= .877

C_i^o = 934 dpm/ml

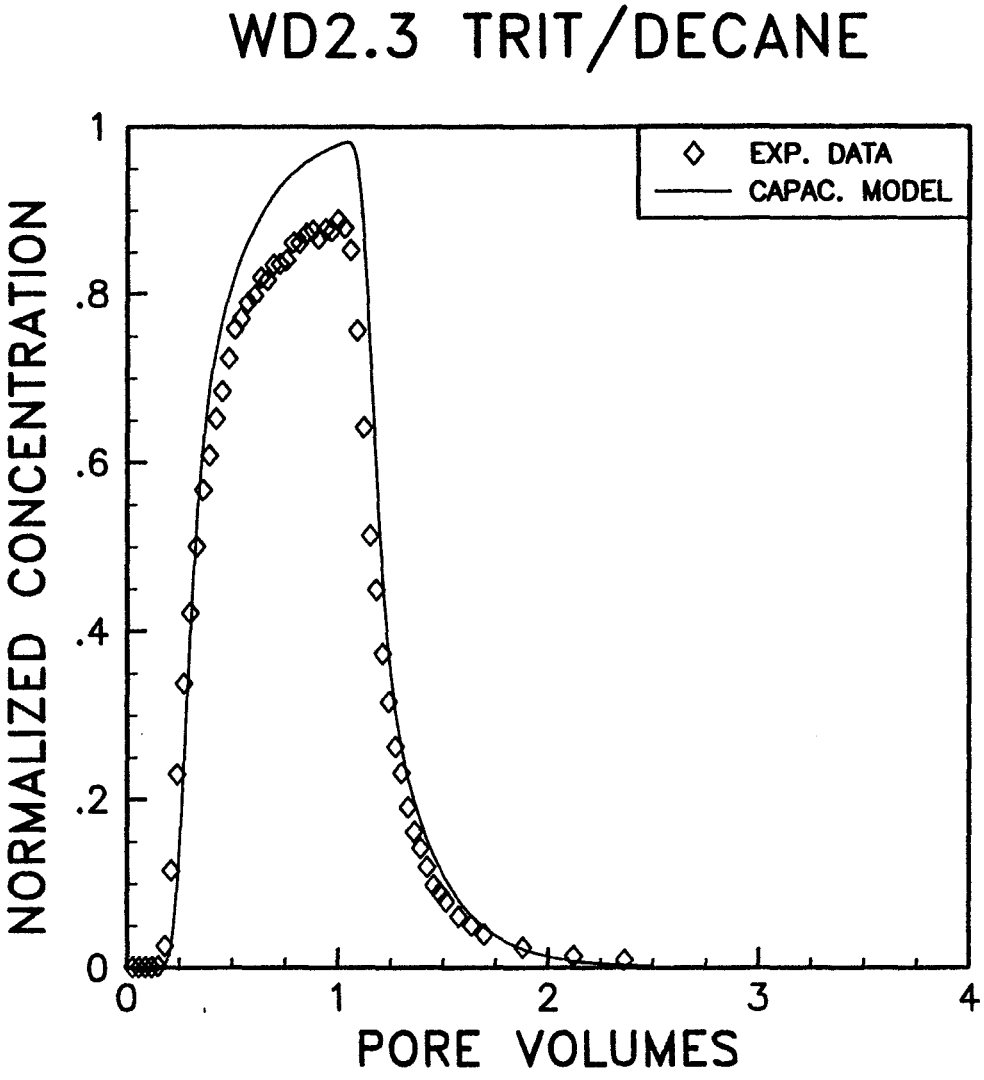

Figure 7-21 Tracer concentration versus pore volumes for treated core. Water saturation of 66.5%, water fractional flow of 0.151, tritiated decane.

S1= .665	S2= .335	F1= .63	F2=1.00
AREA=25.95	L=60.85	POR= .204	
ALPHA1= .50	ALPHA2= 0.00	M1= .6E-03	M2= .0E+00
FF1= .151	FF2= .849	QT= 1.020	PART1= 0.00
NB= 100	NP=7000	PVINJ=10.00	PVS= .877

C_i^o = 1127 dpm/ml

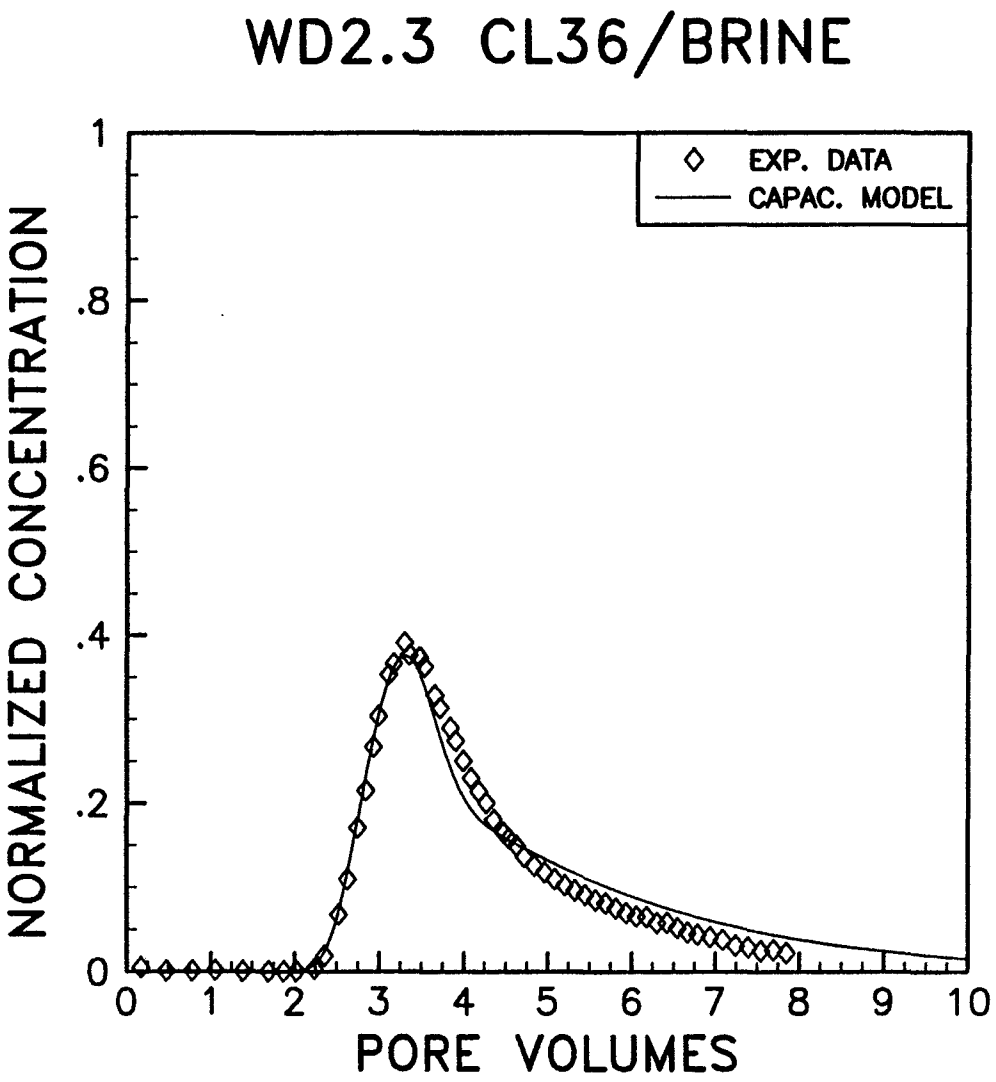

Figure 7-22 Tracer concentration versus pore volumes for treated core. Water saturation of 66.5%, water fractional flow of 0.151, chlorine-36.

S1= .290	S2= .710	F1= .60	F2=1.00
AREA=25.95	L=60.85	POR= .204	
ALPHA1= 5.50	ALPHA2= 0.00	M1= .90E-03	M2= .00E+00
FF1= .699	FF2= .301	QT= 1.014	PART1= 0.00
NB= 50	NP=5000	PVINJ= 4.00	PVS= .217

C_i^o = 915 dpm/ml

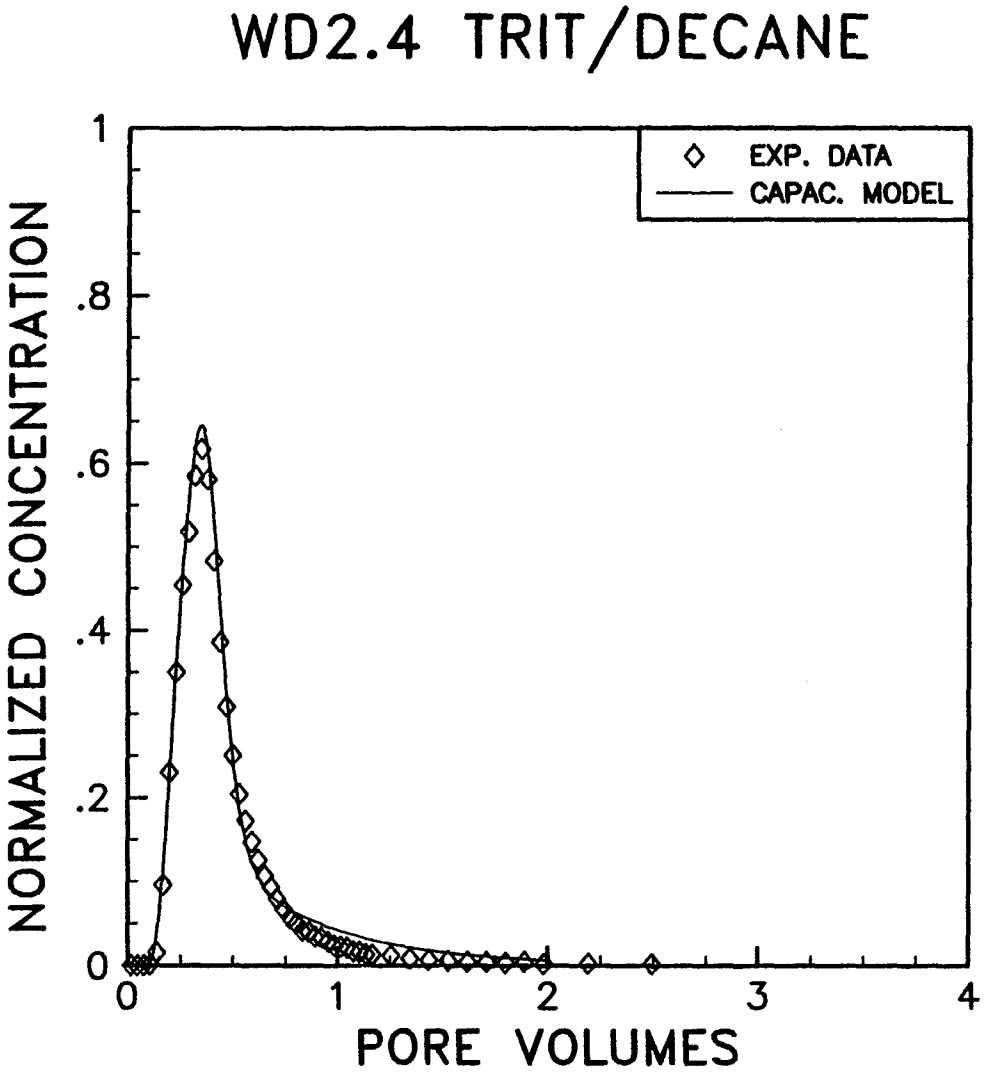

Figure 7-23 Tracer concentration versus pore volumes for treated core. Water saturation of 71%, water fractional flow of 0.301, tritiated decane.

S1= .710	S2= .290	F1= .70	F2=1.00
AREA=25.95	L=60.85	POR= .204	
ALPHA1= .50	ALPHA2= 0.00	M1= .1E-02	M2= .0E+00
FF1= .301	FF2= .699	QT= 1.014	PART1= 0.00
NB= 50	NP=5000	PVINJ= 4.00	PVS= .217

C_i^o = 1141 dpm/ml

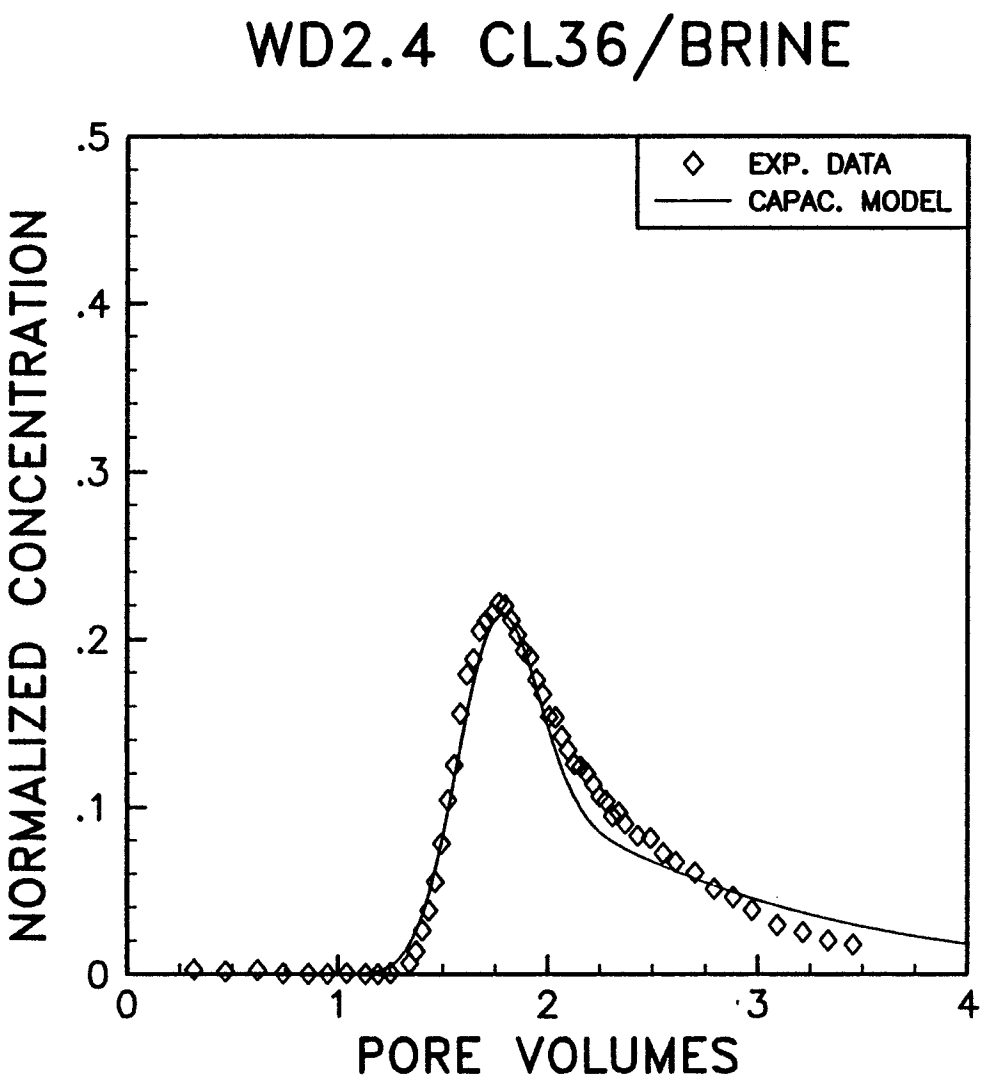

Figure 7-24 Tracer concentration versus pore volumes for treated core. Water saturation of 71%, water fractional flow of 0.301, chlorine-36.

S1= .270	S2= .730	F1= .43	F2=1.00
AREA=25.95	L=60.85	POR= .204	
ALPHA1=12.00	ALPHA2= 0.00	M1= .35E-03	M2= .0E+00
FF1= .298	FF2= .702	QT= .998	PART1= 0.00
NB= 50	NP=5000	PVINJ= 4.00	PVS= .200

C_i^o = 735 dpm/ml

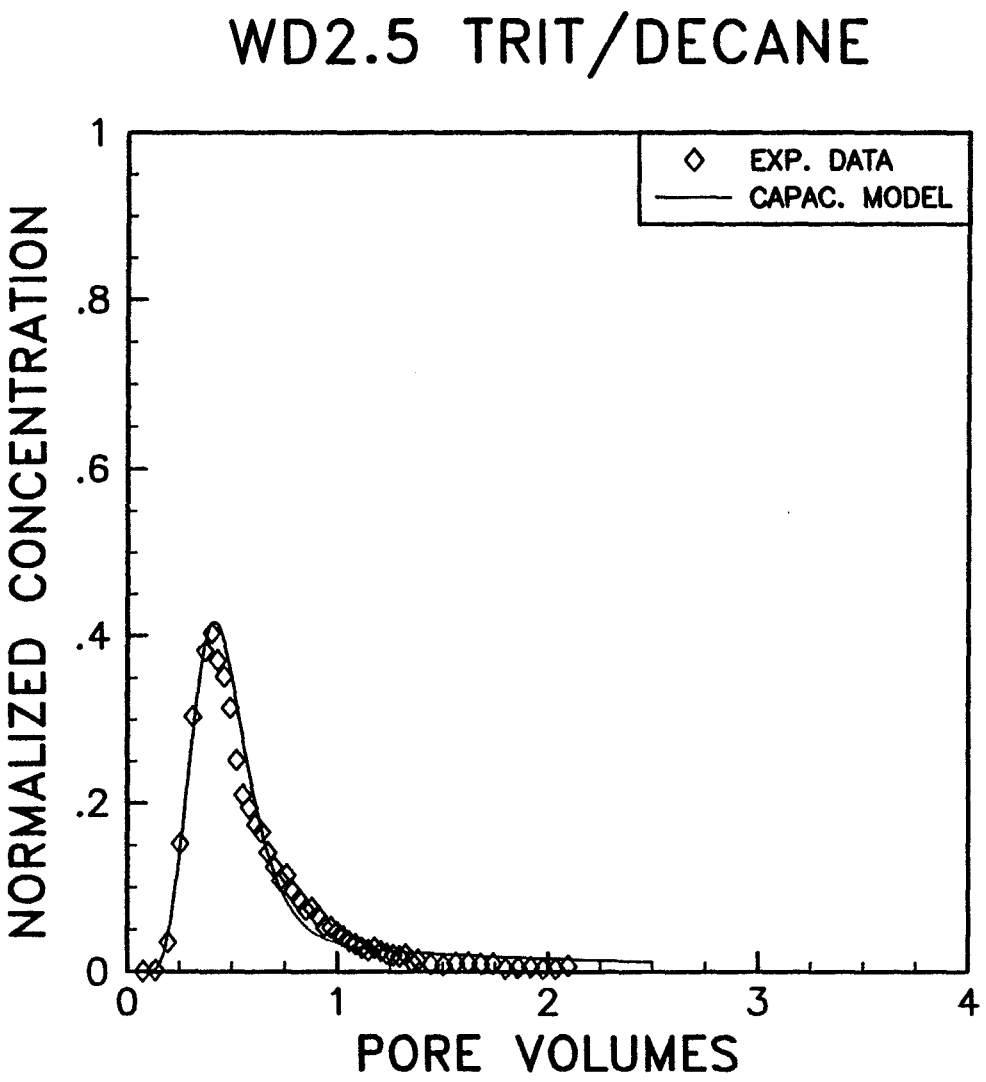

Figure 7-25 Tracer concentration versus pore volumes for treated core. Water saturation of 73%, water fractional flow of 0.702, tritiated decane.

S1= .730	S2= .270	F1= .88	F2=1.00
AREA=25.95	L=60.85	POR= .204	
ALPHA1= 1.30	ALPHA2= 0.00	M1= .3E-03	M2= .0E+00
FF1= .702	FF2= .298	QT= .998	PART1= 0.00
NB= 50	NP=5000	PVINJ= 4.00	PVS= .200

C_i^o = 1141 dpm/ml

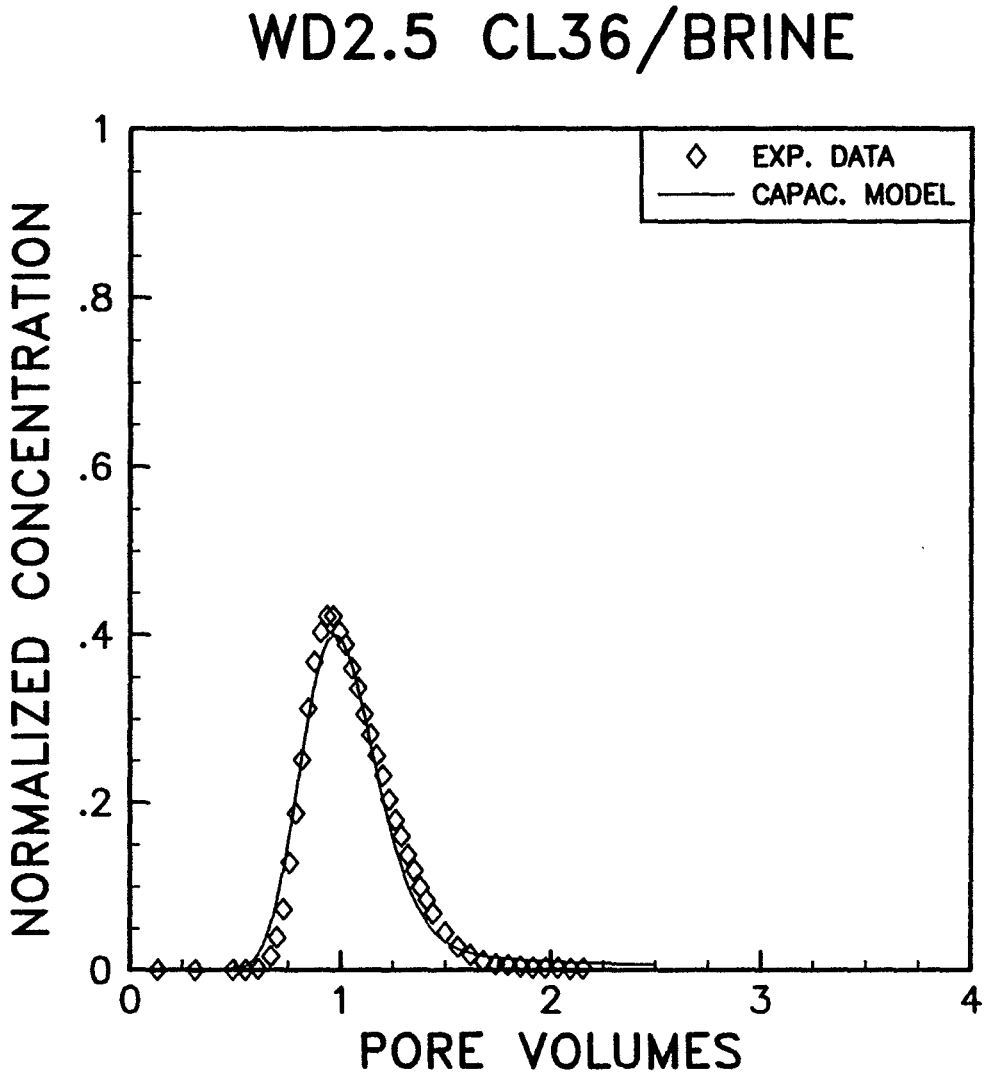

Figure 7-26 Tracer concentration versus pore volumes for treated core. Water saturation of 73%, water fractional flow of 0.702, chlorine-36.

S1= .270	S2= .730	F1= .25	F2=1.00
AREA=25.95	L=60.85	POR= .204	
ALPHA1=13.00	ALPHA2= 0.00	M1= .3E-03	M2= .0E+00
FF1= .124	FF2= .876	QT= .971	PART1= 0.00
NB= 50	NP=5000	PVINJ= 4.00	PVS= .494

C_i^o = 784 dpm/ml

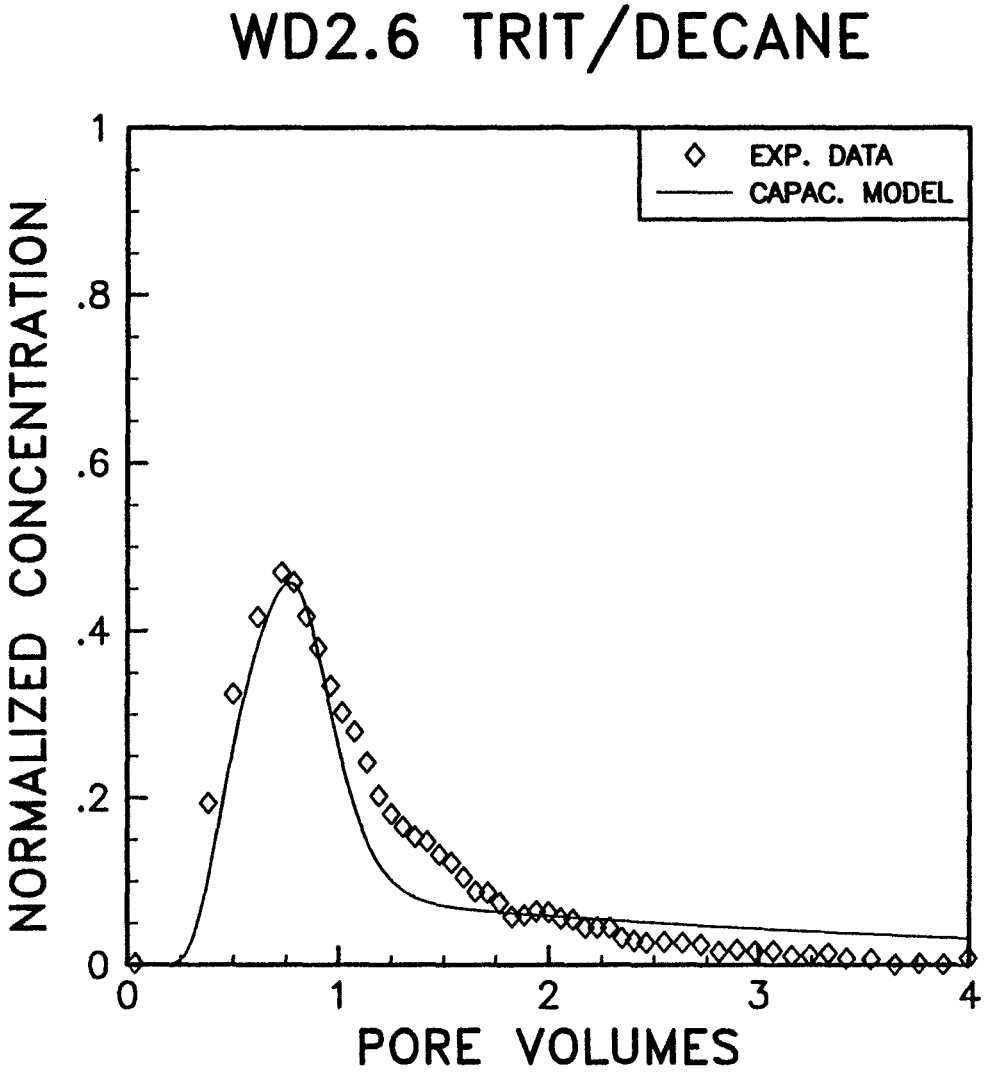

Figure 7-27 Tracer concentration versus pore volumes for treated core. Water saturation of 73%, water fractional flow of 0.876, tritiated decane.

S1= .730	S2= .270	F1= .92	F2=1.00
AREA=25.95	L=60.85	POR= .204	
ALPHA1= 1.20	ALPHA2= 0.00	M1= .5E-04	M2= .0E+00
FF1= .876	FF2= .124	QT= .971	PART1= 0.00
NB= 50	NP=5000	PVINJ= 4.00	PVS= .494

C_i^o = 1136 dpm/ml

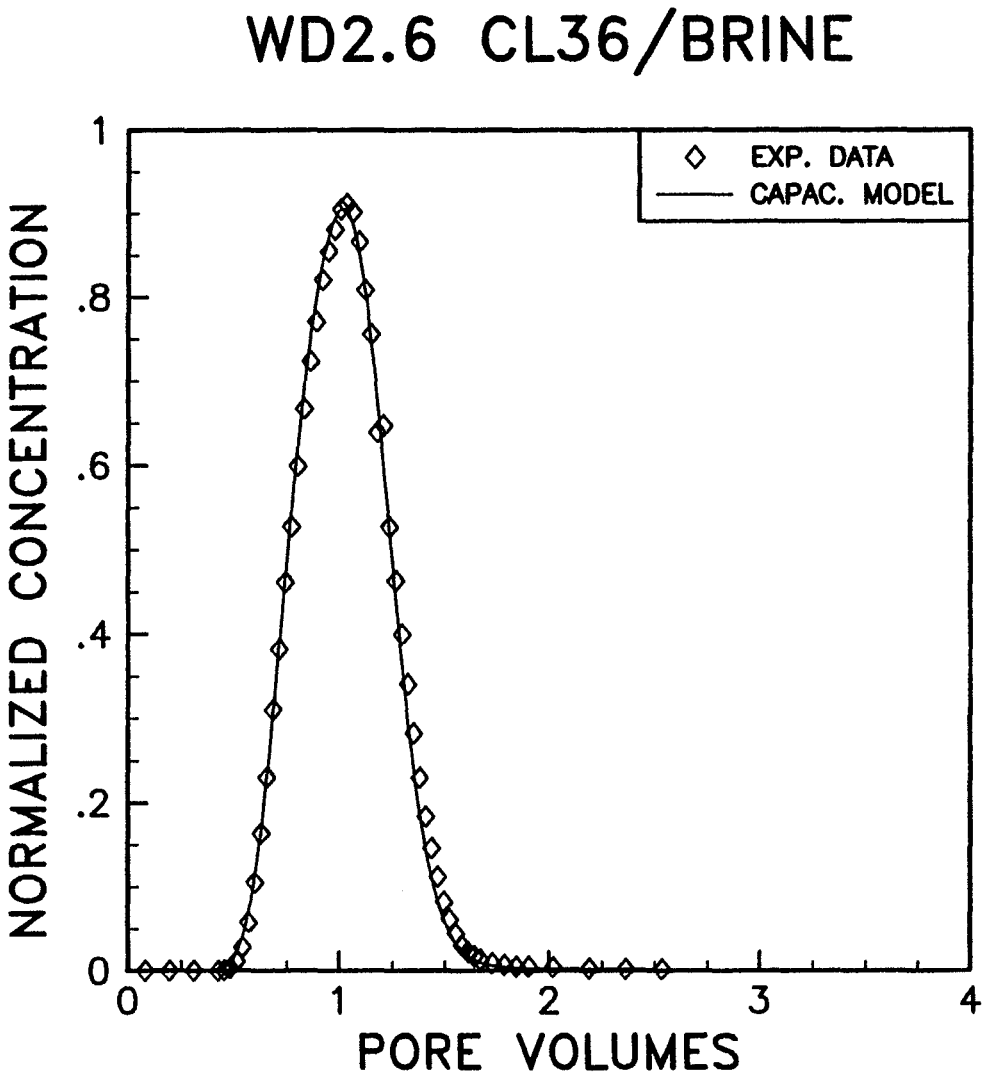

Figure 7-28 Tracer concentration versus pore volumes for treated core. Water saturation of 73%, water fractional flow of 0.876, chlorine-36.

S1= .730	S2= .270	F1= .97	F2=1.00
AREA=25.95	L=60.85	POR= .204	
ALPHA1= 1.60	ALPHA2= 0.00	M1= .10E-04	M2= .00E+00
FF1=1.000	FF2=0.000	QT= .999	PART1= 0.00
NB= 50	NP=5000	PVINJ= 4.00	PVS= .209

C_i^o = 1084 dpm/ml

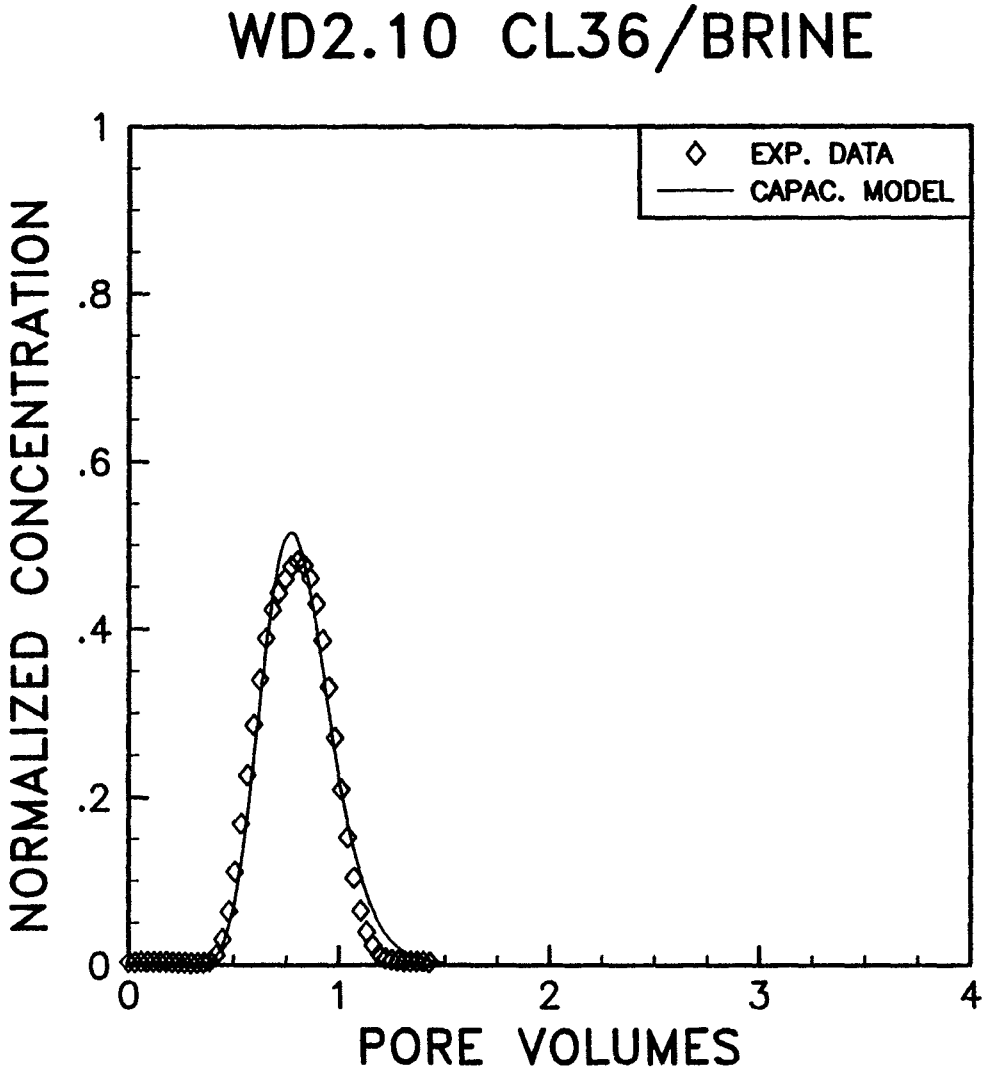

Figure 7-29 Tracer concentration versus pore volumes for treated core. Water saturation of 73%, water fractional flow of 1.0, chlorine-36.

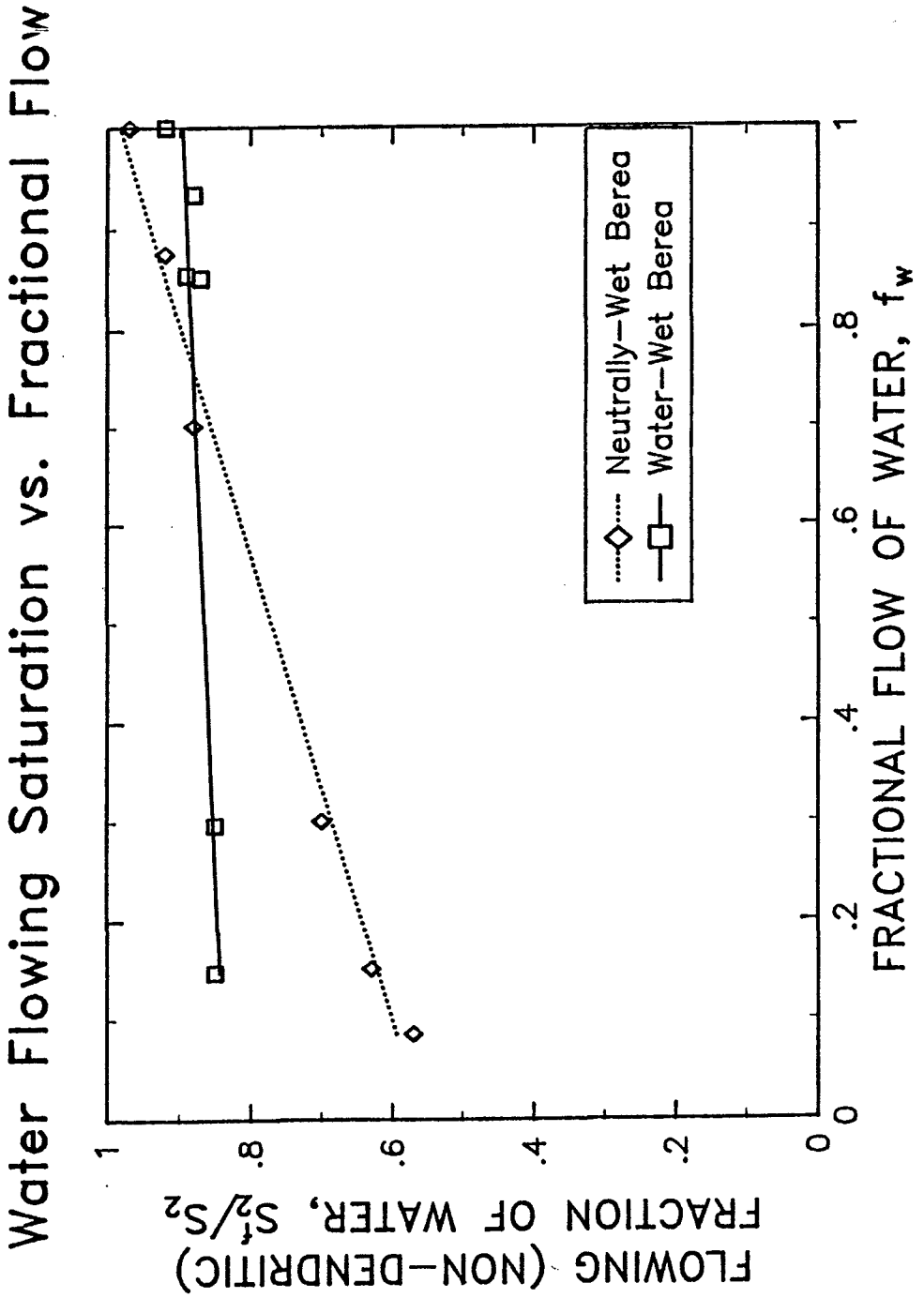

Figure 7-30 Comparison of flowing fraction of water versus water fractional flow for neutrally-wet and water-wet Berea cores.

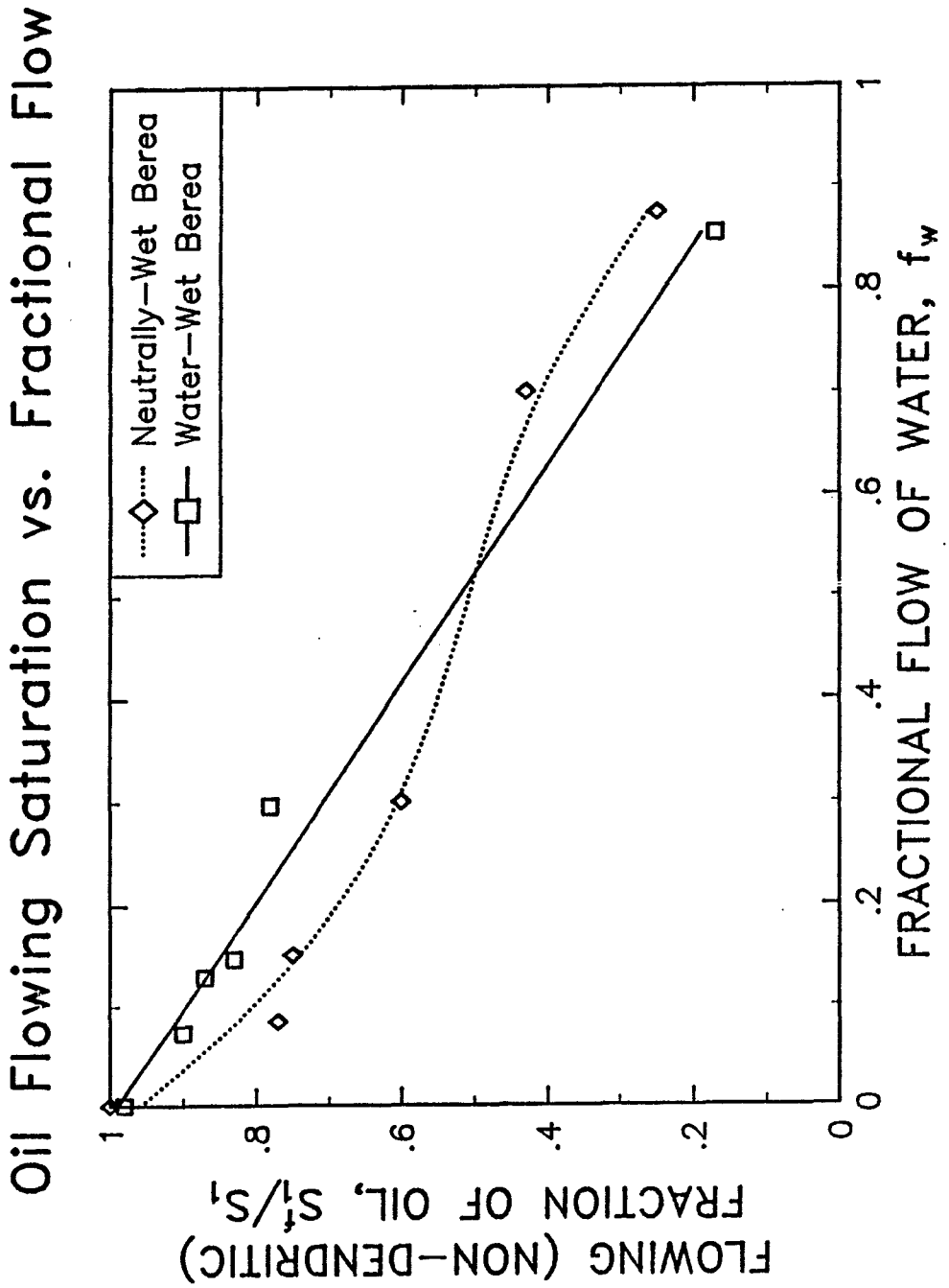

Figure 7-31 Comparison of flowing fraction of oil versus water fractional flow for neutrally-wet and water-wet Berea cores.

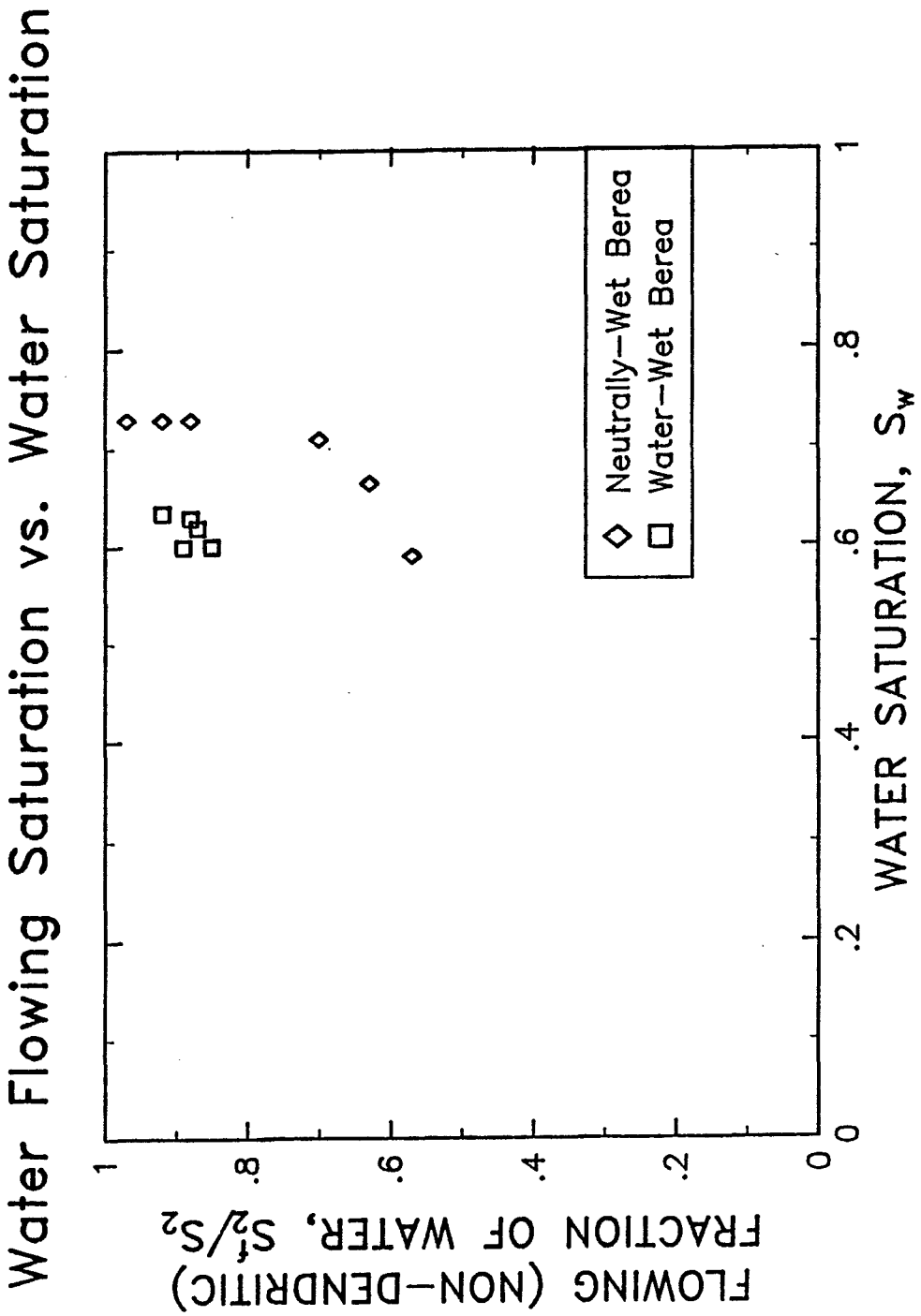

Figure 7-32 Comparison of flowing fraction of water versus water saturation for neutrally-wet and water-wet Berea cores.

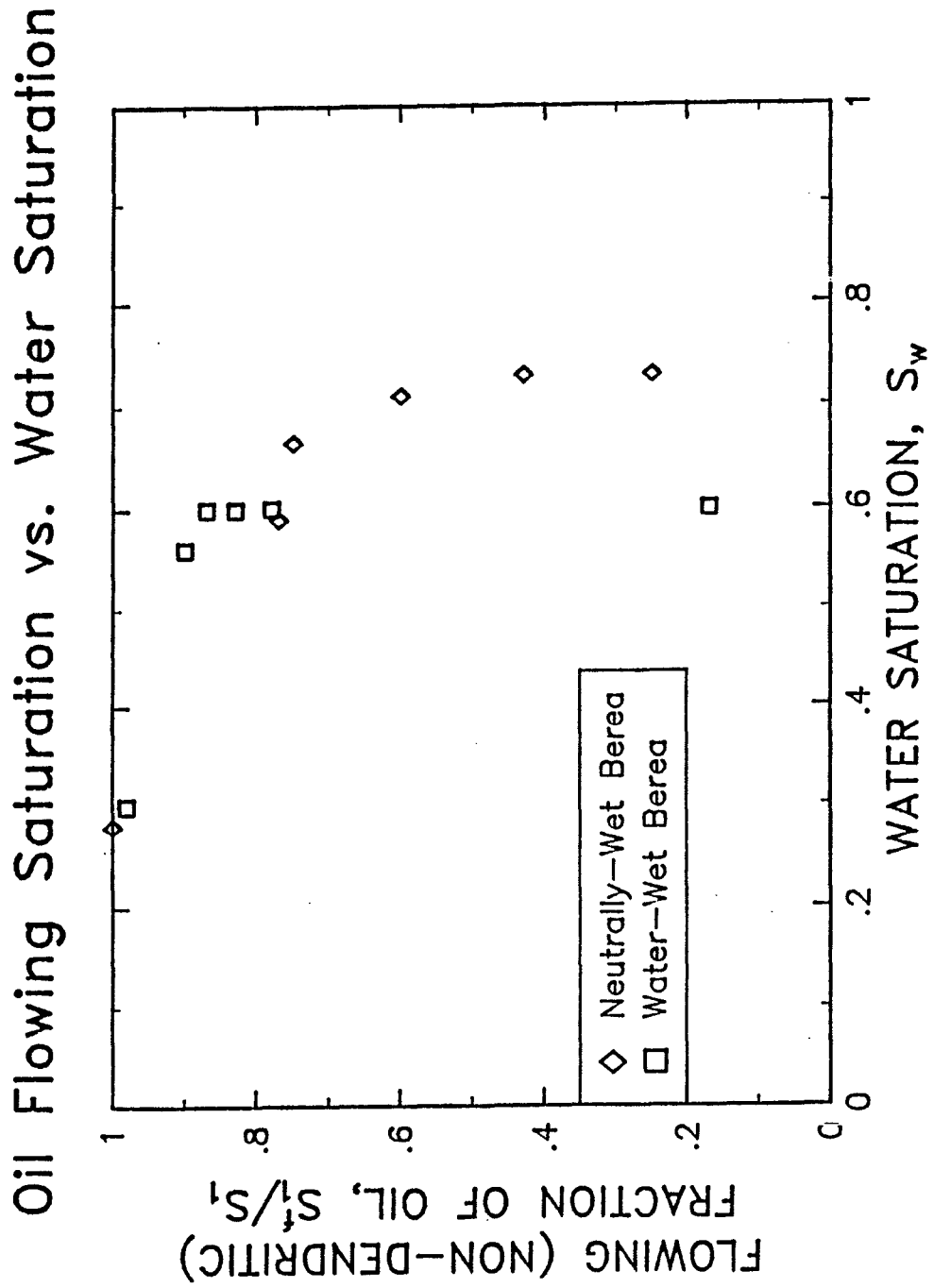

Figure 7-33 Comparison of flowing fraction of oil versus water saturation for neutrally-wet and water-wet Berea cores.

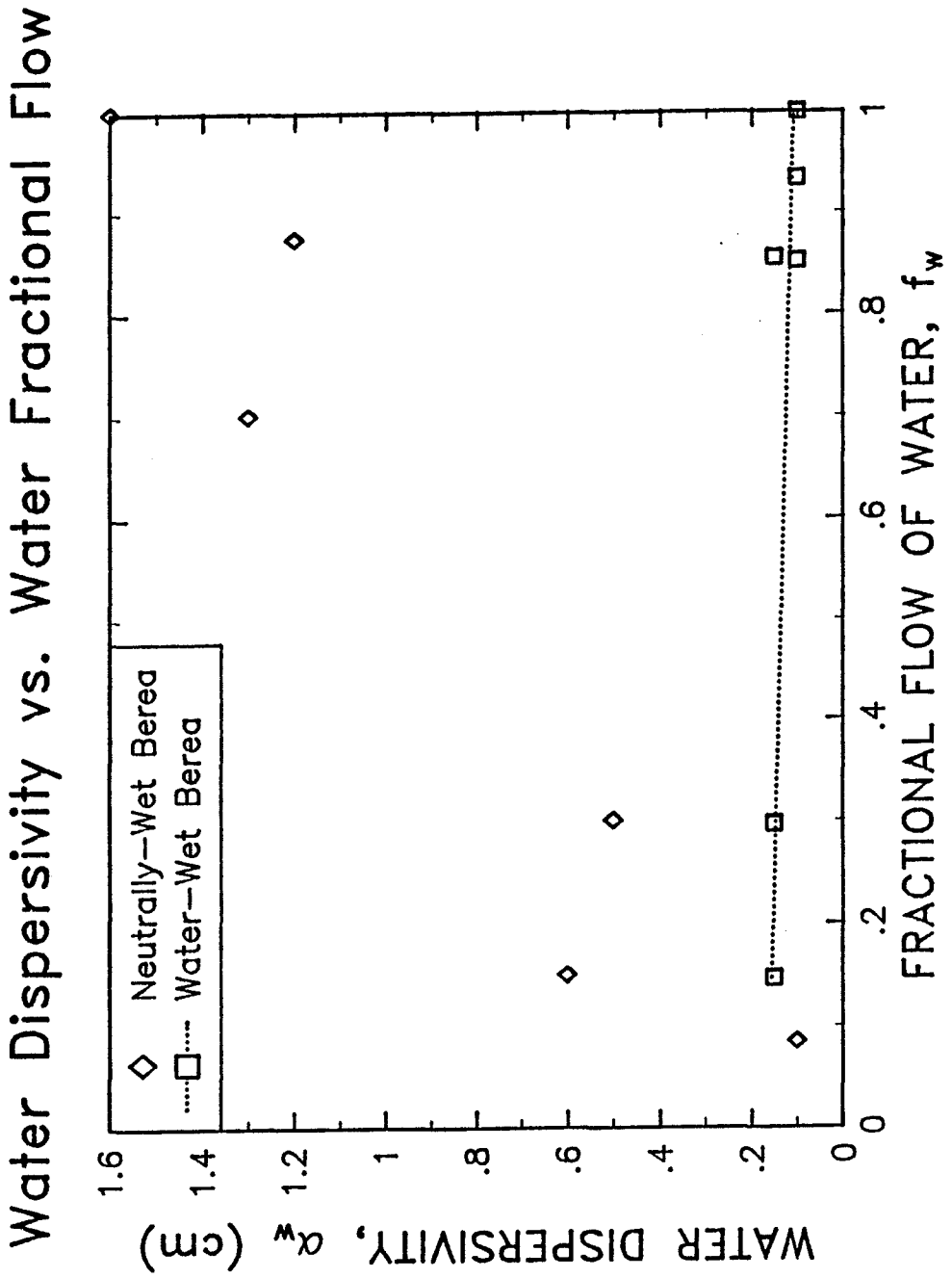

Figure 7-34 Comparison of water dispersivity versus water fractional flow for neutrally-wet and water-wet Berea cores.

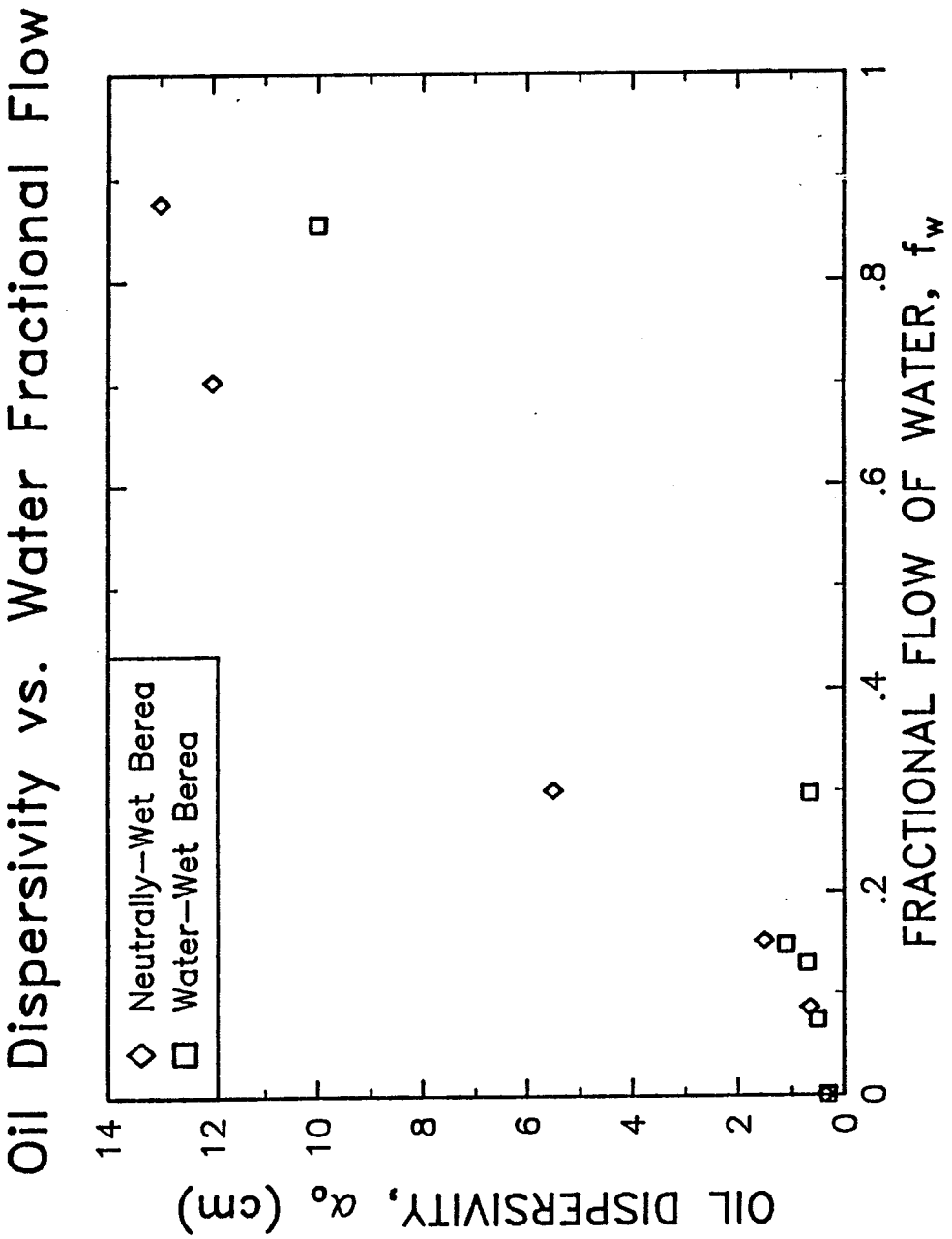

Figure 7-35 Comparison of oil dispersivity versus water fractional flow for neutrally-wet and water-wet Berea cores.

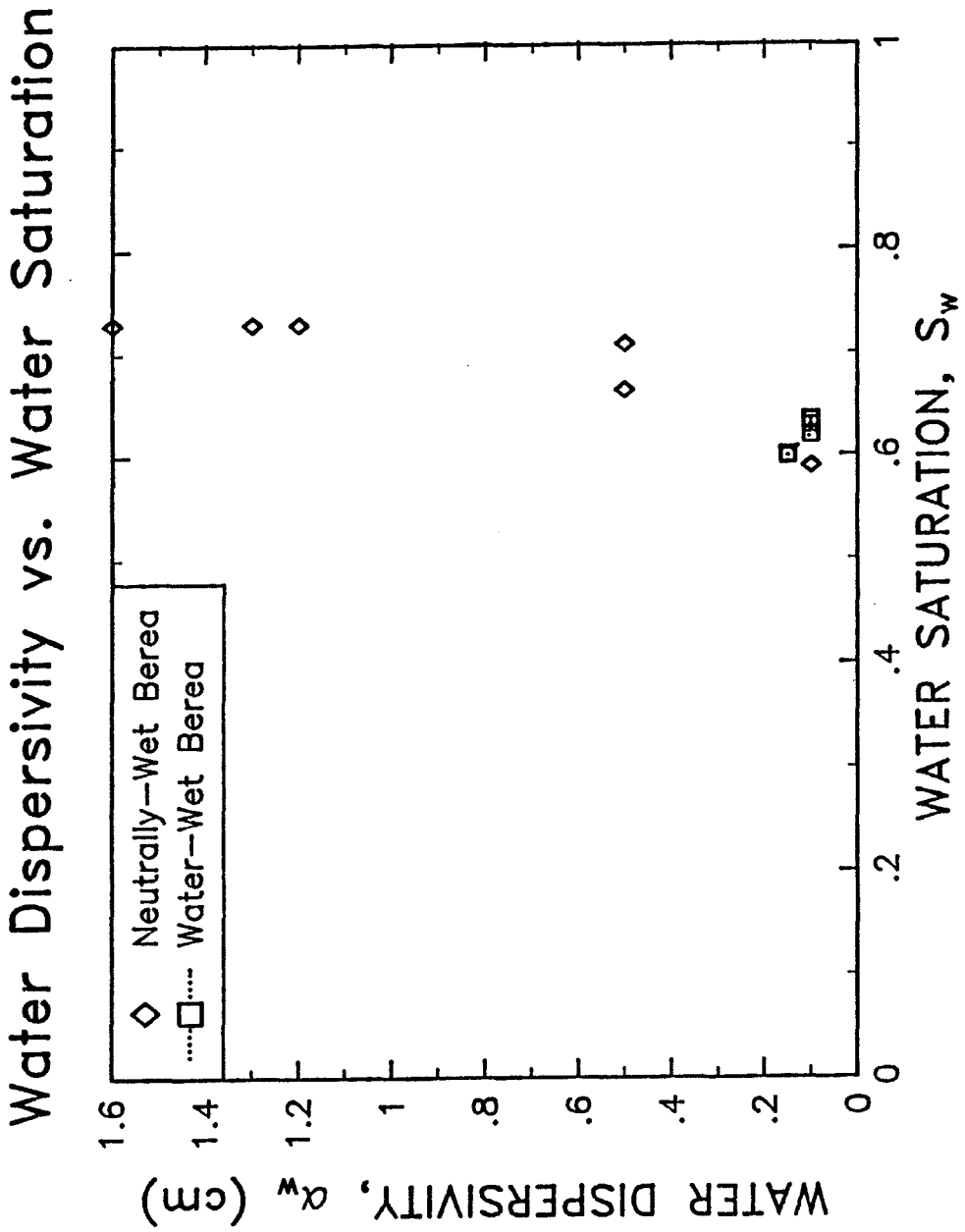

Figure 7-36 Comparison of water dispersivity versus water saturation for neutrally-wet and water-wet Berea cores.

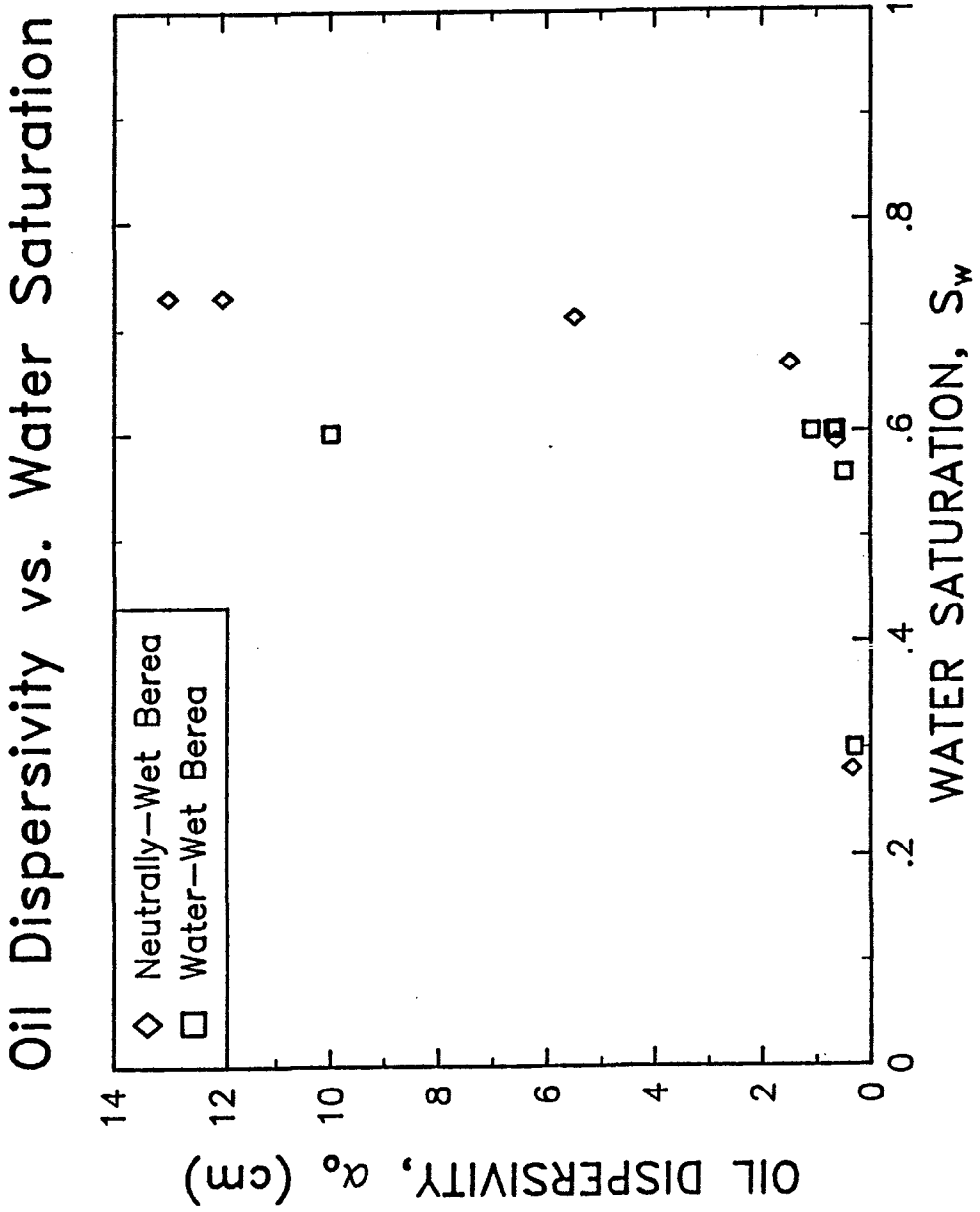

Figure 7-37 Comparison of oil dispersivity versus water saturation for neutrally-wet and water-wet Berea cores.

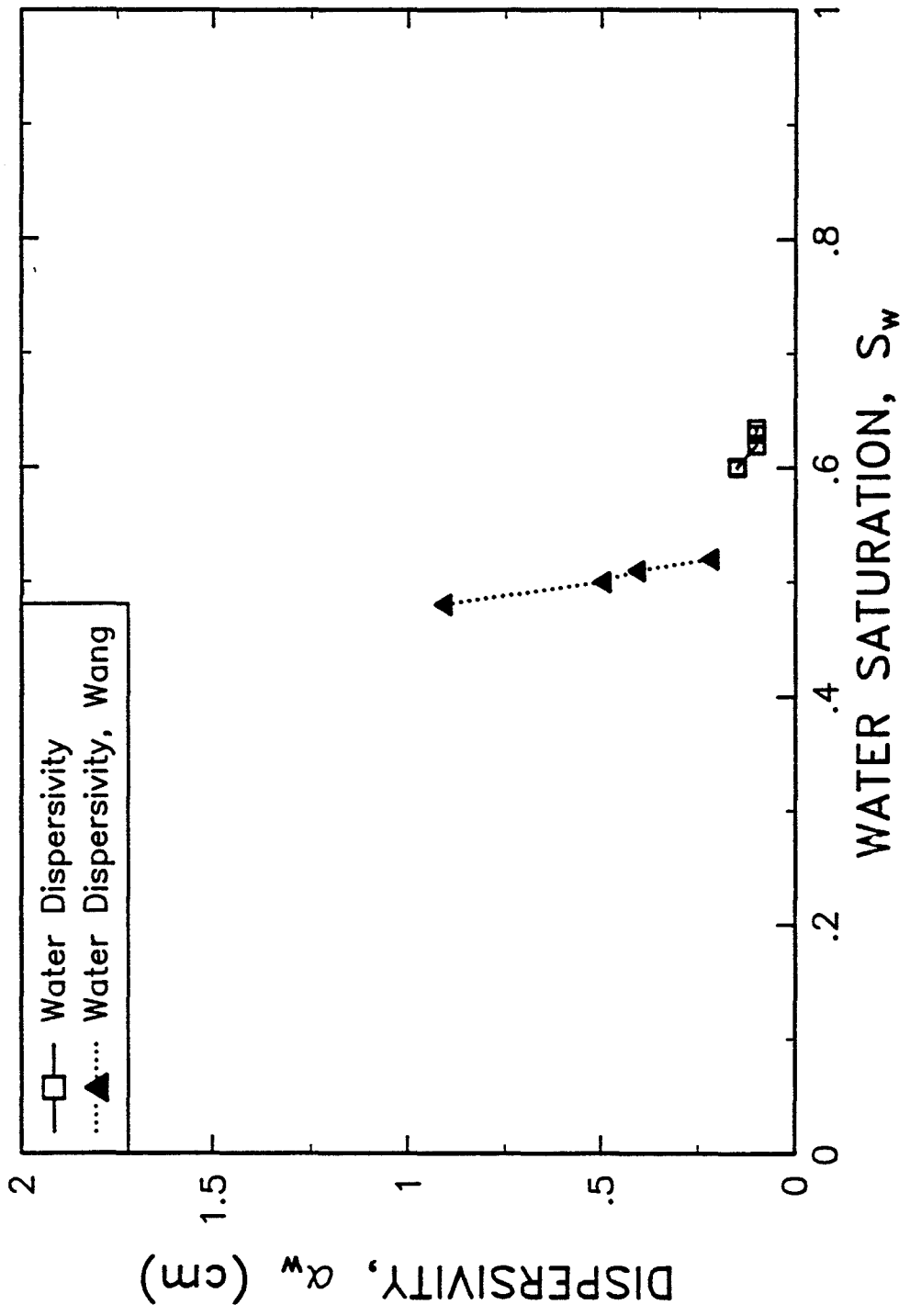

Figure 7-38A Comparison of water dispersivity data for water-wet cores with Wang (1986).

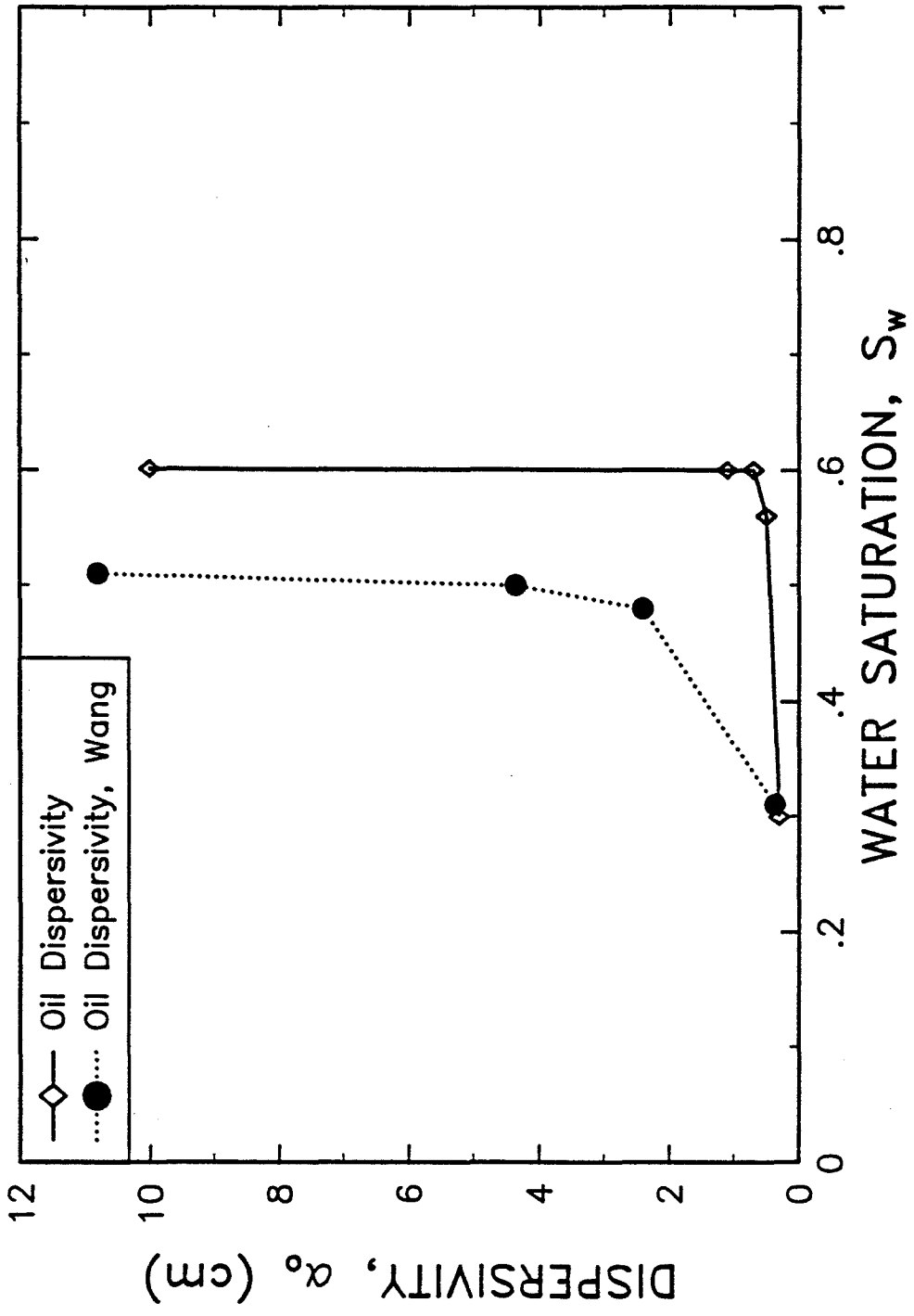

Figure 7-38B Comparison of oil dispersivity data for water-wet cores with Wang (1986).

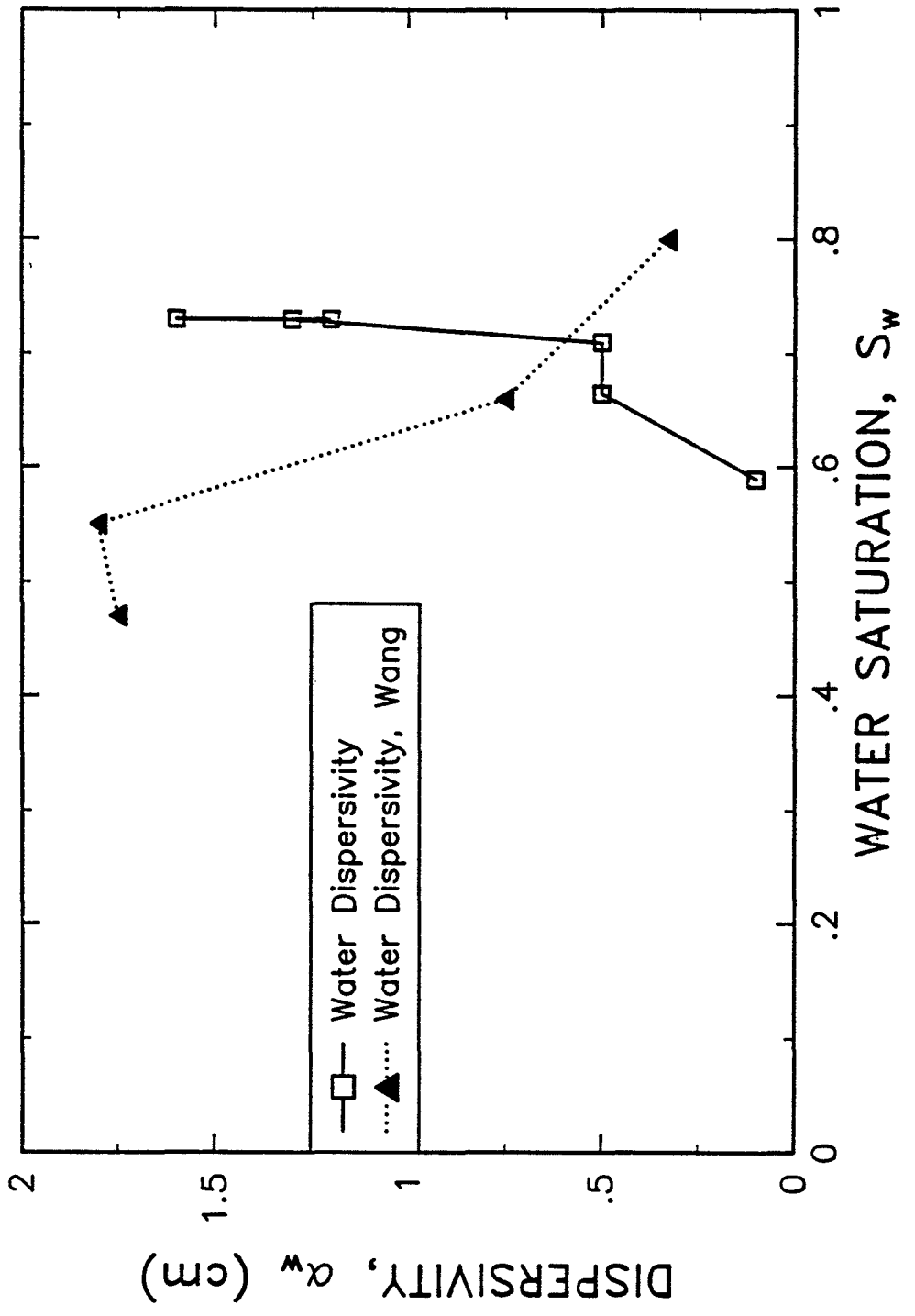

Figure 7-39A Comparison of water dispersivity data for neutrally-wet cores with Wang (1986).

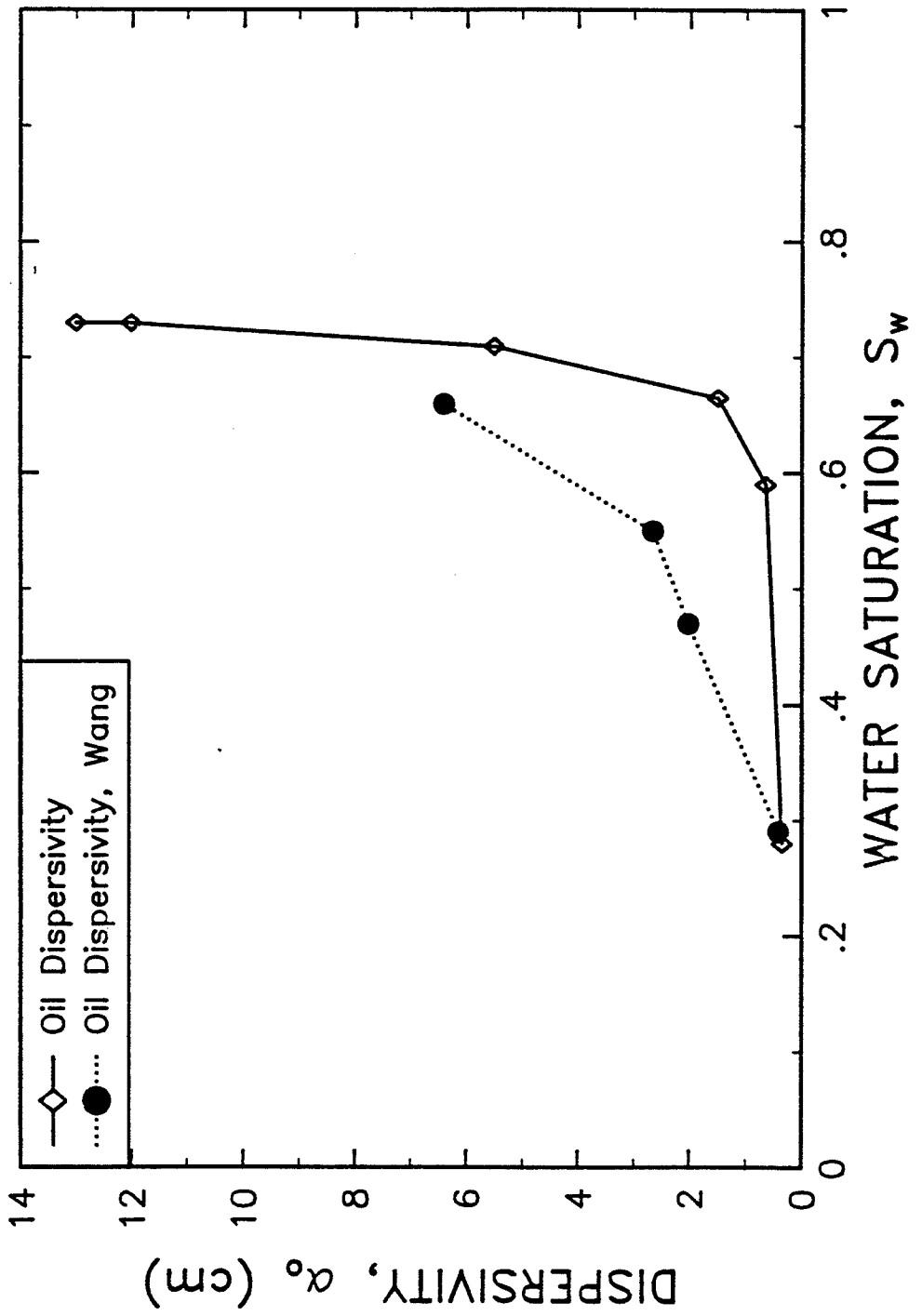

Figure 7-39B Comparison of oil dispersivity data for neutrally-wet cores with Wang (1986).

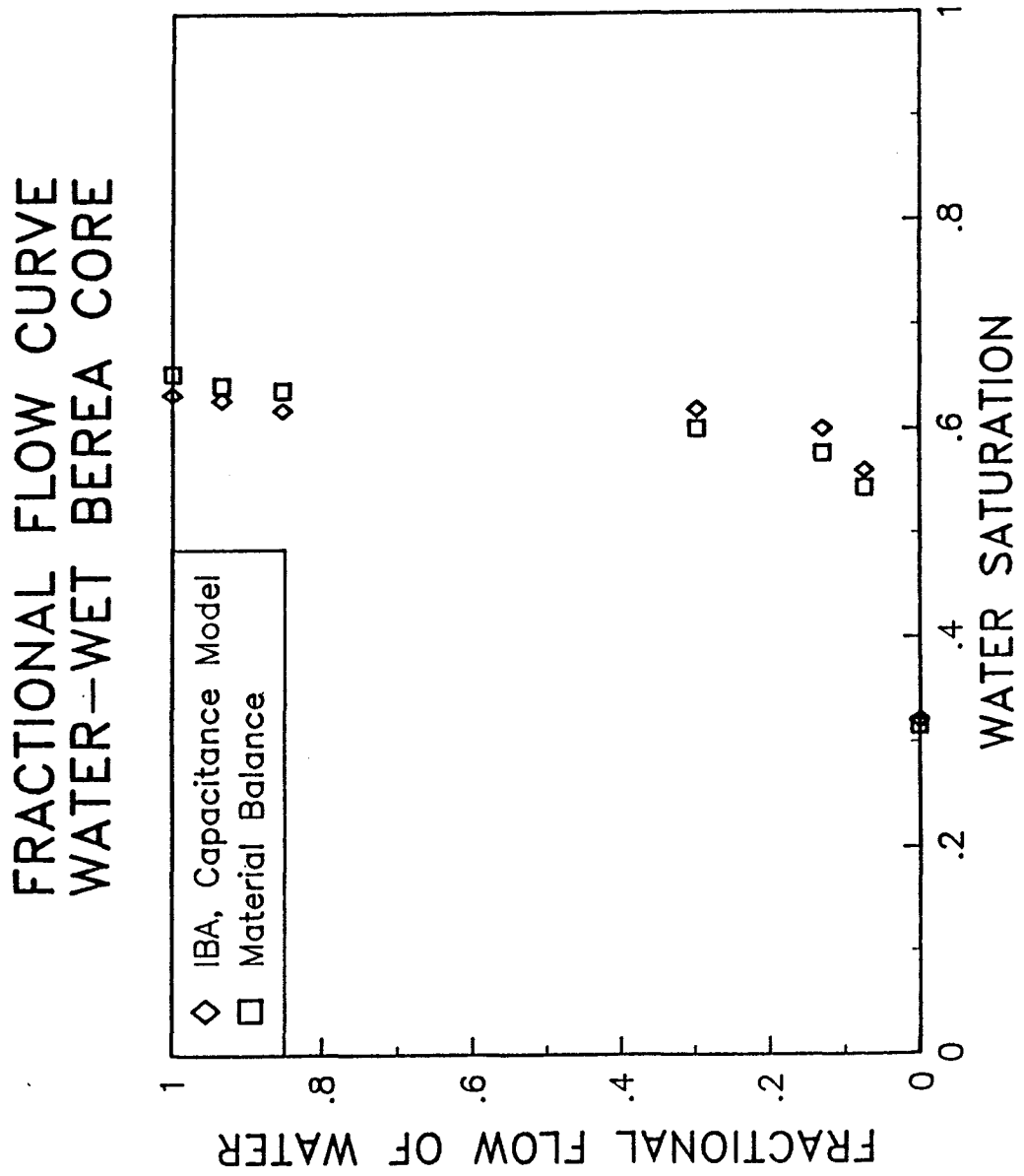

Figure 7-40 Water fractional flow curve for water-wet Berea core. Comparison of partitioning tracer (IBA) and material balance.

S1= .680	S2= .320	F1= .96	F2=1.00
AREA=24.90	L=60.75	POR= .217	
ALPHA1= .20	ALPHA2= 0.00	M1= .60E-02	M2= .00E+00
FF1=1.000	FF2=0.000	QT= 5.060	PART1= 4.80
NB= 100	NP=7000	PVINJ= 4.00	PVS= .200

C_i^o = 4622 ppm

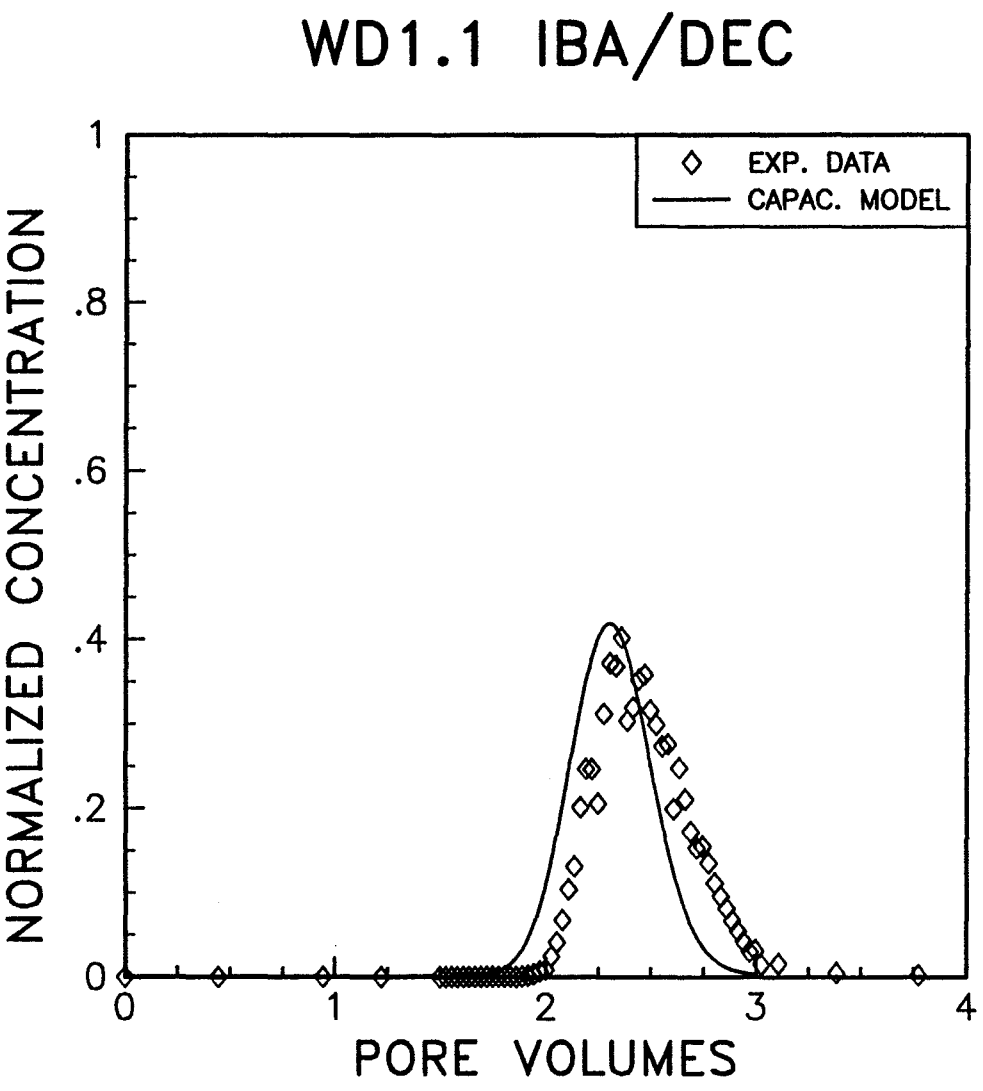

Figure 7-41 Tracer concentration versus pore volumes for water-wet Berea. Water saturation of 32%, water fractional flow of 0.0, IBA in decane.

S1= .680	S2= .320	F1= .98	F2=1.00
AREA=24.90	L=60.75	POR= .217	
ALPHA1= .15	ALPHA2= 0.00	M1= .60E−02	M2= .00E+00
FF1=1.000	FF2=0.000	QT= 1.014	PART1= 4.80
NB= 100	NP=7000	PVINJ= 4.00	PVS= .200

C_i^o = 3079 ppm

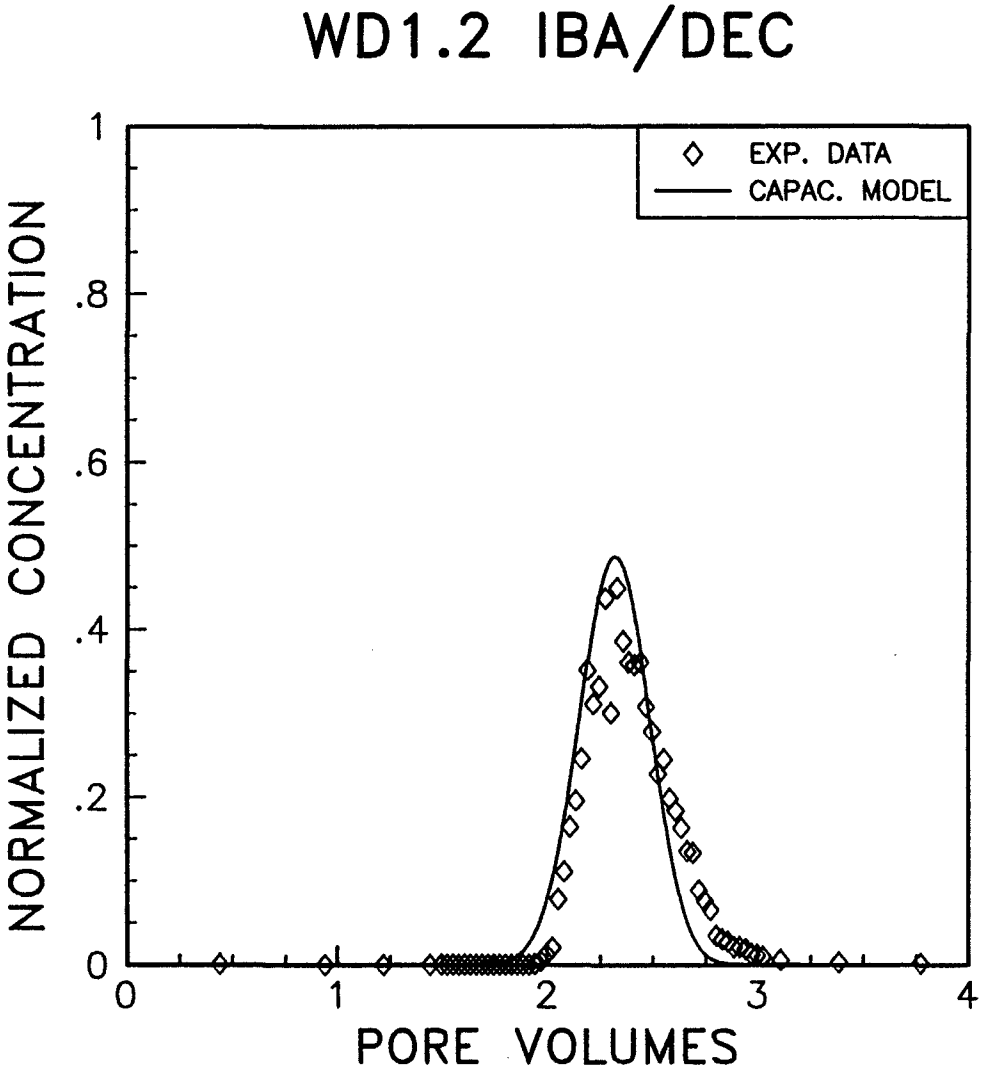

Figure 7-42 Tracer concentration versus pore volumes for water-wet Berea. Water saturation of 32%, water fractional flow of 0.0, IBA in decane.

S1= .440	S2= .560	F1=1.00	F2=1.00
AREA=24.90	L=60.75	POR= .217	
ALPHA1= .10	ALPHA2= .10	M1= .00E+00	M2= .00E+00
FF1= .927	FF2= .073	QT= 1.029	PART1= 4.80
NB= 50	NP=5000	PVINJ= 4.00	PVS= .201

C_i^o = 2882 ppm

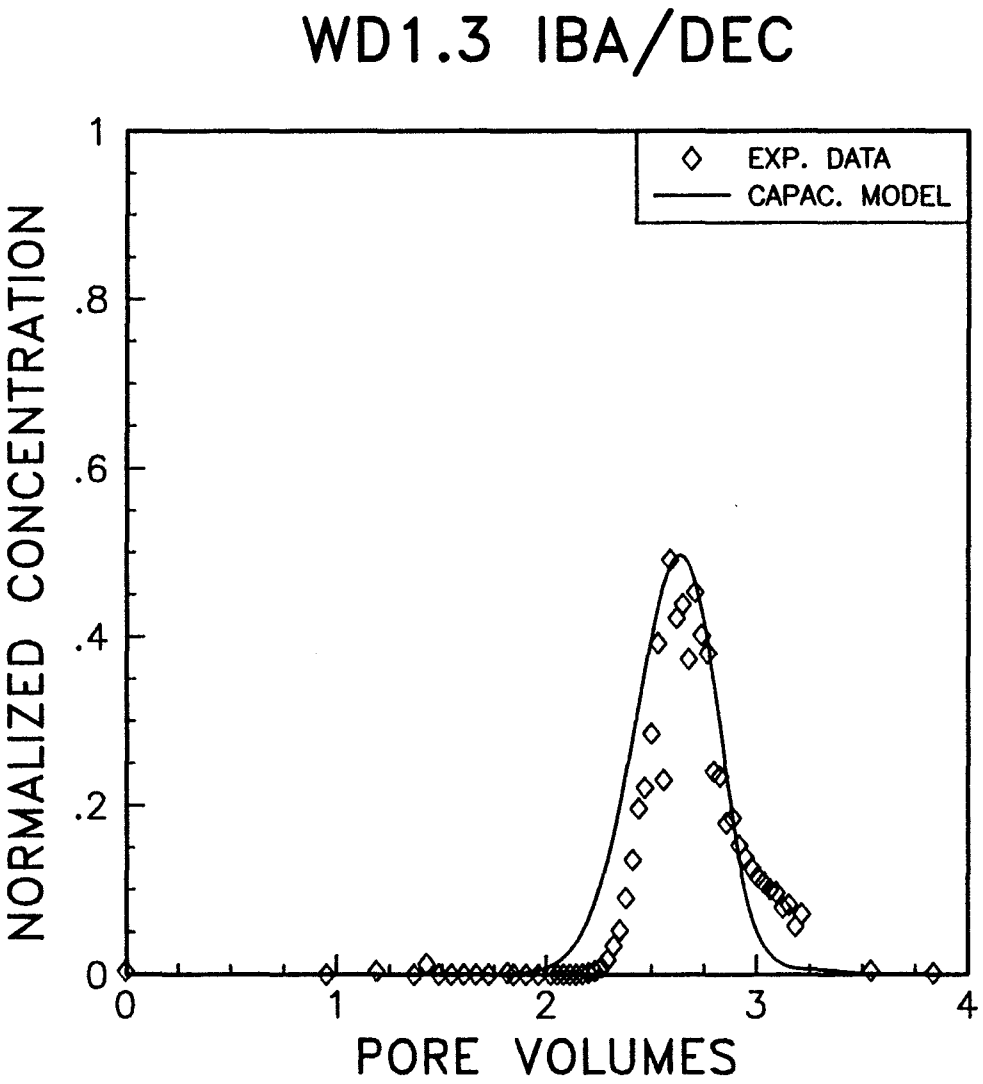

Figure 7-43 Tracer concentration versus pore volumes for water-wet Berea. Water saturation of 56%, water fractional flow of 0.073, IBA in decane.

S1= .560	S2= .440	F1=1.00	F2=1.00
AREA=24.90	L=60.75	POR= .217	
ALPHA1= .10	ALPHA2= .10	M1= .00E+00	M2= .00E+00
FF1= .073	FF2= .927	QT= 1.029	PART1= .21
NB= 50	NP=5000	PVINJ= 4.00	PVS= .201

C_i^o = 10661 ppm

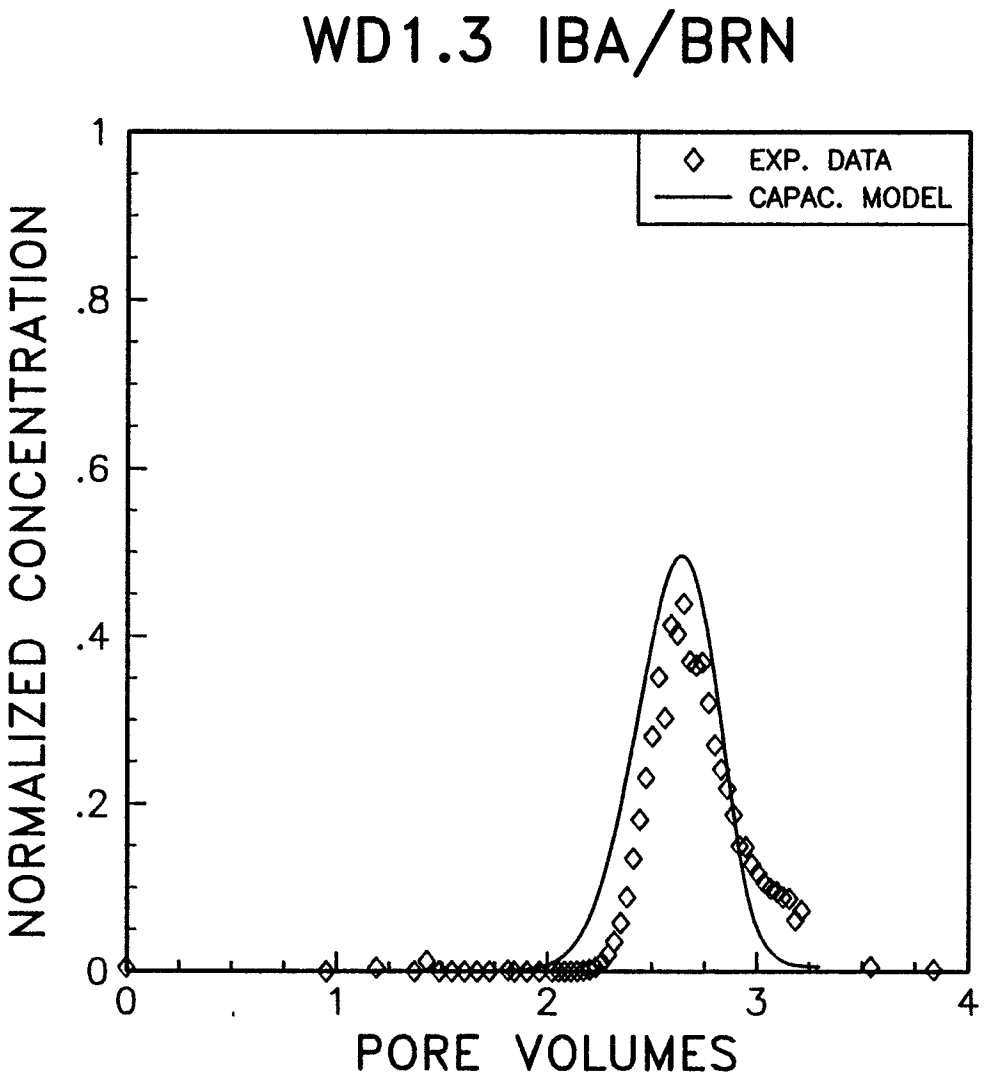

Figure 7-44 Tracer concentration versus pore volumes for water-wet Berea. Water saturation of 56%, water fractional flow of 0.073, IBA in brine.

S1= .400	S2= .600	F1=1.00	F2=1.00
AREA=24.90	L=60.75	POR= .217	
ALPHA1= .15	ALPHA2= .15	M1= .00E+00	M2= .00E+00
FF1= .871	FF2= .129	QT= 1.021	PART1= 4.80
NB= 50	NP=5000	PVINJ= 4.00	PVS= .200

C_i^o = 4796 ppm

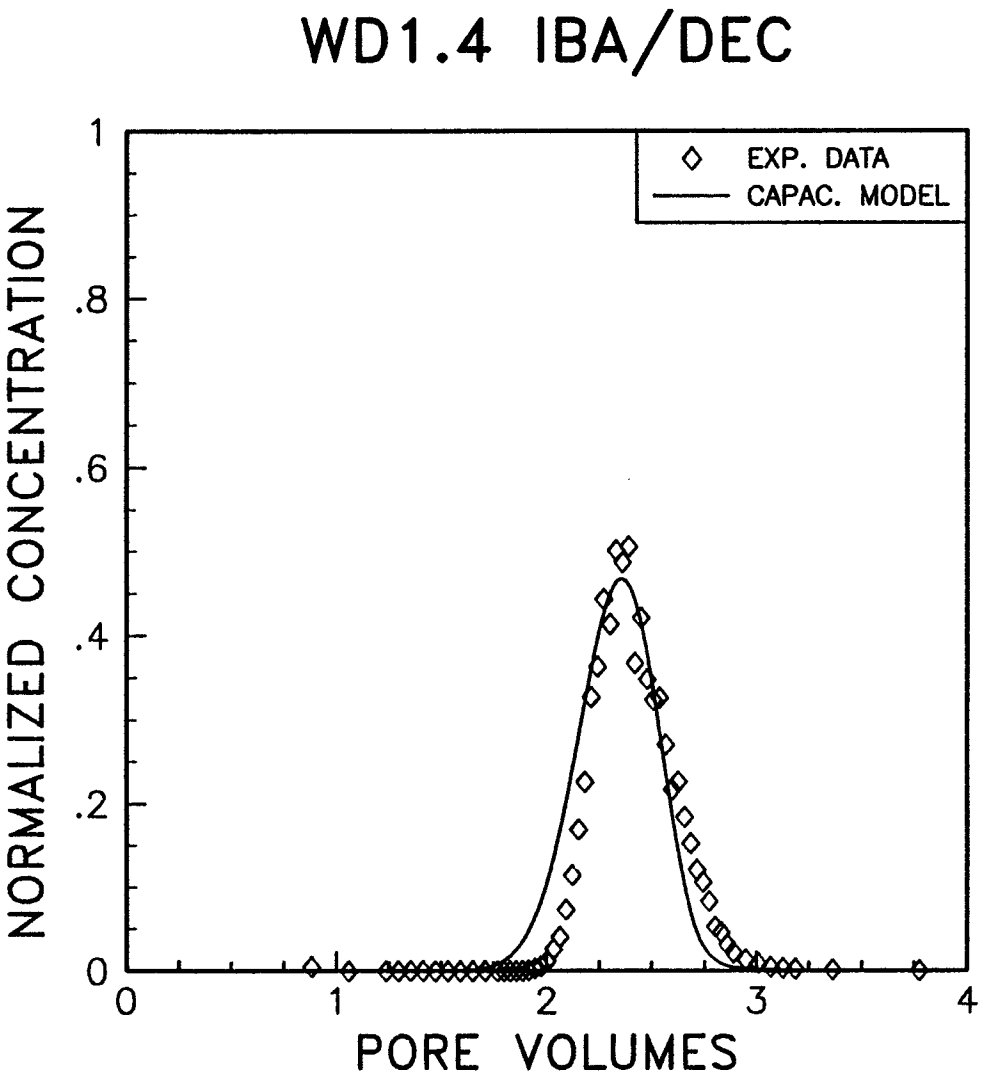

Figure 7-45 Tracer concentration versus pore volumes for water-wet Berea. Water saturation of 60%, water fractional flow of 0.129, IBA in decane.

S1= .600	S2= .400	F1=1.00	F2=1.00
AREA=24.90	L=60.75	POR= .217	
ALPHA1= .15	ALPHA2= .15	M1= .00E+00	M2= .00E+00
FF1= .129	FF2= .871	QT= 1.021	PART1= .21
NB= 50	NP=5000	PVINJ= 4.00	PVS= .200

C_i^o = 10563 ppm

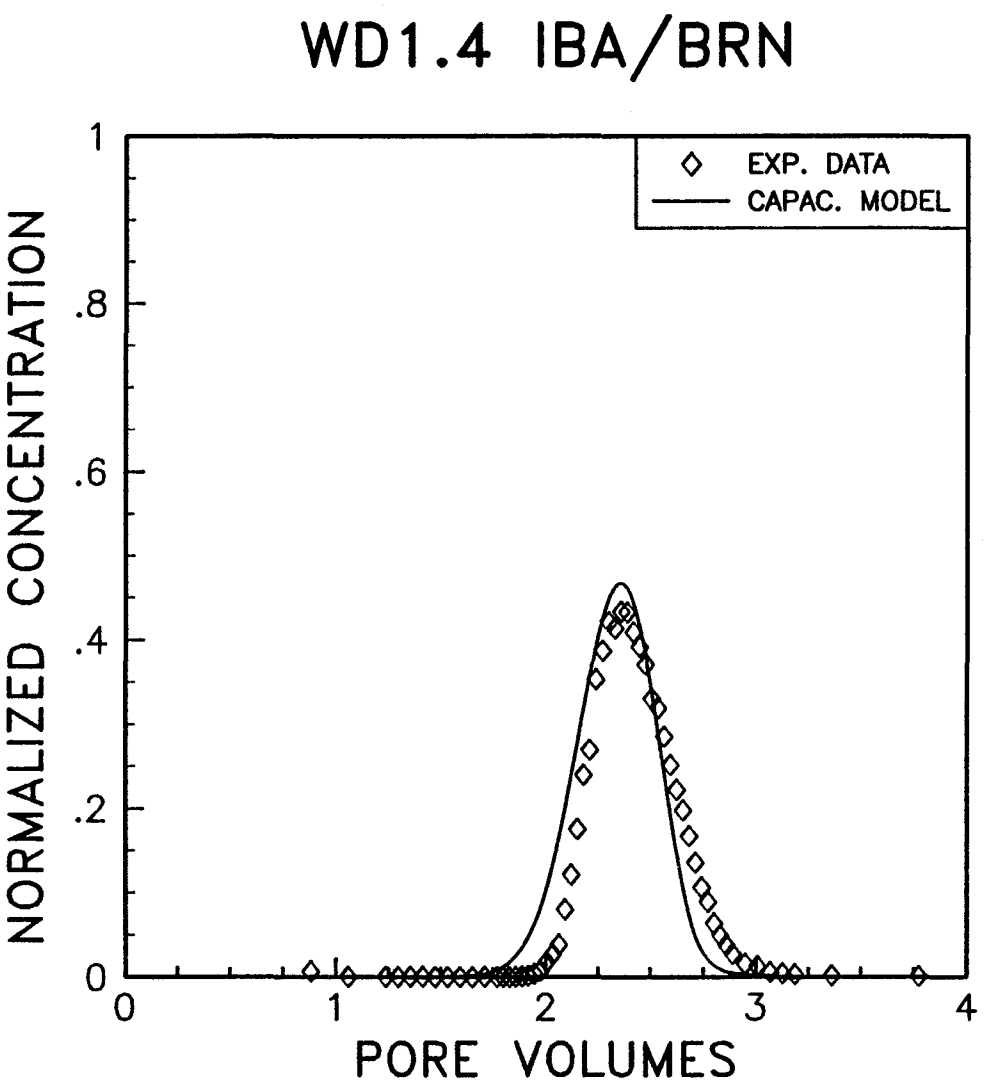

Figure 7-46 Tracer concentration versus pore volumes for water-wet Berea. Water saturation of 60%, water fractional flow of 0.129, IBA in brine.

S1= .380	S2= .620	F1=1.00	F2=1.00
AREA=24.90	L=60.75	POR= .217	
ALPHA1= .10	ALPHA2= .10	M1= .00E+00	M2= .00E+00
FF1= .703	FF2= .297	QT= 1.014	PART1= 4.80
NB= 50	NP=5000	PVINJ= 4.00	PVS= .199

C_i^o = 3641 ppm

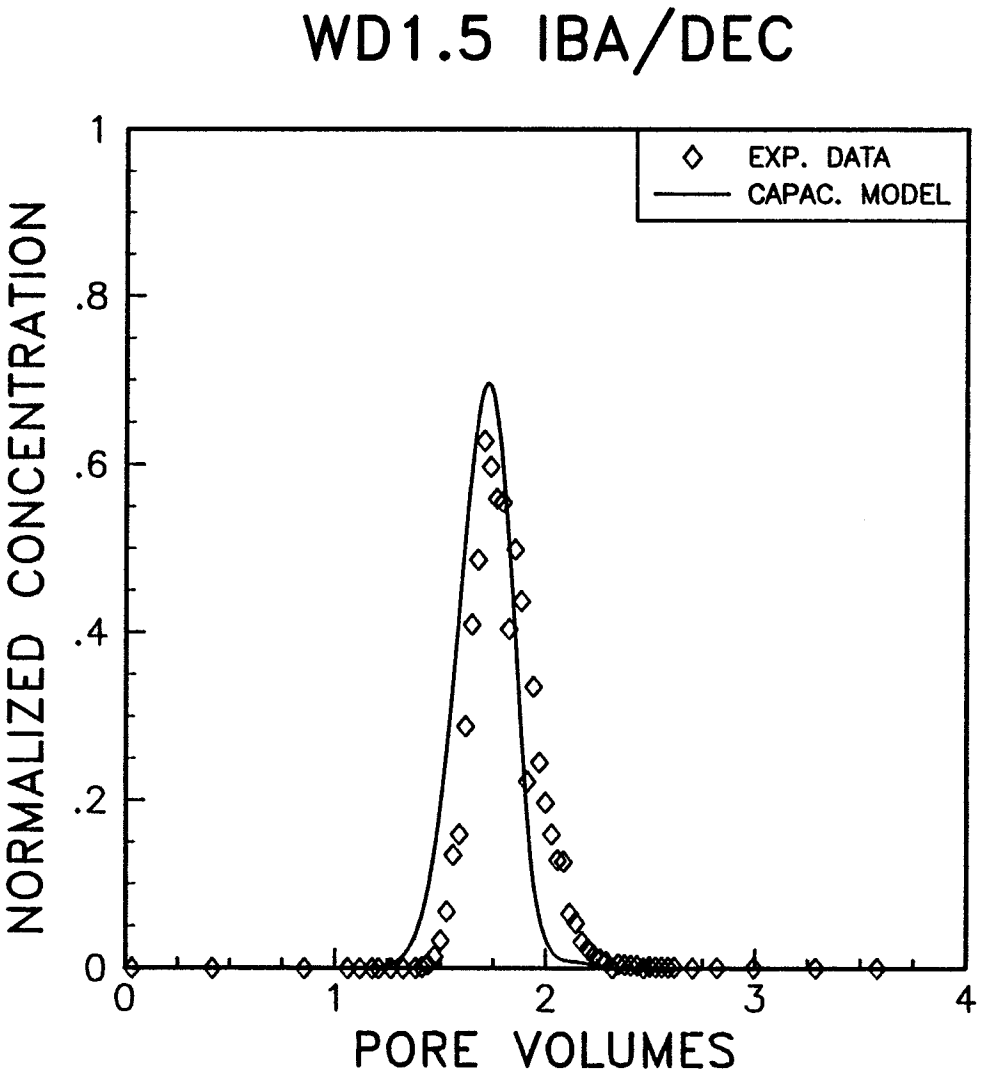

Figure 7-47 Tracer concentration versus pore volumes for water-wet Berea. Water saturation of 62%, water fractional flow of 0.297, IBA in decane.

S1= .620	S2= .380	F1=1.00	F2=1.00
AREA=24.90	L=60.75	POR= .217	
ALPHA1= .10	ALPHA2= .10	M1= .00E+00	M2= .00E+00
FF1= .297	FF2= .703	QT= 1.014	PART1= .21
NB= 50	NP=5000	PVINJ= 4.00	PVS= .199

C_i^o = 11898 ppm

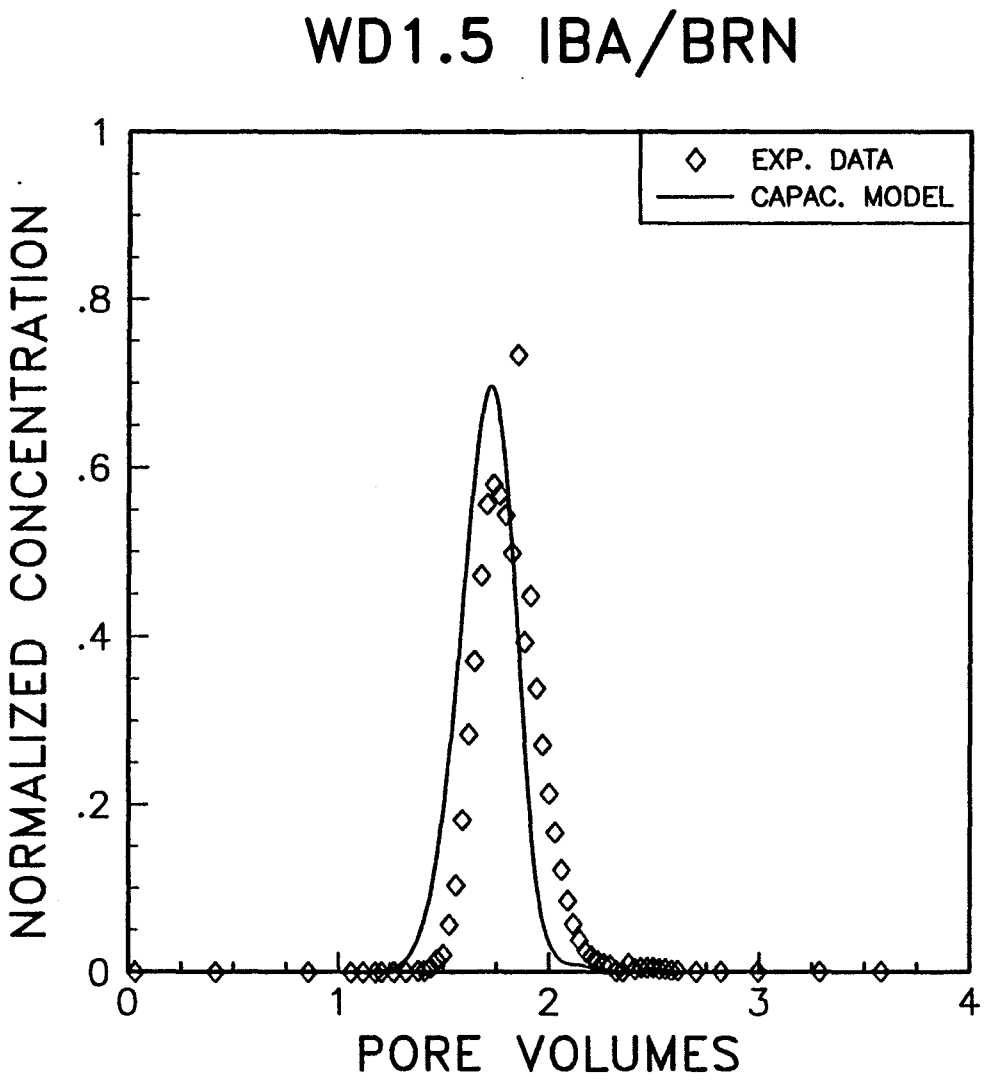

Figure 7-48 Tracer concentration versus pore volumes for water-wet Berea. Water saturation of 62%, water fractional flow of 0.297, IBA in brine.

S1= .380	S2= .620	F1= .20	F2= .90
AREA=24.90	L=60.75	POR= .217	
ALPHA1= 1.00	ALPHA2= .30	M1= .10E−02	M2= .10E−02
FF1= .148	FF2= .852	QT= .994	PART1= 4.80
NB= 100	NP=7000	PVINJ= 4.00	PVS= .210

C_i^o = 3241 ppm

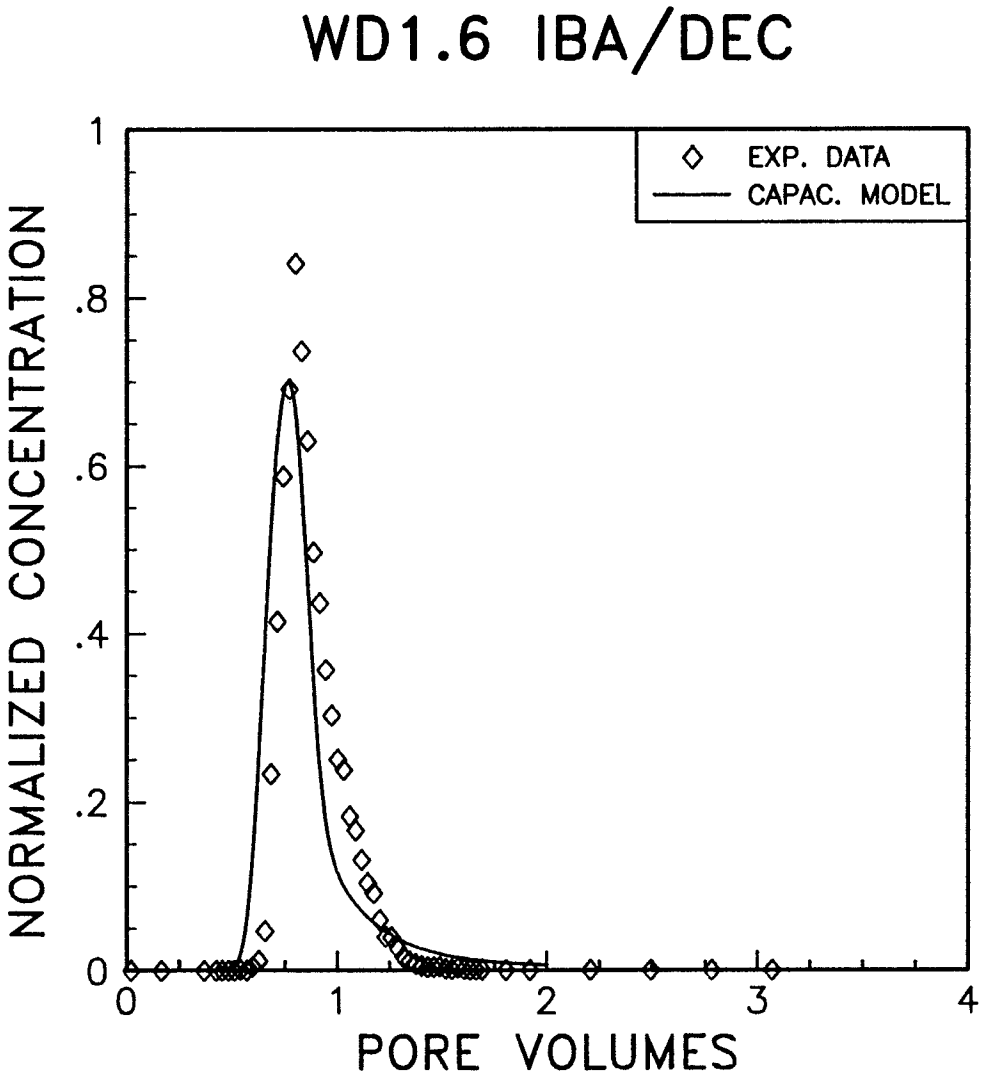

Figure 7-49 Tracer concentration versus pore volumes for water-wet Berea. Water saturation of 62%, water fractional flow of 0.852, IBA in decane.

S1= .620	S2= .380	F1= .90	F2= .20
AREA=24.90	L=60.75	POR= .217	
ALPHA1= .30	ALPHA2= 1.00	M1= .10E−02	M2= .10E−02
FF1= .852	FF2= .148	QT= .994	PART1= .21
NB= 100	NP=7000	PVINJ= 4.00	PVS= .210

C_i^o = 11686 ppm

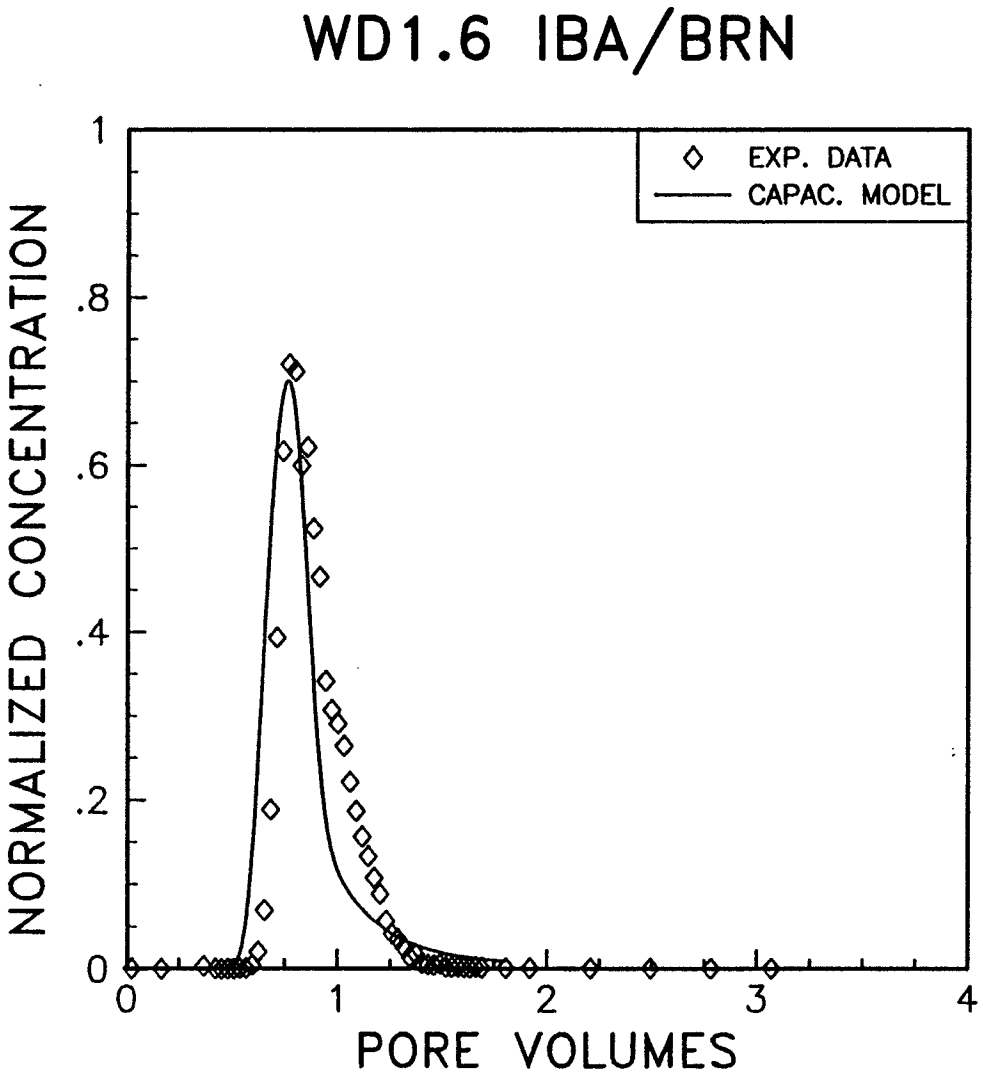

Figure 7-50 Tracer concentration versus pore volumes for water-wet Berea. Water saturation of 62%, water fractional flow of 0.852, IBA in brine.

S1= .370	S2= .630	F1= .20	F2= .88
AREA=24.90	L=60.75	POR= .217	
ALPHA1= 1.00	ALPHA2= .20	M1= .10E−02	M2= .10E−02
FF1= .066	FF2= .934	QT= .996	PART1= 4.80
NB= 100	NP=7000	PVINJ= 4.00	PVS= .199

C_i^o = 3027 ppm

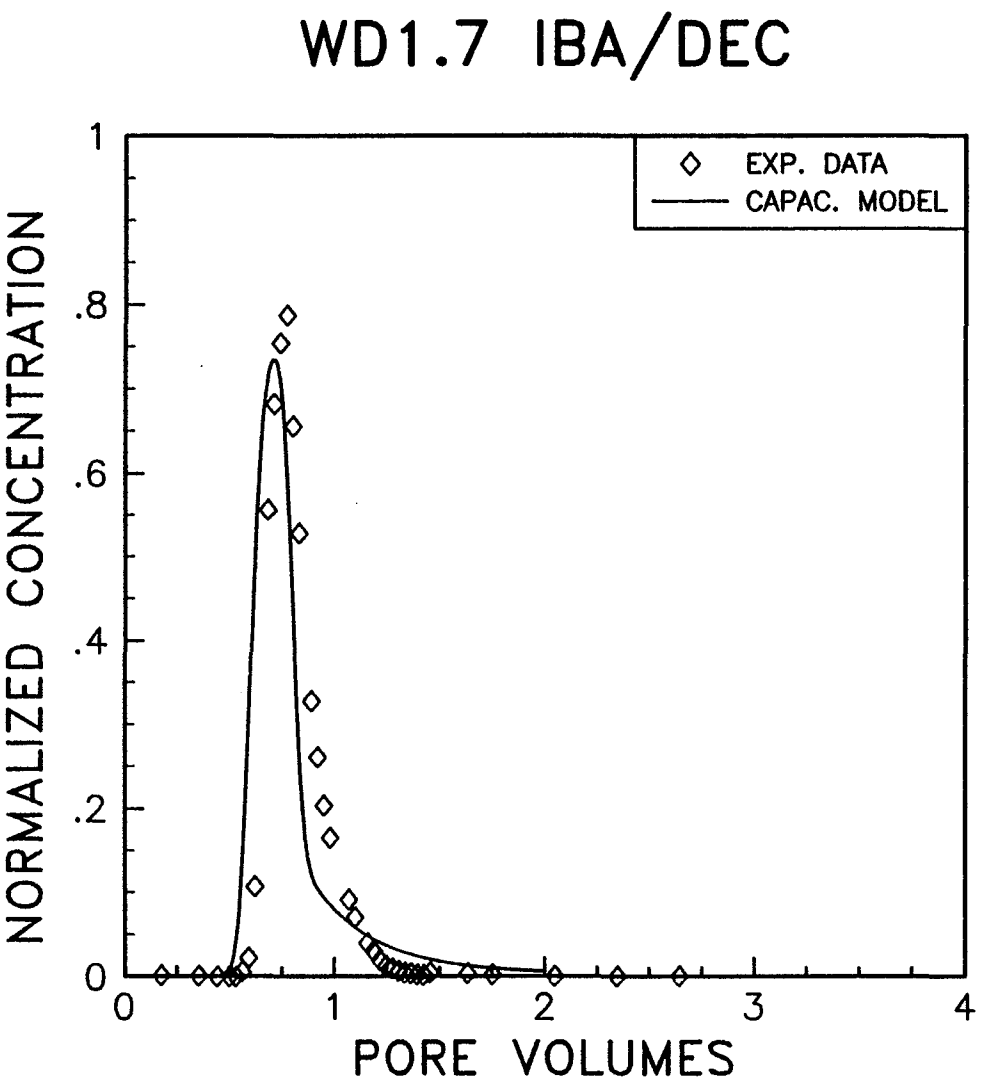

Figure 7-51 Tracer concentration versus pore volumes for water-wet Berea. Water saturation of 63%, water fractional flow of 0.934, IBA in decane.

S1= .630	S2= .370	F1= .88	F2= .20
AREA=24.90	L=60.75	POR= .217	
ALPHA1= .20	ALPHA2= 1.00	M1= .10E−02	M2= .10E−02
FF1= .934	FF2= .066	QT= .996	PART1= .21
NB= 100	NP=7000	PVINJ= 4.00	PVS= .199

C_i^o = 11826 ppm

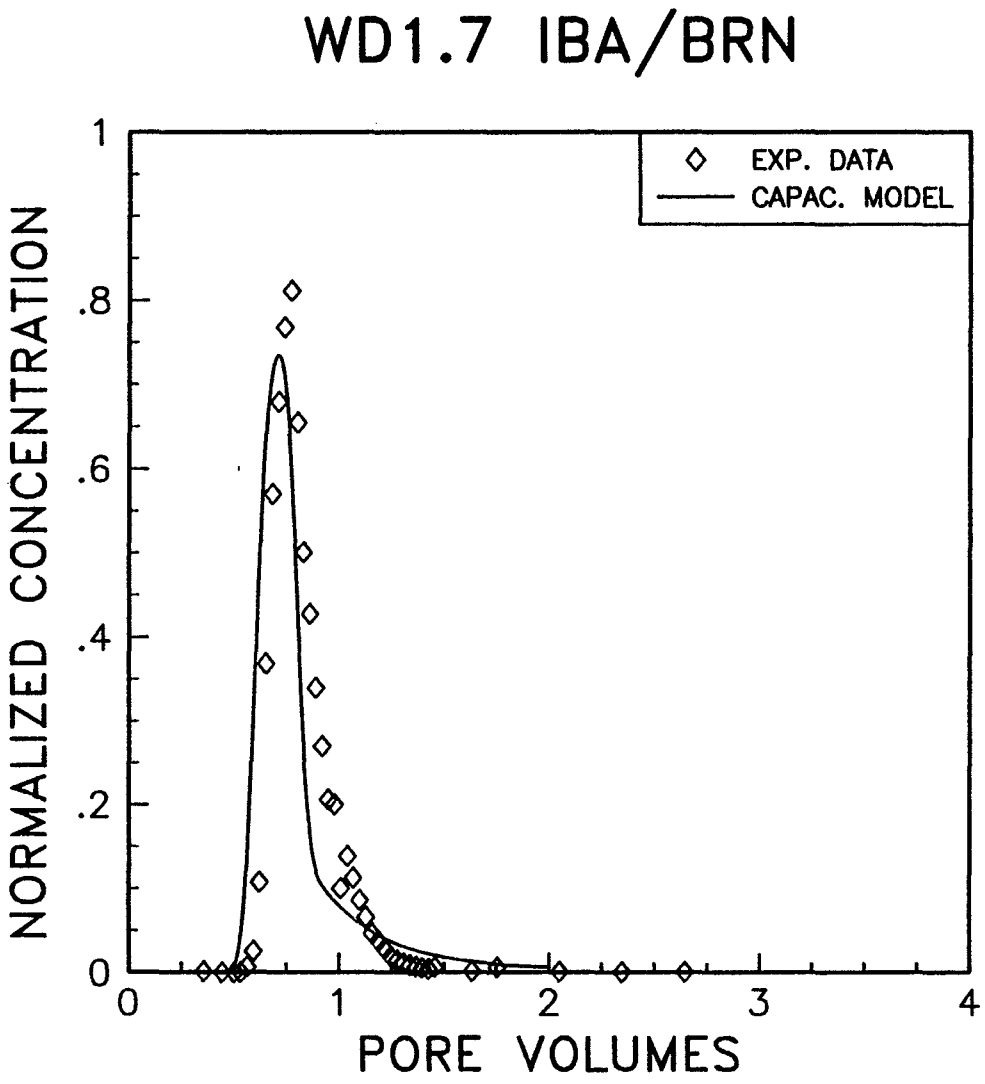

Figure 7-52 Tracer concentration versus pore volumes for water-wet Berea. Water saturation of 63%, water fractional flow of 0.934, IBA in brine.

S1= .635	S2= .365	F1= .92	F2=1.00
AREA=24.90	L=60.75	POR= .217	
ALPHA1= .10	ALPHA2= 0.00	M1= .10E-02	M2= .00E+00
FF1=1.000	FF2=0.000	QT= .997	PART1= .21
NB= 100	NP=7000	PVINJ= 4.00	PVS= .200

C_i^o = 11231 ppm

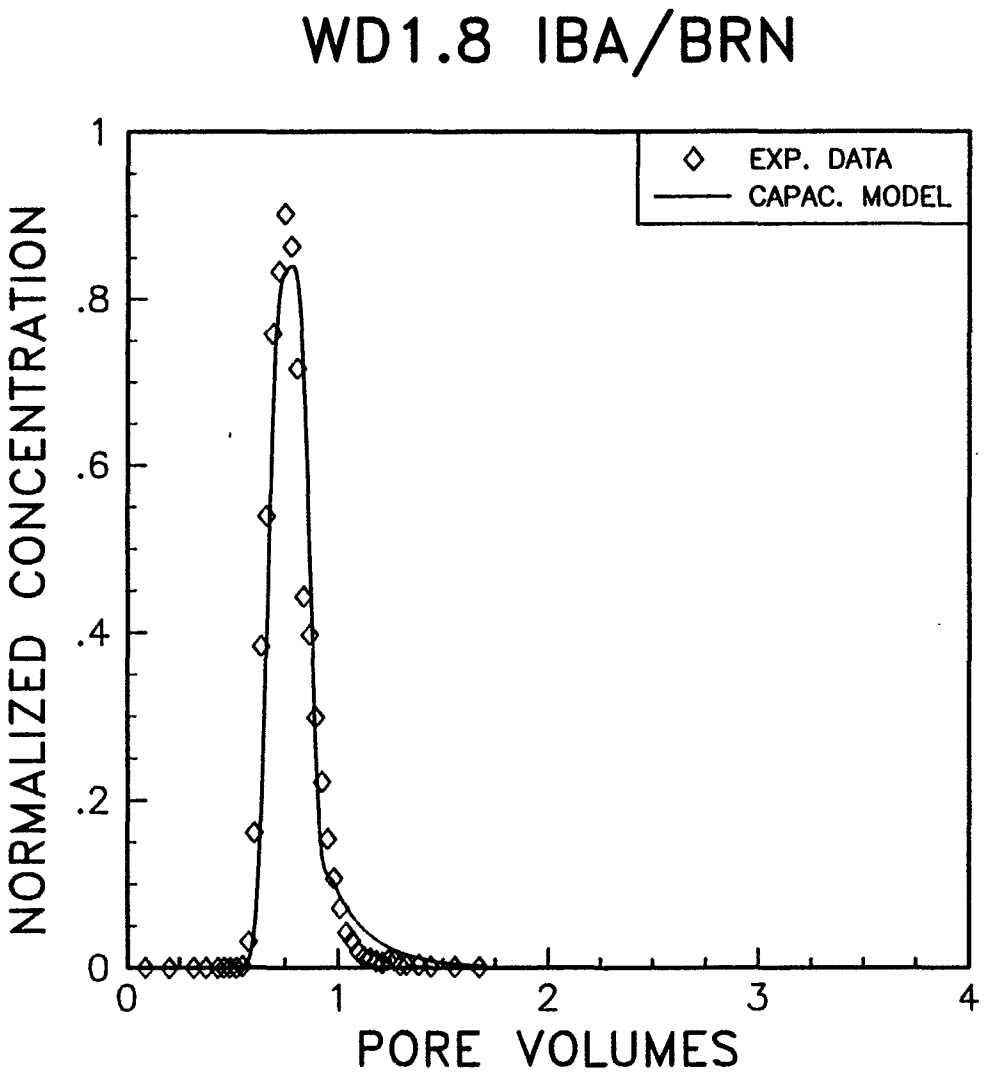

Figure 7-53 Tracer concentration versus pore volumes for water-wet Berea. Water saturation of 63.5%, water fractional flow of 1.0, IBA in brine.

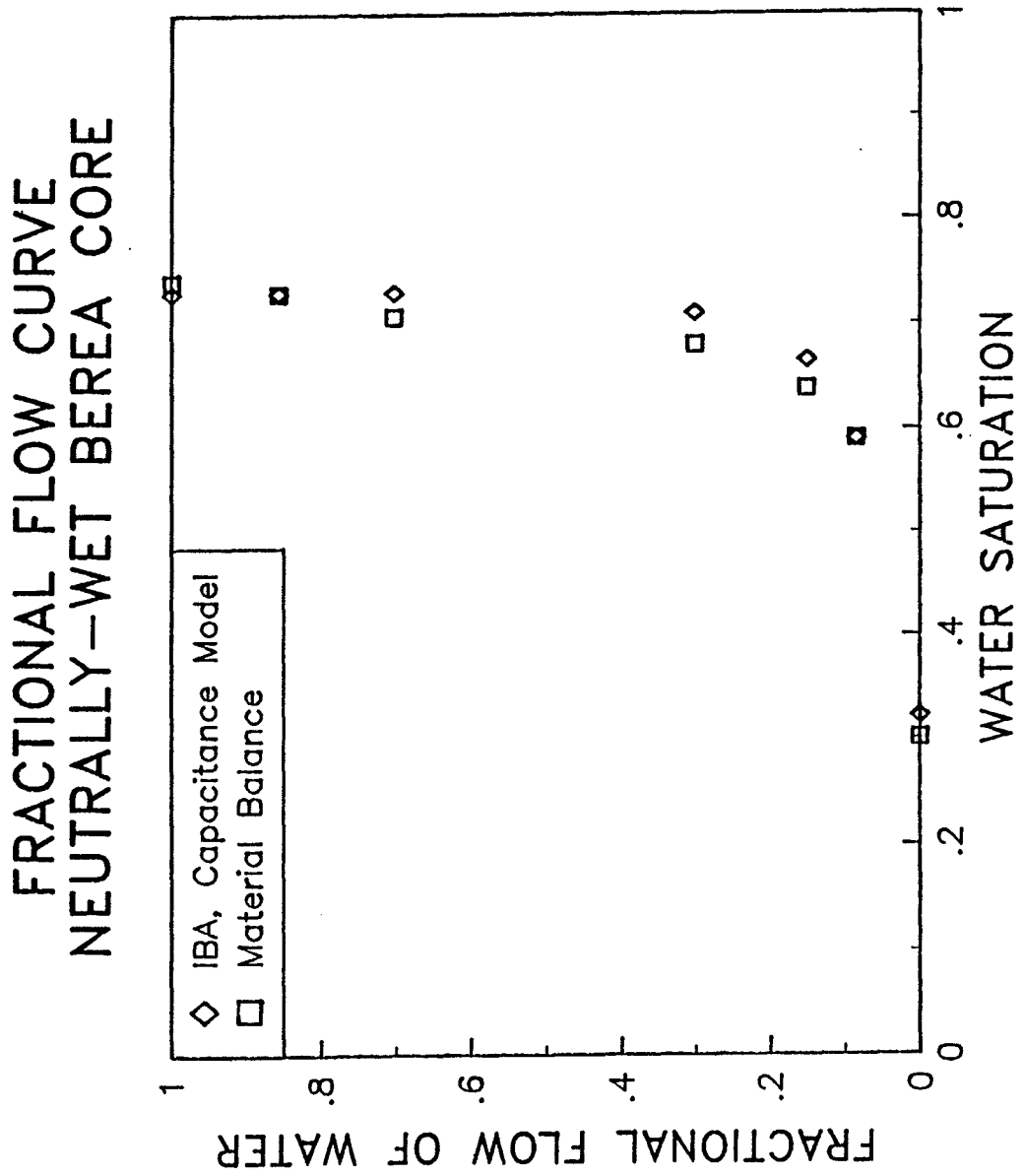

Figure 7-54 Water fractional flow curve for neutrally-wet Berea core. Comparison of partitioning tracer (IBA) and material balance.

S1= .680	S2= .320	F1=1.00	F2=1.00
AREA=25.95	L=60.85	POR= .204	
ALPHA1= .15	ALPHA2= 0.00	M1= .00E+00	M2= .00E+00
FF1=1.000	FF2=0.000	QT= 1.015	PART1= 5.50
NB= 50	NP=5000	PVINJ= 4.00	PVS= .200

C_i^o = 2725 ppm

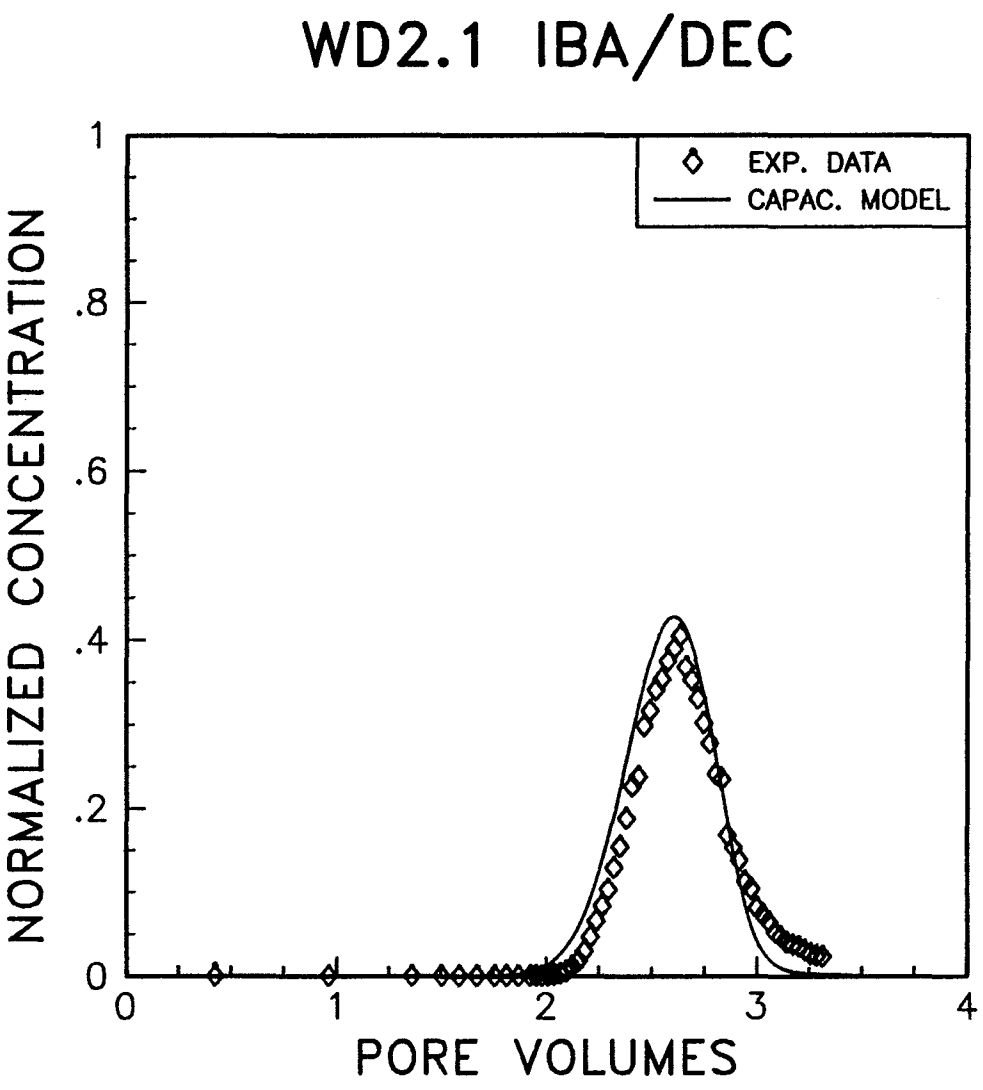

Figure 7-55 Tracer concentration versus pore volumes for treated Berea. Water saturation of 32%, water fractional flow of 0.0, IBA in decane.

S1= .410	S2= .590	F1=1.00	F2=1.00
AREA=25.95	L=60.85	POR= .204	
ALPHA1= 2.00	ALPHA2= 2.00	M1= .00E+00	M2= .00E+00
FF1= .915	FF2= .085	QT= 1.031	PART1= 4.80
NB= 50	NP=5000	PVINJ= 6.00	PVS= .602

C_i^o = 741 ppm

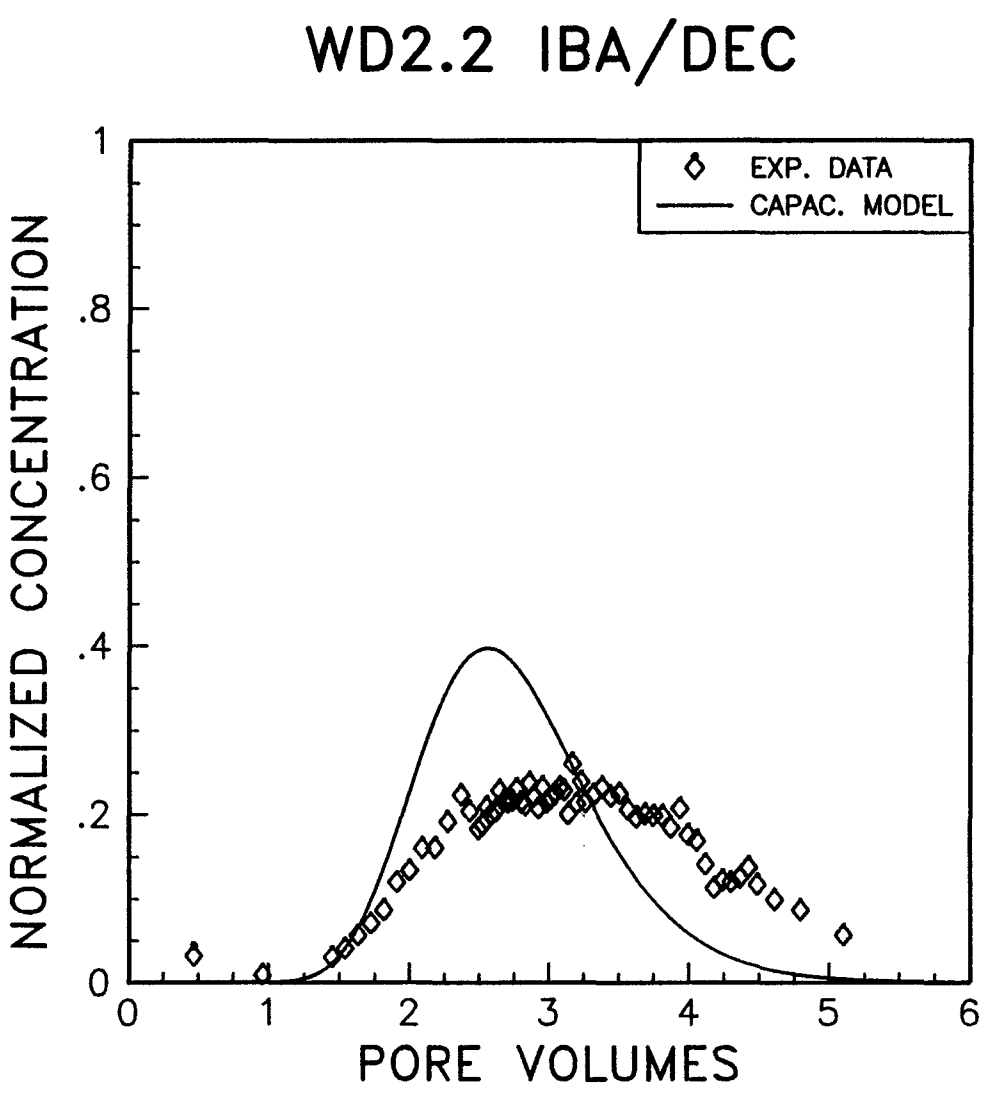

Figure 7-56 Tracer concentration versus pore volumes for treated Berea. Water saturation of 59%, water fractional flow of 0.085, IBA in decane.

S1= .590	S2= .410	F1=1.00	F2=1.00
AREA=25.95	L=60.85	POR= .204	
ALPHA1= 2.00	ALPHA2= 2.00	M1= .00E+00	M2= .00E+00
FF1= .085	FF2= .915	QT= 1.031	PART1= .21
NB= 50	NP=5000	PVINJ= 6.00	PVS= .602

C_i^o = 1936 ppm

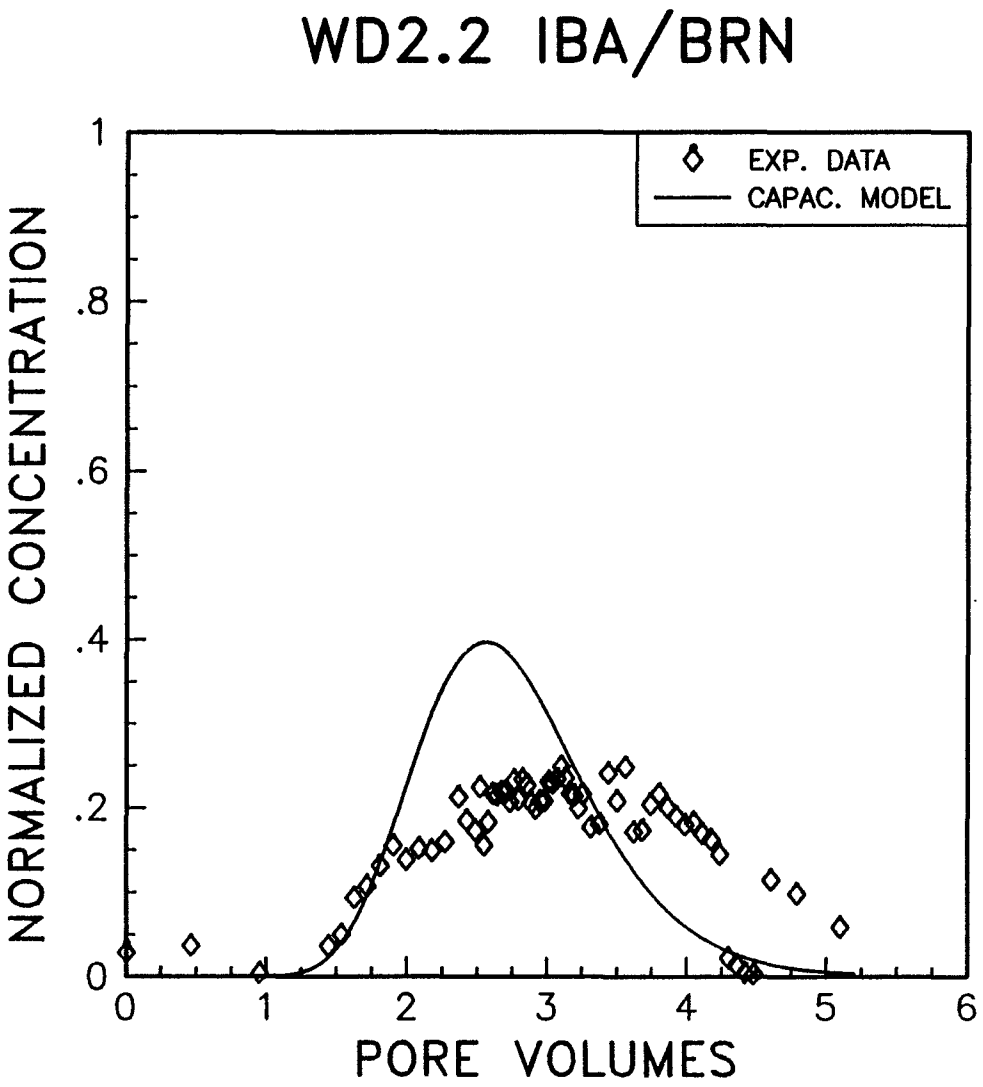

Figure 7-57 Tracer concentration versus pore volumes for treated Berea. Water saturation of 59%, water fractional flow of 0.085, IBA in brine.

S1= .335	S2= .665	F1=1.00	F2=1.00
AREA=25.95	L=60.85	POR= .204	
ALPHA1= 8.00	ALPHA2= 8.00	M1= .00E+00	M2= .00E+00
FF1= .849	FF2= .151	QT= 1.020	PART1= 4.80
NB= 50	NP=3000	PVINJ= 6.00	PVS= .877

C_i^o = 742 ppm

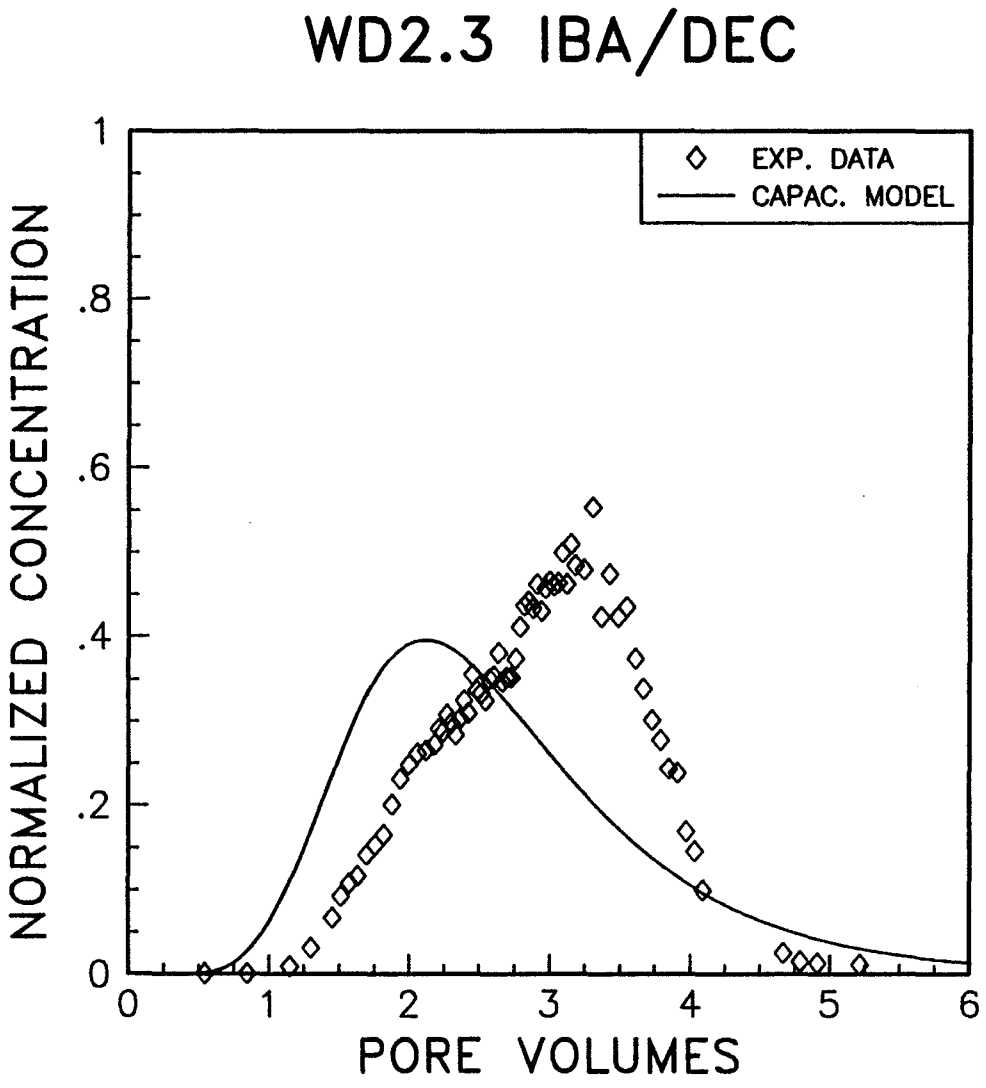

Figure 7-58 Tracer concentration versus pore volumes for treated Berea. Water saturation of 66.5%, water fractional flow of 0.151, IBA in decane.

S1= .665	S2= .335	F1=1.00	F2=1.00
AREA=25.95	L=60.85	POR= .204	
ALPHA1= 8.00	ALPHA2= 8.00	M1= .00E+00	M2= .00E+00
FF1= .151	FF2= .849	QT= 1.020	PART1= .21
NB= 50	NP=5000	PVINJ= 6.00	PVS= .877

C_i^o = 2581 ppm

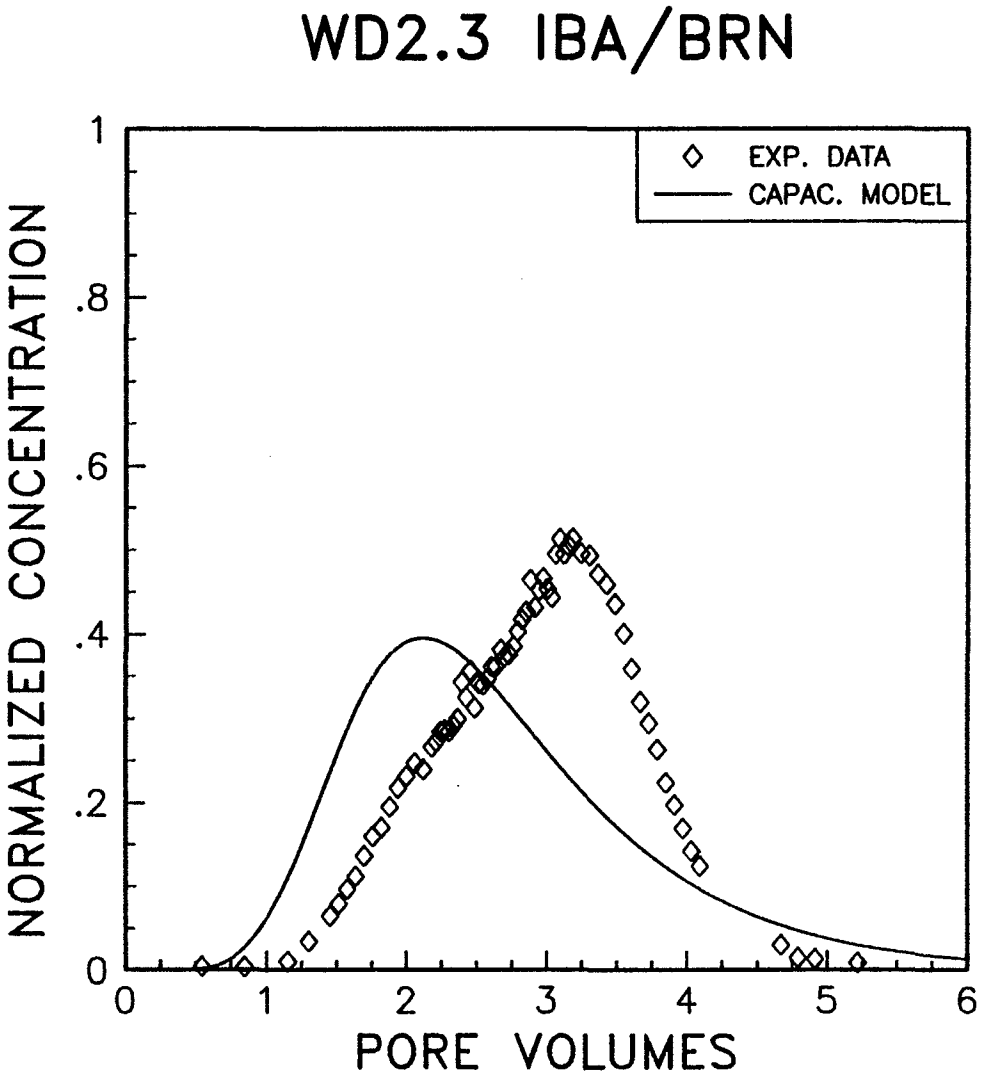

Figure 7-59 Tracer concentration versus pore volumes for treated Berea. Water saturation of 66.5%, water fractional flow of 0.151, IBA in brine.

S1= .290	S2= .710	F1= .90	F2= .90
AREA=25.95	L=60.85	POR= .204	
ALPHA1= 1.50	ALPHA2= 1.50	M1= .80E-04	M2= .80E-04
FF1= .699	FF2= .301	QT= 1.014	PART1= 4.80
NB= 50	NP=5000	PVINJ= 4.00	PVS= .217

C_i^o = 792 ppm

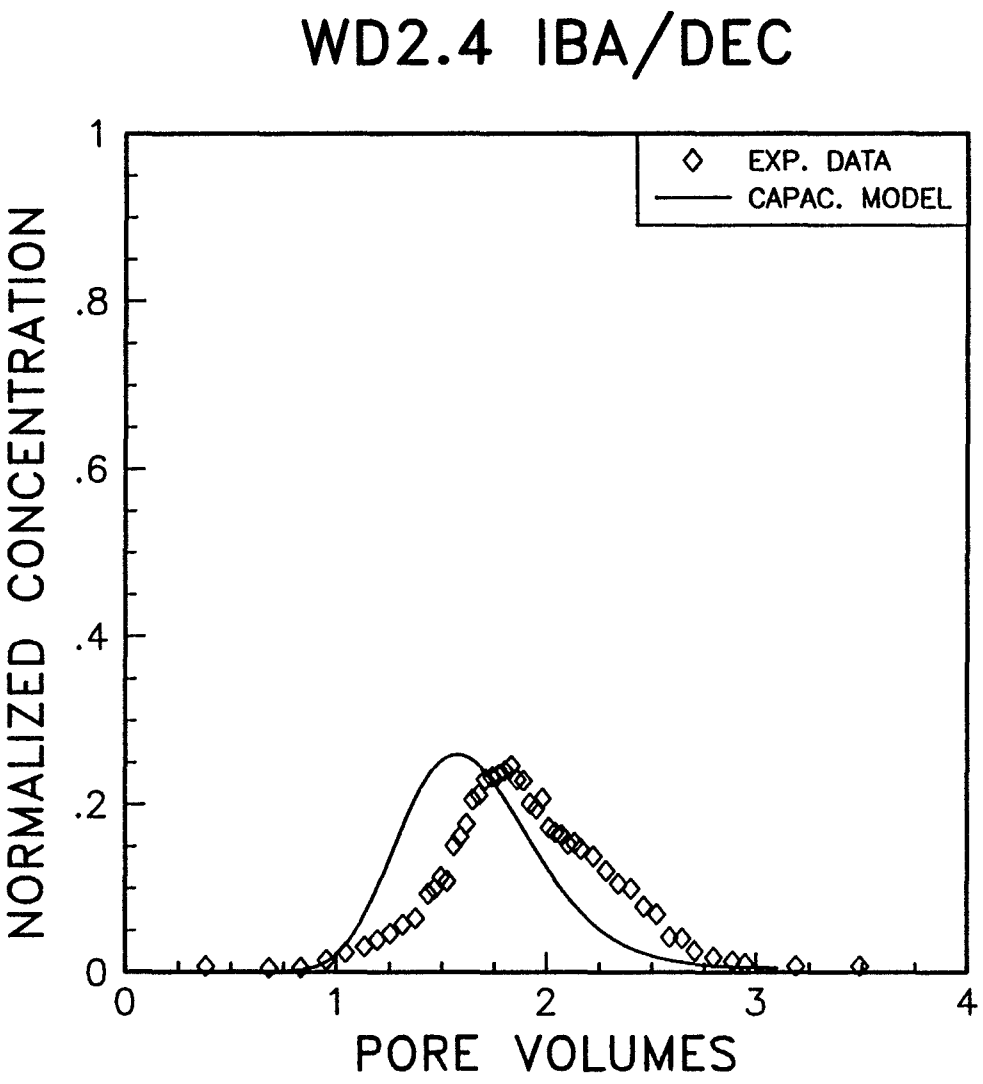

Figure 7-60 Tracer concentration versus pore volumes for treated Berea. Water saturation of 71%, water fractional flow of 0.301, IBA in decane.

S1= .710	S2= .290	F1= .90	F2= .90
AREA=25.95	L=60.85	POR= .204	
ALPHA1= 1.50	ALPHA2= 1.50	M1= .80E-04	M2= .80E-04
FF1= .301	FF2= .699	QT= 1.014	PART1= .21
NB= 50	NP=5000	PVINJ= 4.00	PVS= .217

C_i^o = 2568 ppm

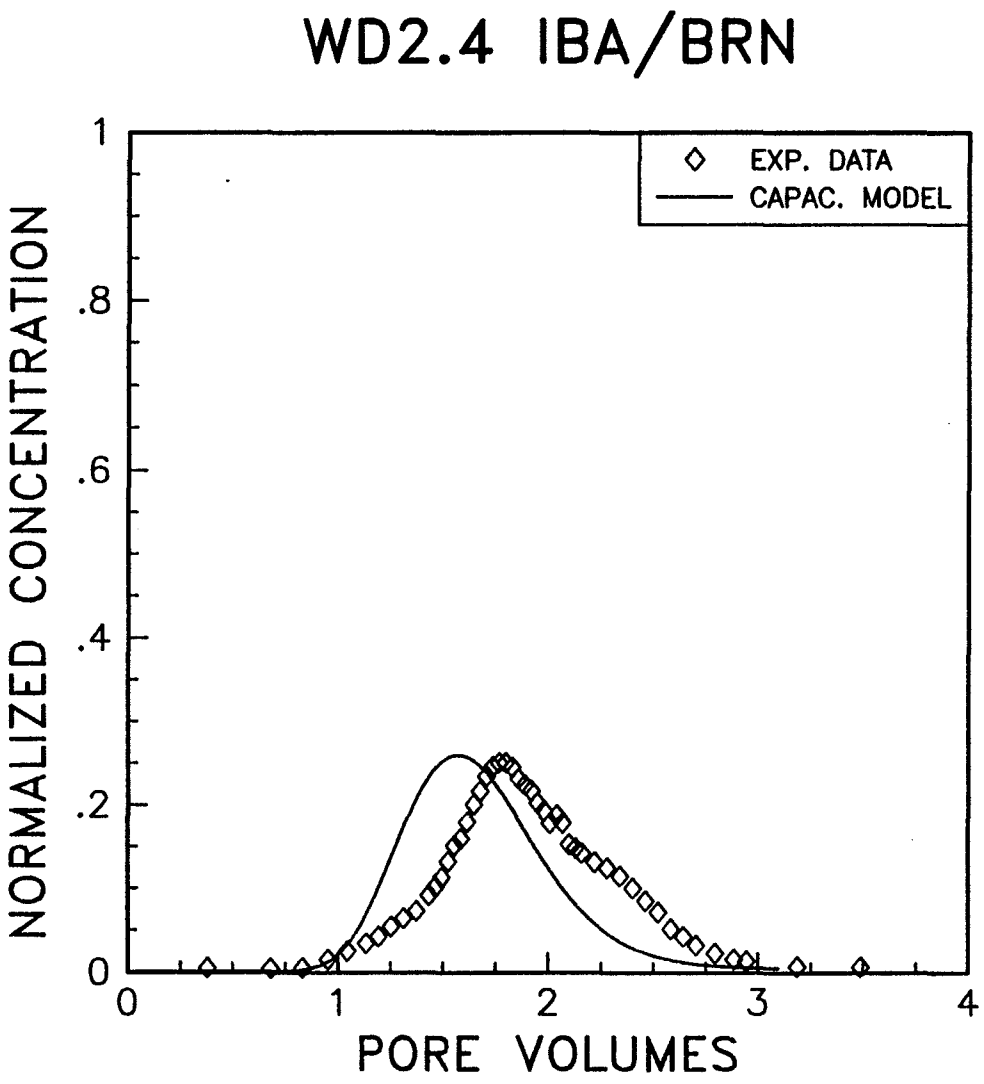

Figure 7-61 Tracer concentration versus pore volumes for treated Berea. Water saturation of 71%, water fractional flow of 0.301, IBA in brine.

S1= .270	S2= .730	F1= .43	F2= .88
AREA=25.95	L=60.85	POR= .204	
ALPHA1= 1.40	ALPHA2= 1.40	M1= .40E−03	M2= .40E−03
FF1= .298	FF2= .702	QT= .998	PART1= 4.80
NB= 50	NP=3000	PVINJ= 4.00	PVS= .200

C_i^o = 790 ppm

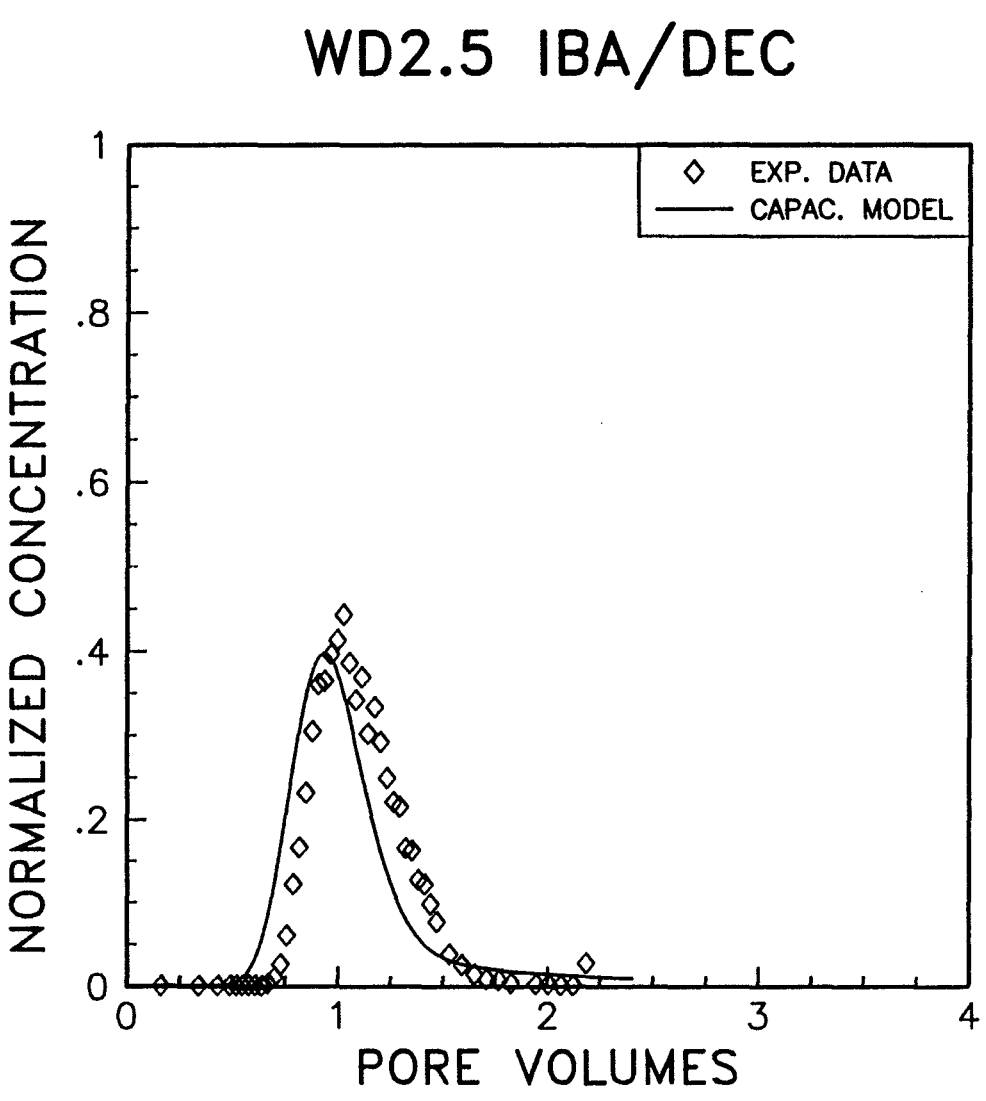

Figure 7-62 Tracer concentration versus pore volumes for treated Berea. Water saturation of 73%, water fractional flow of 0.702, IBA in decane.

S1= .730	S2= .270	F1= .88	F2= .43
AREA=25.95	L=60.85	POR= .204	
ALPHA1= 1.00	ALPHA2= 1.00	M1= .80E−03	M2= .80E−03
FF1= .702	FF2= .298	QT= .998	PART1= .21
NB= 50	NP=3000	PVINJ= 4.00	PVS= .200

C_i^o = 2413 ppm

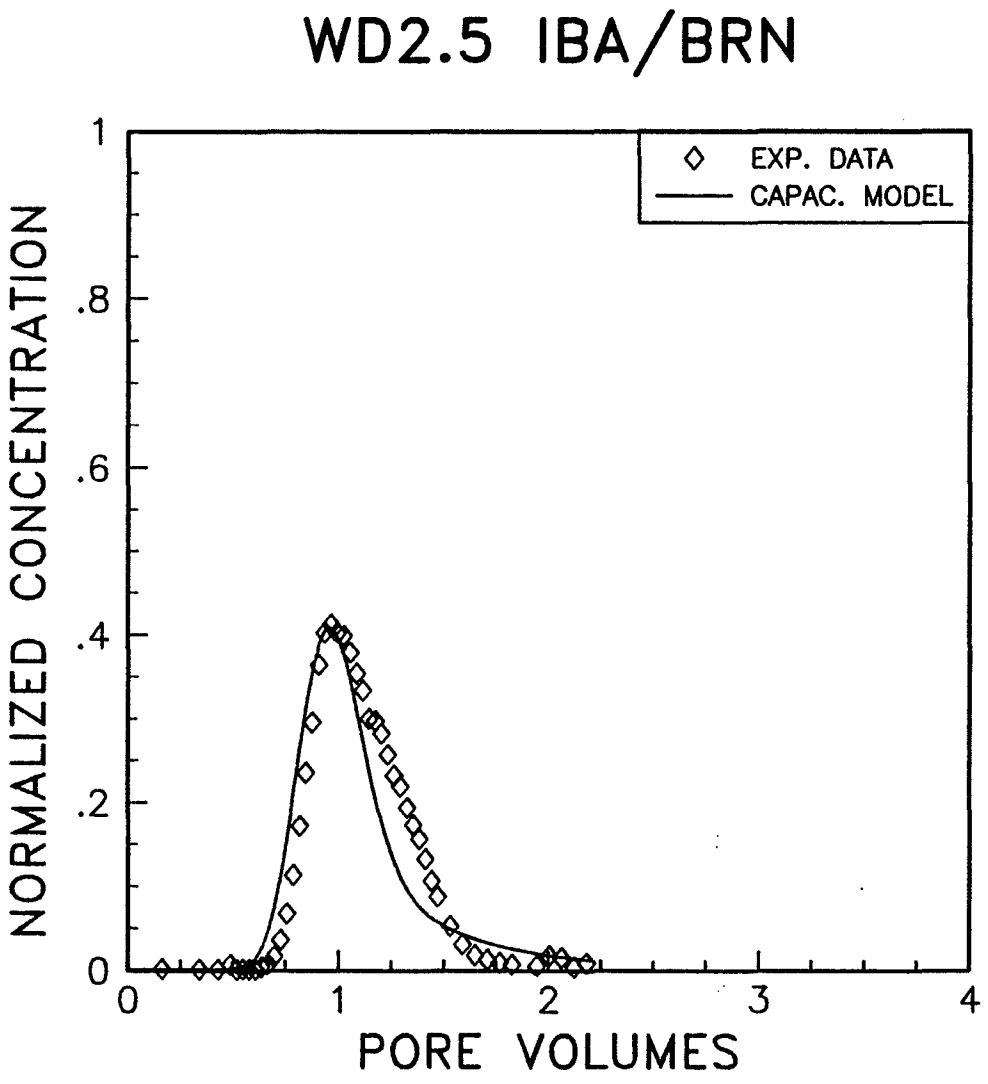

Figure 7-63 Tracer concentration versus pore volumes for treated Berea. Water saturation of 73%, water fractional flow of 0.702, IBA in brine.

S1= .270	S2= .730	F1= .25	F2= .92
AREA=25.95	L=60.85	POR= .204	
ALPHA1= 1.20	ALPHA2= 1.20	M1= .30E−03	M2= .30E−03
FF1= .124	FF2= .876	QT= .971	PART1= 4.80
NB= 50	NP=3000	PVINJ= 4.00	PVS= .494

C_i^o = 763 ppm

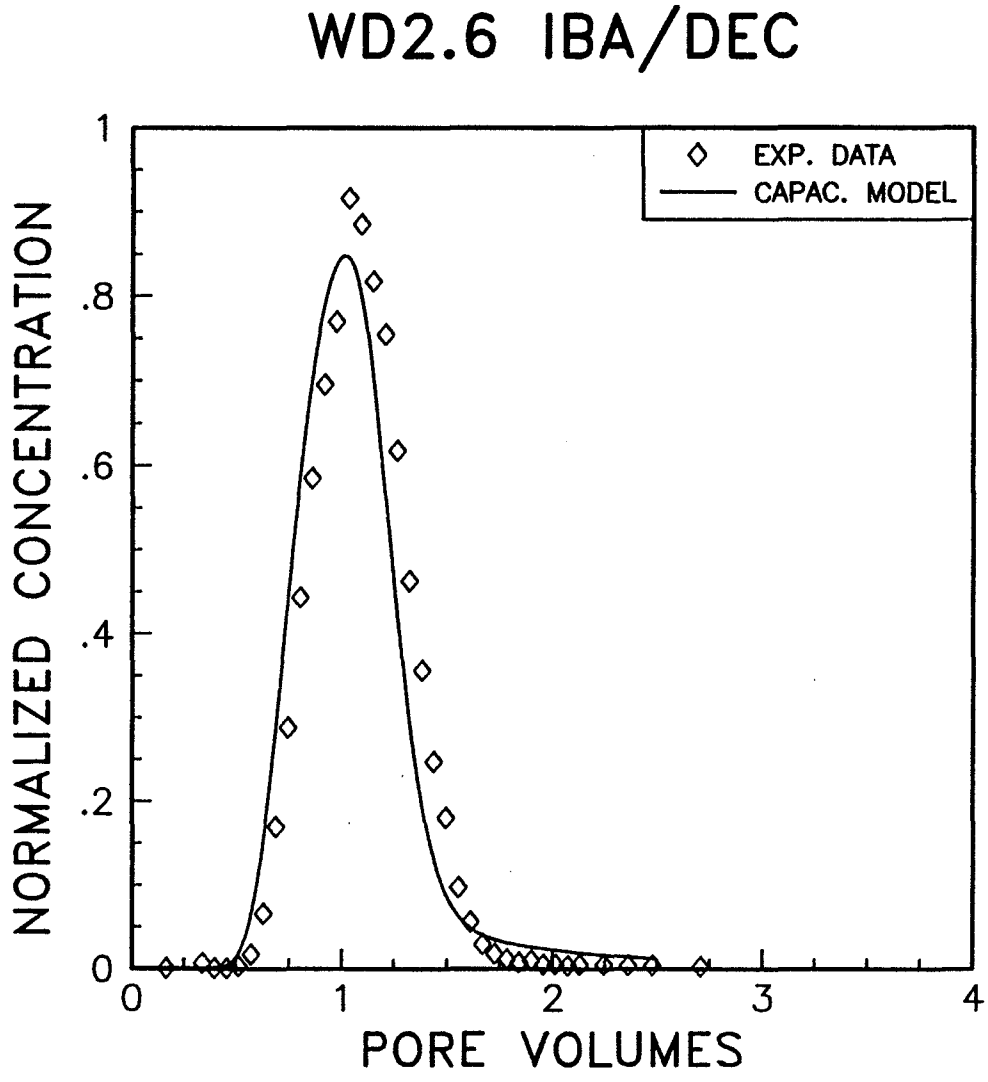

Figure 7-64 Tracer concentration versus pore volumes for treated Berea. Water saturation of 73%, water fractional flow of 0.876, IBA in decane.

S1= .730	S2= .270	F1= .92	F2= .25
AREA=25.95	L=60.85	POR= .204	
ALPHA1= 1.20	ALPHA2= 1.20	M1= .30E-03	M2= .30E-03
FF1= .876	FF2= .124	QT= .971	PART1= .21
NB= 50	NP=3000	PVINJ= 4.00	PVS= .494

C_i^o = 2474 ppm

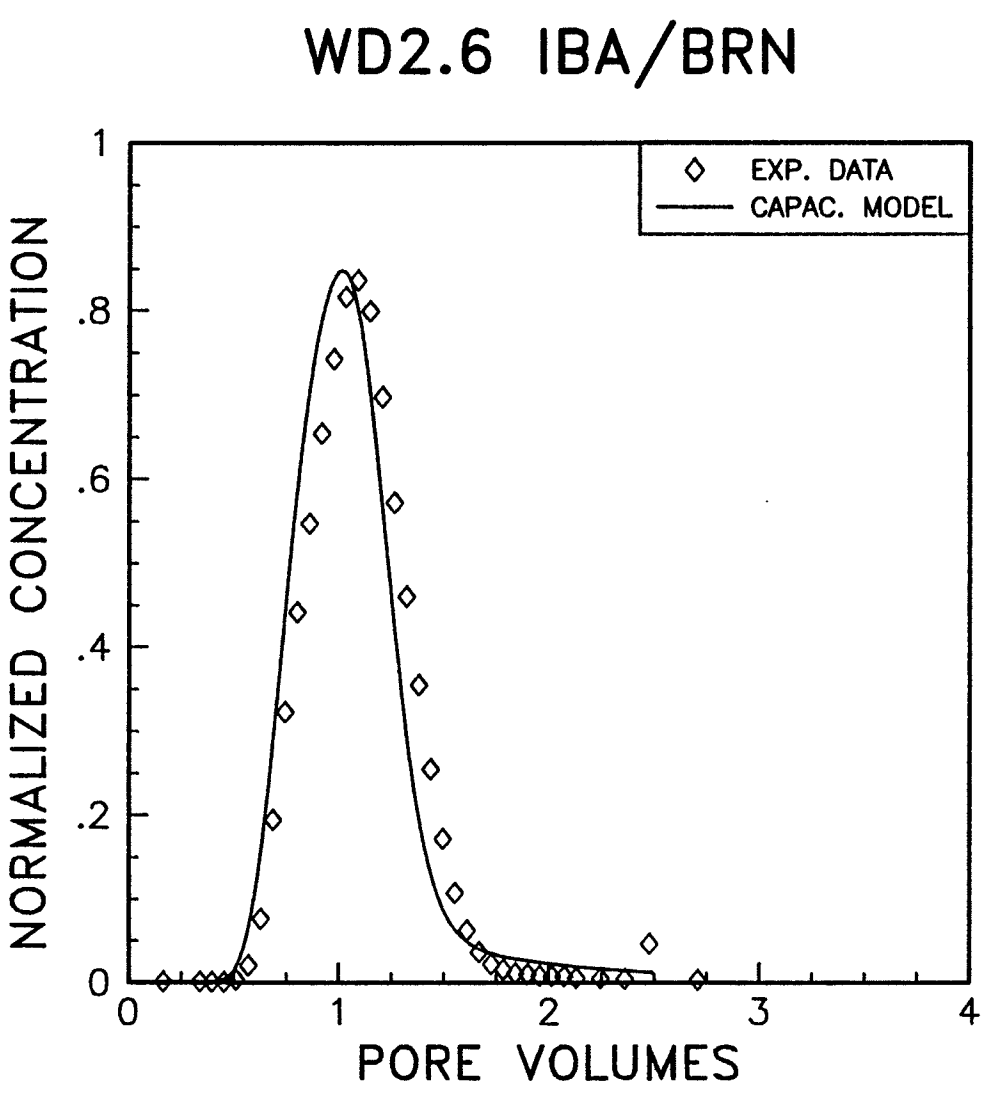

Figure 7-65 Tracer concentration versus pore volumes for treated Berea. Water saturation of 73%, water fractional flow of 0.876, IBA in brine.

S1= .730	S2= .270	F1= .97	F2=1.00
AREA=25.95	L=60.85	POR= .204	
ALPHA1= 1.80	ALPHA2= 0.00	M1= .80E-04	M2= .00E+00
FF1=1.000	FF2=0.000	QT= .999	PART1= .21
NB= 50	NP=5000	PVINJ= 4.00	PVS= .209

C_i^o = 2638 ppm

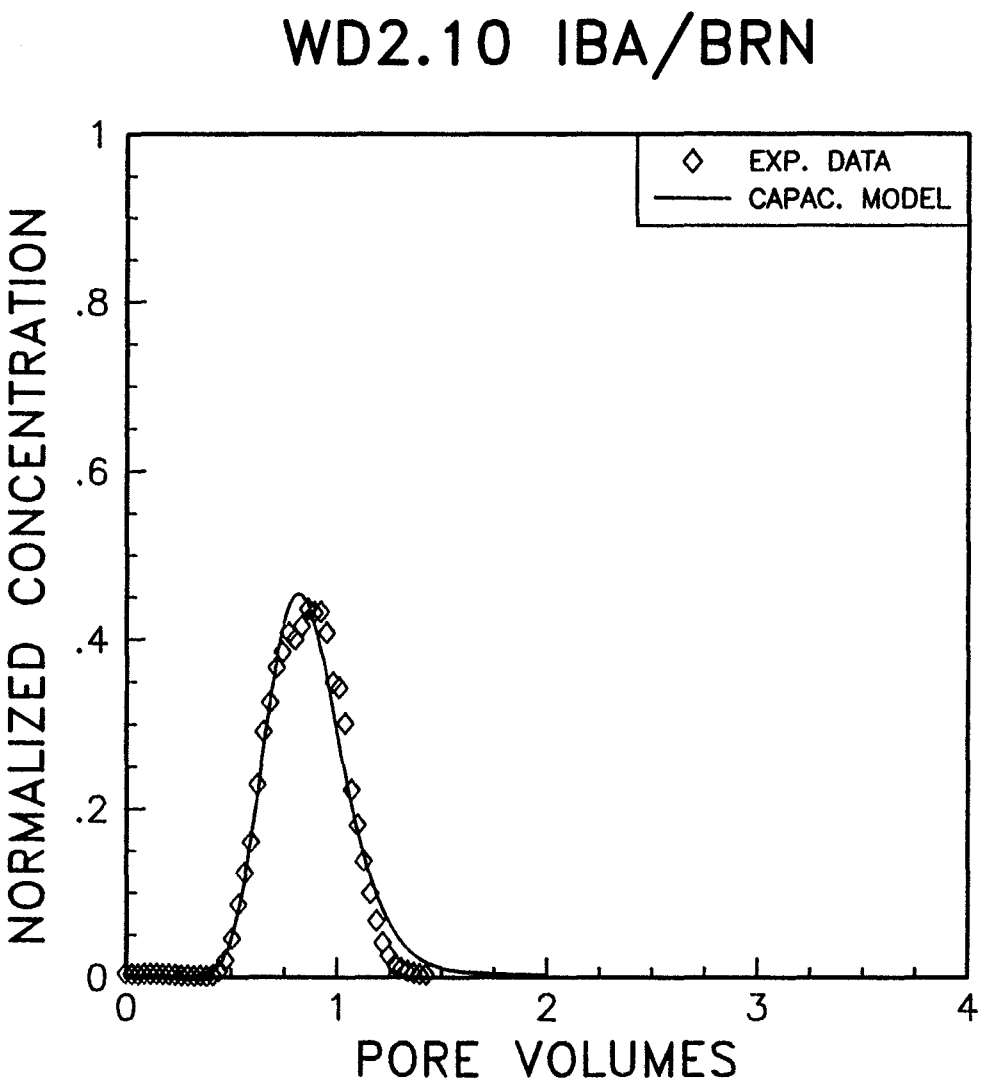

Figure 7-66 Tracer concentration versus pore volumes for treated Berea. Water saturation of 73%, water fractional flow of 1.0, IBA in brine.

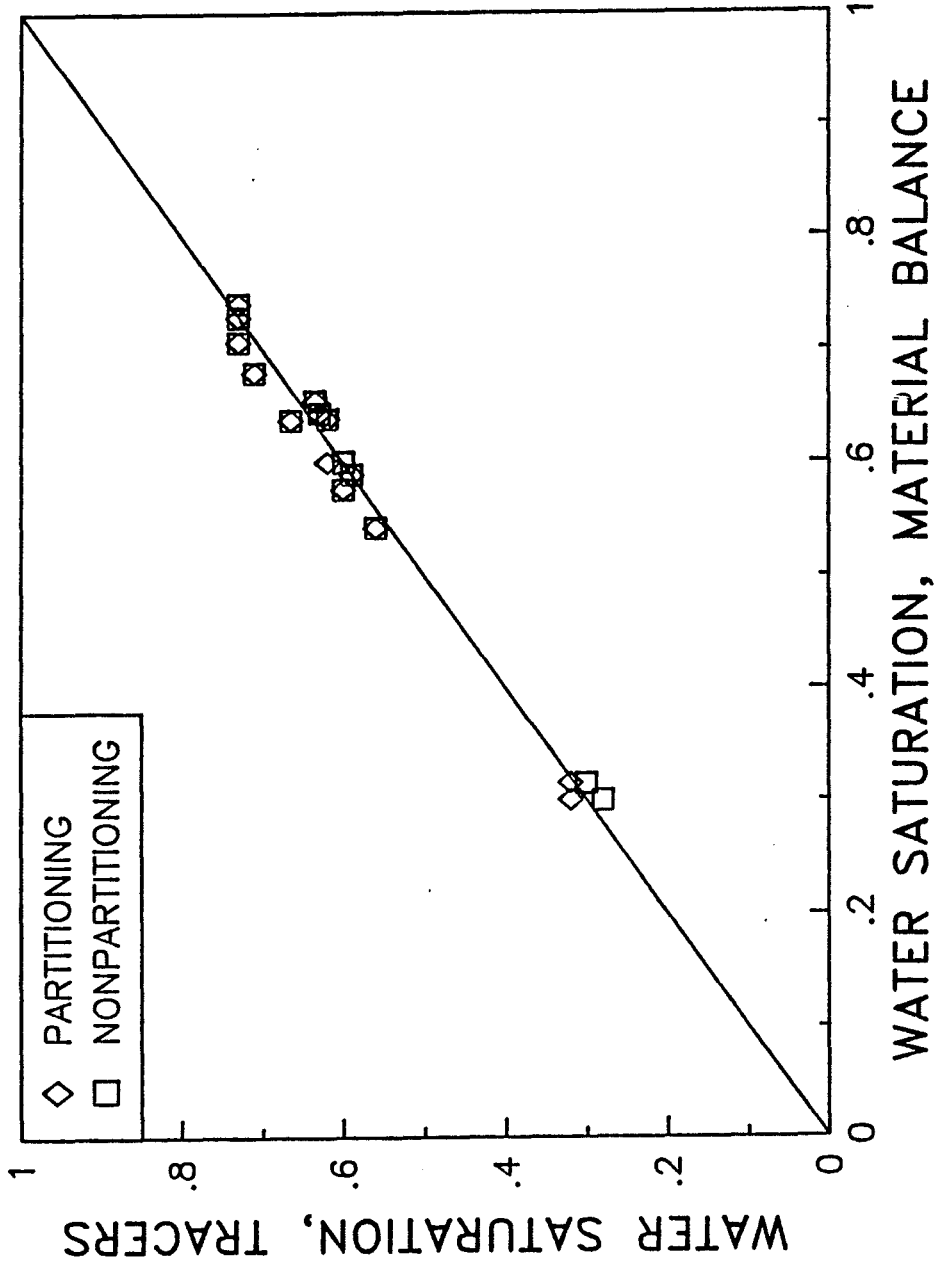

Figure 7-67 Comparison of water saturation by partitioning and non-partitioning tracers versus water saturation by material balance.

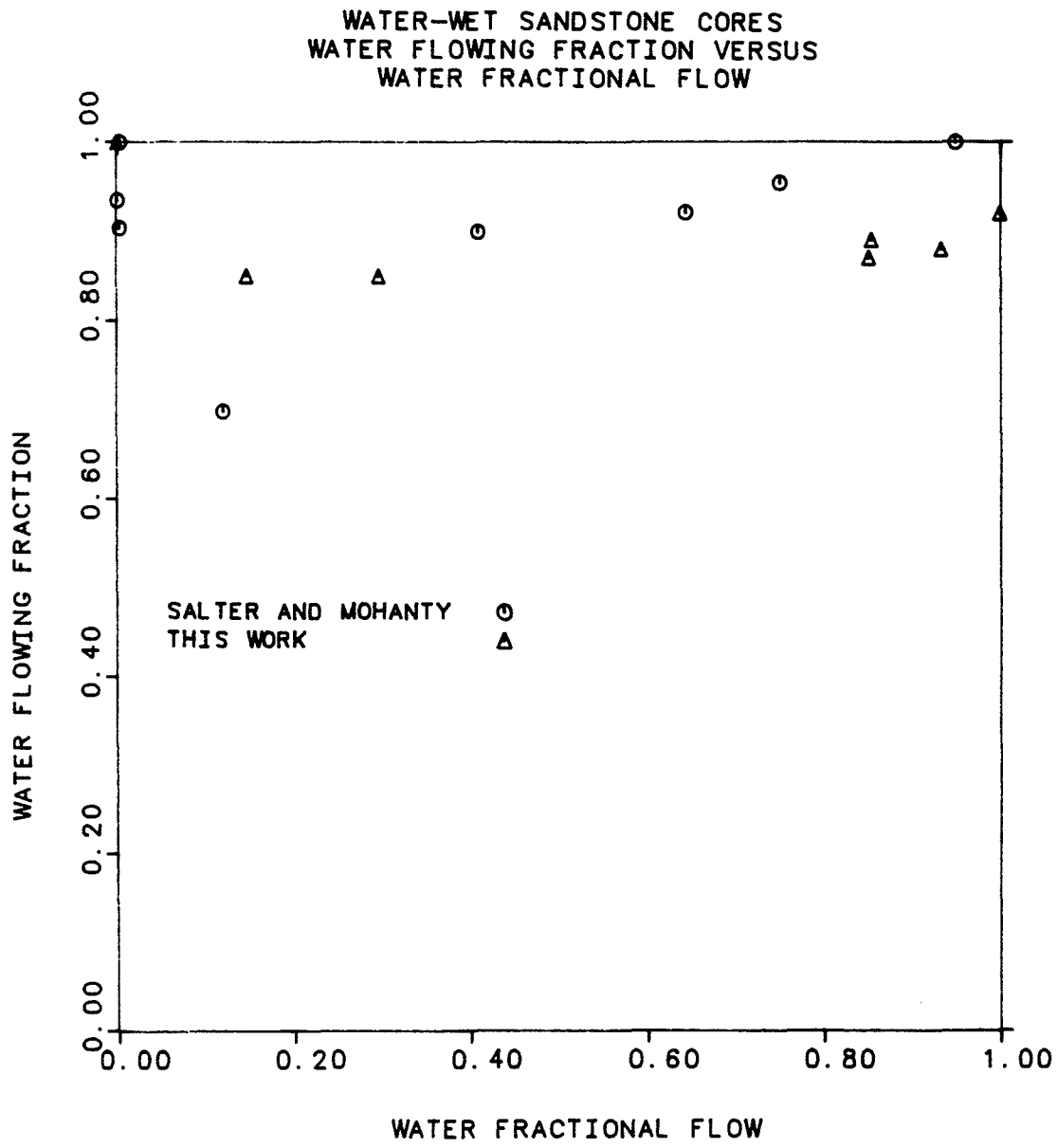

Figure 7-68 Comparison of water flowing fraction data versus water fractional flow for water-wet cores.

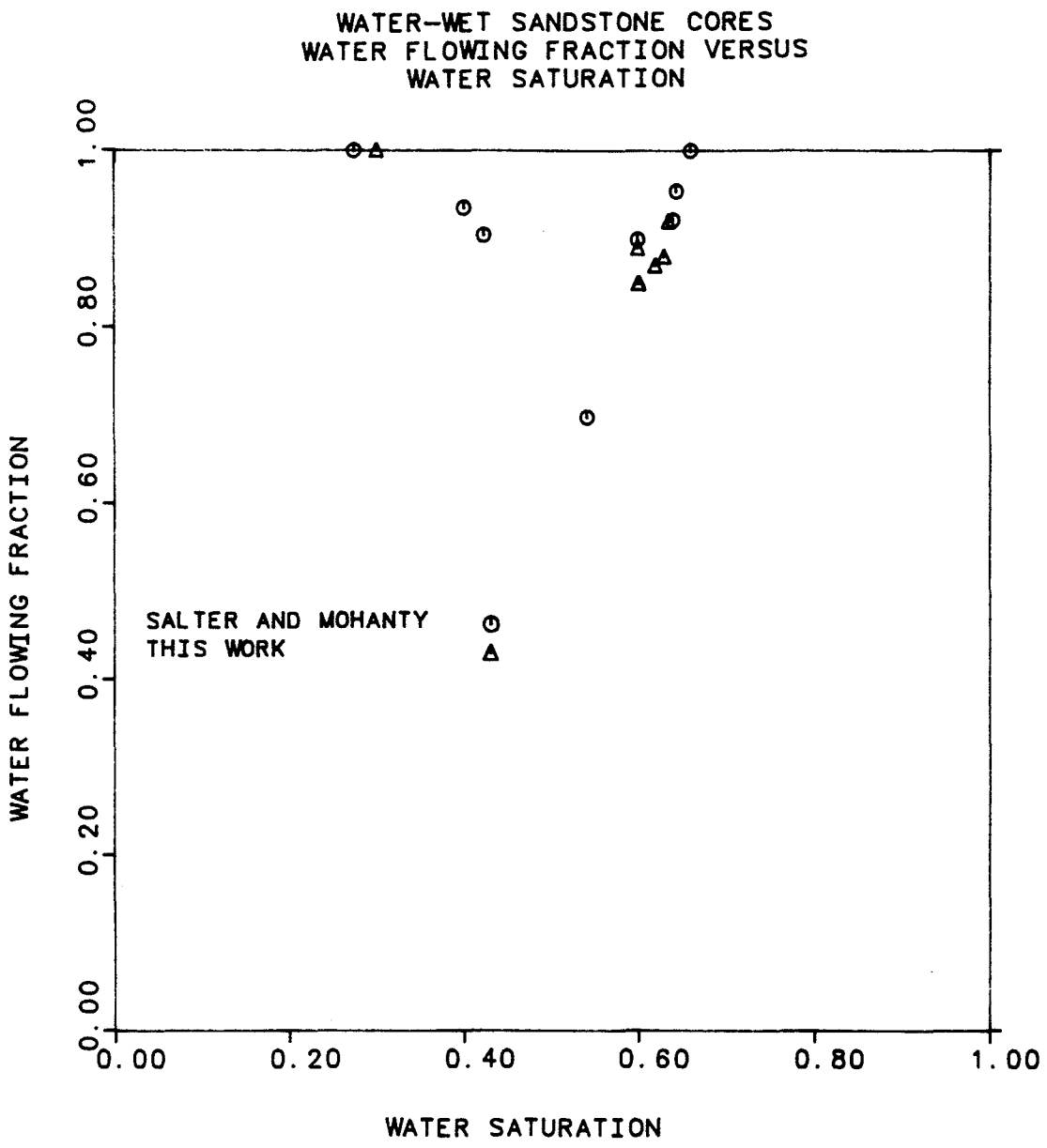

Figure 7-69 Comparison of water flowing fraction data versus water saturation for water-wet cores.

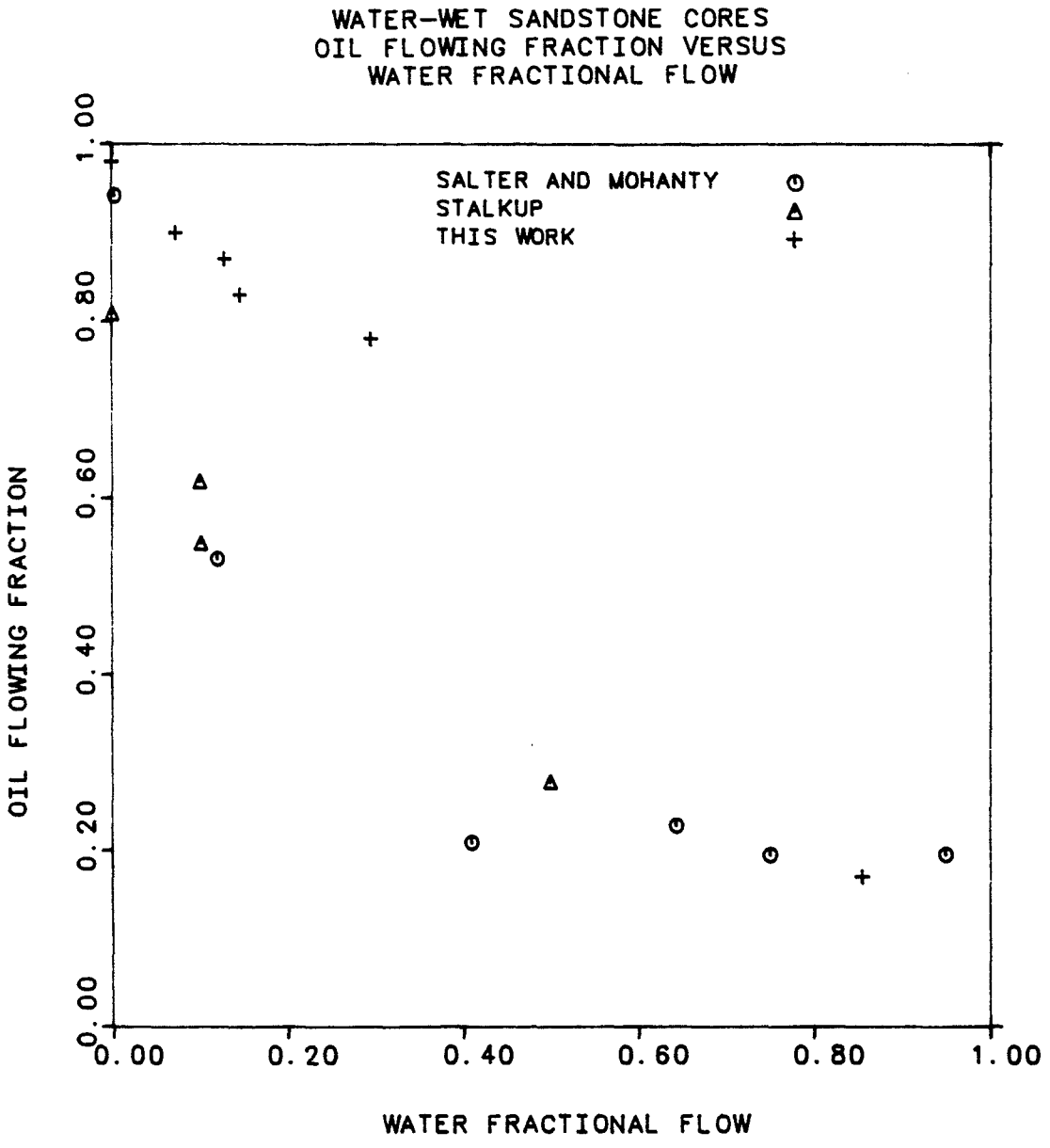

Figure 7-70 Comparison of oil flowing fraction data versus water fractional flow for water-wet cores.

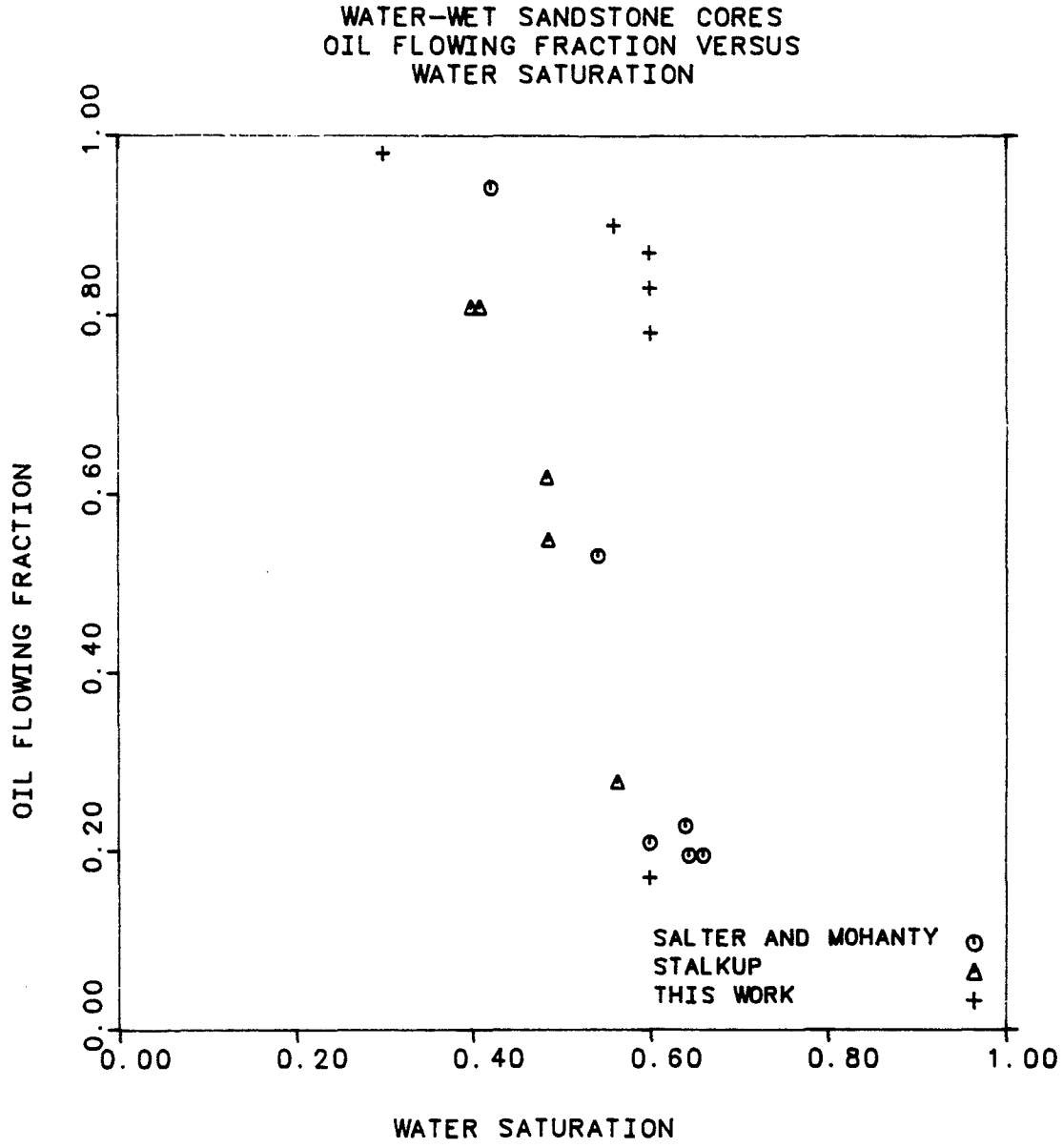

Figure 7-71 Comparison of oil flowing fraction data versus water saturation for water-wet cores.

CHAPTER 8

UNSTEADY-STATE EXPERIMENTAL RESULTS

After the two-phase experiments were completed, the core was driven to irreducible water saturation (IWS), then a steady-state decane flood was made and tracer data were fit with the steady-state capacitance model as before. This was done to compare material balance saturation values with those obtained from the model. Following this, an unsteady-state waterflood was performed. These experiments used the same two Berea cores as the steady-state experiments, see Table 7-1. Brine labeled with Cl-36 was the nonpartitioning tracer. IBA and C-14 labeled IPA, both partitioning tracers, were also injected. Experimental procedures are discussed in Chapter 5.

EXPERIMENT USS.1: WATER-WET CORE

After IWS had been reached, a slug of tritiated decane was injected into the core at 1 mL/min to obtain values of saturation, dispersivity, and flowing fraction prior to beginning the unsteady-state experiment. The effluent tracer data were fit with the steady-state capacitance model as shown in Figure 8-1. The results are given in Table 8-1 along with values obtained from material balance calculations.

The values of saturation, dispersivity, and flowing fraction obtained from the model compare very well with those obtained from Experiment WD1.2 (see Table 7-2). The values for IWS are identical at 30 percent. Oil dispersivity from Experiment WD1.2 was 0.30 cm, whereas a value of 0.20 cm was obtained from this experiment. Oil flowing fraction was 0.98 from WD1.2 and 0.95 from this experiment. However, Table 8-1

shows that saturation from material balance did not agree well with saturation obtained from the model for this experiment. It is suspected that the accumulation of errors from the many previous experiments performed on this core is the probable cause for this discrepancy. Therefore, the model-determined estimate for IWS of 30 percent is probably more accurate than the material balance estimate.

Following the steady-state decane flood, a waterflood, Experiment USS.1, was performed on the core. A slug of labeled brine was injected into the core at a constant rate. Brine injection continued until well after ROS had been reached. Plug flow was observed with no additional oil production after water breakthrough.

The effluent tracer data of Cl-36, IPA labeled with C-14, and IBA were curve-fit with the unsteady-state model described in Chapter 3 and Appendix J. Normalized tracer concentration versus pore volumes are shown for the three tracers in Figures 8-2, 8-3, and 8-4. The results are summarized in Table 8-2, while material balance on tracers is given in Table 7-7.

Identical values for saturation, dispersivity, and flowing fractions were used to achieve good fits for all three tracers. Additionally, these values agreed very well with those obtained from steady-state Experiments WD1.2 and WD1.8 at IWS and ROS, respectively (see Table 7-2). From Experiment WD1.2: IWS was 30 percent and identical to the value used to fit Experiment USS.1; oil flowing fraction was 0.98, while a value of 1.0 was used to fit Experiment USS.1; oil dispersivity was 0.30 cm, while a value of 0.35 cm was used to fit USS.1. From Experiment WD1.8: ROS was 36.5 percent, while a value of 34 percent was used to fit USS.1; water flowing fraction was 0.92 and identical to the value used to fit USS.1; water dispersivity was 0.1 cm, while 0.35 cm was used to fit USS.1.

EXPERIMENT USS.2: NEUTRALLY WET CORE

After IWS had been reached, a slug of tritiated decane was injected into the core at 1 mL/min, to obtain values of saturation, dispersivity, and flowing fraction prior to beginning the unsteady-state experiment. The effluent tracer data was fit with the steady-state capacitance model as shown in Figure 8-5. The results are given in Table 8-1 along with values obtained from material balance calculations.

The values of saturation, dispersivity, and flowing fraction obtained from the model compare very well with those obtained from Experiment WD2.1 (see Table 7-2). IWS from Experiment WD2.1 was 28 percent, while a value of 30 percent was obtained from this experiment. Oil dispersivity from Experiment WD2.1 was 0.35 cm, while a value of 0.3 cm was obtained from this experiment. Values for oil flowing fraction were 1.0 for both experiments. However, Table 8-1 shows that saturation from material balance did not agree with saturation obtained from the model for this experiment. This is the same thing that was observed with the water-wet core.

Following the steady-state decane flood, a waterflood, Experiment USS.2, was performed on the core. Plug flow was observed with no additional oil production after water breakthrough.

The effluent tracer data of Cl-36, C-14 labeled IPA, and IBA were curve-fit with the unsteady-state model. Normalized concentration versus pore volumes are shown in Figures 8-6, 8-7, and 8-8. The results are summarized in Table 8-2, while material balance on tracers is given in Table 7-7.

Identical values for saturation, dispersivity, and flowing fractions were used to achieve good fits for all three tracers. Again, these values agreed very well with those obtained from steady-state Experiments WD2.1 and WD2.10 at IWS and ROS, respectively (see Table 7-4). From Experiment WD2.1: IWS was 28 percent, while a value of 30 percent was used to fit Experiment USS.2; oil flowing fraction was 1.0 and

identical to the value used to fit USS.2: oil dispersivity was 0.35 cm, while a value of 1.3 cm was used to fit USS.2 (the model was not sensitive to this parameter). From Experiment WD2.10: ROS was 27 percent, while a value of 26 percent was used to fit USS.2; water flowing fraction was 0.97, while 0.96 was used to fit USS.2: water dispersivity was 1.6 cm, while a value of 1.3 cm was used to fit USS.2.

For both experiments described in this chapter, the simple relative permeability equations in the model were used to fit the experimental data (see Appendix J). The relative permeability exponents were obtained by fitting the steady-state relative permeability data, as shown in Figures 8-9 and 8-10, for the water-wet and treated cores, respectively.

HIGH MOBILITY RATIO SIMULATIONS

The end-point mobility ratios for the unsteady-state experiments reported here were very low, less than 0.1, resulting in plug flow. Therefore, simulations were run using a high mobility ratio of about 10.0 in order to further test the unsteady-state model. Input data for the model were identical to the data from the low mobility ratio simulations with the following exceptions: a value of 150 cp was used for the oil viscosity, and values used for oil and water flowing fractions were those obtained from the steady-state experiments. For the water-wet core, water flowing fraction ranged from 0.85 to 0.92, whereas the oil flowing fraction ranged from 0.17 to 0.98 (see Table 7-2). For the treated core, water flowing fraction ranged from 0.57 to 0.97, whereas the oil flowing fraction ranged from 0.25 to 1.0 (see Table 7-4). Appendix J discusses the function used in the model for phase flowing fraction. Simulations were run using data from both the water-wet and treated cores and for both partitioning and nonpartitioning tracers.

High mobility ratio fractional flow curves for both the water-wet and treated cores were calculated and are shown in Figures 8-11 and 8-12, respectively. Both curves indicate a shock front followed by simultaneous two-phase flow or Buckley-Leverett tail.

Figures 8-13 and 8-14 show the results of the water-wet core simulations for partitioning and nonpartitioning tracers, respectively. For the partitioning case, a partition coefficient of 0.21 was used as if IBA had been the tracer. The results look very similar to the low mobility ratio simulations, Figures 8-2 and 8-4, except that tracer breakthrough is earlier. This is expected since the shock front for a high mobility ratio case breaks through earlier than for a low mobility ratio case.

Figures 8-15 and 8-16 show the results of the organochlorosilane-treated core simulations for nonpartitioning and partitioning (IBA) tracers, respectively. Again, the results look similar to the low mobility ratio simulations, Figures 8-6 and 8-8, except that tracer breakthrough is earlier.

TABLE 8-1

DISPERSION DATA FOR TRITIATED n-DECANE,

STEADY-STATE FLOODS PRIOR TO WATERFLOODS,

WATER-WET AND NEUTRALLY WET CORES

Core	Water Fractional Flow	Water Saturation[1]	Water Saturation[2]	Oil Dispersivity (cm)	Oil Flowing Fraction
Water wet	0.0	0.30	0.357	0.20	0.95
Neutrally wet	0.0	0.30	0.352	0.30	1.0

[1]Determined by the steady-state model
[2]Determined by material balance

TABLE 8-2

RESULTS OF WATERFLOODS ON WATER-WET AND NEUTRALLY WET CORES, UNSTEADY-STATE MODEL

Tracer	IWS	ROS	Water Dispersivity (cm)	Oil Dispersivity (cm)	Water Flowing Fraction	Oil Flowing Fraction
			Water-Wet Core			
Cl-36	0.30	0.34	0.35	—	0.92	—
C-14 IPA	0.30	0.34	0.35	0.35	0.92	1.0
IBA	0.30	0.34	0.35	0.35	0.92	1.0
			Neutrally-Wet Core			
Cl-36	0.30	0.26	1.3	—	—	—
C-14 IPA	0.30	0.26	1.3	1.3	0.96	1.0
IBA	0.30	0.26	1.3	1.3	0.96	1.0

S1= .700	S2= .300	F1= .95	F2=1.00
AREA=24.90	L=60.75	POR= .217	
ALPHA1= .20	ALPHA2= 0.00	M1= .60E-02	M2= .00E+00
FF1=1.000	FF2=0.000	QT= 1.026	PART1= 0.00
NB= 100	NP=7000	PVINJ= 4.00	PVS= .200

C_i^o = 1387 dpm/ml

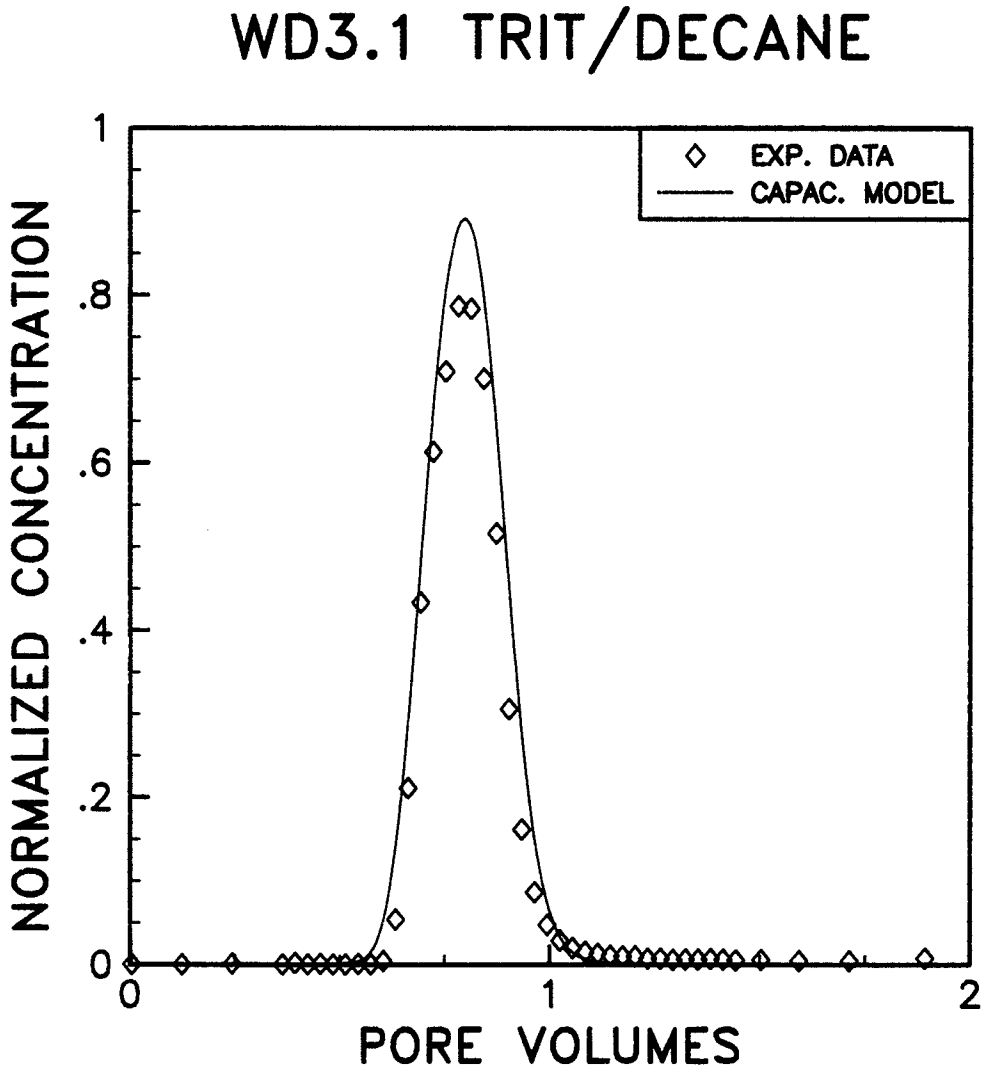

Figure 8-1 Tracer concentration versus pore volumes for water-wet Berea prior to experiment USS.1. Tritiated decane.

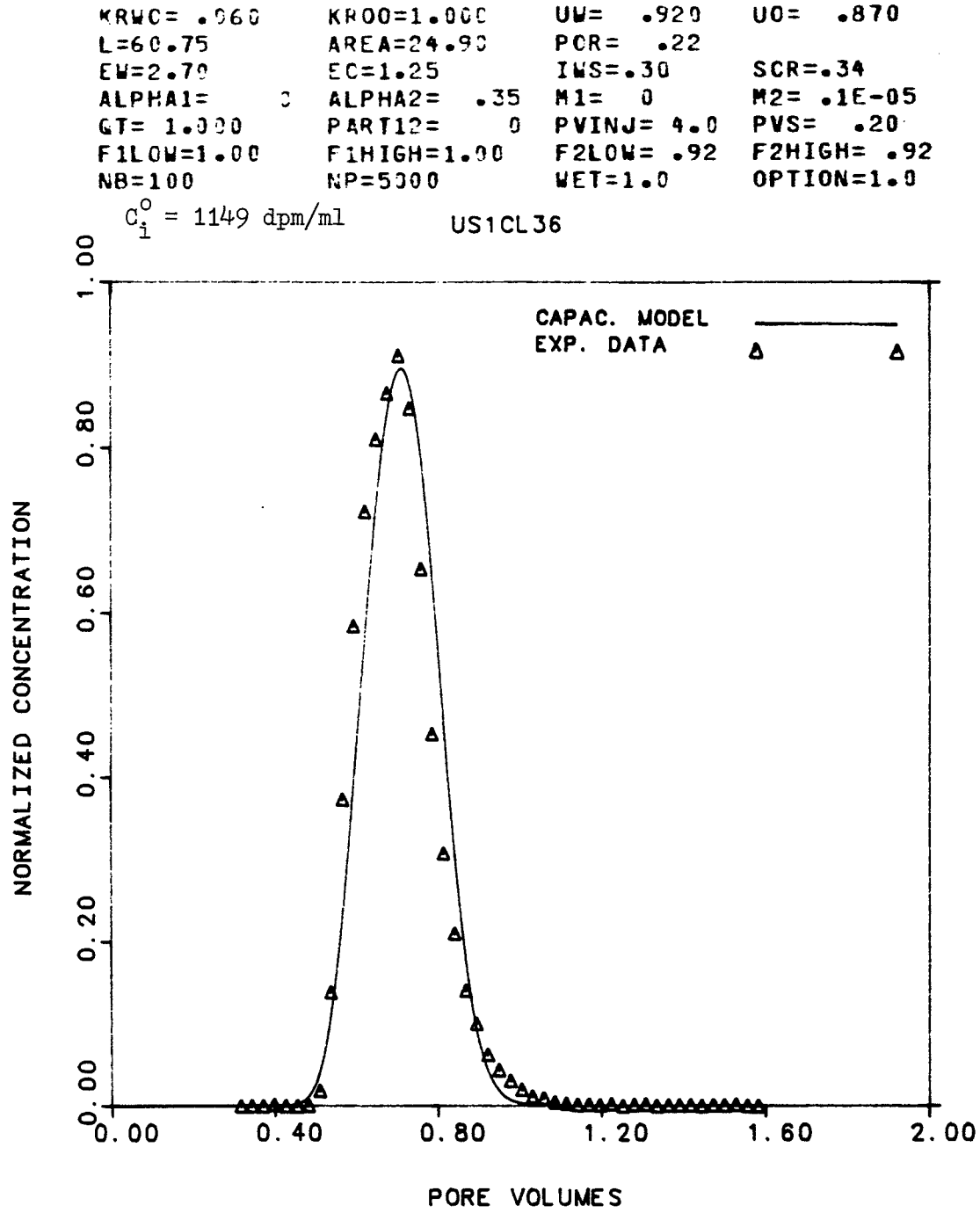

Figure 8-2 Tracer concentration versus pore volumes for water-wet Berea, waterflood experiment USS.1. Chlorine-36.

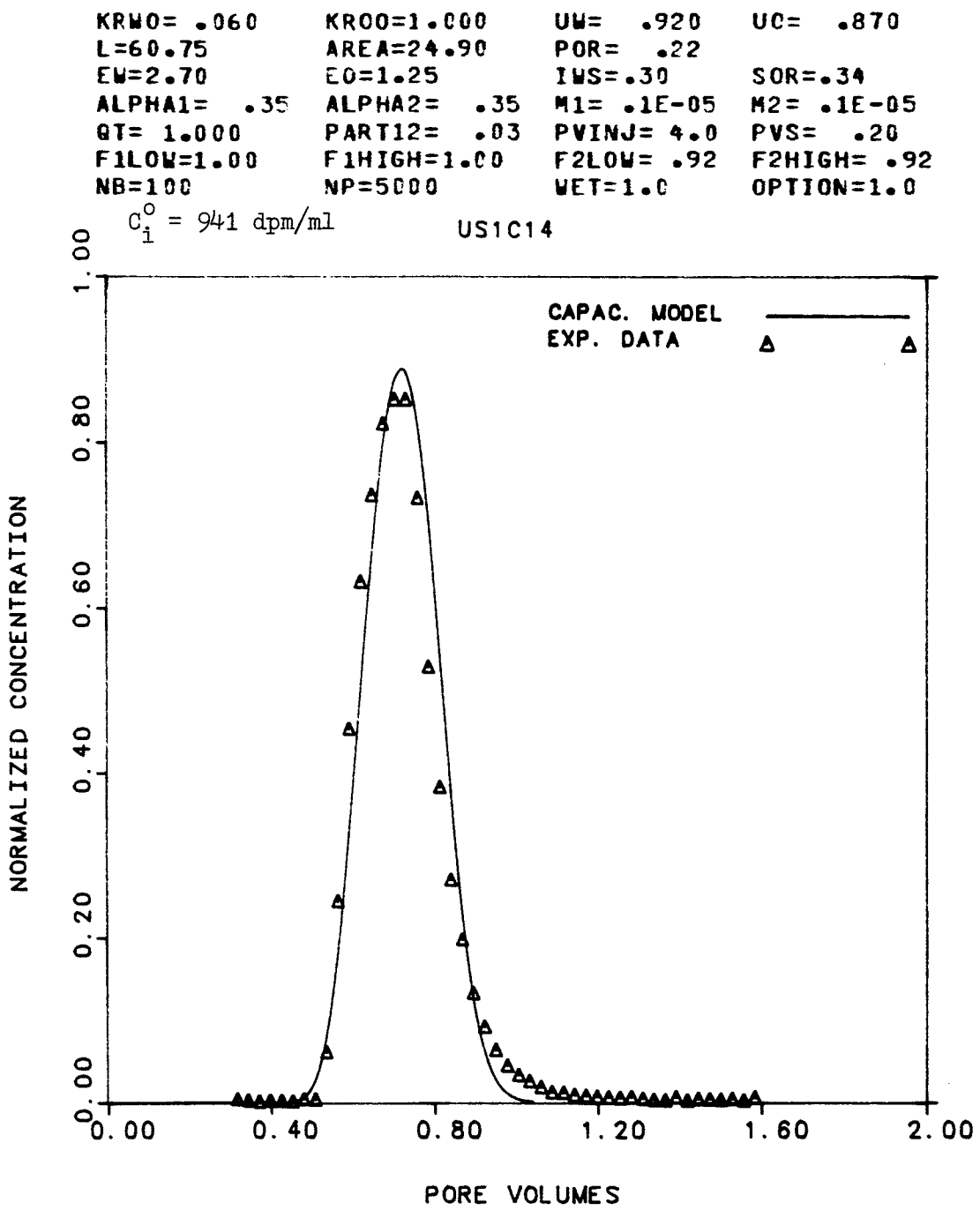

Figure 8-3 Tracer concentration versus pore volumes for water-wet Berea, waterflood experiment USS.1. Carbon-14 labelled IPA.

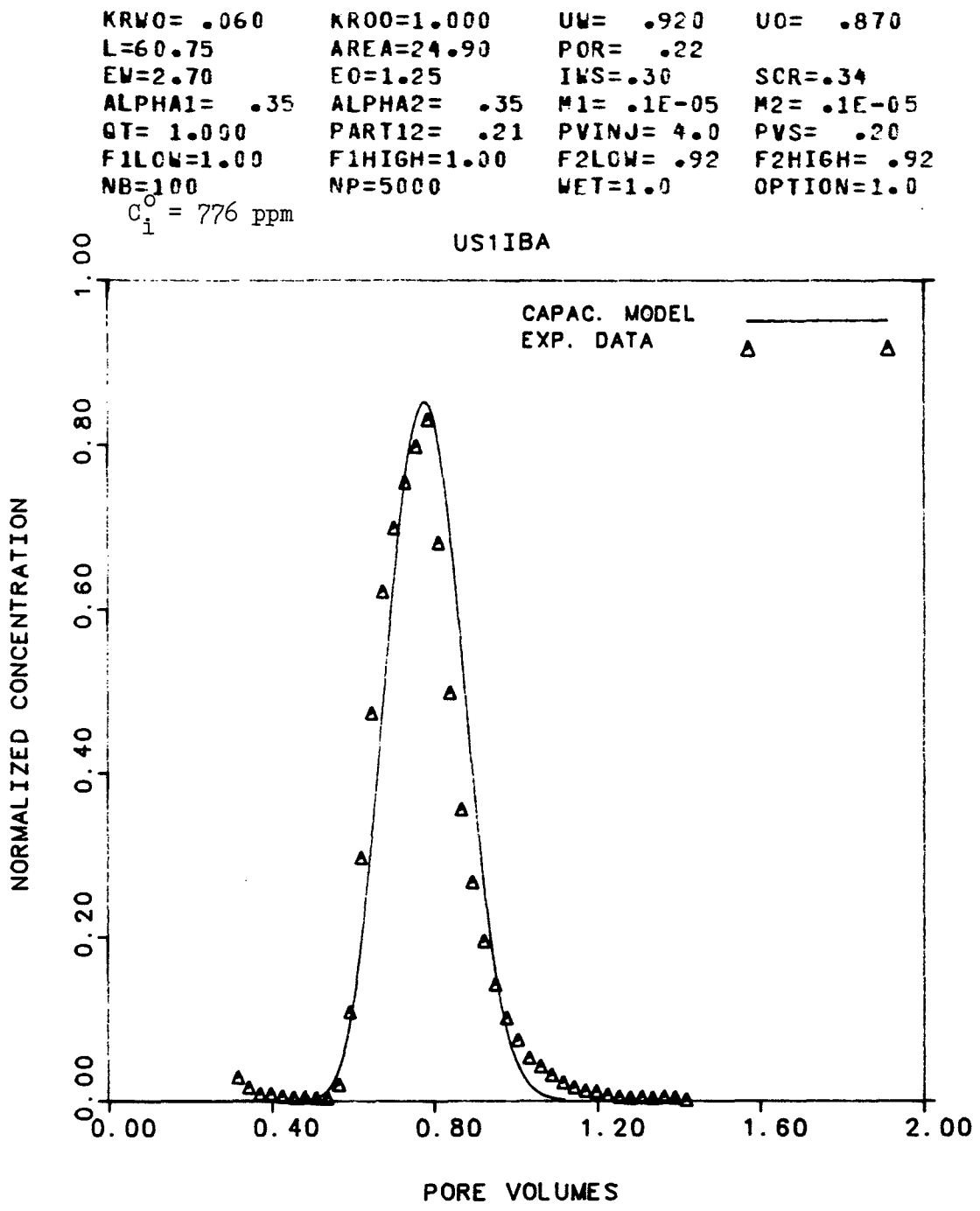

Figure 8-4 Tracer concentration versus pore volumes for water-wet Berea, waterflood experiment USS.1. IBA.

S1= .700	S2= .300	F1=1.00	F2=1.00
AREA=25.95	L=60.85	POR= .204	
ALPHA1= .30	ALPHA2= 0.00	M1= .00E+00	M2= .00E+00
FF1=1.000	FF2=0.000	QT= 1.022	PART1= 0.00
NB= 50	NP=5000	PVINJ= 4.00	PVS= .200

C_i^o = 1388 dpm/ml

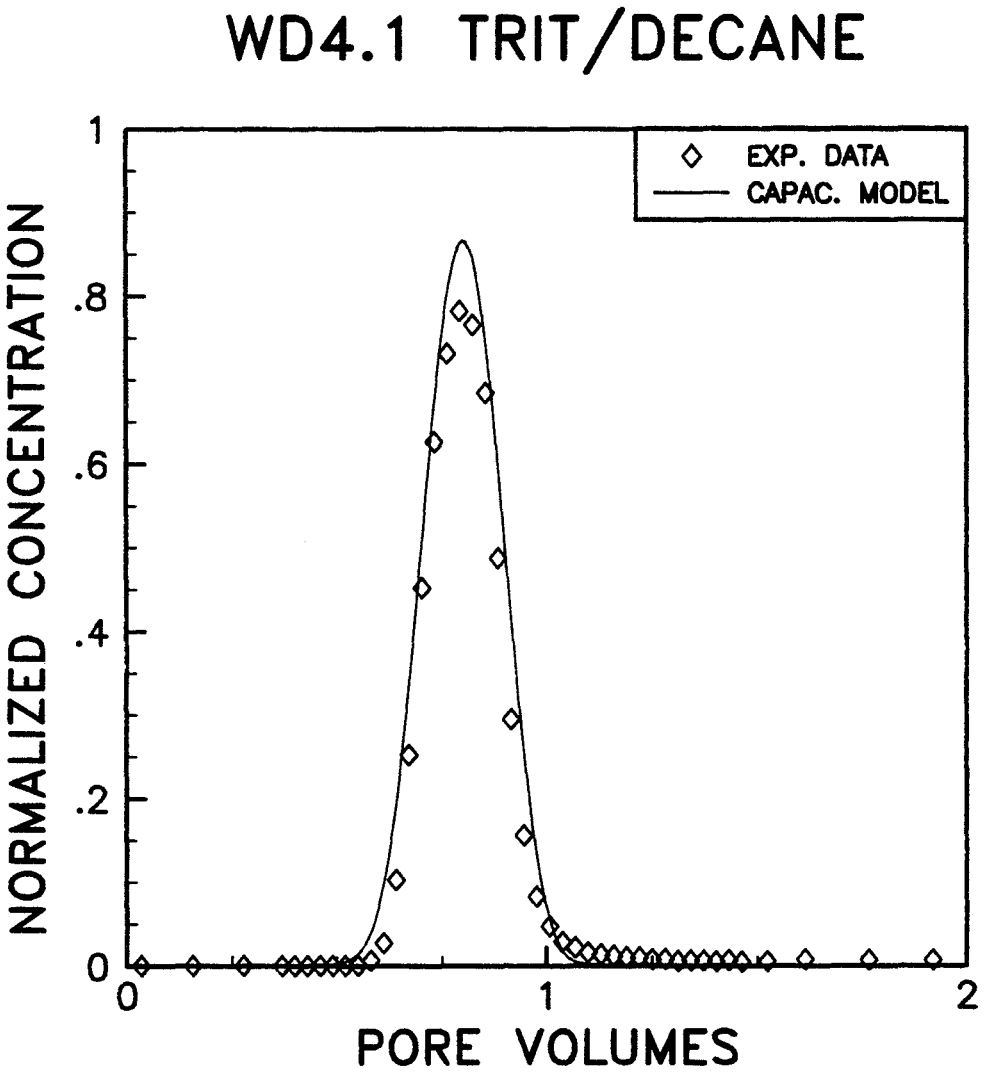

Figure 8-5 Tracer concentration versus pore volumes for treated core prior to experiment USS.2. Tritiated decane.

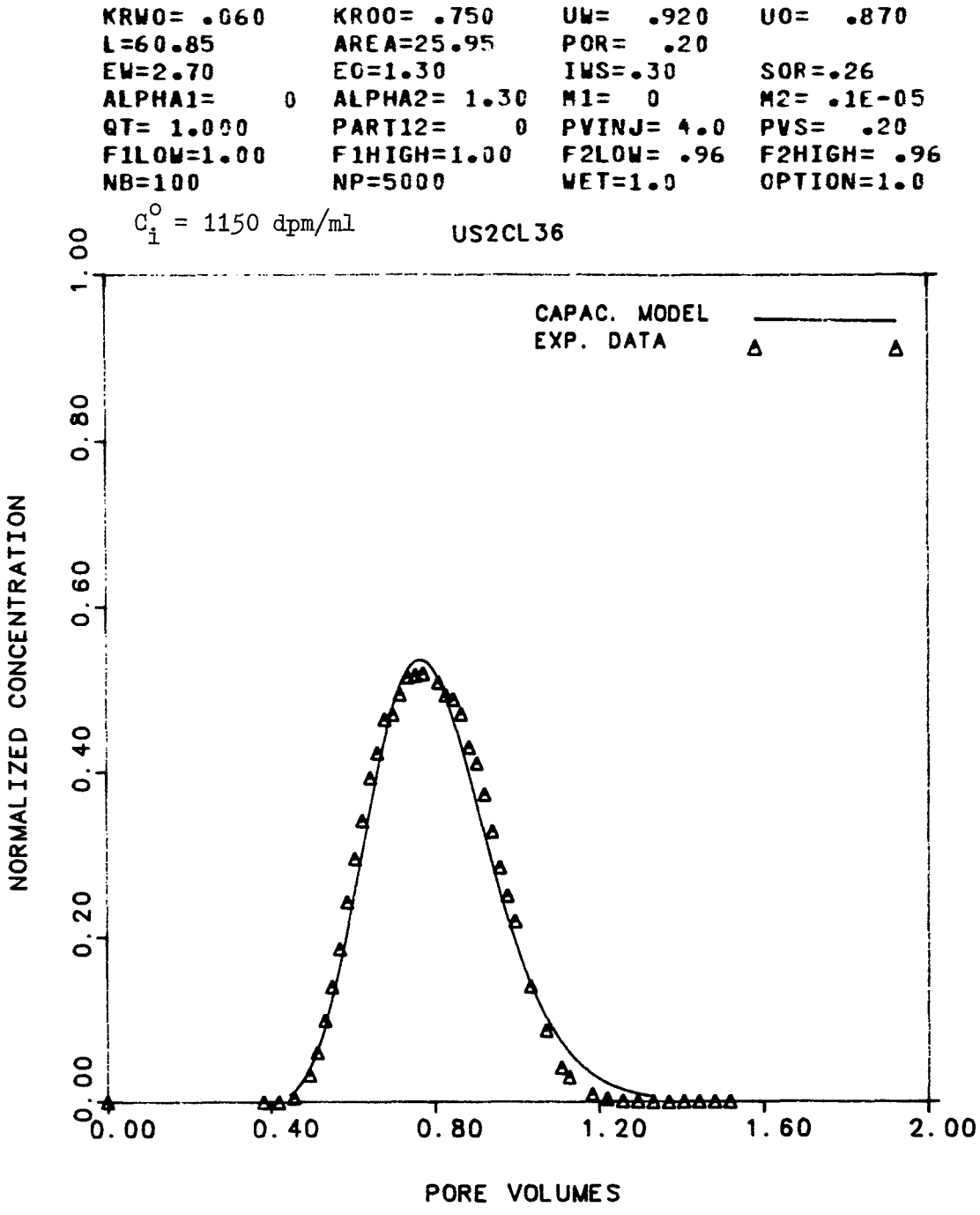

Figure 8-6 Tracer concentration versus pore volumes for treated core, waterflood experiment USS.2. Chlorine-36.

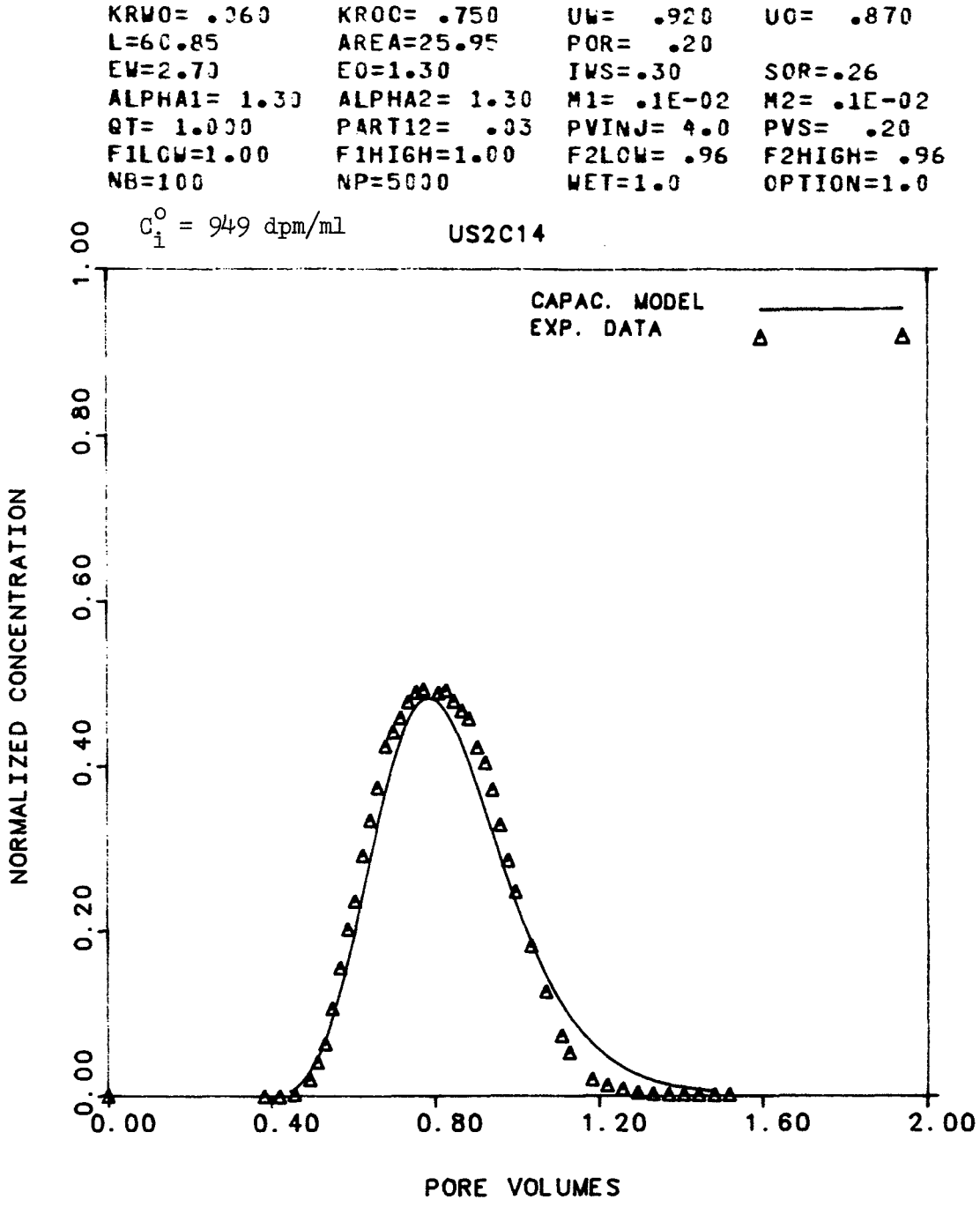

Figure 8-7 Tracer concentration versus pore volumes for treated core, waterflood experiment USS.2. Carbon-14 labelled IPA.

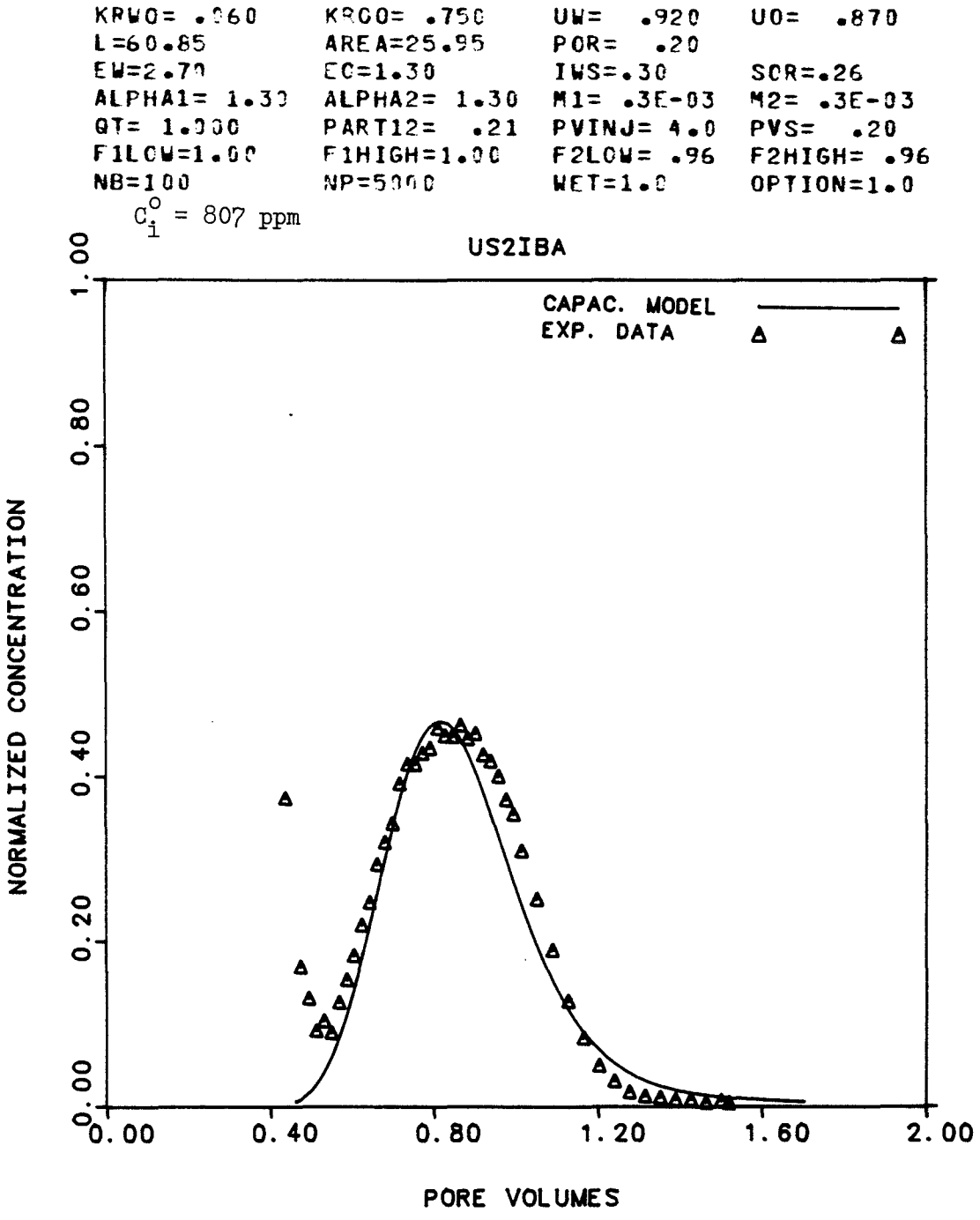

Figure 8-8 Tracer concentration versus pore volumes for treated core, waterflood experiment USS.2. IBA.

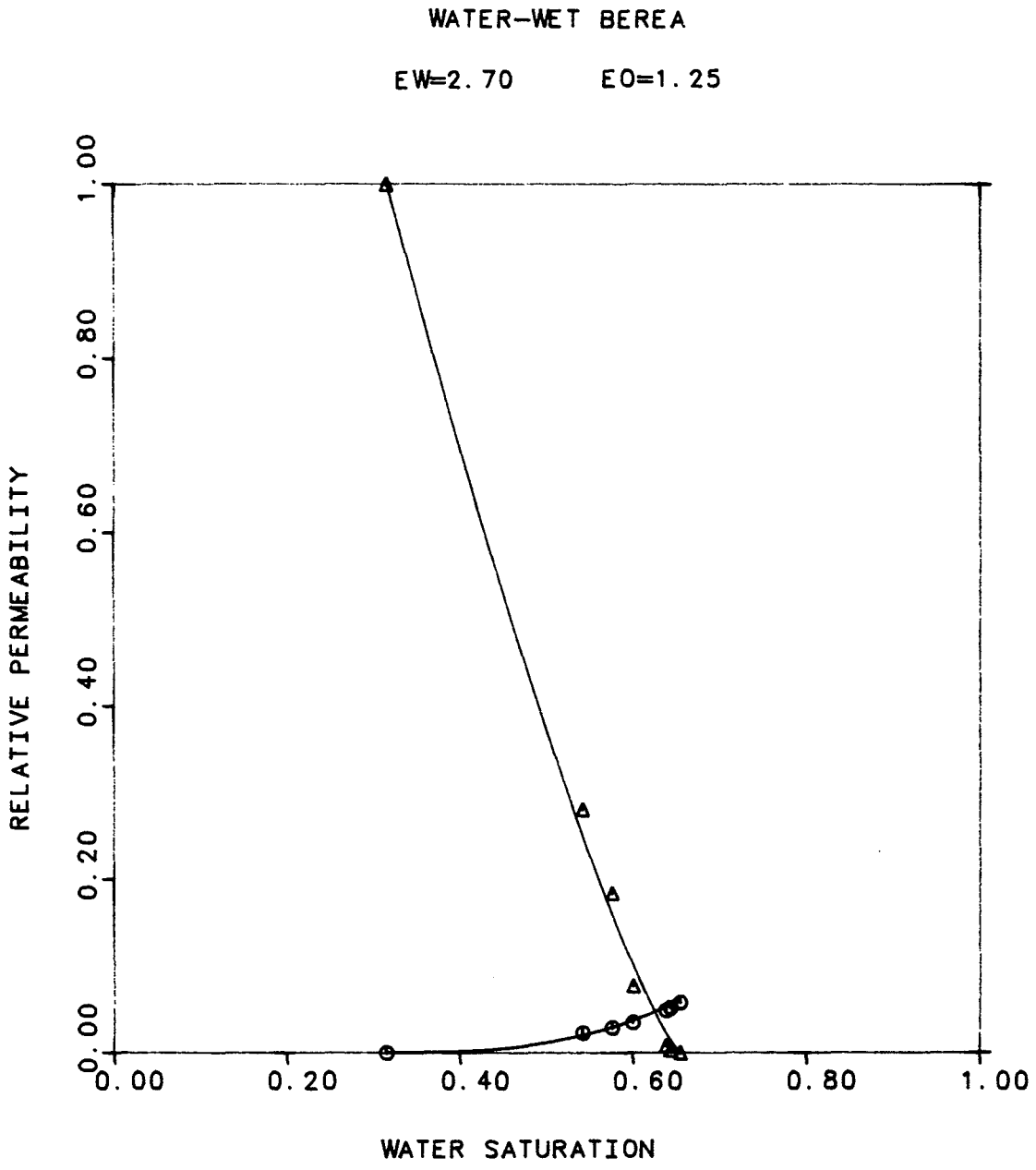

Figure 8-9 Fit of relative permeability data of water-wet core using simple equations.

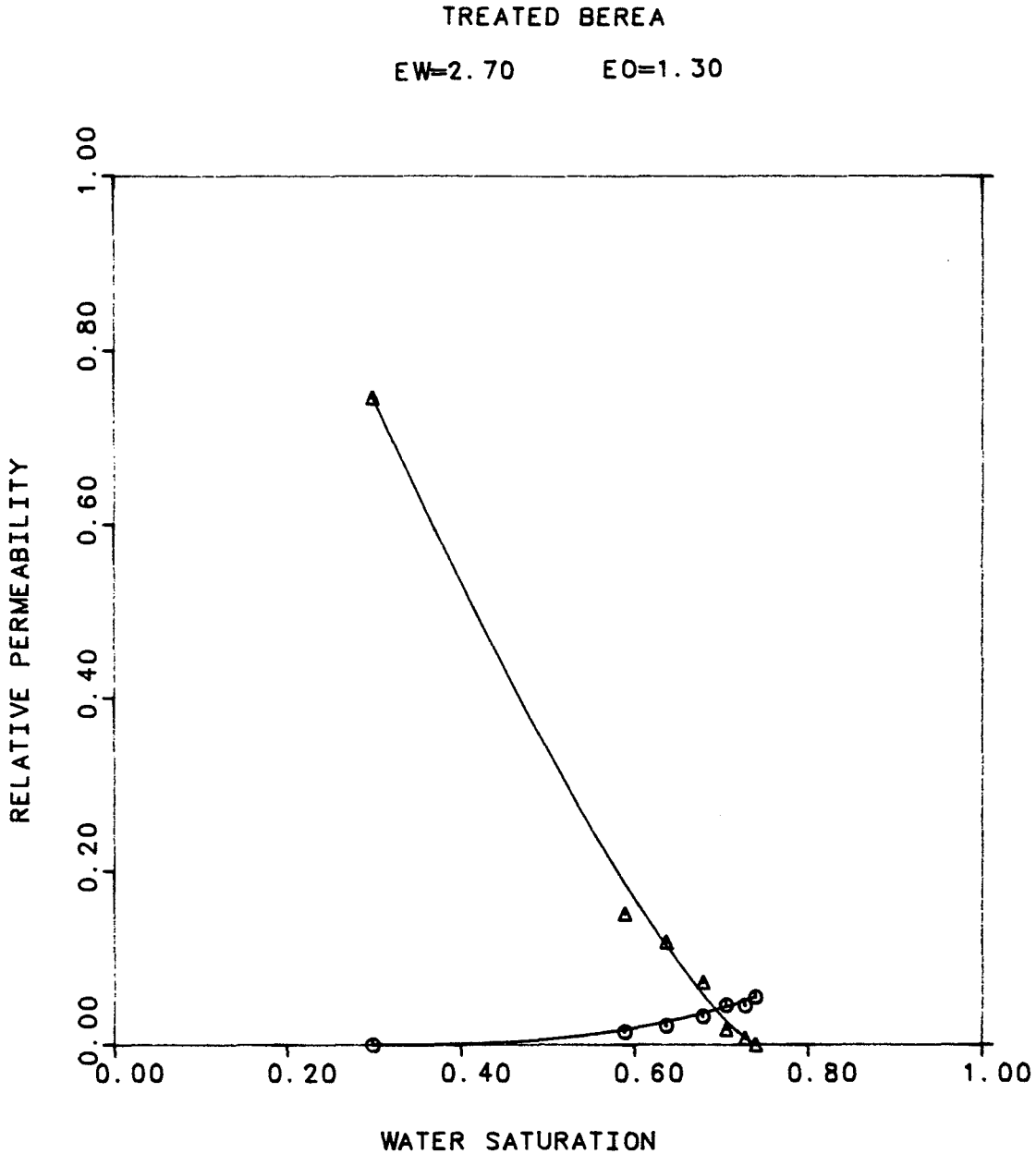

Figure 8-10 Fit of relative permeability data of treated core using simple equations.

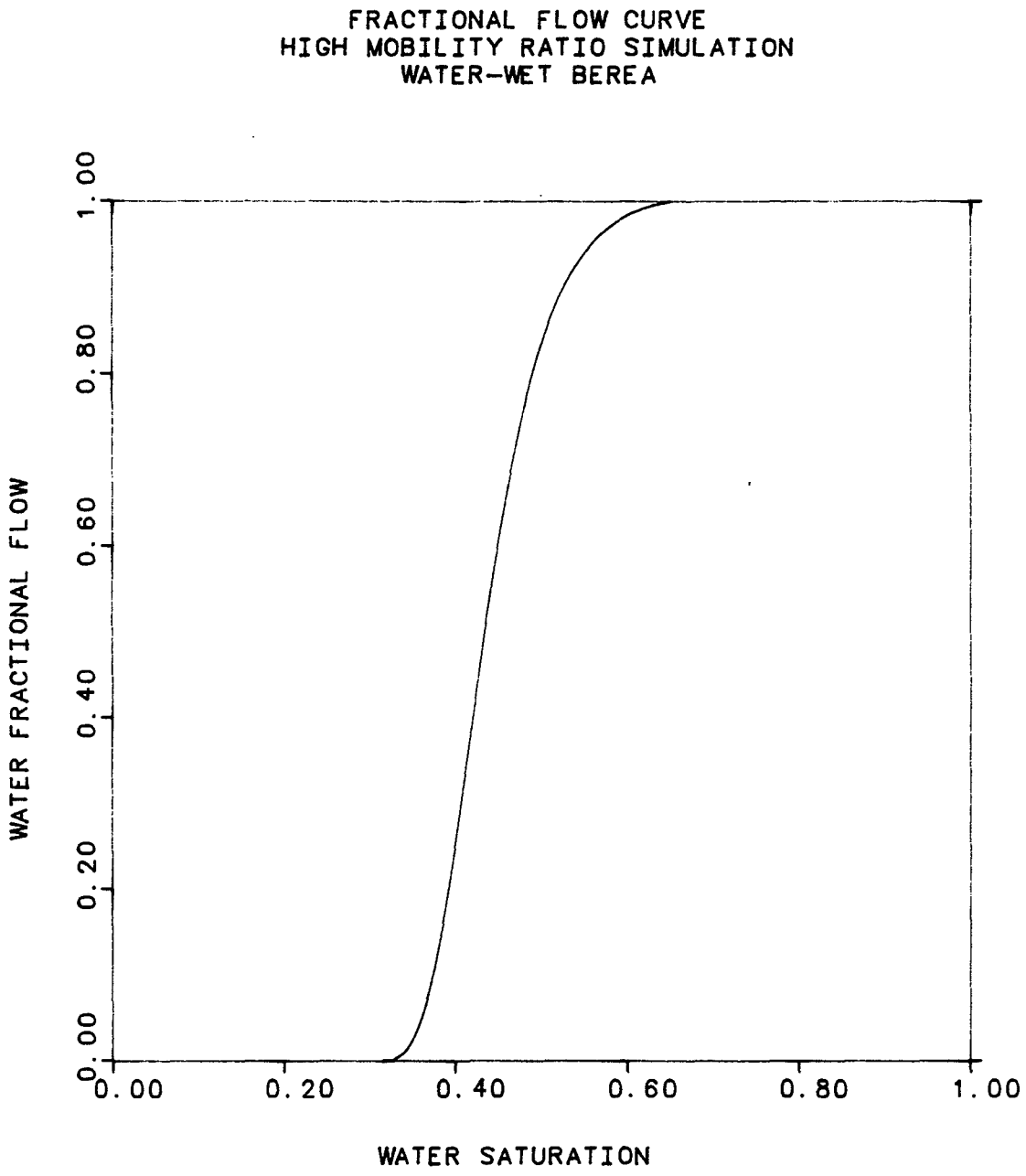

Figure 8-11 Calculated fractional flow curve for high mobility ratio simulation, water-wet core.

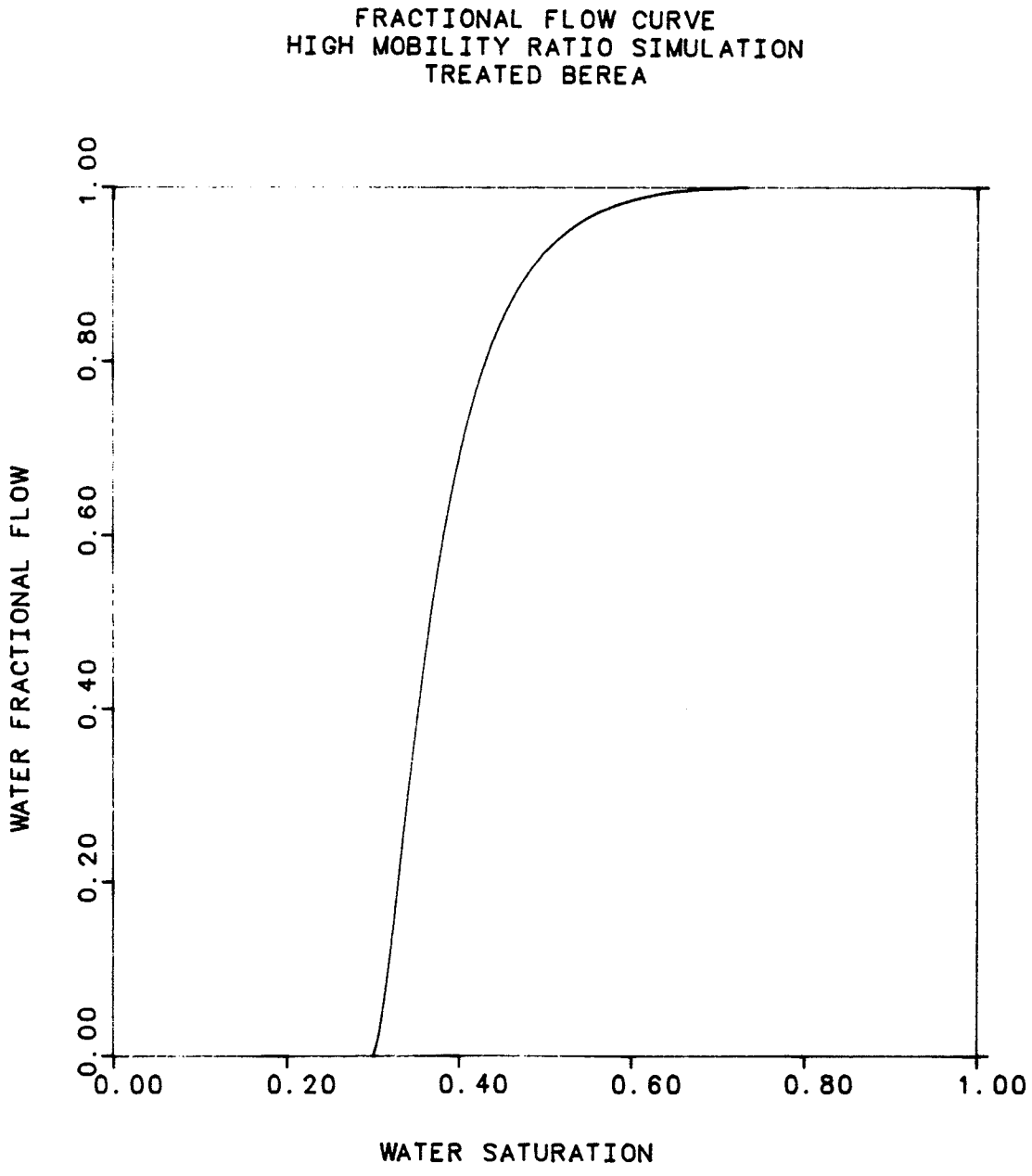

Figure 8-12 Calculated fractional flow curve for high mobility ratio simulation, treated core.

KRWC= .060	KRCC=1.000	UW= .920	UO=150.
L=60.75	AREA=24.90	POR= .22	
SW=2.70	SO=1.25	IWS=.30	SOR=.34
ALPHA1= 0	ALPHA2= .35	M1= 0	M2= .1E-05
QT= 1.000	PART12= 0	PVINJ= 4.0	PVS= .20
F1LOW= .17	F1HIGH= .98	F2LOW= .85	F2HIGH= .92
NB=100	NP=5000	WET=1.0	OPTION=1.0

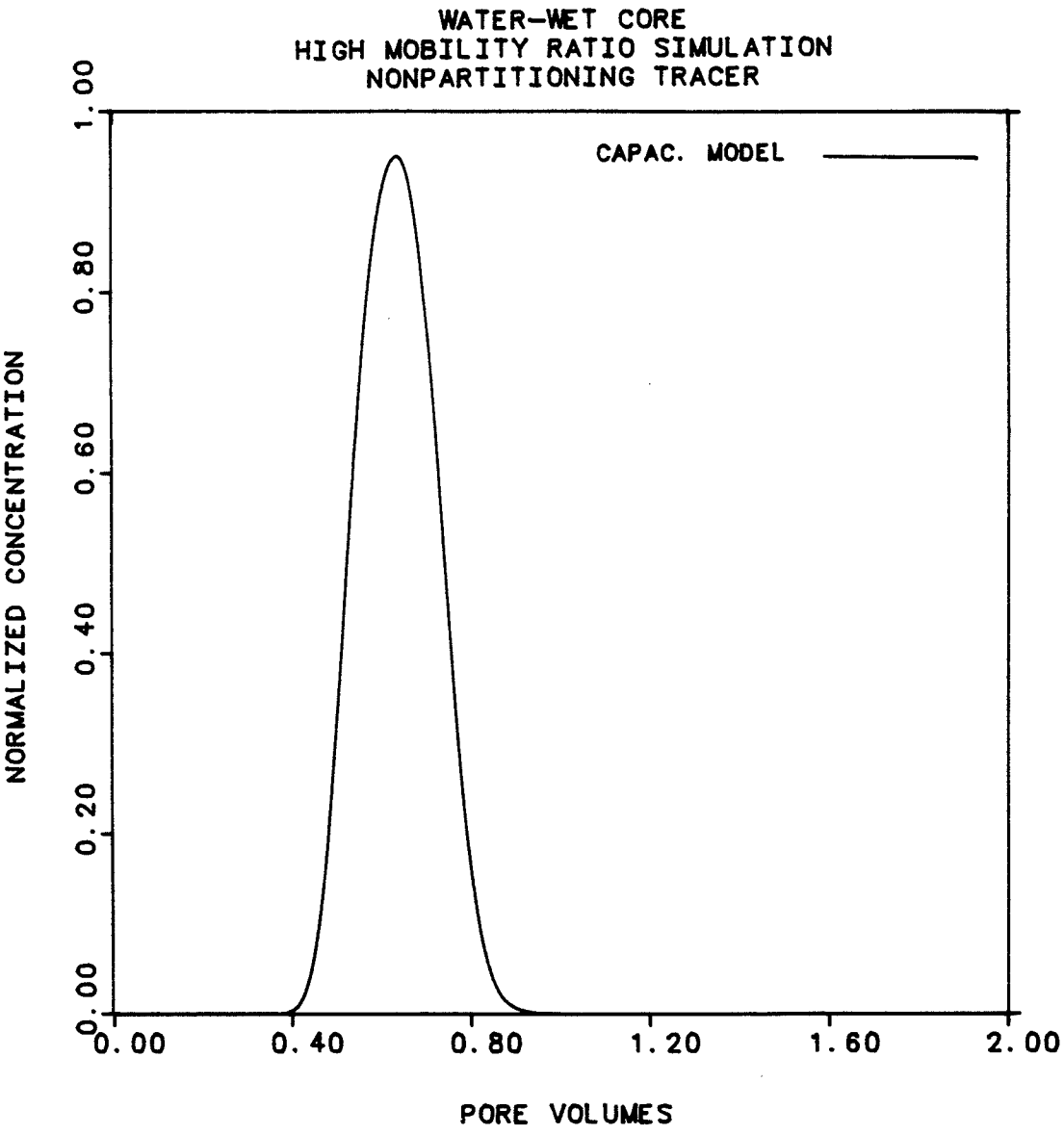

Figure 8-13 High mobility ratio waterflood simulation. Water-wet core, non-partitioning tracer.

KRWO= .060	KROO=1.000	UW= .920	UO=150.
L=60.75	AREA=24.90	POR= .22	
EW=2.70	EO=1.25	IWS=.30	SOR=.34
ALPHA1= .35	ALPHA2= .35	M1= .1E-05	M2= .1E-05
QT= 1.000	PART12= .21	PVINJ= 4.0	PVS= .20
F1LOW= .17	F1HIGH= .98	F2LOW= .85	F2HIGH= .92
NB=100	NP=5000	WET=1.0	OPTION=1.0

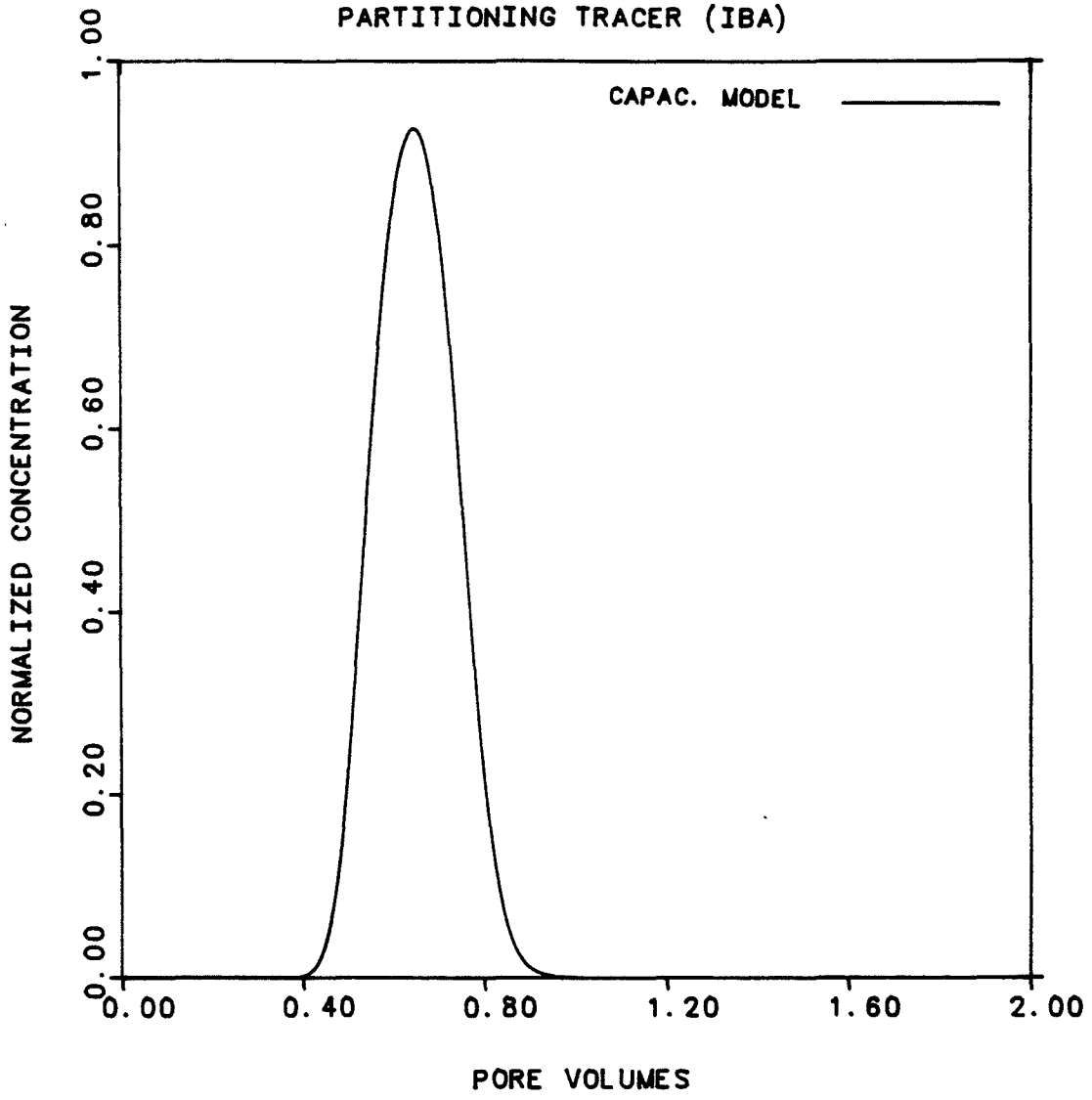

Figure 8-14 High mobility ratio waterflood simulation. Water-wet core, partitioning tracer.

KRWO= .360	KROO= .750	UW= .920	UO=150.
L=60.85	AREA=25.95	POR= .20	
FW=2.70	EO=1.30	IWS=.30	SOR=.26
ALPHA1= 0	ALPHA2= 1.30	M1= 0	M2= .1E-05
QT= 1.000	PART12= 0	PVINJ= 4.0	PVS= .20
F1LOW= .25	F1HIGH=1.00	F2LOW= .57	F2HIGH= .97
NB=100	NP=5000	WET=1.0	OPTION=1.0

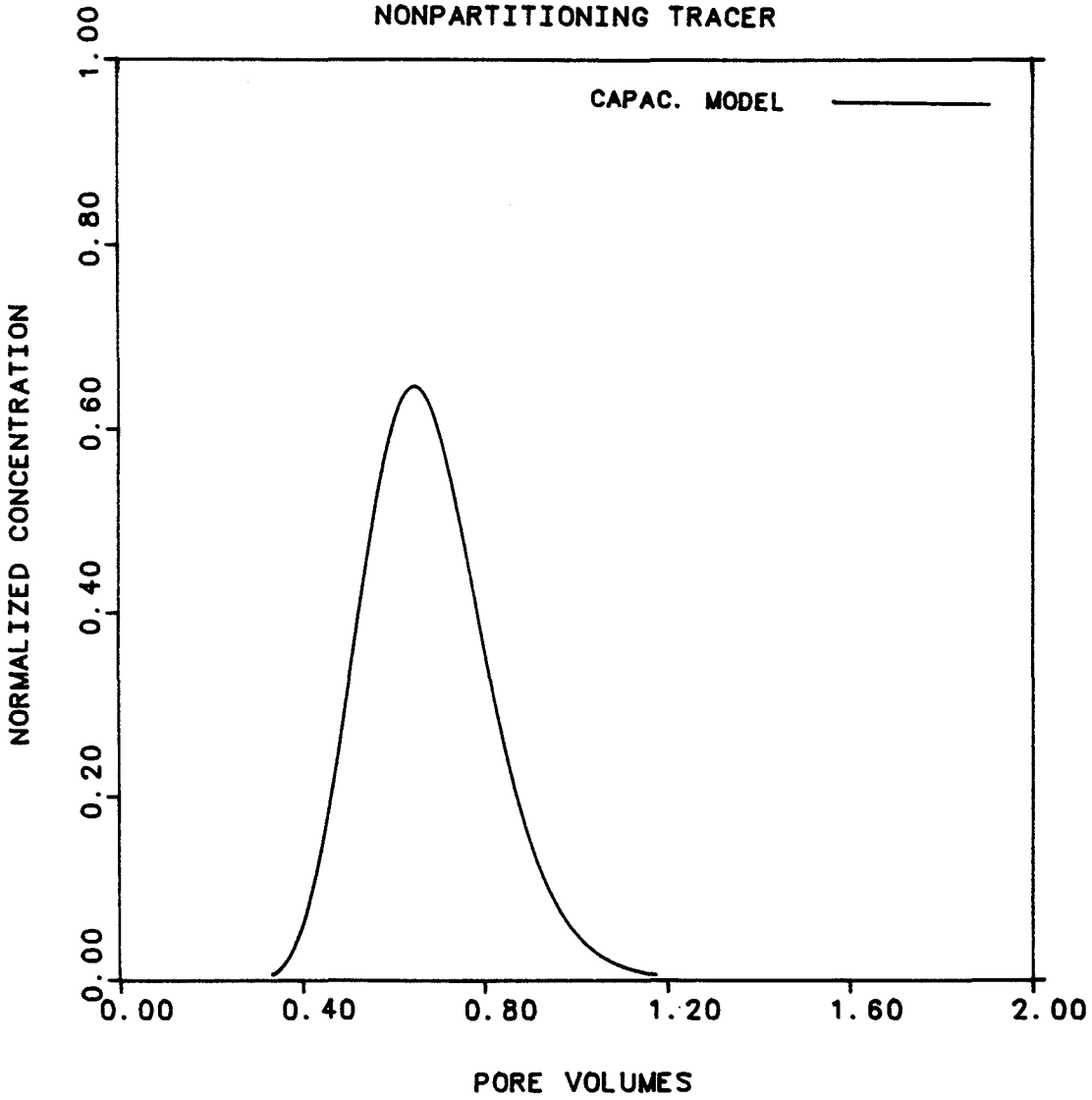

Figure 8-15 High mobility ratio waterflood simulation. Treated core, non-partitioning tracer.

KRWC= .960	KROO= .750	UW= .920	UO=150.
L=60.85	AREA=25.95	POR= .20	
DW=2.70	DO=1.30	IWS=.30	SOR=.26
ALPHA1= 1.30	ALPHA2= 1.30	M1= .3E-03	M2= .3E-03
QT= 1.000	PART12= .21	PVINJ= 4.0	PVS= .20
F1LOW= .25	F1HIGH=1.00	F2LOW= .57	F2HIGH= .97
NB=100	NP=5000	WET=1.0	OPTION=1.0

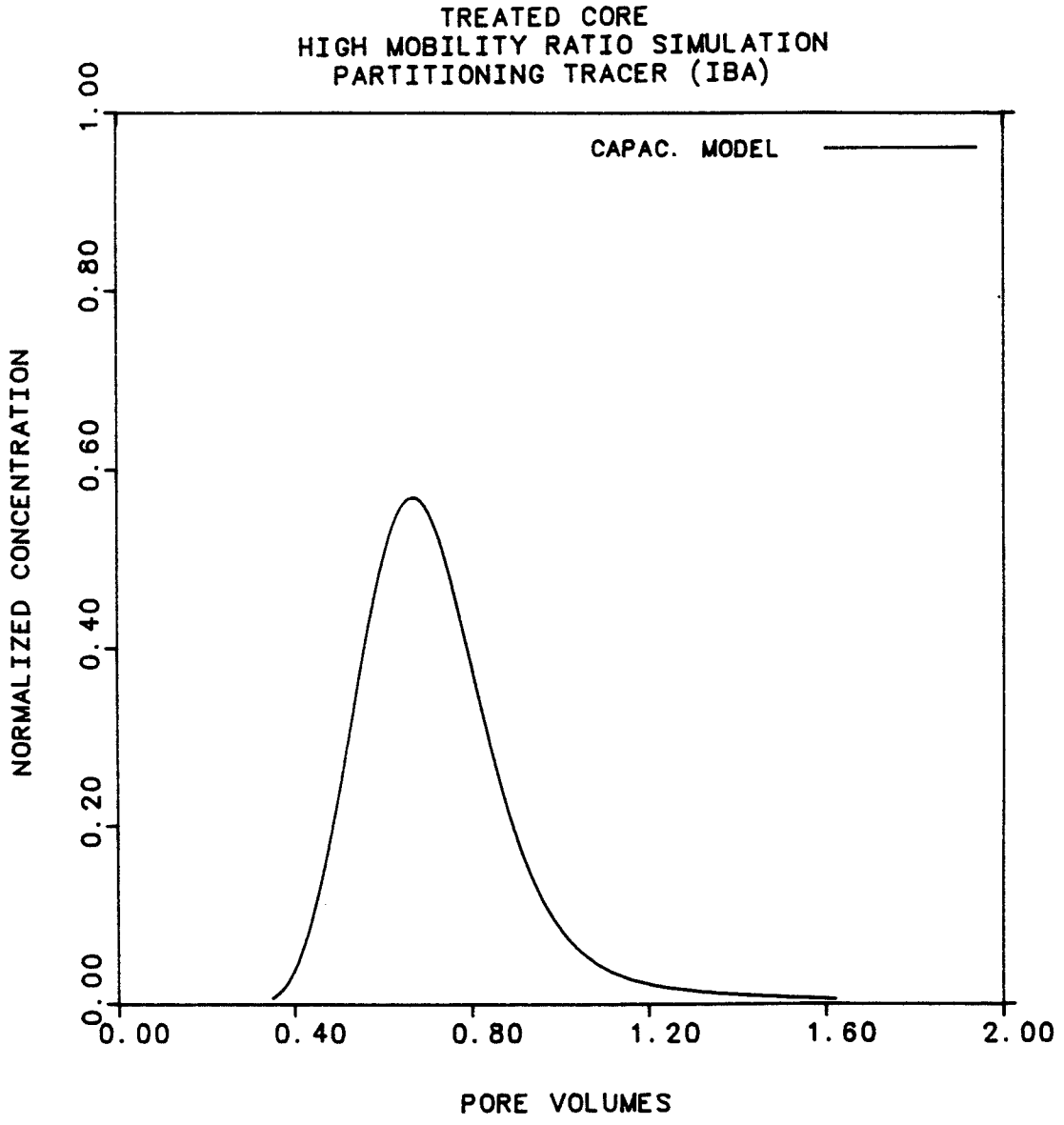

Figure 8-16 High mobility ratio waterflood simulation. Treated core, partitioning tracer.

CHAPTER 9

CONCLUSIONS

Computer models have been used successfully to predict the behavior of tracers during steady- and unsteady-state measurements. It has been shown that partitioning and nonpartitioning tracers can be used to determine saturations during steady-state measurements and at the endpoints of unsteady-state measurements. Instantaneous values of saturation can also be determined at any time during the unsteady-state measurements.

Parameter values determined from steady-state measurements can be used as input for a computer model that predicts tracer behavior during waterfloods. These parameters include endpoint saturation, dispersivity, flowing fraction, and mass transfer coefficient. Thus it has been shown that the unsteady-state model discussed here can be used to characterize cores and gives parameter values very close to those determined from a steady-state model.

Wettability has been shown to affect capacitance behavior, dispersion, and endpoint saturation. A linear dependence of phase flowing (nondendritic) fraction on fractional flow was observed, confirming an assumption made in the unsteady-state model. A stronger dependence was seen in the neutrally wet core. For both cores, as the saturation of a phase increased, the dendritic fraction of that phase decreased. A dependence of water dispersivity on saturation was seen for the neutrally wet core, but not for the water-wet core. A dependence of oil dispersivity on saturation was seen for both cores and was stronger for the neutrally wet core.

With the steady-state dispersion-capacitance model, good fits of experimental data were difficult to achieve when the flowing fraction was less than 0.3 for the particular phase that was being modeled. Future work is needed, for example, to determine if better fits can be obtained by considering more than one mass transfer rate for a particular experiment.

A very low endpoint mobility ratio existed for the unsteady-state waterflood experiments reported here. This resulted in plug flow; therefore, simultaneous two-phase flow did not occur in any part of the core. To further determine the validity of the unsteady-state model presented here, waterflood experiments with a high mobility ratio should be carried out.

A method proposed by Deans (1978) that would allow independent saturation determination was examined. As discussed in Appendix K, predictions of the Deans' model were compared with those of the unsteady-state model given here. It was found that the results did not agree at all, and therefore, Deans' model is probably not valid.

NOMENCLATURE

a	$\frac{\phi ML}{v}$, Equation (2-18).
A	Cross-sectional area.
A_1	Area under the oil-drive centrifugal capillary pressure curve, USBM method.
A_2	Area under the brine-drive centrifugal capillary pressure curve, USBM method.
C_D	Normalized (dimensionless) tracer concentration.
C_i	Concentration of tracer i, single-phase experiment.
C_i^0	Concentration of tracer i in the injected slug.
C_{ij}^f, C_{ij}^d	Concentration of tracer i in the flowing and dendritic fractions of Phase j.
C_{i2}^0	Concentration of tracer i in the injected slug of water.
D	Molecular diffusion coefficient.
F	Flowing fraction, single-phase, Coats-Smith model, Equation (2-17).
F_j	Flowing fraction of Phase j (Coats-Smith model). F is the fraction of the fluid that is flowing, and (1 − F) is the dendritic fraction.
F_R	Formation electrical resistivity factor, Equation (2-1).
f_j	Fractional flow of Phase j.
$\bar{f}$	Weighted average fractional flow, Equation (4-10).
k_w	Permeability to 100 percent water.
k_j	Effective permeability of Phase j.
k_{rj}	Relative permeability of Phase j.
K_l	Longitudinal dispersion coefficient.
K_t	Transverse dispersion coefficient.
K_{ij}	Dispersion coefficient of tracer i in Phase j.
$\bar{K}_i$	Weighted average dispersion coefficient, Equation (A-10).

L	Length.
M_{ij}	Mass transfer coefficient of tracer i in Phase j.
$M_{D_{ij}}$	Damkohler number.
N_{Pe}	Peclet Number.
P	Pressure.
P_{ijk}	Partition coefficient of tracer i between Phases j and k.
q	Total flow rate of water and oil.
S_j	Total saturation of Phase j (flowing and dendritic).
S_j^f, S_j^d	Saturation of the flowing and dendritic fractions of Phase j.
$\bar{S}$	Weighted average saturation, Equation (4-9).
SOR	Residual oil saturation.
SWI	Irreducible water saturation.
t	Time.
t_D	Dimensionless time (pore volumes).
t_i^{BT}	Breakthrough time of tracer i (at 50 percent concentration).
t_{Di}^{BT}	Dimensionless breakthrough time of tracer i.
t_{DS}	Dimensionless slug size (pore volumes).
v	Velocity = $q/A\phi$.
v_j	Frontal velocity of Phase j.
v_T	Modified frontal velocity, Equation (A-5).
V_E	Volume of fluid between the outlet of the core and the collector.
V_P	Pore volume.
$(V_o)_{spontaneous}$	Volume of oil displaced by spontaneous imbibition of water, Amott method.
$(V_w)_{spontaneous}$	Volume of water displaced by spontaneous imbibition of oil, Amott method.
$(V_o)_{total}$	Total volume of oil displaced, Amott method.
$(V_w)_{total}$	Total volume of water displaced, Amott method.
W	U.S. Bureau of Mines (USBM) wettability index.

W_I	Cumulative water injected.
x	Distance.
x_D	Dimensionless distance.
α_l	Longitudinal dispersivity.
α_t	Transverse dispersivity.
α_{ij}	Dispersivity of tracer i in Phase j.
$\alpha_{D_{ij}}$	Dimensionless dispersivity of tracer i in Phase j.
$\bar{\alpha}_D$	Weighted average dimensionless dispersivity, Equation (4-8).
β_l, β_t	Dispersion parameters.
μ_1	Oil viscosity.
μ_2	Water viscosity.
ϕ	Porosity.

SUBSCRIPTS

i	Tracer i.
j	Fluid j, 1 = oil, 2 = water.
k	Fluid k, 1 = oil, 2 = water.

FORTRAN NOMENCLATURE

ALPHA1	Oil dispersivity (cm).
ALPHA2	Water dispersivity (cm).
AREA	Cross-sectional area of core (cm^2).
EO,EW	Relative permeability exponents for oil, water.
FF1, FF2	Fractional flow of oil, water.
F1, F2	Flowing fraction of oil, water.
F1HIGH	Maximum flowing fraction of oil.
F1LOW	Minimum flowing fraction of oil.
F2HIGH	Maximum flowing fraction of water.
F2LOW	Minimum flowing fraction of water.
IWS	Irreducible water saturation.
KROO	Endpoint relative permeability of oil.
KRWO	Endpoint relative permeability of water.
L	Length of core (cm).
M1, M2	Mass transfer coefficient of oil, water.
NB	Number of blocks.
NP	Number of time steps.
OPTION	Choice of relative permeability equations.
PART12	Partition coefficient.
POR	Porosity of core.
PVINJ	Total pore volumes injected.
PVS	Pore volume of tracer slug.
QT	Total flow rate (cm^3/s).

S1, S2	Oil, water saturation.
SOR	Residual oil saturation.
UW, UO	Water, oil viscosity (cp).
WET	Choice of water- or oil-wet equations.

APPENDIX A

TWO-PHASE CONVECTION-DIFFUSION EQUATION

In the Introductory section, we derived the single-phase convection-diffusion equation. A similar equation can be derived for two-phase flow, with partitioning or nonpartitioning tracers. This equation is helpful in *qualitatively* modeling the flow of tracers in porous media. It can also be used to estimate some of the flow parameters, as explained in Appendix D. However, it should *not* be used to determine dispersivity and other parameters, since neglecting capacitance effects can cause serious errors. For example, Delshad (Mohammad Delshad, 1984) found errors of 30 percent in estimating saturation when capacitance was neglected. For this reason, the convection-diffusion equation should only be used for rough estimates. The capacitance-dispersion model should be used to obtain more accurate numbers.

For two-phase flow, the convection-diffusion equation is similar to the equation for the single-phase flow case, Equation (2-3). The material balance equation for a partitioning tracer of concentration C_{ij} is given by:*

$$\phi A \frac{\partial}{\partial t}\left(S_1 C_{i1} + S_2 C_{i2}\right) + q \frac{\partial}{\partial x}\left(f_1 C_{i1} + f_2 C_{i2}\right) = \phi A \frac{\partial}{\partial x}\left(S_1 K_{i1} \frac{\partial C_{i1}}{\partial x} + S_2 K_{i2} \frac{\partial C_{i2}}{\partial x}\right) \tag{A-1}$$

*See Equations (3-1) to (3-6) for derivation of the more general case with dendritic and flowing saturations.

where we have made the assumption that there is no dendritic fluid. Phase saturations and fractional flows are constant, and only the tracer concentrations are functions of x and t. The relationship between the tracer concentrations in the two phases is given by the equation for the partitioning coefficient:

$$C_{i1} = P_{i12}\, C_{i2} \tag{A-2}$$

Substituting into Equation (A-1):

$$\phi A \left(S_1 P_{i12} + S_2\right) \frac{\partial}{\partial t} C_{i2} + q \left(f_1 P_{i12} + f_2\right) \frac{\partial}{\partial x} C_{i2} = \phi A \left(S_1 K_{i1} P_{i12} + S_2 K_{i2}\right) \frac{\partial^2}{\partial x^2} C_{i2} \tag{A-3}$$

By defining the appropriate variables, Equation (A-1) can be reduced to the dimensionless single-phase equation (Delshad, MacAllister, Pope, and Rouse, 1985):

1. Dimensionless time

$$t_{DT} = \frac{qt}{AL\phi}\left(\frac{f_1 P_{i12} + f_2}{S_1 P_{i12} + S_2}\right) = \frac{t\, v_T}{L} \tag{A-4}$$

Where v_T is the modified frontal velocity:

$$v_T = \frac{q}{A\phi}\left(\frac{f_1 P_{i12} + f_2}{S_1 P_{i12} + S_2}\right) \tag{A-5}$$

2. Dimensionless distance

$$X_D = \frac{X}{L} \tag{A-6}$$

3. Dimensionless tracer concentration

$$C_D = \frac{C_{i2}}{C_{i2}^0} \tag{A-7}$$

where C_{i2}^0 is the injected tracer concentration in Phase 2. Substituting Equations (A-4) to (A-7) into the convection-diffusion equation (Equation (A-3)) and simplifying the coefficients:

$$\frac{C_{i2}^0\, q\, (f_1 P_{i12} + f_2)}{L} \frac{\partial C_D}{\partial t_{DT}} + \frac{C_{i2}^0\, q\, (f_1 P_{i12} + f_2)}{L} \frac{\partial C_D}{\partial x_D} = \frac{C_{i2}^0\, \phi A\, (S_1 K_1 P_{i12} + S_2 K_2)}{L^2} \frac{\partial^2 C_D}{\partial x_D^2} \tag{A-8}$$

which can be written as:

$$\frac{\partial C_D}{\partial t_{DT}} + \frac{\partial C_D}{\partial x_D} = \frac{\phi A\, (S_1 K_1 P_{i12} + S_2 K_2)}{q\, (f_1 P_{i12} + f_2)} \frac{(S_1 P_{i12} + S_2)}{(S_1 P_{i12} + S_2)} \frac{\partial C_D^2}{\partial x_D^2} \tag{A-9}$$

Define the weighted average of the dispersion coefficient $\bar{K}_i$ as:

$$\bar{K}_i = \frac{S_1 K_1 P_{i12} + S_2 K_2}{S_1 P_{i12} + S_2} \tag{A-10}$$

Substituting Equations (A-5) and (A-10) into Equation (A-9) and simplifying:

$$\frac{\partial C_D}{\partial t_{DT}} + \frac{\partial C_D}{\partial x_D} = \frac{\bar{K}_i}{L v_T} \frac{\partial^2 C_D}{\partial x_D^2} \tag{A-11}$$

Defining a weighted average Peclet Number:

$$\bar{N}_{Pe} = \frac{L\, v_T}{\bar{K}_l} \tag{A-12}$$

Substituting Equation (A-12) into Equation (A-11):

$$\frac{\partial C_D}{\partial t_{DT}} + \frac{\partial C_D}{\partial x_D} = \frac{1}{\bar{N}_{Pe}} \frac{\partial^2 C_D}{\partial x_D^2} \tag{A-13}$$

This equation has the same form as the single-phase convection-diffusion equation.

APPENDIX B

FINITE DIFFERENCE EQUATIONS FOR THE UNSTEADY-STATE MODEL

The dimensionless equations for the unsteady-state model are summarized in Table 3-1. Before converting the equations to the finite difference form, the following equations are introduced for computational convenience:

$$\bar{S} = S_1^f P_{i12} + S_2^f \tag{B-1a}$$

$$\bar{f} = f_1 P_{i12} + f_2 \tag{B-2a}$$

Introducing these into the tracer material balance equation (Equation (3-40)), we have:

$$\frac{\partial}{\partial t_D}(C_{D_{i2}}^f \bar{S}) + \frac{\partial}{\partial t_D}(C_{D_{i1}}^d S_1^d) + \frac{\partial}{\partial t_D}(C_{D_{i2}}^d S_2^d) + \frac{\partial}{\partial x_D}(C_{D_{i2}}^f \bar{f}) = \frac{\partial}{\partial x_D}\bar{\alpha}_D\left(\frac{\partial}{\partial x_D} C_{D_{i2}}^f\right) \tag{B-3}$$

DERIVATIVES IN FINITE DIFFERENCE FORM

The equations must be put into finite difference form before they can be solved. There are NB blocks in the core, with Block 1 at the inlet end and Block NB at the outlet end. Block 0 is the inlet, and Block NB + 1 is the outlet.

The finite difference forms of the partial derivatives will be written using a forwards-in-time, backwards-in-space formulation. The following finite difference forms of the partial derivatives will be used:

$$\frac{\partial}{\partial x} u = \frac{[u]_K^N - [u]_{K-1}^N}{\Delta x} \tag{B-4}$$

where the superscript N refers to the time step and the subscript K to the block.

$$\frac{\partial^2}{\partial x^2} u = \frac{[u]_{K-1}^N - 2\,[u]_K^N + [u]_{K-1}^N}{(\Delta x)^2} \tag{B-5}$$

$$\frac{\partial^2}{\partial t} u = \frac{[u]_K^{N-1} - [u]_K^N}{\Delta t} \tag{B-6}$$

The dimensionless model equations can now be written in finite difference form using Equations (B-4) to (B-6). The subscript D indicating that the equations are nondimensionless will be *dropped*.

Tracer Material Balance

Using Equations (B-4) to (B-6), the tracer material balance equation (Equation (B-3)) becomes:

$$\frac{([C^f_{i2}\,\bar{S}]^{N-1}_K - [C^f_{i2}\,\bar{S}]^N_K)}{\Delta t} + \frac{([C^d_{i1}\,S^d_1]^{N+1}_K - [C^d_{i1}\,S^d_1]^N_K)}{\Delta t} +$$

$$\frac{([C^d_{i2}\,S^d_2]^{N-1}_K - [C^d_{i2}\,S^d_2]^N_K}{\Delta t} + \frac{([C^f_{i2}\,\bar{f}]^N_K - [C^f_{i2}\,\bar{f}]^N_{K-1})}{\Delta x} =$$

$$\frac{1}{(\Delta x)^2}\,\{[\bar{\alpha}]^N_K\,([C^f_{i2}]^N_{K-1} - [C^f_{i2}]^N_K) - [\bar{\alpha}]^N_{K-1}\,([C^f_{i2}]^N_K - [C^f_{i2}]^N_{K-1})\} \qquad \text{(B-7)}$$

One point upstream weighting is used on the dispersivity term.

Equation (B-7) involves three terms at the new time step (N + 1), with the remaining terms at the old time step. Solving for $C^f_{i2}\,\bar{S}$ at the new time step:

$$[C^f_{i2}\,\bar{S}]^{N-1}_K = [C^f_{i2}\,\bar{S}]^N_K - ([C^d_{i1}\,S^d_1]^{N-1}_K - [C^d_{i1}\,S^d_1]^N_K) -$$

$$([C^d_{i2}\,S^d_2]^{N-1}_K - [C^d_{i2}\,S^d_2]^N_K) - \frac{([C^f_{i2}\,\bar{f}]^N_K - [C^f_{i2}\,\bar{f}]^N_{K-1})}{\Delta x}\,\Delta t +$$

$$\frac{\Delta t}{(\Delta x)^2}\,\{[\bar{\alpha}]^N_K\,([C^f_{i2}]^N_{K-1} - [C^f_{i2}]^N_K) - [\bar{\alpha}]^N_{K-1}\,([C^f_{i2}]^N_K - [C^f_{i2}]^N_{K-1})\} \qquad \text{(B-8)}$$

2. Partitioning Coefficient

Equation (3-41) for the partitioning coefficient is written at the new time step, N + 1:

$$[C^f_{i1}]^{N-1}_K = P_{i12}\,[C^f_{i2}]^{N-1}_K \qquad \text{(B-9)}$$

3, 4. Rate Equations for Mass Transfer Between the Flowing and Dendritic Fractions

Equation (3-43) for the mass transfer in the oil becomes:

$$\frac{([C^d_{i1}\,S^d_1]^{N-1}_K - [C^d_{i1}\,S^d_1]^N_K)}{\Delta t} = M_{i1}\,([C^f_{i1}]^N_K - [C^d_{i1}]^N_K) \qquad \text{(B-10)}$$

Solving for $C_{i1}^d\ S_1^d$ at the new time step:

$$[C_{i1}^d\ S_1^d]_K^{N-1} = [C_{i1}^d\ S_1^d]_K^N + M_{i1}\ ([C_{i1}^f]_K^N - [C_{i1}^d]_K^N)\ \Delta t \qquad \text{(B-11)}$$

Similarly, Equation (3-44) for the mass transfer in the water becomes:

$$[C_{i2}^d\ S_2^d]_K^{N+1} = [C_{i2}^d\ S_2^d]_K^N + M_{i2}\ ([C_{i2}^f]_K^N - [C_{i2}^d]_K^N)\ \Delta t \qquad \text{(B-12)}$$

5, 6. Relationship Between Flowing and Dendritic Fractions

At the new time step, Equations (3-14) and (3-15) are:

$$[S_1^f]_K^{N-1} = \text{function}_1\ ([S_1]_K^{N-1}) \qquad \text{(B-13)}$$

$$[S_2^f]_K^{N-1} = \text{function}_2\ ([S_2]_K^{N-1}) \qquad \text{(B-14)}$$

7. Saturation Material Balance

Using Equations (B-4) to (B-6), the saturation material balance equation (Equation (3-46)) becomes:

$$\frac{([S_2]_K^{N-1} - [S_2]_K^N)}{\Delta t} + \frac{([f_2]_K^N - [f_2]_{K-1}^N)}{\Delta x} = 0 \qquad \text{(B-15)}$$

Solving for S_2 at the new time step:

$$[S_2]_K^{N-1} = [S_2]_K^N - \frac{([f_2]_K^N - [f_2]_{K-1}^N)}{\Delta x}\ \Delta t = 0 \qquad \text{(B-16)}$$

8, 9, 10. Saturation Constraints

Writing the saturation constraints, Equations (3-17) to (3-20), at the new time step and rearranging:

$$[S_1^d]_K^{N-1} = [S_1]_K^{N-1} - [S_1^f]_K^{N-1} \tag{B-17}$$

$$[S_2^d]_K^{N-1} = [S_2]_K^{N-1} - [S_2^f]_K^{N-1} \tag{B-18}$$

$$[S_1]_K^{N-1} = 1 - [S_2]_K^{N-1} \tag{B-19}$$

where Equation (3-20) is used instead of Equation (3-19).

11. Fractional Flow Versus Water Saturation

Writing the fractional flow equation (Equation (3-21)) at the new time step:

$$[f_2]_K^{N-1} = \frac{1}{1 + \frac{(\mu_2 [k_{r1}]_K^{N-1})}{(\mu_1 [k_{r2}]_K^{N-1})}} \tag{B-20}$$

12. Fractional Flow Constraint

Writing the fractional flow constraint (Equation (3-21)) at the new time step and rearranging:

$$[f_1]_K^{N-1} = 1 - [f_2]_K^{N-1} \tag{B-21}$$

13. 14. Relative Permeability Relations

The oil and water relative permeability versus water saturation relationships are determined from steady-state relative permeability measurements or from mathematical relationships. Writing the relative permeabilities (Equations (3-23) and (3-24)) at the new time step:

$$[k_{r1}]_K^{N-1} = \text{function}_3\,([S_2]_K^{N-1}) \tag{B-22}$$

$$[k_{r2}]_K^{N-1} = \text{function}_4\,([S_2]_K^{N-1}) \tag{B-23}$$

15. Average Dimensionless Dispersivity

The average dimensionless dispersivity (Equation (3-37)) is

$$[\bar{\alpha}]_K^N = \frac{\alpha_{i1} P_{i12} [f_1]_K^N + \alpha_{i2} [f_2]_K^N}{L} \tag{B-24}$$

where $\alpha_{i1} + \alpha_{i2}$ are parameters.

16, 17. Average Saturation and Fractional Flow

Finally, the last two equations in the model are for the average saturation and fractional flow:

$$[\bar{S}]_K^{N-1} = P_{i12} [S_1']_K^{N-1} + [S_2']_K^{N-1} \tag{B-1b}$$

$$[\bar{f}]_K^{N-1} = P_{i12} [f_1]_K^{N-1} + [f_2]_K^{N-1} \tag{B-2b}$$

Initial and Boundary Conditions

There are NB blocks, with Block 1 at the inlet end and Block NB at the outlet end. Block 0 is the inlet, and Block NB + 1 is the outlet. The core is initially at IWS and contains no tracer. The initial conditions (Equations (3-47) and (3-48)) in finite difference form become:

$$[S_2]_K^0 = (S_2)_{IWS} \qquad N = 0,\ 1 \le K \le NB \qquad \text{(B-25)}$$

$$[C_{i1}^t]_K^0 = [C_{i1}^d]_K^0 = [C_{i2}^t]_K^0 = [C_{i2}^d]_K^0 = 0 \qquad N = 0,\ 1 \le K \le NB \qquad \text{(B-26)}$$

Start water injection at t = 0 and inject a slug of tracer for dimensionless time t_s. The boundary conditions (Equations (3-49) and (3-50)) become:

$$[f_2]_0^N = 1.0 \qquad \text{(B-27)}$$

$$[C_{i2}^t]_0^N = 1 \qquad K = 0,\ 0 < N\,\Delta t \le t_s \qquad \text{(B-28a)}$$

$$[C_{i2}^t]_0^N = 0 \qquad K = 0,\ N\,\Delta t > t_s \qquad \text{(B-28b)}$$

METHOD OF SOLUTION OF THE UNSTEADY-STATE MODEL

The unsteady-state model equations listed above are solved at each new time step in a two-step process. First, the saturation and fractional flow equations are used to determine the new distribution of oil and water in the core. These equations are *not* dependent on the tracer concentrations, so they can be solved first. The tracer concentrations at the new time step are then determined once the fractional flows and saturations are known.

The following describes the loop that is used to update the model at each new time step:

1. Update the saturations:

$$[S_2]_K^{N+1} = [S_2]_K^N - \frac{([f_2]_K^N - [f_2]_{K-1}^N)}{\Delta x} \Delta t = 0 \qquad \text{(B-16)}$$

$$[S_1]_K^{N-1} = 1 - [S_2]_K^{N-1} \qquad \text{(B-19)}$$

2. Calculate updated relative permeabilities:

$$[k_{r1}]_K^{N-1} = \text{function}_3\,([S_2]_K^{N-1}) \qquad \text{(B-22)}$$

$$[k_{r2}]_K^{N-1} = \text{function}_4\,([S_2]_K^{N-1}) \qquad \text{(B-23)}$$

The actual relative permeability-saturation relation used can be varied in the program as a user option (see Appendix J).

3. Calculate updated fractional flows:

$$[f_2]_K^{N-1} = \frac{1}{1 + \frac{(\mu_2\,[k_{r1}]_K^{N-1})}{(\mu_1\,[k_{r2}]_K^{N-1})}} \qquad \text{(B-20)}$$

$$[f_1]_K^{N-1} = 1 - [f_2]_K^{N-1} \qquad \text{(B-21)}$$

4. Update dendritic and flowing fraction saturations:

$$[S_1^f]_K^{N-1} = \text{function}_1\,([S_1]_K^{N-1}) \qquad \text{(B-13)}$$

$$[S_1^d]_K^{N+1} = [S_1]_K^{N-1} - [S_1^f]_K^{N-1} \qquad \text{(B-17)}$$

$$[S_2^f]_K^{N-1} = \text{function}_2\,([S_2]_K^{N-1}) \tag{B-14}$$

$$[S_2^d]_K^{N-1} = [S_2]_K^{N-1} - [S_2^f]_K^{N-1} \tag{B-18}$$

5. Calculate average saturation, fractional flow, and dimensionless dispersivity:

$$[\bar{S}]_K^{N-1} = P_{i12}\,[S_1^f]_K^{N-1} + [S_2^f]_K^{N-1} \tag{B-1b}$$

$$[\bar{f}\,]_K^{N-1} = P_{i12}\,[f_1]_K^{N-1} + [f_2]_K^{N-1} \tag{B-2b}$$

$$[\bar{\alpha}]_K^N = \frac{\alpha_{i1}\,P_{i12}\,[f_1]_K^N + \alpha_{i2}\,[f_2]_K^N}{L} \tag{B-24}$$

All of the flow variables are now updated, and the new tracer concentrations can be calculated.

6. Calculate new dendritic concentrations:

$$[C_{i1}^d\,S_1^d]_K^{N-1} = [C_{i1}^d\,S_1^d]_K^N + M_{i1}\,([C_{i1}^f]_K^N - [C_{i1}^d]_K^N)\,\Delta t \tag{B-11}$$

$$[C_{i2}^d\,S_2^d]_K^{N-1} = [C_{i2}^d\,S_2^d]_K^N + M_{i2}\,([C_{i2}^f]_K^N - [C_{i2}^d]_K^N)\,\Delta t \tag{B-12}$$

7. Calculate new flowing concentrations:

$$[C_{i2}^f\,\bar{S}]_K^{N-1} = [C_{i2}^f\,\bar{S}]_K^N - ([C_{i1}^d\,S_1^d]_K^{N-1} - [C_{i1}^d\,S_1^d]_K^N) -$$

$$([C_{i2}^d\,S_2^d]_K^{N-1} - [C_{i2}^d\,S_2^d]_K^N) - \frac{([C_{i2}^f\,\bar{f}]_K^N - [C_{i2}^f\,\bar{f}]_{K-1}^N)}{\Delta x}\,\Delta t +$$

$$\frac{\Delta t}{(\Delta x)^2}\,\{[\bar{\alpha}]_K^N\,([C_{i2}^f]_{K-1}^N - [C_{i2}^f]_K^N) - [\bar{\alpha}]_{K-1}^N\,([C_{i2}^f]_K^N - [C_{i2}^f]_{K-1}^N)\} \tag{B-8}$$

$$[C_{i1}^f]_K^{N-1} = P_{i12}\,[C_{i2}^f]_K^{N-1} \tag{B-9}$$

8. Return to Step 1 for the next time step.

APPENDIX C

FINITE DIFFERENCE EQUATIONS FOR THE STEADY, TWO-PHASE FLOW MODEL

EQUATIONS IN FINITE DIFFERENCE FORM

The capacitance-dispersion equations derived in Chapter 4 must be put into finite difference form before they can be solved. There are NB blocks in the core, with Block 1 at the inlet end and Block NB at the outlet end. Block 0 is the inlet,* and Block NB + 1 is the outlet. The finite difference forms of the partial derivatives will be written using a forwards-in-time, backwards-in-space formulation using Equations (B-4) to (B-6). The Subscript D, indicating that the equations are dimensionless, will be dropped.

*In the program, Block NB + 2 is the inlet.

1. Partitioning Coefficient

Equation (4-1) for the partitioning coefficient is written at the new time step, N + 1, in Block K:

$$[C_{i1}^{f}]_K^{N+1} = P_{i12}\,[C_{i2}^{f}]_K^{N+1} \qquad \text{(C-1)}$$

2, 3. Rate Equations for Mass Transfer Between the Flowing and Dendritic Fractions

Using Equation (B-6), Equation (4-4) for the tracer mass transfer in the oil becomes:

$$S_1^d \frac{([C_{i1}^d]_K^{N-1} - [C_{i1}^d]_K^N)}{\Delta t} = M_{i1} ([C_{i1}^f]_K^N - [C_{i1}^d]_K^N) \qquad \text{(C-2)}$$

Solving for C_{i1}^d at the new time step:

$$[C_{i1}^d]_K^{N-1} = [C_{i1}^d]_K^N + \frac{M_{i1} ([C_{i1}^f]_K^N - [C_{i1}^d]_K^N) \Delta t}{S_1^d} \qquad \text{(C-3)}$$

Similarly, Equation (4-5) for the mass transfer in the water becomes:

$$[C_{i2}^d]_K^{N-1} = [C_{i2}^d]_K^N + \frac{M_{i2}([C_{i2}^f]_K^N - [C_{i2}^d]_K^N) \Delta t}{S_2^d} \qquad \text{(C-4)}$$

Tracer Material Balance

Using Equations (B-4) to (B-6), the tracer material balance equation (Equation (4-11)) becomes:

$$\bar{S} \frac{([C_{i2}^f]_K^{N-1} - [C_{i2}^f]_K^N)}{\Delta t} + S_1^d \frac{([C_{i1}^d]_K^{N-1} - [C_{i1}^d]_K^N)}{\Delta t} + S_2^d \frac{([C_{i2}^d]_K^{N-1} - [C_{i2}^d]_K^N)}{\Delta t} +$$

$$\bar{f} \frac{([C_{i2}^f]_K^N - [C_{i2}^f]_{K-1}^N)}{\Delta x} = \bar{\alpha} \frac{([C_{i2}^f]_{K-1}^N - 2[C_{i2}^f]_K^N + [C_{i2}^f]_{K-1}^N)}{(\Delta x)^2} \qquad \text{(C-5)}$$

This involves three terms at the new time step (N + 1), with the remaining terms at the old time step. Solving for C^f_{i2} at the new time step:

$$[C^f_{i2}]^{N-1}_K = [C^f_{i2}]^N_K - \frac{S^d_1}{\bar{S}}([C^d_{i1}]^{N-1}_K - [C^d_{i1}]^N_K) - \frac{S^d_2}{\bar{S}}([C^d_{i2}]^{N-1}_K - [C^d_{i2}]^N_K) -$$

$$\frac{\bar{f}([C^f_{i2}]^N_K - [C^f_{i2}]^N_{K-1})\,\Delta t}{\bar{S}\,\Delta x} + \frac{}{\alpha}\frac{([C^f_{i2}]^N_{K-1} - 2\,[C^f_{i2}]^N_K + [C^f_{i2}]^N_{K-1})}{\bar{S}(\Delta x)^2}\Delta t \qquad \text{(C-6)}$$

Initial and Boundary Conditions

There are NB blocks, with Block 1 at the inlet end and Block NB at the outlet end. Block 0 is the inlet, and Block NB + 1 is the outlet. The core is initially at IWS and contains no tracer. The initial conditions (Equation (4-18)) in finite difference form become:

$$[C^f_{i1}]^0_K = [C^d_{i1}]^0_K = [C^f_{i2}]^0_K = [C^d_{i2}]^0_K = 0 \qquad N=0,\ 1 \le K \le NB \qquad \text{(C-7)}$$

Start water injection at t = 0, and inject a slug of tracer for dimensionless time t_s. The boundary conditions (Equations (4-21) and (4-22)) become:

$$[C^f_{i2}]^N_0 = 1 \qquad K = 0,\ 0 < N\,\Delta t \le t_s \qquad \text{(C-8)}$$

$$[C^f_{i2}]^N_0 = 0 \qquad K = 0,\ N\,\Delta t > t_s \qquad \text{(C-9)}$$

METHOD OF SOLUTION OF THE STEADY, TWO-PHASE FLOW MODEL

The following describes the loop that is used to update the model at each new time step:

1. Calculate new dendritic concentrations:

$$[C_{i1}^{d}]_K^{N+1} = [C_{i1}^{d}]_K^{N} + \frac{M_{i1}\,([C_{i1}^{f}]_K^{N} - [C_{i1}^{d}]_K^{N})\,\Delta t}{S_1^{d}} \tag{C-3}$$

$$[C_{i2}^{d}]_K^{N-1} = [C_{i2}^{d}]_K^{N} + \frac{M_{i2}\,([C_{i2}^{f}]_K^{N} - [C_{i2}^{d}]_K^{N})}{S_2^{d}} \tag{C-4}$$

2. Calculate new flowing concentrations of tracer in the water:

$$[C_{i2}^{f}]_K^{N-1} = [C_{i2}^{f}]_K^{N} - \frac{S_1^{d}}{\bar{S}}([C_{i1}^{d}]_K^{N-1} - [C_{i1}^{d}]_K^{N}) - \frac{S_2^{d}}{\bar{S}}([C_{i2}^{d}]_K^{N-1} - [C_{i2}^{d}]_K^{N}) -$$

$$\frac{\bar{f}([C_{i2}^{f}]_K^{N} - [C_{i2}^{f}]_{K-1}^{N})\,\Delta t}{\bar{S}\,\Delta x} + \frac{}{}\alpha\,\frac{([C_{i2}^{f}]_{K-1}^{N} - 2\,[C_{i2}^{f}]_K^{N} + [C_{i2}^{f}]_{K-1}^{N})}{\bar{S}\,(\Delta x)^2}\,\Delta t \tag{C-6}$$

3. Calculate new flowing concentrations of tracer in the oil:

$$[C_{i1}^{f}]_K^{N-1} = P_{i12}\,[C_{i2}^{f}]_K^{N-1} \tag{C-1}$$

4. Return to Step 1 for the next time step.

APPENDIX D

ESTIMATING MODEL PARAMETERS

Estimates of core properties, such as dispersion, can be obtained from the single- and two-phase convection-diffusion equations. Since capacitance effects are ignored, the estimations are only qualitative, particularly for two-phase flow. When capacitance is taken into account, the dispersion coefficient is generally lower than the rough estimates provided here, because the capacitance behavior contributes to the tracer mixing. Separating the effects is important, particularly when the laboratory experiments are performed to determine dispersion coefficients that will subsequently be used in field studies. On a field scale, flow velocity is usually much smaller and system length hundreds of times greater than in laboratory experiments. In the experiments, there may be a significant amount of mixing due to capacitance effects, while in the field, the capacitance effects may be small or negligible. Considerable error will arise if the total mixing observed in laboratory flow tests is attributed to the dispersion process alone. Using a capacitance-dispersion model for the laboratory experiments enables one to determine effects due to capacitance versus dispersion, making it possible to scale up to the field.

While the equations in this Appendix will provide only rough estimates of core properties, these estimates are useful in providing starting values for computer matching with the more accurate capacitance-dispersion model.

SINGLE-PHASE DISPERSION COEFFICIENT

An estimate of the dispersivity in single-phase flow can be obtained from the analytical solution of the convection-diffusion equation for a step change in tracer concentration in an infinite porous medium (Aronofsky and Heller, 1957). As discussed in Chapter 2, the nondimensional form of the convection-diffusion equation is:

$$\frac{\partial C_D}{\partial t_D} + \frac{\partial C_D}{\partial x_D} = \frac{1}{N_{Pe}} \frac{\partial^2}{\partial x_D^2} C_D \tag{2-8}$$

For a step-change in tracer concentration in an infinite porous media, the solution to Equation (2-8) is:

$$C_D = \frac{1}{2}\left[1 - \text{erf}\left(\frac{x_D - t_D}{\sqrt{\frac{4t_D}{N_{Pe}}}}\right)\right] \tag{2-10}$$

At the endpoint of a finite core, $X = L$, $x_D = 1$, and Equation (2-10) become:

$$C_D = \frac{1}{2}\left[1 - \text{erf}\left(\frac{1 - t_D}{\sqrt{\frac{4t_D}{N_{Pe}}}}\right)\right] \tag{2-11}$$

To obtain an estimate of the dispersion coefficient K, we introduce

$$\lambda = \frac{t_D - 1}{\sqrt{t_D}} \tag{D-1}$$

Substituting into Equation (2-11),

$$C_D = \frac{1}{2}\left[1 - \text{erf}\left(\frac{-\lambda\sqrt{N_{Pe}}}{2}\right)\right] \tag{D-2}$$

The most common way of estimating dispersivity is to solve Equation (D-2) at two different values of λ, generally λ_{90} and λ_{10}, the values corresponding the 90 and 10 percent values of C_D.

When $C_D = 0.9$, a table of the error function shows that the argument of the error function is -0.9062. Similarly, when $C_D = 0.1$, the argument is $+0.9062$. Substituting into Equation (D-2),

$$\frac{\lambda_{90}\sqrt{N_{Pe}}}{2} = 0.9062 \tag{D-3}$$

$$\frac{\lambda_{10}\sqrt{N_{Pe}}}{2} = -0.9062 \tag{D-4}$$

Subtracting Equation (D-4) from Equation (D-3) and multiplying by 2,

$$(\lambda_{90} - \lambda_{10}) \sqrt{N_{Pe}} = 3.625 \tag{D-5}$$

Solving for $1/N_{Pe}$,

$$\frac{1}{N_{Pe}} = \left(\frac{\lambda_{90} - \lambda_{10}}{3.625}\right)^2 \tag{D-6}$$

Substituting in Equation (2-7) which defined the Peclet Number,

$$\alpha = \frac{K}{v_T} = L\left(\frac{\lambda_{90} - \lambda_{10}}{3.625}\right)^2 \tag{D-7}$$

where α is the dispersivity, K / v_T.

Other values besides λ_{10} and λ_{90} may be used, and only the constant in Equation (D-7) changes. The most common method of solving Equation (D-7) is to plot C_D versus λ on probability paper. Ideally, such a plot should give a straight line from which smooth values of λ_{10} and λ_{90} can be read.

TWO-PHASE DISPERSION COEFFICIENT

A similar procedure is used to estimate the average dispersion coefficient during two-phase flow. In Appendix A, the nondimensional form of the two-phase convection-diffusion equation was derived:

$$\frac{\partial C_D}{\partial t_{DT}} + \frac{\partial C_D}{\partial x_D} = \frac{1}{\bar{N}_{Pe}} \frac{\partial^2}{\partial x_D^2} C_D \qquad \text{(A-13)}$$

where

$$\bar{N}_{Pe} = \frac{L v_T}{\bar{K}_i} \qquad \text{(A-12)}$$

and

$$\bar{K}_i = \frac{S_1 K_1 P_{i12} + S_2 K_2}{S_1 P_{i12} + S_2} \qquad \text{(A-10)}$$

For a step-change in tracer concentration in an infinite porous medium, the solution is the same as Equation (2-10) for the single-phase case, using the averaged Peclet Number.

$$C_D = \frac{1}{2}\left[1 - \text{erf}\left(\frac{x_D - t_{DT}}{\sqrt{\frac{4 t_{DT}}{\bar{N}_{Pe}}}}\right)\right] \qquad \text{(D-8)}$$

where the dimensionless time, t_{DT}, was defined in Equation (A-4). To obtain an estimate of the dispersion coefficient K, we introduce

$$\lambda = \frac{t_{DT} - 1}{\sqrt{t_{DT}}} \tag{D-9}$$

Substituting into Equation (D-8) and solving for the tracer concentration at the end of the core, where $x_D = 1$, gives:

$$C_D = \frac{1}{2}\left[1 - \text{erf}\left(\frac{-\lambda\sqrt{\bar{N}_{Pe}}}{2}\right)\right] \tag{D-11}$$

As in the single-phase case, Equation (D-11) can be solved for the averaged dispersivity,

$$\bar{\alpha} = \frac{\bar{K}}{v_T} = L\left[\frac{(\lambda_1)_{90} - (\lambda_1)_{10}}{3.625}\right]^2 \tag{D-12}$$

The determination of the actual dispersion coefficient for each phase is not as easy as before since $\bar{K}$ is a weighted average of K_1 and K_2. Therefore, at least one of the tracers should be nonpartitioning. For example, a nonpartitioning tracer in the water could be used to estimate K_2. Once K_2 is known, $\bar{K}$ can be estimated from Equation (D-12) and K_1 can be estimated from Equation (A-30).

ESTIMATING SATURATIONS

In addition to estimating dispersivity, the two-phase convection-diffusion equation can also be used to estimate fluid saturations (Delshad, MacAllister, Pope, and Rouse, 1985). Note, however, that the convection-diffusion equation neglects capacitance effects, which can cause serious errors in the esti-

mated parameters (Mohammed Delshad, 1984). For this reason, the capacitance-dispersion computer model must be used to obtain the final numbers.

Nonpartitioning Tracer

Nonpartitioning tracers can be used to estimate saturation from the travel time of the tracer through the core (Delshad et al., 1985). The average velocity of a fluid flowing through the core is determined by the injection rate and the cross-sectional area available for flow. For fluid j, the injection rate is:

$$q_j = q\, f_j \tag{D-13}$$

where q is the total flow rate and f_j is the fractional flow of fluid j. The cross-sectional area available for the flow of all the fluids is $A\phi$. For fluid j with saturation S_j, the cross-sectional area available for flow is:

$$A_j = A\, \phi\, S_j \tag{D-14}$$

where we have assumed that all of the fluid is flowing. The average velocity of fluid j is:

$$v_j = \frac{q_j}{A_j} = \frac{q\, f_j}{A\, \phi\, S_j} \tag{D-15}$$

or solving for S_j,

$$S_j = \frac{q\, f_j}{A\, \phi\, v_j} \tag{D-15}$$

Since q, f_j, A, and ϕ are all known, Equation (D-15) shows that the saturation can be estimated, once the average velocity is known.

The average velocity is obtained by measuring the time for a nonpartitioning tracer to travel through the core. Consider a tracer i that is present in only one phase, j. When a step-change in tracer concentration is made at the inlet, the change in tracer concentration will travel through the core, gradually being smeared out due to dispersion. Define the midpoint breakthrough time (t_i^{BT}) of a tracer as the time which the tracer concentration reaches 50 percent of its injected value. Since the tracer traveled at an average speed of v_j through the length of the core,

$$v_j\, t_i^{BT} = L \tag{D-16}$$

Converting t_i^{BT} to pore volumes to nondimensionalize the equation:

$$t_{Di}^{BT} = \frac{t_i^{BT}}{AL\phi/q} \tag{D-17}$$

Substituting Equations (D-16) and (D-17) into Equation (D-15) and then solving for t_{Di}^{BT} gives:

$$t_{Di}^{BT} = \frac{S_j}{f_j} \tag{D-18}$$

From the tracer dispersion curve, t_{Di}^{BT} is estimated and Equation (D-18) is used to calculate a first approximation for S_j. The fractional flow of phase j, f_j, is taken to be the average of the final steady-state produced cuts. For the injection of a finite slug, saturation is determined in a similar manner. In this case, the breakthrough time of tracer i, t_i^{BT}, is defined as the time corresponding to the peak tracer concentration. Equation (D-18) is then used as before.

Partitioning Tracer

The dimensionless breakthrough time for a partitioning tracer can also be used to estimate saturations when the assumption is made that there is no dendritic fluid (Delshad et al., 1985). In Chapter 4, the tracer material balance equation during steady-state flow was developed:

$$A\phi\,(S_1^f\,P_{i12} + S_2^f)\,\frac{\partial}{\partial t}\,C_{i2}^f + A\,\phi\,S_1^d\,\frac{\partial}{\partial t}C_{i1}^d + A\,\phi\,S_2^d\,\frac{\partial}{\partial t}\,C_{i2}^d + q\,(f_1P_{i12} + f_2)\,\frac{\partial}{\partial x}\,C_{i2}^f = q\,(f_1\,\alpha_{i1}\,P_{i12} + f_2\,\alpha_{i2})\,\frac{\partial^2}{\partial x^2}\,C_{i2}^f \tag{4-6}$$

Assuming that all of the fluid is flowing, with no dendritic saturations, Equation (4-6) becomes:

$$A\phi\,(S_1\,P_{i12} + S_2)\,\frac{\partial}{\partial t}\,C_{i2} + q\,(f_1P_{i12} + f_2)\,\frac{\partial}{\partial x}\,C_{i2} = q\,(f_1\,\alpha_{i1}\,P_{i12} + f_2\,\alpha_{i1})\,\frac{\partial^2}{\partial x^2}\,C_{i2} \tag{D-19}$$

Neglecting dispersion, the material balance equation becomes:

$$A\phi\,(S_1\,P_{i12} + S_2)\,\frac{\partial}{\partial t}\,C_{i2} + q\,(f_1P_{i12} + f_2)\,\frac{\partial}{\partial x}\,C_{i2} = 0 \tag{D-20}$$

From Equation (D-20), the velocity, v_T, of a given tracer concentration, C_i, in Phase 2 can be calculated:

$$v_T = \left(\frac{dx}{dt}\right)_{C_{i2}} = \frac{q}{A\phi}\left(\frac{f_1P_{i12} + f_2}{S_1P_{i12} + S_2}\right) \tag{D-21}$$

As in the nonpartitioning case, Equation (D-16) provides a relationship between the dimensionless breakthrough time, the average velocity, and the core length.

$$t_i^{BT} = \frac{L}{v_T} \tag{D-22}$$

Nondimensionalizing the time based on pore volumes injected,

$$t_{Di}^{BT} = \frac{t_i^{BT}}{\left(\frac{AL\phi}{q}\right)} = \frac{L/v_T}{\left(\frac{AL\phi}{q}\right)} = \frac{q}{A\phi}\left(\frac{1}{v_T}\right) \tag{D-23}$$

Substituting for v_T from Equation (D-21), the relationship between the dimensionless breakthrough time and the saturation becomes:

$$t_{Di}^{BT} = \frac{S_1 P_{i12} + S_2}{f_1 P_{i12} + f_2} \tag{D-24}$$

This is the tracer breakthrough equation which was used to estimate saturations from partitioning tracer breakthrough times. In this equation, there is only one unknown, since P_{i12}, f_1, and $f_2 = 1 - f_1$ are all measured quantities and $S_1 + S_2 = 1$.

At the endpoints of relative permeability measurements, where Phase 2 is flowing and Phase 1 is at residual saturation S_{1r}, Equation (11) reduces to

$$t_{Di}^{BT} = S_{1r} P_{i12} + S_2 \tag{D-25}$$

For a finite slug, t_i^{BT} is defined as before and Equation (D-24) or (D-25) is used, depending on whether the core is at the residual saturation.

APPENDIX E

WETTABILITY ALTERATION AND MEASUREMENT

WETTABILITY ALTERATION

Tracer measurements were made in strongly water-wet and neutrally wet Berea cores. The strongly water-wet core was cut from outcrop Berea sandstone and was not treated. The neutrally wet Berea core was treated with several organochlorosilanes using a procedure described in Salter and Mohanty (1982). The detailed procedure is given in Table E-1 and Figure E-2. Note that it is necessary to remove all of the organochlorosilanes from the core before water is injected, otherwise a gel and gas will form inside the core.

Companion plugs for wettability measurement were cut for both the water-wet and neutrally wet Berea cores. The water-wet plugs were not treated, while the procedure described in Table E-1 was used to treat the neutrally wet plugs. Wettability was measured by the combined USBM-Amott method described below. The results are given in Table 5-1.

Although treatment with organochlorosilanes was the procedure selected to alter wettability, it was actually the second method considered. The first, discussed in Sharma and Wunderlich (1985), used dry Berea samples that are saturated with an asphaltic crude oil. The samples are then flushed with pentane to precipitate asphaltenes, leaving an oil-wet surface. This procedure was dropped when static tests showed that the pentane formed a gel with the crude used, Loco crude, which is very asphaltic.

WETTABILITY MEASUREMENT PROCEDURE

There are two quantitative wettability indices used to measure the wettability of core (Anderson): the Amott index (Amott, 1959) and the U.S. Bureau of Mines (USBM) index (Donaldson et al., 1969, 1980, 1981). The procedure that we used to assay wettability was the combined procedure of Sharma and Wunderlich (1985), which determines both the Amott and USBM wettability indices. The procedure shown in Figure E-1 has the following five steps: (1) initial oil drive, (2) spontaneous (free) imbibition of brine, (3) brine drive, (4) spontaneous (free) imbibition of oil, and (5) oil drive. The areas under the brine and oil drive curves are used to calculate the USBM index, while the Amott index uses the volumes of free and total water and oil displacements.

Prior to the wettability measurement, the dry Berea plugs are saturated with brine. Note that this wettability measurement method can also be used with plugs initially at ROS, as shown in Figure E-1. During the initial oil drive step of the measurement, Curve 1, the plugs are driven to IWS. Next, the cores are immersed in water, and the volume of water that imbibes freely is measured, Curve 2. During the brine drive step, Curve 3, the average saturation of the plug is determined from the amount of expelled oil at each incremental capillary pressure.* This data is used to calculate the area under the brine drive curve, A_2, for the USBM method. At the end of the brine drive step, the plug is left at ROS. In the fourth step, Curve 4, the plug is immersed in oil and the volume of oil that imbibes spontaneously is measured. The final step is the oil drive, Curve 5, where the capillary pressures and average saturations are used to calculate A_1 for the USBM method. A detailed description of the procedure is given in Table E-2.

---

*The USBM method uses the average saturation in the core (Donaldson et al., 1980). In contrast, the centrifugal capillary pressure curve is based on the saturation at the face of the core, which is calculated from the average saturation (Hassler and Brunner, 1945; Slobod et al., 1951).

The USBM method uses the ratio of the areas under the brine drive and oil drive capillary pressure curves to calculate a wettability index, according to the equation:

$$W = \log(A_1/A_2) \tag{E-1}$$

where A_1 and A_2 are the areas under the oil and brine drive curves, respectively. As shown in Table E-3, when W is greater than 0, the core is water-wet, and when W is less than 0, the core is oil-wet. A wettability index near 0 means that the core is neutrally wet. The larger the absolute value of W, the greater the wetting preference.

The Amott method gives two indices: (1) the "displacement-by-oil ratio," which is the ratio of the water volume displaced by spontaneous (free) oil imbibition alone, $(V_w)_{spontaneous}$, to the total displaced by oil imbibition and centrifugal displacement, $(V_w)_{total}$:

$$D_{by\text{-}oil} = \frac{(V_w)_{spontaneous}}{(V_w)_{total}} \tag{E-2}$$

and (2) the "displacement-by-water ratio," which is the ratio of the oil volume displaced by spontaneous water imbibition, $(V_o)_{spontaneous}$, to the total oil volume displaced by imbibition and centrifugal displacement, $(V_o)_{total}$:

$$D_{by\text{-}water} = \frac{(V_o)_{spontaneous}}{(V_o)_{total}} \tag{E-3}$$

As shown in Table E-3, preferentially water-wet cores have a positive displacement-by-water ratio and a zero value for the displacement-by-oil ratio. The displacement-by-water ratio approaches 1 as the water-wetness increases. Similarly, oil-wet cores have a positive displacement-by-oil ratio and a zero displacement-by-water ratio. Both values are zero for neutrally wet cores.

There are several advantages of the combined USBM-Amott method over either of the methods alone (Anderson, 1987; Sharma and Wunderlich, 1985). First, the resolution of the USBM method is improved by accounting for the saturation changes which occur at zero capillary pressure. Second, the USBM method is sensitive near neutral wettability, whereas the Amott method is not. Finally, the Amott method will *sometimes* indicate that a rock-oil-brine system is nonuniformly wetted, while the USBM test cannot determine if a system has fractional or mixed wettability. In some fractional- or mixed-wet systems, both oil and water will imbibe freely. The Amott method will have positive displacement-by-water and displacement-by-oil ratios, indicating that the system is nonuniformly wetted (Anderson, 1985, 1986).

TABLE E-1

ORGANOCHLOROSILANE TREATMENT OF BEREA CORE

1. Place plugs in Hassler core holder, evacuate them with a vacuum pump, then saturate with hexane.

2. Inject 5 pore volumes of a 7 weight percent dichlorodiphenyl silane solution.* Allow the silane solution to remain in the plugs for approximately 24 hours. The apparatus shown in Figure E-2 was used to treat the core.

3. Flush with 5 pore volumes of hexane.

4. Inject 5 pore volumes of a 7 weight percent chlorotrimethyl silane solution.* Allow the silane solution to remain in the plugs for approximately 24 hours.

5. Flush with at least 5 pore volumes of hexane to remove all of the unreacted silanes. These unreacted silanes must be removed since they will form a gel with water. Test the effluent for silanes by mixing a small amount with water. If no reaction is seen, stop hexane injection.

6. Flood plugs with nitrogen gas until dry.

7. Evacuate the plugs and saturate with brine.

---

*Dichlorodiphenyl silane and chlorotrimethyl silane are available from Aldrich Chemical Company, Milwaukee, Wisconsin.

TABLE E-2

PROCEDURES TO MEASURE USBM AND

AMOTT WETTABILITY INDICES

1. Cut 1-inch-diameter by 2-inch-long plugs with brine. Dry plugs in oven at 250°F (120°C) for 24 hours.

2. Treat the neutrally wet plugs using the procedure described in Table E-1.

3. Evacuate the plugs for approximately 24 hours to remove air, then saturate with brine.

4. Initial Oil Drive: Immerse the plugs in decane and use the Beckmann L5-50P ultracentrifuge to drive the plugs to IWS (Curve 1, Figure E-1). A capillary pressure of 10 psi (70 kPa) was used (2400 rpm).

5. Free Imbibition of Brine: Immerse the plugs in brine and measure the volume of oil displaced by the spontaneous (free) imbibition of brine, $(V_o)_{spontaneous}$ (Curve 2, Figure E-1). Brine was allowed to imbibe for at least 1 week. The plugs were monitored daily until production of oil stopped.

6. Brine Drive: Place the plugs in centrifuge tubes, immerse the plugs in brine, and centrifuge the cores at incrementally increasing speeds until a capillary pressure of -10 psi (-70 kPa) is reached. At each incremental pressure, the average saturation of the plug is calculated from the volume of expelled oil (Curve 3, Figure E-1). A_2 is the area under the plot of capillary pressure versus the average saturation of the brine drive. $(V_o)_{total}$, the total volume of oil expelled, is calculated by adding the amount of oil expelled during the brine drive to $(V_o)_{spontaneous}$.

TABLE E-2 (CONTINUED)

PROCEDURES TO MEASURE USBM AND

AMOTT WETTABILITY INDICES

7. Free Imbibition of Oil: Immerse the plugs in oil, and measure the volume of brine displaced by the spontaneous (free) imbibition of oil, $(V_w)_{spontaneous}$ (Curve 4, Figure E-1). Oil was allowed to imbibe for at least 1 week. Brine production was monitored daily until it stopped.

8. Oil Drive: Place the plugs in centrifuge tubes, immerse the plugs in oil, and centrifuge the cores at incrementally increasing speeds until a capillary pressure of +10 psi (+70 kPa) is reached. At each incremental pressure, the average saturation of the plug is calculated from the volume of expelled brine (Curve 5, Figure E-1). A_1 is the area under the plot of capillary pressure versus the average saturation of the oil drive. $(V_w)_{total}$, the total volume of brine expelled, is calculated by adding the amount of brine expelled during the oil drive to $(V_w)_{spontaneous}$.

9. Use Equation (E-1) to calculate the USBM wettability index and Equations (E-2) and (E-3) to calculate the Amott wettability indices.

TABLE E-3

APPROXIMATE RELATIONSHIP BETWEEN WETTABILITY, CONTACT ANGLE, AND THE USBM AND AMOTT WETTABILITY INDICES (ANDERSON, 1986)

	Water-Wet	Neutrally Wet	Oil-Wet
Contact angle			
Minimum	0°	60° to 75°	105° to 120°
Maximum	60° to 75°	105° to 120°	180°
USBM wettability index	W near 1	W near 0	W near −1
Amott wettability index			
Displacement-by-water ratio	Positive	Zero	Zero
Displacement-by-oil ratio	Zero	Zero	Positive

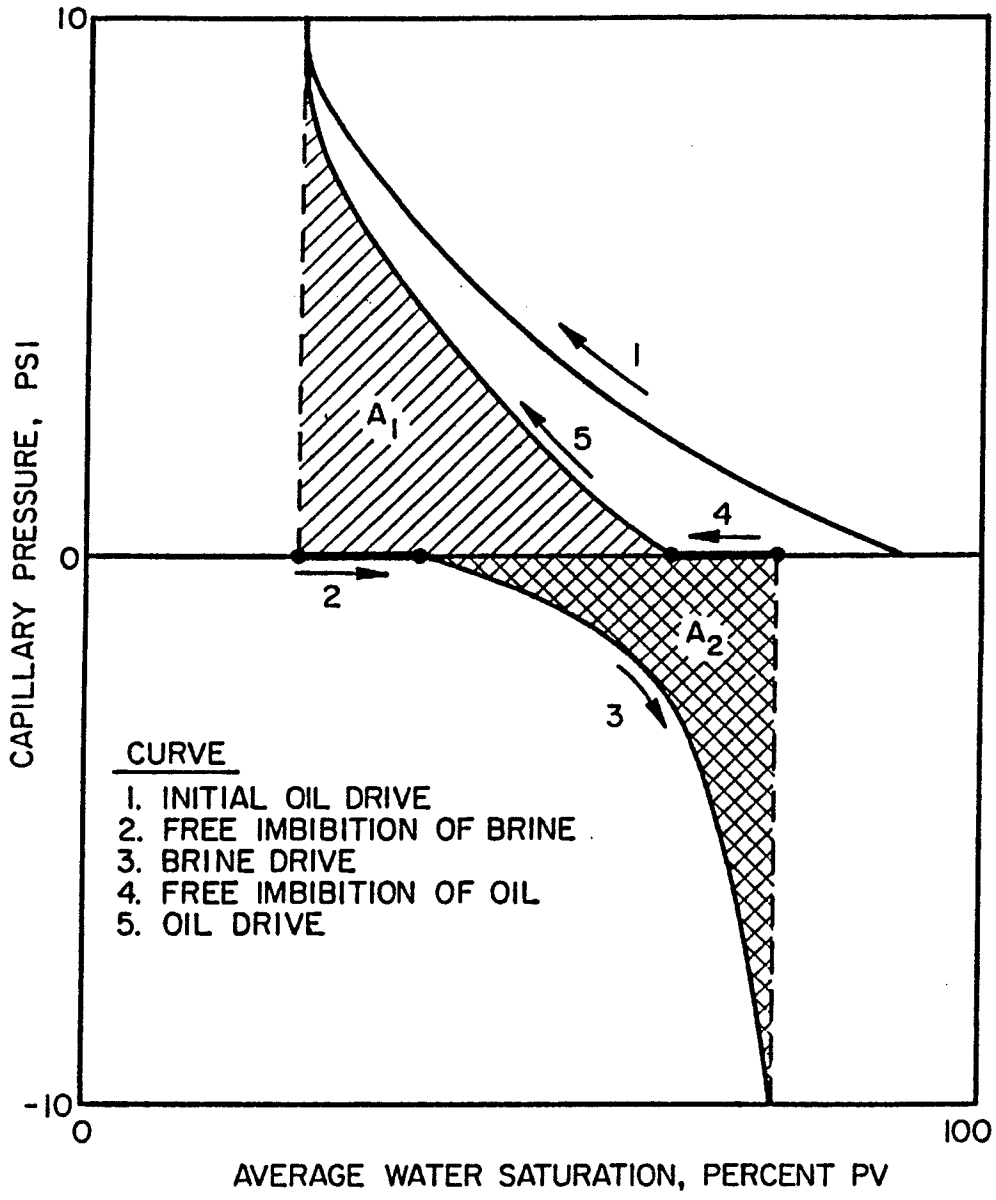

Figure E-1 Combined USBM-Amott wettability measurement (Sharma and Wunderlich, 1985). Taken from Anderson (1986).

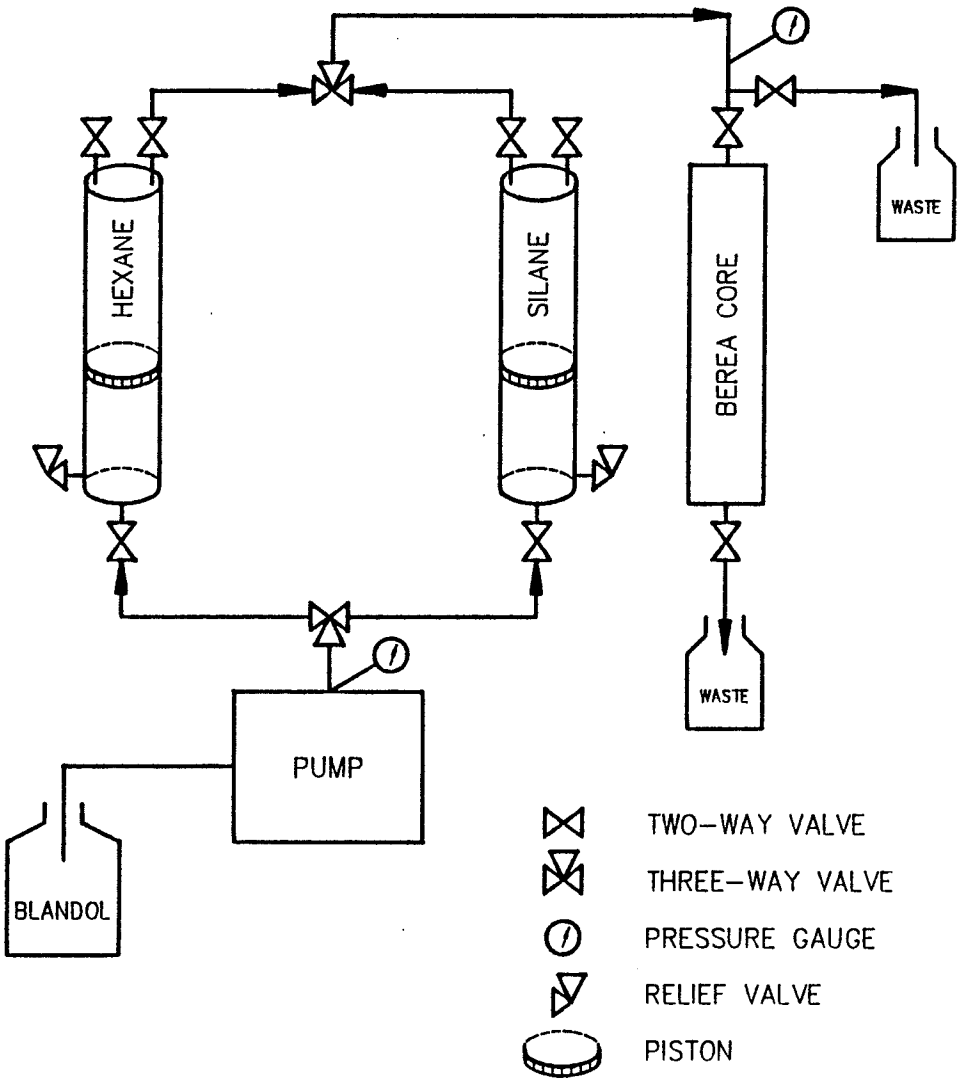

Figure E-2 Experimental apparatus used to treat Berea cores with organochlorosilanes to render them neutrally wet.

APPENDIX F

CORE PREPARATION

The Berea cores used in the experiments were mounted in epoxy with Plexiglas headers, as shown in Figure F-1. The 2-foot-long by 2-inch-square, high permeability (roughly 660 md) Berea sandstone cores were cut and faced off square with a dry rock saw. The Plexiglas headers, shown in Figure F-2, were milled to a depth of 1/64 inch on the side facing the core, to allow even distribution of the fluids entering and leaving the core. The headers were drilled and tapped to allow for 1/8-inch stainless steel bulkhead fittings. Two fittings were used on each header to allow circulation into and out of each end when connecting the core to the pump. Intermediate pressure taps, constructed of a stainless steel plate to which a Swagelok fitting was soldered, were mounted 12 inches apart.

The four-electrode method was used to measure electrical resistivity. The outer two electrodes were silver screens placed between the core and headers. A silver screen (180 mesh, 0.0023-inch-diameter wire) was cut to fit in the milled area of each header, whereas a silver wire (1-mm diameter) was soldered to each screen. With the screen in place, a small amount of "5-Minute Epoxy" was placed on the unmilled edge of each header. The headers were held firmly in place against the ends of the core for several minutes until the epoxy had set.

The inner two electrodes were silver wires wrapped around the core as shown in Figure F-1. An ice pick was used to scratch a notch approximately 1-mm deep and 1-mm wide around the perimeter of the core. Thin silver wire (0.1-mm diameter) was wrapped around the notch six times. A piece of 1-mm-diameter wire was then soldered to the loop and extended from the core for use as a lead. To do this, a small gouge was made

in the rock under the thin wire loop and the end of the wire that was to be soldered was hammered flat. The flattened end was placed in this gouge and the wires soldered together (Figure F-1). To prevent epoxy from insulating the wire loop, cellophane tape was wrapped once around the loop, adhesive side up. The edges of the tape were trimmed to make the tape approximately 1/4-inch wide, and hot air was used to shrink the tape a small amount. "5-Minute Epoxy" was then smeared over the tape, and any air bubbles under the tape were forced out. The core was now ready for epoxy mounting, which consists of the following three steps: (1) a thin layer of epoxy was applied over the entire core, (2) the pressure taps shown in Figure F-1 were mounted, and (3) a thick layer of epoxy was applied over the entire core. The detailed procedure is shown in Table F-1.

TABLE F-1

EPOXY MOUNTING PROCEDURE

1. Weigh out 300 grams of epoxy at a time and mix in a shallow dish. The epoxy consists of R-828 Resin and Versamid 125 hardener mixed in the proportion of 70/30 by weight, respectively.

2. Heat the mixture to about 100°F (40°C) with a heat lamp during mixing to decrease the viscosity and allow air bubbles to come out of the mixture. The epoxy is ready to be applied to the core when all of the air bubbles are gone and the mixture just begins to thicken from the chemical reaction between the resin and hardener, about 10 minutes.

3. To apply the first thin coat of epoxy, place the core on a device that allows the core to be rotated slowly. With the core stationary, apply a thin layer of epoxy to one side and allow it to run off. Turn the core and repeat the procedure until all four sides have been coated. Rotate the core slowly and continuously until dry, allowing any excess epoxy to drip off. This method allows the application of a thin first coat to the core with good adhesion and the elimination of any air bubbles.

4. Mount the intermediate pressure taps 12 inches apart on the same side of the core as the silver resistivity wires. The pressure taps are constructed from a 1-inch-square, 1/16-inch-thick plate of stainless steel with a 1/8-inch Swagelok fitting silver-soldered to one side. After the fitting is soldered in place, drill a 1/16-inch hole through the plate. Cement the pressure taps in place on the core with "5-Minute Epoxy." After the epoxy dries, drill a 1 1/16-inch hole through the pressure tap and epoxy until the drill bit just comes in contact with the sandstone. Pack modeling clay closely around the fitting to allow space between the fitting and the next coat of epoxy. Place a cap over the fitting to prevent matter from entering the core.

5. Sand the epoxy surface of the core to provide a good bonding surface for the next coat of epoxy.

TABLE F-1 (CONTINUED)

EPOXY MOUNTING PROCEDURE

6. A mold made from a 3-inch-wide cardboard core box is used to apply the final coat of epoxy. The sides of the box are coated with Vaseline to allow easy separation of the mold from the epoxy coating of the core. Place the core in the mold with a space of 1/2 inch between the core and the sides and bottom of the mold. The side of the core with the wires and pressure taps must face up out of the mold. Mix several batches of epoxy as described in Step 1. Slightly tilt the mold on one side, and pour epoxy slowly into the low side. This allows the epoxy to run under the core from one side and push air out the other side, reducing the possibility of trapping air bubbles in the epoxy. Continue pouring epoxy into the mold until a layer 1/2-inch thick has formed on top of the core. Level the mold, and use two heat lamps to heat the epoxy while curing for about 4 hours.

7. After the mold is removed, pressure the core to 50 psi with air and use a pressure gauge to check for leaks. The pressure taps are also tested to insure good communication with the core.

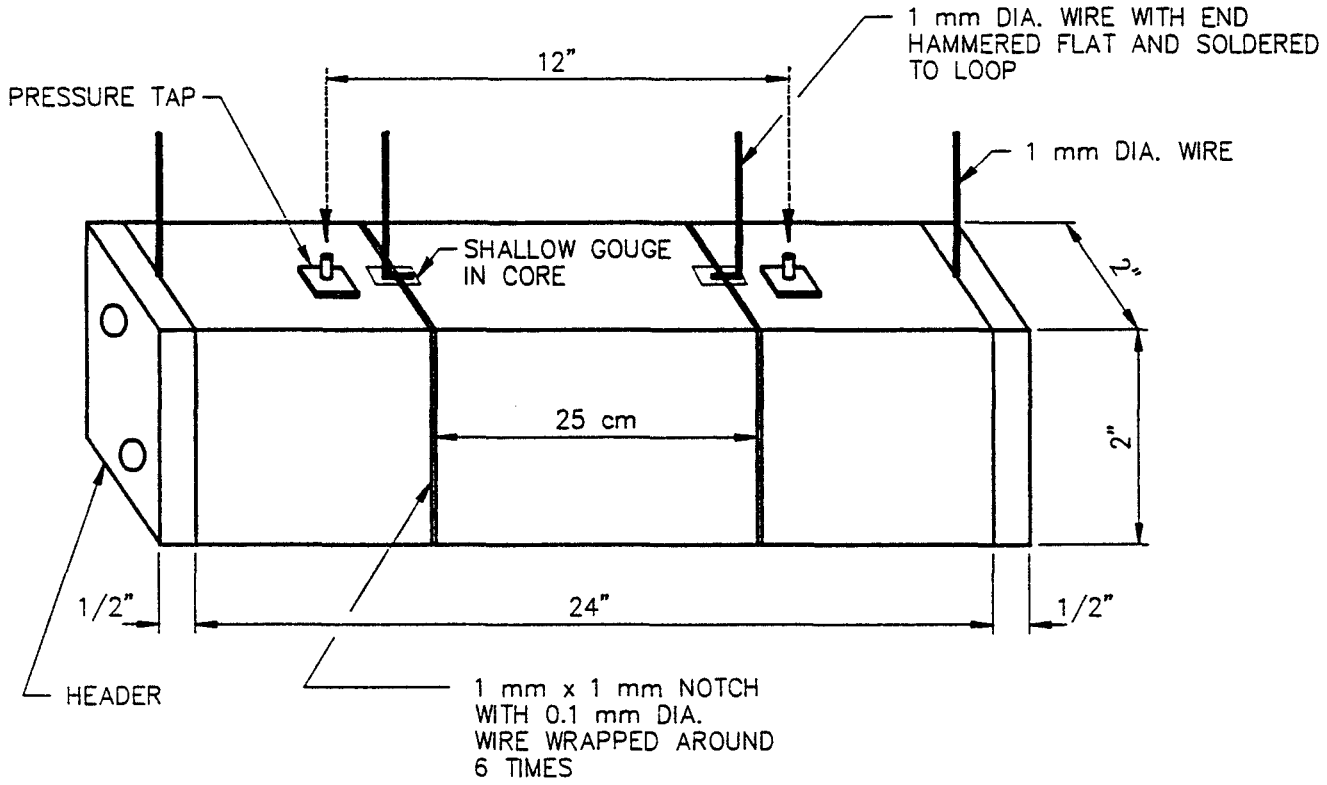

Figure F-1 Diagram of core.

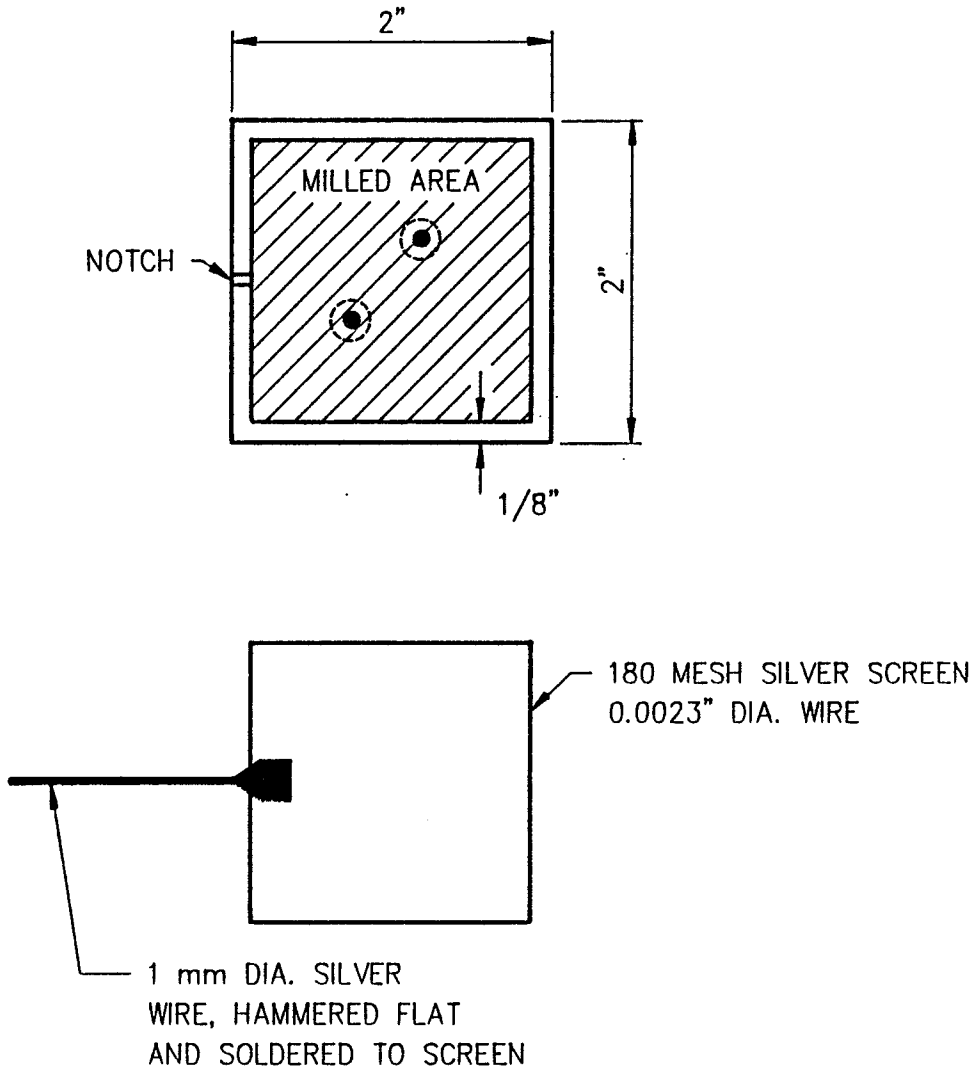

Figure F-2 Diagram of plexiglas header for the core and silver mesh screen.

APPENDIX G

DATA ACQUISITION

During the two-phase tracer experiments, pressure and electrical resistivity measurements were made. The pressure transducer was a Rosemount Alphaline pressure transducer, powered by an HP 6218B power supply. Manual pressure readings were taken with an HP 3476B digital multimeter. Electrical resistivity measurements were made with an HP 4262A LCR meter.

The data acquisition program listed below was used to take pressure and resistivity measurements, then store them on an HP-1000 computer in a form that could be plotted. An HP 59500A Multiprogrammer Interface and an HP 6940B Multiprogrammer were used to communicate between the computer and the pressure transducer and LCR meter.

After the program is initialized, it enters a loop to make pressure and resistivity measurements at an operator-specified interval. Pressure readings are read as voltages using a voltmeter in the multiprogrammer. Electrical resistivity readings are made on the LCR meter at frequencies of 100, 1,000, and 10,000 Hz. The readings are then extrapolated to a reading at infinite frequency using the method in Walther (1968).

APPENDIX H

PROGRAM FOR NORMALIZING TRACER DATA

```
FTN7X,Q
$FILES(0,3)
$EMA /OUTPUT/
      PROGRAM RAWDATA
C     ************************************************************************
C     THIS PROGRAM TAKES RAW DATA OF THE TRACER EFFLUENT CONCENTRATION
C     IN GROSS DPM PER ML AND CONVERTS IT TO NORMALIZED TRACER
C     CONCENTRATION RANGING FROM 0 TO 1.  IT ALSO CORRECTS FOR DEAD VOLUME
C     IN THE SYSTEM.
C
C     JEFF SMITH          APRIL 14, 1987
C     ************************************************************************
      CHARACTER*64 INPUT_FILE_NAME, OUTPUT_FILE_NAME
      CHARACTER    START*2
      COMMON /OUTPUT/PV,CD
C
C     GET INPUT AND OUTPUT FILE NAMES
C
      CALL SETUP(INPUT_FILE_NAME, OUTPUT_FILE_NAME)
C
C     OPEN INPUT AND OUTPUT FILE NAMES
C
      OPEN (60, FILE = INPUT_FILE_NAME, STATUS='OLD')
      OPEN (80, FILE = OUTPUT_FILE_NAME)
C
C     READ IN DATA AND ECHO IT TO THE OUTPUT FILE WITH A LEADING !
C
      START = '!'
C
C     READ NO. OF DATA POINTS, CMIN AND CMAX
C
      READ (60,*)N,CMIN,CMAX
      WRITE(80,600)START,N,CMIN,CMAX
C
C     READ VOL, DEADVOL, AND COREPV
C
      READ (60,*)VOL,DEADVOL,COREPV
      WRITE(80,610)START,VOL,DEADVOL,COREPV
C
C     PRINT HEADINGS
C
      WRITE(80,625)START
C
C     DESIGNATE RAW DATA AS COLUMNS 3 AND 4 FOR GRAF.CMD
C
      WRITE(80,620)
C
C
C
C
C     READ TUBE NUMBER AND THE TRACER CONCENTRATION, AND CALCULATE
C     NORMALIZED CONCENTRATION
C
      DO 10 I=1,N
```

```
          READ(60,*)TNO,C
C
          VOLINJ=(TNO-1.)*VOL + VOL/2. - DEADVOL
C
          IF(VOLINJ.LT.0.)THEN
          CD=0.
          PV=0.
          ELSE
          END IF
C
          PV=VOLINJ/COREPV
C
          CD=(C-CMIN)/(CMAX-CMIN)
C
          WRITE(80,630)PV,CD
C
10      CONTINUE
C
C       INDICATE THE END OF THE DATA FILE FOR GRAF.CMD
C
        WRITE(80,640)
C
C       CLOSE INPUT AND OUTPUT FILES
C
        CLOSE(60)
        CLOSE(80)
C
        STOP
C
600     FORMAT(A2,8HNO. PTS=,I3,5X,5HCMIN=,F8.2,5X,5HCMAX=,F8.2)
610     FORMAT(A2,4HVOL=,F5.2,5X,8HDEADVOL=,F6.2,5X,7HCOREPV=,F8.2)
620     FORMAT(5X,"DATA DEST C3")
625     FORMAT(A2,5X,"PV INJ",5X,"TRACER CONC.")
630     FORMAT(7X,F7.4,10X,F6.4)
640     FORMAT(5X,"END")
C
C
        END
C
C



C
        SUBROUTINE SETUP (INPUT_FILE_NAME, OUTPUT_FILE_NAME)
C       **********************************************************************
C       THIS SUBROUTINE HAS THREE TASKS:
C           1.PRINT OUT THE INITIAL INSTRUCTIONS
C
C           2. READ IN THE NAME OF THE FILE CONTAINING THE EXPERIMENTAL
C           DATA.
C
C           3. READ IN THE NAME OF THE FILE USED TO STORE THE OUTPUT.  IF
C           THE FILE ALREADY EXISTS, WARN THE USER THAT HE WILL DESTROY
C           HIS OLD DATA IF HE PROCEEDS.
```

```
C
C     INPUT:
C         NONE
C
C     OUTPUT:
C         INPUT_FILE_NAME, OUTPUT_FILE NAME, THE NAMES OF THE INPUT AND
C         OUTPUT FILES.
C
C
C     SUBROUTINE SETUP
C     BILL ANDERSON                          MARCH 8, 1985
C     ******************************************************************
      LOGICAL       DEBUG, EXISTING_FILE
      INTEGER       FLAG, PERIOD
      CHARACTER     JUNK*72, DECIDE*3
      CHARACTER*64  INPUT_FILE_NAME, OUTPUT_FILE_NAME, FILE_NAME
C
      DEBUG = .FALSE.
C
C
      WRITE(1,'(/,"THIS PROGRAM CALCULATES THE TRACER CONCENTRATIONS",
     1 " VERSUS PORE VOLUMES",/,"INJECTED. TRACER CONCENTRATION",
     2 " IS NORMALIZED.             THE OUTPUT IS STORED IN",/,
     3 "A FILE THAT CAN BE PLOTTED WITH GRAFIT/1000.")')
C
C
C                                    INPUT FILE NAME
      FLAG = 0
100   WRITE(1,'(/,"ENTER THE INPUT FILE NAME.")')
      READ (1,'(A64)')    INPUT_FILE_NAME
                          ! SEE IF FILE ALREADY EXISTS
      INQUIRE ( FILE = INPUT_FILE_NAME, EXIST = EXISTING_FILE )
      IF (EXISTING_FILE .EQV. .FALSE. ) THEN
          FLAG = FLAG + 1
          IF (FLAG .LT. 3) THEN
              WRITE(1,'(/,"THE FILE YOU HAVE ENTERED,",/,A64,/,"CAN ",
     1        "NOT BE FOUND.  PLEASE RE-ENTER THE NAME",/)')
     2        INPUT_FILE_NAME
              GO TO 100
          ELSE
              WRITE(1,'(/,"CANNOT FIND FILE, PROGRAM ABORTING.")')
              STOP
          END IF
      END IF
C
      WRITE (1,'(//,"THE DATA WILL BE READ FROM ",A64)') INPUT_FILE_NAME
C
      WRITE(1,'(/,"ENTER THE OUTPUT FILE NAME.")')
300   READ (1,'(A64)')    OUTPUT_FILE_NAME

                                    ! SEE IF FILE ALREADY EXISTS
      INQUIRE (FILE = OUTPUT_FILE_NAME, EXIST = EXISTING_FILE)
      IF (EXISTING_FILE) THEN
          WRITE(1,'(/,"THE OUTPUT FILE NAME YOU HAVE ENTERED,"./,
     1    A64,/,"ALREADY EXISTS. WRITE OVER THE OLD FILE? (Y/N) _")')
```

```
     2    OUTPUT_FILE_NAME
          READ (1,'(A3)') DECIDE
          IF (INDEX(DECIDE,'Y') .GT. 0 .OR.
     1        INDEX(DECIDE,'y') .GT. 0 ) THEN
              CONTINUE
          ELSE
              WRITE(1,'("ENTER THE FILE NAME.")')
              GO TO 300             ! THE USER WILL RE-ENTER THE FILE NAME.
          END IF
      END IF
C
C
                                    ! HAVE AN ACCEPTABLE FILE
      WRITE(1,'(//,"THE DATA WILL BE WRITTEN TO ",A64)')
     1  OUTPUT_FILE_NAME
C
C
C
      RETURN
C
C
      END                       ! END SUBROUTINE SETUP
```

APPENDIX I

PROGRAM FOR STEADY, TWO-PHASE FLOW

```
FTN7X,Q
$FILES(0,3)
$EMA /OUTPUT/
      PROGRAM CAPSLUG
C     ***********************************************************************
C     STEADY-STATE FLOW, CAPACITANCE-DISPERSION MODEL FOR INJECTION OF A
C     FINITE SLUG.
C
C     JEFF SMITH      APRIL 14, 1987
C     ***********************************************************************
      CHARACTER*64 INPUT_FILE_NAME, OUTPUT_FILE_NAME
      CHARACTER    START*2
      DIMENSION C1(202), C3(202), C1P(202), C3P(202), C4(202)
      REAL L,M1,M3,MD1,MD3
      COMMON /OUTPUT/ CNT, PVI
C

C     GET INPUT AND OUTPUT FILE NAMES.
      CALL SETUP(INPUT_FILE_NAME, OUTPUT_FILE_NAME)
C
C     OPEN INPUT AND OUTPUT FILES
      OPEN (60, FILE = INPUT_FILE_NAME, STATUS = 'OLD')
      OPEN (80, FILE = OUTPUT_FILE_NAME)
C
C     INPUT DATA, AND ECHO IT TO THE OUTPUT FILE
      START = '! '
C
C     READ STP: NO. OF PVINJ WHEN YOU WANT CALCULATIONS TO STOP
C
      READ(60,*)STP
C
C     READ SATURATIONS(S1,S3), FLOWING FRAC.(F1,F3)
C
      READ (60,*) S1,S3,F1,F3
      WRITE(80,330) S1,S3,F1,F3
C
C     READ AREA, LENGTH, POROSITY OF THE CORE
C
      READ (60,*) A,L,POR
      WRITE(80,340)A,L,POR
C
C     READ DISPERSIVITIES AND MASS TRANS. COEFFS., AND PARTITION COEFF.
C
      READ (60,*) ALPHA1,ALPHA3,M1,M3,PART1
      WRITE(80,350) ALPHA1,ALPHA3,M1,M3
C
C     READ FRACTIONAL FLOW, FLOW RATE
C
      READ (60,*) FF1,FF3,TFLOW
      WRITE(80,360)FF1,FF3,TFLOW,PART1
C
C     READ NO. OF BLOCKS, NO. OF POE VOL.  ???
C
      READ (60,*) NB,NP,PORN,PVS
```

```
      WRITE(80,370)NB,NP,PORN,PVS
C
C
C
C
C     DEFINE THE NON-DIMENSIONAL PARAMETERS
C
      DX=1./FLOAT(NB)
      DT=PORN/FLOAT(NP)
      UT=TFLOW/(A*POR)
      DISD1=ALPHA1*F1/L
      DISD3=ALPHA3*F3/L
      DISPN=1./(2.*NB)
      DIS1=DISD1-DISPN
      DIS3=DISD3-DISPN
      MD1=L*M1/UT
      MD3=L*M3/UT
      SB=S1*F1+S3*F3*PART1
      FFB=FF1+FF3*PART1
      DISPB=DIS1*FF1+DIS3*FF3*PART1
C
C     IN-SITU CONCENTRATION AT T=0
C
      NBB=NB+1
      DO 100 I=1,NBB
         C1(I)=0.0
         C3(I)=0.0
         C1P(I)=0.0
         C3P(I)=0.0
         C4(I)=0.0
100   CONTINUE
C
C     SOLVE THE CAP. EQ. FOR TRACER I USING 3-P EXPLICIT FORM.
C
      COUNT = 0.0
      NBP=NB+2
      PV=0.0
      NB1=NB-1
110   PV=PV+DT
      COUNT = COUNT + 1.0
      C4(NBP)=FFB*C1(1)
      DO 140 I=2,NB1
         DISPT=DISPB*(C1(I-1)-2.*C1(I)+C1(I+1))*FLOAT(NB)
         CONVT=FFB*(C1(I)-C1(I+1))
         CAPT=1.*(MD1*(C1(I)-C1P(I))+MD3*(C3(I)-C3P(I)))
         IF (F1.EQ.1.0) GO TO 120
         C1P(I)=C1P(I)+MD1/(S1*(1.-F1))*(C1(I)-C1P(I))*DT
120      IF (F3.EQ.1.0) GO TO 130
         C3P(I)=C3P(I)+MD3/(S3*(1.-F3))*(C3(I)-C3P(I))*DT
130      C4(I)=C4(I)+DT/DX*(DISPT-CONVT)-DT*CAPT
         IF (C4(I).GE.0.0) GO TO 140
         C4(I)=0.0
140   CONTINUE
C
C     NEXT TO THE PRODUCER
```

```
C        I = 1
C
      DISPT=-DISPB*(C1(1)-C1(2))*FLOAT(NB)
      CONVT=FFB*(C1(1)-C1(2))
      CAPT=1.*(MD1*(C1(1)-C1P(1))+MD3*(C3(1)-C3P(1)))
      IF (F1.EQ.1.0) GO TO 150
      C1P(1)=C1P(1)+MD1/(S1*(1.-F1))*(C1(1)-C1P(1))*DT
150   IF (F3.EQ.1.0) GO TO 160
      C3P(1)=C3P(1)+MD3/(S3*(1.-F3))*(C3(1)-C3P(1))*DT
160   C4(1)=C4(1)+DT/DX*(DISPT-CONVT)-DT*CAPT
C
C     NEXT TO THE INJECTOR  I=NB
C
      IF (PV.LE.PVS) GO TO 170
      C1(NB+1)=0.0
      GO TO 180
170   C1(NB+1)=1.0
180   DISPT=DISPB*(C1(NB-1)-C1(NB))*FLOAT(NB)
      CONVT=FFB*(C1(NB)-C1(NB+1))
      CAPT=1.*(MD1*(C1(NB)-C1P(NB))+MD3*(C3(NB)-C3P(NB)))
      IF (F1.EQ.1.0) GO TO 190
      C1P(NB)=C1P(NB)+MD1/(S1*(1.-F1))*(C1(NB)-C1P(NB))*DT
190   IF (F3.EQ.1.0) GO TO 200
      C3P(NB)=C3P(NB)+MD3/(S3*(1.-F3))*(C3(NB)-C3P(NB))*DT
200   C4(NB)=C4(NB)+DT/DX*(DISPT-CONVT)-DT*CAPT
      DO 210 K=1,NB
         C1(K)=C4(K)/SB
         C3(K)=C1(K)*PART1
210   CONTINUE
      C1(NBP)=C4(NBP)/FFB
      C3(NBP)=C1(NBP)*PART1
C
C
C     PRINT OUTPUT
C
      IF (PV.EQ.DT) GO TO 220
      GO TO 230
220   WRITE(80,400)START
      WRITE(80,405)
C
C
C
230   CNT=C1(NBP)
      PVI=PV
      IF(COUNT.EQ.10.)THEN
           WRITE (80,410) PVI,CNT
           COUNT = 0.0
      ELSE
      END IF
C
      IF (DT.GT.(PORN-PV)) DT=PORN-PV
      IF (PV.EQ.PORN) GO TO 290
      IF (PV.GT.STP) THEN        ! STOP WHEN PV GT STP
         WRITE(80,420)
         STOP
```

```
      ELSE
      END IF
      GO TO 110
C
C     CLOSE INPUT AND OUTPUT FILES, 60 AND 80
C
290   WRITE(80,420)
      CLOSE(60)
      CLOSE(80)
C
C
      STOP
C
C
330   FORMAT ("TEXT 1",3X,"'S1=",F5.3,6X,"S2=",F5.3,6X,"F1=",F4.2,6X,
     1"F2=",F4.2,"'")
340   FORMAT (9X,"'AREA=",F5.2,4X,"L=",F5.2,7X,"POR=",F5.3,"'")
350   FORMAT (9X,"'ALPHA1=",F5.2,2X,"ALPHA2=",F5.2,2X,"M1=",E8.2,2X,
     1"M2=",E8.2,"'")
360   FORMAT (9X,"'FF1=",F5.3,5X,"FF2=",F5.3,5X,"QT=",F6.3,4X,"PART1=",
     1F5.2,"'")
370   FORMAT (9X,"'NB=",I4,6X,"NP=",I4,6X,"PVINJ=",F5.2,3X,"PVS=",F5.3,
     1"'")
380   FORMAT (A2,3X,40A1)
390   FORMAT (A2,3X,10A1,2X,10A1)
400   FORMAT (A2,T17,2HPV,T29,5HC1(I))
405   FORMAT (5X,12HDATA DEST C1)
410   FORMAT (T18,F6.4,T30,F10.6)
420   FORMAT (5X, 3HEND)
C
      END
C
C
      SUBROUTINE SETUP (INPUT_FILE_NAME, OUTPUT_FILE_NAME)
C     ****************************************************************
C     THIS SUBROUTINE HAS THREE TASKS:
C         1.PRINT OUT THE INITIAL INSTRUCTIONS
C
C         2. READ IN THE NAME OF THE FILE CONTAINING THE EXPERIMENTAL
C         DATA.
C
C         3. READ IN THE NAME OF THE FILE USED TO STORE THE OUTPUT.  IF
C         THE FILE ALREADY EXISTS, WARN THE USER THAT HE WILL DESTROY
C         HIS OLD DATA IF HE PROCEEDS.
C
C     INPUT:
C         NONE
C
C     OUTPUT:
C         INPUT_FILE_NAME, OUTPUT_FILE NAME, THE NAMES OF THE INPUT AND
C         OUTPUT FILES.
C
C
C     SUBROUTINE SETUP
C     BILL ANDERSON                    MARCH 8, 1985
```

```
C     ***************************************************************************
      LOGICAL       DEBUG, EXISTING_FILE
      INTEGER       FLAG, PERIOD
      CHARACTER     JUNK*72, DECIDE*3
      CHARACTER*64 INPUT_FILE_NAME, OUTPUT_FILE_NAME, FILE_NAME
C
      DEBUG = .FALSE.
C
C
      WRITE(1,'(/,"THIS PROGRAM CALCULATES THE TRACER CONCENTRATIONS",
     1 " VERSUS PORE VOLUMES",/,"INJECTED FOR PARTITIONING AND",
     2 " NONPARTITIONING TRACERS.  THE OUTPUT IS STORED IN",/,
     3 "A FILE THAT CAN BE PLOTTED WITH GRAFIT/1000.")')
C
C
C                                     INPUT FILE NAME
      FLAG = 0
100   WRITE(1,'(/,"ENTER THE INPUT FILE NAME.")')
      READ (1,'(A64)')    INPUT_FILE_NAME
                          ! SEE IF FILE ALREADY EXISTS
      INQUIRE ( FILE = INPUT_FILE_NAME, EXIST = EXISTING_FILE )
      IF (EXISTING_FILE .EQV. .FALSE. ) THEN
          FLAG = FLAG + 1
          IF (FLAG .LT. 3) THEN
              WRITE(1,'(/,"THE FILE YOU HAVE ENTERED,",/,A64,/,"CAN ",
     1        "NOT BE FOUND.  PLEASE RE-ENTER THE NAME",/)')
     2        INPUT_FILE_NAME
              GO TO 100
          ELSE
              WRITE(1,'(/,"CANNOT FIND FILE, PROGRAM ABORTING.")')
              STOP
          END IF
      END IF
C
      WRITE (1,'(//,"THE DATA WILL BE READ FROM ",A64)') INPUT_FILE_NAME
C
      WRITE(1,'(/,"ENTER THE OUTPUT FILE NAME.")')
300   READ (1,'(A64)')    OUTPUT_FILE_NAME

                                ! SEE IF FILE ALREADY EXISTS
      INQUIRE (FILE = OUTPUT_FILE_NAME, EXIST = EXISTING_FILE)
      IF (EXISTING_FILE) THEN
          WRITE(1,'(/,"THE OUTPUT FILE NAME YOU HAVE ENTERED,",/,
     1    A64,/,"ALREADY EXISTS. WRITE OVER THE OLD FILE? (Y/N) _")')
     2    OUTPUT_FILE_NAME
          READ (1,'(A3)') DECIDE
          IF (INDEX(DECIDE,'Y') .GT. 0 .OR.
     1        INDEX(DECIDE,'y') .GT. 0 ) THEN
              CONTINUE
          ELSE
              WRITE(1,'("ENTER THE FILE NAME.")')
              GO TO 300             ! THE USER WILL RE-ENTER THE FILE NAME.
          END IF
      END IF
C
```

```
C
                                        ! HAVE AN ACCEPTABLE FILE
      WRITE(1,'(//,"THE DATA WILL BE WRITTEN TO ",A64)')
     1  OUTPUT_FILE_NAME
C
C
C
      RETURN
C
C
      END                          ! END SUBROUTINE SETUP
```

APPENDIX J

PROGRAM FOR UNSTEADY, TWO-PHASE FLOW

Program CAPSAT calculates the effluent tracer concentration for a finite upward slug during an unsteady-state waterflood. Both partitioning and nonpartitioning tracers can be modeled.

The program assumes a linear relationship between flowing (nondendritic) fraction and fractional flow. The user must choose the minimum and maximum flowing fractions for both oil and water. The data from the steady-state experiments show that this is a good assumption.

The user has a choice between two different relative permeability functions, simple and complicated (Honarpour et. al., 1982). The simple equations are given as:

$$k_{rw} = k^{o}_{rw}\left(\frac{S_w - S_{wr}}{1 - S_{wr} - S_{or}}\right)^{e_w} \tag{J-1}$$

$$k_{ro} = k^{o}_{ro}\left(\frac{1 - S_w - S_{or}}{1 - S_{wr} - S_{or}}\right)^{e_o} \tag{J-2}$$

If the user inputs OPTION = 1.0, then the simple equations are used. For this option, WET = 1.0 for both water- and oil-wet cases.

If the more complicated equations are chosen, the user has a choice between water-wet and oil-wet conditions. If the user inputs WET = 1.0, then the water-wet equations are used. Equation (J-3) is for a

water-wet sandstone, Equation (J-4) is for an intermediate or oil-wet sandstone, and Equation (J-5) is for either case.

$$k_{rw} = 0.0354 \frac{(S_w - S_{wr})}{(1 - S_{wr} - S_{or})} - 0.0109 \left(\frac{(S_w - S_{or})}{(1 - S_{wr} - S_{or})} \right)^{2.9}$$

$$+ 0.566 (S_w)^{3.6} (S_w - S_{wr}) \qquad \text{(J-3)}$$

$$\{(S_w - S_{or}) \geq 0\}$$

$$k_{rw} = 1.58 \left(\frac{S_w - S_{wr}}{1 - S_{wr}} \right)^{1.91} - 0.586 \left(\frac{S_w - S_{or}}{1 - S_{wr} - S_{or}} \right) (S_w - S_{wr})$$

$$- 1.25 \phi (1 - S_{wr}) (S_w - S_{wr}) \qquad \text{(J-4)}$$

$$k_{ro} = 0.761 \left(\frac{(S_o / (1 - S_{wr})) - S_{or}}{1 - S_{or}} \right)^{1.8} \left(\frac{S_o - S_{or}}{1 - S_{wr} - S_{or}} \right)^{2.0}$$

$$+ 2.63 \phi (1 - S_{or}) (S_o - S_{or}) \qquad \text{(J-5)}$$

```
      PROGRAM CAPSAT(INPUT,OUTPUT,PLT,TAPE5=INPUT,TAPE6=OUTPUT,
     /               TAPE7=PLT)
C
C
C     THIS IS THE UNSTEADY-STATE MODEL FOR A FINITE UPWARDS SLUG.
C     CAPACITANCE-DISPERSION BEHAVIOR IS MODELLED.
C
C     BY JEFFREY C. SMITH    1986-1987
C
C
C
      DIMENSION C1F(101),C1D(101),C2F(101),C2D(101),C2FNEW(101),
     /C1FNEW(101),S1F(101),S1D(101),S2F(101),S2D(101),SB(101),FF1(101),
     /FF2(101),FFB(101),F1(101),F2(101)
C
      DIMENSION S1FNEW(101),S1DNEW(101),S2FNEW(101),S2DNEW(101),
     /F1NEW(101),F2NEW(101),SAT(101),SATO(101),FF1NEW(101),FF2NEW(101),
     /FFBNEW(101),SBNEW(101)
C
      DIMENSION FW(101),SW(101),FFW(101),DISPB(101)
      DIMENSION XPV(400), YCON(400), PVI(100), CD(100)
C
      REAL L,M1,M2,MD1,MD2,KRWO,KROO
C
C
      READ(5,*)RUNNO
      WRITE(6,*)RUNNO
C
C
C     READ  END POINT PERMS
      READ (5,*)KRWO,KROO
C
C     READ VISCOSITIES
C
      READ (5,*)UW,UO
      WRITE(6,121)KRWO,KROO,UW,UO
C
C     READ LENGTH, AREA, AND POROSITY OF THE CORE
C
      READ(5,*)L,AREA,POR
      WRITE(6,141)L,AREA,POR
C
C     READ RELATIVE PERM EXPONENTS FOR SIMPLE EQUATION
C
      READ(5,*)EW,EO
C
C     READ RESIDUAL SATURATIONS
C
      READ (5,*)SWR,SOR
      WRITE(6,171)EW,EO,SWR,SOR
      SWI = SWR
C
C
C     READ DISPERSIVITIES ALPHA1, ALPHA2
C
      READ(5,*)ALPHA1,ALPHA2
C
C     READ MASS TRANSFER COEFFICIENTS M1, M2
C
      READ(5,*)M1,M2
      WRITE(6,201)ALPHA1,ALPHA2,M1,M2
```

```
C
C     READ PARTITIONING COEFFICIENT PART12
C
      READ(5,*)PART12
C
C     READ TOTAL FLOWRATE QT
C
      READ(5,*)QT
C
C     READ TOTAL PV INJECTED AND SLUG SIZE
C
      READ(5,*)PVINJ,PVS
      WRITE(6,231)QT,PART12,PVINJ,PVS
C
C     READ LOW AND HIGH OIL FLOWING FRACTION
C
      READ(5,*) F1LOW,F1HIGH
C
C     READ LOW AND HIGH WATER FLOWING FRACTION
C
      READ(5,*)F2LOW,F2HIGH
      WRITE(6,251)F1LOW,F1HIGH,F2LOW,F2HIGH
C
C
C     READ NO. OF BLOCKS AND NO. OF TIME STEPS
C
      READ(5,*)NB,NP
C
C     READ WETABILITY AND REL. PERM EQ. OPTION
C     IF WET = 1.0 CORE IS WATER-WET
C     IF OPTION = 1.0 USE SIMPLE REL. PERM EQS
C
      READ(5,*)WET,OPTION
      WRITE(6,261)NB,NP,WET,OPTION
C
C     READ THE RAWDATA AND NORMALIZE IT
C
      CALL RAWDATA(PVI,CD,NDAT)
C
C     ***************************************************************
C     IN-SITU CONDITIONS AT T=0
C
      C2FINJ = 0.0
      NBB = NB+1
      DO 10 I=1,NBB
C
          C1F(I) = 0.0
          C1D(I) = 0.0
          C2F(I) = 0.0
          C2D(I) = 0.0
          C2FNEW(I) = 0.0
C
          S1F(I) = 1. - SWI
C         ASSUME NO DENDRITIC OIL AT SWI
          S1D(I) = 0.0
          S2F(I) = SWI
C         ASSUME NO DENDRITIC WATER AT SWI
          S2D(I) = 0.0
          SB(I) = S1F(I)*PART12 + S2F(I)
C
C         ONLY OIL FLOWING
          FF1(I) = 1.0
```

```
            FF2(I) = 0.0
C           NO DENDRITIC OIL OR WATER
            F1(I) = 1.0
            F2(I) = 1.0
            FFB(I) = PART12
            FFW(I) = 0.0
C
10      CONTINUE
C
C       ********************************************************************
C       DEFINE THE NON-DIMENSIONAL PARAMETERS
C
        DX = 1.0/FLOAT(NB)
        DT = PVINJ/FLOAT(NP)
        UT = QT/(AREA*POR)
        MD1 = M1*L/UT
        MD2 = M2*L/UT
        DISD1 = ALPHA1/L
        DISD2 = ALPHA2/L
        DISPN = 1./(2.*FLOAT(NB))
        DIS1 = DISD1 - DISPN
        DIS2 = DISD2 - DISPN
C
C       INITIALIZE
C
        NUMDATA = 0
C
C       PRINT DATA EVERY 10TH TIME THRU LOOP
        ICOUNT = 0
        PV = 0.0
C       SUBROUTINE SATCALC HAS NOT BEEN CALLED YET
        FIT = 0.0
        NB1 = NB-1
C       AREA UNDER CURVE BY TRAP RULE-- INITIALIZE
        TRAP = 0.0
C
C       USE TO CALCULATE FLOWING FRACTION FOR EACH PHASE
C
        SLOPE1 = -(F1HIGH - F1LOW)
        SLOPE2 = F2HIGH - F2LOW
C
C
C
C       ********************************************************************
C       ********************************************************************
C
C       THIS IS THE BEGINNING OF THE LOOP THAT IS RUN FOR EACH TIME STEP
C
C
C       INCREMENT PV INJECTED
100     PV = PV + DT
C       PRINT DATA EVERY 10TH TIME THRU LOOP
        ICOUNT = ICOUNT + 1
C
C       CALCULATE WEIGHTED AVERAGE DISPERSIVITY FOR EACH BLOCK
C
        DO 11 I=1,NB
          DISPB(I)=(1.-FFW(I))*DIS1*PART12 + FFW(I)*DIS2
11      CONTINUE
C
C
C       CALCULATE THE NEW SATURATION PROFILE.  OUTPUT VARIABLES FROM THIS
```

```
C     SUBROUTINE ARE SAT(I), FFW(I) FOR I=1,NB
C
      CALL SATCALC(FIT,SWR,SOR,PVINJ,NB,NP,KRWO,KROO,EW,EO,UW,UO,
     1SW,FW,SAT,FFW,WET,OPTION,POR)
C
C
C     DETERMINE NEW CONDITIONS IN EACH BLOCK
C     **************************************
C
      DO 20 I=1,NB
C         TOTAL OIL SATURATION
          SATO(I) = 1. - SAT(I)
C
C
C     DETERMINE DENDRITIC FRACTIONS AND SATURATIONS FOR OIL AND WATER
C     OIL = 1 WATER = 2
C
C     OIL
C     ***
      F1NEW(I) = SLOPE1*FFW(I) + F1HIGH
      IF(FFW(I).EQ.1.0)F1NEW(I)=1.0
      IF(F1NEW(I).GT.(F1HIGH - 0.005)) F1NEW(I) = F1HIGH
      S1FNEW(I) = SATO(I)*F1NEW(I)
      S1DNEW(I) = SATO(I) - S1FNEW(I)
C
C     WATER
C     *****
      F2NEW(I) = SLOPE2*FFW(I) + F2LOW
      IF(FFW(I).EQ.0.0)F2NEW(I)=1.0
      IF(F2NEW(I).GT.(F2HIGH - 0.005)) F2NEW(I) = F2HIGH
      S2FNEW(I) = SAT(I)*F2NEW(I)
      S2DNEW(I) = SAT(I) - S2FNEW(I)
C
C         DETERMINE FLOWING FRACTIONS, AVERAGE FLOWING FRACTION, AND
C         AVERAGE SATURATION FOR EACH BLOCK
C         ************************************************************
C
          FF1NEW(I) = 1.0 - FFW(I)
          FF2NEW(I) = FFW(I)
          FFBNEW(I) = FF1NEW(I)*PART12 + FF2NEW(I)
          SBNEW(I) = S1FNEW(I)*PART12 + S2FNEW(I)
C
C
20    CONTINUE
C
C
C     SOLVE THE CAPACITANCE-DESPERSION EQUATION FOR BLOCKS 2 THRU NB-1
C     ***************************************************************
C
      DO 120 I=2,NB1
C
          DISPT=(DISPB(I)*(C2F(I+1)-C2F(I))
     /           -DISPB(I-1)*(C2F(I)-C2F(I-1)))*FLOAT(NB)
C
          CONVT = C2F(I)*FFB(I) - C2F(I-1)*FFB(I-1)
C
          CAPT = MD1*(C1F(I) - C1D(I)) + MD2*(C2F(I) - C2D(I))
C
C         CALCULATE NEW DENDRITIC CONCENTRATIONS
C
          IF(S1DNEW(I).EQ.0.0) THEN
              C1D(I) = 0.0
```

```
          ELSE
             C1D(I) = (MD1*(C1F(I)-C1D(I))*DT + C1D(I)*S1D(I))/S1DNEW(I)
          END IF
C
          IF(S2DNEW(I).EQ.0.0) THEN
             C2D(I) = 0.0
          ELSE
             C2D(I) = (MD2*(C2F(I)-C2D(I))*DT + C2D(I)*S2D(I))/S2DNEW(I)
          END IF
C
C
C     CALCULATE NEW FLOWING CONCENTRATIONS
C     ************************************
C
      C2FNEW(I) =((DISPT-CONVT)*DT/DX - CAPT*DT + C2F(I)*SB(I))/SBNEW(I)
C
      IF(C2FNEW(I).LT.0.0) C2FNEW(I) = 0.0
C
      C1FNEW(I) = C2FNEW(I)*PART12
C
120   CONTINUE
C
C
C     NEXT TO THE INJECTOR: I=1
C     *********************
C
      IF(PV.GT.PVS) THEN
          C2FINJ = 0.0
      ELSE
          C2FINJ = 1.0
      END IF
C
C
      DISPT=(DISPB(1)*(C2F(2)-C2F(1))-DIS2*(C2F(1)-C2FINJ))*FLOAT(NB)
C
C     FFB(0) = 1.0
      CONVT = C2F(1)*FFB(1) - C2FINJ
C
      CAPT = MD1*(C1F(1) - C1D(1)) + MD2*(C2F(1) - C2D(1))
C
C     CALCULATE NEW DENDRITIC CONCENTRATIONS NEXT TO THE INJECTOR
C
      IF(S1DNEW(1).EQ.0.0) THEN
          C1D(1) = 0.0
      ELSE
          C1D(1) = (MD1*(C1F(1) - C1D(1))*DT + C1D(1)*S1D(1))/S1DNEW(1)
      END IF
C
      IF(S2DNEW(1).EQ.0.0) THEN
          C2D(1) = 0.0
      ELSE
          C2D(1) = (MD2*(C2F(1) - C2D(1))*DT + C2D(1)*S2D(1))/S2DNEW(1)
      END IF
C
C     CALCULATE NEW FLOWING CONCENTRATIONS NEXT TO THE INJECTOR
C
      C2FNEW(1) =((DISPT-CONVT)*DT/DX - CAPT*DT + C2F(1)*SB(1))/SBNEW(1)
C
      IF(C2FNEW(1).LT.0.0) C2FNEW(1) = 0.0
C
      C1FNEW(1) = C2FNEW(1)*PART12
C
```

```
C
C     NEXT TO THE PRODUCER: I = NB
C     ****************************
C
C     USING BOUNDARY CONDITION (C(NB+1)-C(NB))/DX = 0.0
C     NO-FLOW BOUNDARY
C
      DISPT=-DISPB(NB-1)*(C2F(NB)-C2F(NB-1))*FLOAT(NB)
C
      CONVT = C2F(NB)*FFB(NB) - C2F(NB-1)*FFB(NB-1)
C
      CAPT = MD1*(C1F(NB) - C1D(NB)) + MD2*(C2F(NB) - C2D(NB))
C
C     CALCULATE NEW DENDRITIC CONCENTRATIONS NEXT TO THE PRODUCER
C
      IF(S1DNEW(NB).EQ.0.0) THEN
          C1D(NB) = 0.0
      ELSE
          C1D(NB)=(MD1*(C1F(NB)-C1D(NB))*DT+C1D(NB)*S1D(NB))/S1DNEW(NB)
      END IF
C
      IF(S2DNEW(NB).EQ.0.0) THEN
          C2D(NB) = 0.0
      ELSE
          C2D(NB)=(MD2*(C2F(NB)-C2D(NB))*DT+C2D(NB)*S2D(NB))/S2DNEW(NB)
      END IF
C
C     CALCULATE NEW FLOWING CONCENTRATIONS NEXT TO THE PRODUCER
C
      C2FNEW(NB)=((DISPT-CONVT)*DT/DX-CAPT*DT+C2F(NB)*SB(NB))/SBNEW(NB)
C
      IF(C2FNEW(NB).LT.0.0) C2FNEW(NB) = 0.0
C
      C1FNEW(NB) = C2FNEW(NB)*PART12
C
C     SET CONCENTRATION IN BLOCK NB+1 = CONCENTRATION IN BLOCK NB
C
      C2FNEW(NB+1) = C2FNEW(NB)
C
C     DO SUMMATION TERM FOR AREA UNDER THE CURVE, TRAP. RULE
C
      TRAP = TRAP + C2FNEW(NB+1)
C
C     PRINT OUTPUT
C     ************
C
      IF(ICOUNT.EQ.10) THEN
          WRITE(6,281)PV,C2FNEW(NB+1),SAT(NB),FFW(NB)
281       FORMAT(F7.4,5X,F7.5,5X,F7.5,5X,F7.5)
C
C         NUMDATA,XPV,YCON USED FOR PLOTTING
C
          NUMDATA = NUMDATA + 1
          XPV(NUMDATA) = PV
          YCON(NUMDATA) = C2FNEW(NB+1)
          IF(YCON(NUMDATA) .LT. 0.001) YCON(NUMDATA) = 0.0
C
C          REINITIALIZE
          ICOUNT = 0
      ELSE
      END IF
C
```

```
C     RENAME NEW TO OLD AND RETURN FOR NEXT TIME STEP
C     ***********************************************
C
      DO 666 I=1,NB
          C1F(I) = C1FNEW(I)
          C2F(I) = C2FNEW(I)
C
          S1F(I) = S1FNEW(I)
          S1D(I) = S1DNEW(I)
          S2F(I) = S2FNEW(I)
          S2D(I) = S2DNEW(I)
          SB(I) = SBNEW(I)
C
          FF1(I) = FF1NEW(I)
          FF2(I) = FF2NEW(I)
          FFB(I) = FFBNEW(I)
666   CONTINUE
C
      IF(DT.GT.(PVINJ-PV)) DT = PVINJ - PV
C
      IF(PV.GT.1.0 .AND. C2FNEW(NB+1).LT..001) THEN
C     ACTUAL AREA UNDER CURVE
          TRAP = DT*TRAP
          WRITE(6,271)
          WRITE(6,*)TRAP
C
C         WRITE DATA TO FILE PLT TO BE PLOTTED
C
          NCURVES = 2
          WRITE(7,*) NCURVES
          WRITE(7,*) NUMDATA
          DO 987 I=1,NUMDATA
             WRITE(7,*) XPV(I), YCON(I)
987       CONTINUE
          WRITE(7,*) NDAT
          DO 986 I=1,NDAT
             WRITE(7,*) PVI(I), CD(I)
986       CONTINUE
C
C
         WRITE(7,282)
282      FORMAT(1X,12HPORE VOLUMES,/,1X,24HNORMALIZED CONCENTRATION,
     /           /,1X,12HCAPAC. MODEL,/,1X,9HEXP. DATA)
C
         WRITE(7,283)RUNNO
283      FORMAT(1X,F4.1,3/)
C
          STOP
      ELSE
      END IF
C
      IF(PV.LT.PVINJ) GO TO 100
C
C     ***********************************************************************
C     ***********************************************************************
C
C
      STOP
C
C     FORMAT STATEMENTS
C
121   FORMAT(1X,"      ",2X,"*KRW0=",F5.3,4X,"KRO0=",F5.3,4X,"UW=",F6.3,
```

```
     13X,"UO=",F6.3,"")
141   FORMAT(9X,""L=",F5.2,7X,"AREA=",F5.2,4X,"POR=",F5.2,"")
171   FORMAT(9X,""EW=",F4.2,7X,"EO=",F4.2,7X,"SWR=",F3.2,5X,"SOR=",F3.2,
     1"")
201   FORMAT(9X,""ALPHA1=",F5.2,2X,"ALPHA2=",F5.2,2X,"M1=",E7.1,2X,"M2="
     1,E7.1,"")
231   FORMAT(9X,""QT=",F6.3,5X,"PART12=",F5.2,2X,"PVINJ=",F4.1,2X,"PVS="
     1,F5.2,"")
251   FORMAT(9X,""F1LOW=",F4.2,4X,"F1HIGH=",F4.2,3X,"F2LOW=",F4.2,2X,"F2
     1HIGH=",F4.2,"")
261   FORMAT(9X,""NB=",I3,8X,"NP=",I4,7X,"WET=",F3.1,5X,"OPTION=",F3.1,
     1"")
271   FORMAT("1",8X,"AREA UNDER CURVE = ")
C
C
C     END OF MAIN PROGRAM
C
      END
C
C
C     ****************************************************************
C     ****************************************************************
C
C     THIS SUBROUTINE CALCULATES FW AND SW FOR EACH BLOCK I=1,NB
C     BY FINITE DIFFERENCE
C
      SUBROUTINE SATCALC(FIT,SWR,SOR,PVINJ,NB,NP,KRWO,KROO,EW,EO,UW,UO,
     /SW,FW,SAT,FFW,WET,OPTION,POR)
C
C
      REAL KRW, KRO, KRWO, KROO
C
C
      DIMENSION SW(101),FW(101),KRW(101),KRO(101)
      DIMENSION SWB(101),SOB(101),SAT(101),FFW(101),SO(101)
C
C
C
C
C
C     INITIALIZE
C
C     IF THIS IS FIRST TIME THROUGH SUBROUTINE, SET INITIAL VALUES TO
C     SW(I) = SWR, FW(I) = 0.0
C
      IF(FIT.EQ.0.) THEN
C
          DO 10 I=1,NB
              SW(I) = SWR
              FW(I) = 0.0
10        CONTINUE
          FIT = 1.0
C
      ELSE
C         SET NEW TO OLD
          DO 15 I=1,NB
              SW(I) = SAT(I)
              FW(I) = FFW(I)
15        CONTINUE
      END IF
C
C     100% WATER INJECTED
```

```
      FWINJ = 1.0
      DTDX = PVINJ*FLOAT(NB)/FLOAT(NP)
C
C
C     CALCULATE SATURATION IN EACH BLOCK
C
      DO 20 I=1,NB
C         CALC. NEW SATURATION IN EACH BLOCK
C
          IF(I.EQ.1)THEN
              SAT(I) = SW(I) + (FWINJ - FW(I))*DTDX
          ELSE
              SAT(I) = SW(I) + (FW(I-1) - FW(I))*DTDX
          END IF
C
          SO(I) = 1. - SAT(I)
C
C         CALC. NEW FRACTIONAL FLOW IN EACH BLOCK FFW(I)
C
C     DETERMINE WHICH RELATIVE PERM EQUATION TO USE
C
      IF(OPTION.EQ.1.) THEN
C     USE SIMPLE EQUATION
C
C         SIMPLE REL. PERM EQ.
C         ********************
C
          SWB(I) = (SAT(I) - SWR)/(1. - SWR - SOR)
          IF(SWB(I).EQ.0.)THEN
              KRW(I) = 0.
          ELSE
              KRW(I) = KRWO*(SWB(I)**EW)
          END IF
C
          SOB(I) = (1. - SAT(I) - SOR)/(1. - SWR - SOR)
          IF(SOB(I).EQ.0.)THEN
              KRO(I) = 0.
          ELSE
              KRO(I) = KROO*(SOB(I)**EO)
          END IF
C
C
      ELSE
C     USE COMPLICATED EQS.
C
C         COMPLICATED REL. PERM. EQ. (HONARPOUR ET. AL)
C         *********************************************
C
          IF(WET.EQ.1.) THEN
C     CORE IS WATER WET
              IF((SW(I)-SOR).LT.0.) THEN
                  WRITE(6,200)
200               FORMAT(2X,'ERROR: SW(I) - SOR) IS LESS THAN 0.0  SW=')
                  WRITE(6,*)SW(I)
                  STOP
              ELSE
              END IF

              TERM1 = 1. - SWR - SOR
              ARG1 = 0.035388*(SW(I) - SWR)/TERM1
              ARG2 = 0.018874*((SW(I) - SOR)/TERM1)**2.9
              ARG3 = 0.56556*(SW(I) - SWR)*(SW(I))**3.6
```

```
            KRW(I) = ARG1 - ARG2 + ARG3
C
        ELSE
C     CORE IS OIL-WET
C
            TERM1 = 1. - SWR
            ARG1 = 1.5814*((SW(I) - SWR)/TERM1)**1.91
            ARG2 = 0.58617*(SW(I) - SWR)*((SW(I) - SOR)/(TERM1 - SOR))
            ARG3 = 1.2484*POR*TERM1*(SW(I) - SWR)
            KRW(I) = ARG1 - ARG2 - ARG3
C
        END IF
C
C       CALC KRO(I)
C
C
        TERM1 = 1. - SWR
        TERM2 = 1. - SOR
        TERM3 = SO(I) - SOR
        ARG1 = (((SO(I)/TERM1) - SOR)/TERM2)**1.8
        ARG2 = TERM3/(TERM1 - SOR)
        ARG3 = 2.6318*POR*TERM2*TERM3
        KRO(I) = 0.76067*ARG1*ARG2*ARG2 + ARG3
C
    END IF
C
C     CALC FFW(I)
C     ***********
C
        IF(KRW(I).EQ.0.) THEN
            FFW(I) = 0.0
        ELSE
            FFW(I) = 1.0/(1. + (UW*KRO(I))/(UO*KRW(I)))
        END IF
C
20  CONTINUE
C
C
C
C     ****************************************************************
C
C     RETURN TO MAIN PROGRAM
C
      RETURN
C
C     END SUBROUTINE SATCALC
C
      END
C
C
C
C
      SUBROUTINE RAWDATA(PVI,CD,NDAT)
C
      DIMENSION CD(100), PVI(100)
C
C     THIS ROUTINE READS THE RAWDATA AND NORMALIZES IT.  IT ALSO
C     ACCOUNTS FOR DEADVOLUME IN THE TUBING.
C
C     READ NUMBER OF DATA PTS, MIN CONCENTRATION, MAX CONCENTRATION
C
      READ(5,*)NDAT,CMIN,CMAX
```

```
C
C     READ TESTTUBE VOLUME,DEADVOL,CORE POREVOLUME
C
      READ(5,*)VOL,DEADVOL,COREPV
C
C     READ TESTTUBE NUMBER AND TRACER CONCENTRATION, THEN NORMALIZE
C
      DO 10 I=1,NDAT
         READ(5,*)TNO,C
         VOLINJ = (TNO-1.)*VOL + VOL/2. - DEADVOL
C
         IF(VOLINJ.LT.0.0)THEN
            CD(I) = 0.0
            PVI(I) = 0.0
         ELSE
            PVI(I) = VOLINJ/COREPV
            CD(I) = (C-CMIN)/(CMAX-CMIN)
         END IF
10    CONTINUE
C
      RETURN
      END
```

APPENDIX K

INVESTIGATION OF A METHOD PROPOSED BY DEANS (1978)

THAT ALLOWS INDEPENDENT SATURATION DETERMINATION

Deans (1978) proposed a method that uses chemical tracers flowing with oil and brine to give an independent measure of saturation. Multiple partitioning tracers with different partition coefficients would be used during unsteady-state waterfloods to give points on the fractional flow versus saturation curve.

The relevant equations for core floods are:

$$S_o = \frac{d}{d(1/PV_i)} \quad \frac{PV_i - 1}{PV_i(P_{ijk} - 1)} \tag{K-1}$$

$$f_o = \frac{1}{PV^2} \quad \frac{d}{d(1/PV_i)} \quad \frac{PV_i - 1}{P_{ijk} - 1} \tag{K-2}$$

where PV_i is the pore volume of brine injected when tracer i breaks through, usually defined to be when the concentration of tracer i equals one-half its initial concentration. P_{ijk} is the partition coefficient of tracer i defined as the concentration of i in oil divided by the concentration of i in brine. These relationships require differentiation of experimental results.

This method was tested by using the unsteady-state model developed earlier in this report. Computer runs were made using several different values for this partition coefficient, and PV_i was determined for each run.

The appropriate plots were made, and Equations (K-1) and (K-2) were used to determine the fractional flow curve. This curve was compared with the one calculated by the unsteady-state model, and it was found that the two fractional flow curves were not in agreement.

This indicates that Dean's method is probably not valid. Even if it were, it would be difficult to use when one considers the experimental difficulties involved in using multiple partitioning tracers in a waterflood and the problem of finding enough tracers with the appropriate partitioning coefficient.

APPENDIX L

ELECTRICAL RESISTIVITY DATA

To eliminate the effects of polarization, resistance across the center of 25 cm of each core was measured at three frequencies: 100, 1,000, and 10,000 Hz. The values are given in Tables L-1 and L-2. To correct for polarization effects, an extrapolation is made to infinite frequency, plotting resistivity versus one over the square root of frequency. The extrapolated resistance is the value at the y-intercept when $1/f = 0$. The method is explained in Walther (1968).

As shown in Tables L-1 and L-2, resistance was measured under varying conditions, either with or without flow. Unfortunately, partway through the experiments we realized that the resistance was generally lower during fluid injection. Similar results have been reported by Graham (1958). The effect of flow on electrical resistivity should be kept in mind when evaluating the data.

It is apparent that the silane treatment had almost no influence on resistance in the core.

TABLE L-1

RESISTANCE DATA FOR WATER-WET BEREA CORE

Experiment	f_w	S_w**	Resistance* (ohms) at: 100 Hz	1,000 Hz	10,000 Hz	Comment	Brine Conductivity (millimhos/cm)
W1.1	1.0	1.0	746	718	716	Not flowing.	19.6
WD1.2	0.0	0.315	8,100	6,850	6,530	Not flowing.	19.6
WD1.3	0.073	0.543	3,280	2,620	2,470	Not flowing.	19.6
WD1.4	0.129	0.577	2,930	2,290	2,130	Not flowing.	19.6
WD1.5	0.297	0.601	2,790	2,190	2,040	Not flowing.	18.4
WD1.6	0.852	0.639	1,990	1,770	1,642	Flowing, before slug injection	18.4
WD1.6	0.852	0.639	2,150	1,770	1,619	Not flowing, after experiment.	18.4
WD1.7	0.934	0.644	2,030	1,746	1,633	Flowing, slug containing IBA has entered core.	18.4
WD1.7	0.934	0.644	1,990	1,720	1,606	Flowing, slug is out of core.	18.4
WD1.8	1.0	0.655	1,930	1,602	1,512	Not flowing, after experiment.	18.4

*Measured across center 25 cm of core. Cross-sectional area of core = 24.90 cm^2.
**Material balance.

TABLE L-2

RESISTANCE DATA FOR TREATED BEREA CORE

Experiment	f_w	S_w**	Resistance* (ohms) at: 100 Hz	1,000 Hz	10,000 Hz	Comment	Brine Conductivity (millimhos/cm)
W2.1	1.0	1.0	746	718	716	Not flowing, before silane treatment.	18.4
W3.1	1.0	1.0	738	714	712	Not flowing, after silane treatment.	18.4
WD2.1	0.0	0.300	1,424	1,344	1,331	Not flowing, after experiment.	18.4
WD2.2	0.085	0.590	5,510	5,220	4,190	Not flowing, before experiment.	18.4
WD2.2	0.085	0.590	4,560	4,370	3,220	Flowing, after experiment.	18.4
WD2.3	0.151	0.638	3,240	3,160	2,520	Flowing, before experiment	18.4
WD2.3	0.151	0.638	3,360	3,250	2,430	Flowing, after experiment.	18.4
WD2.4	0.301	0.680	2,700	2,660	2,510	Flowing, before experiment.	18.4
WD2.4	0.301	0.680	4,150	4,000	3,140	Not flowing, after experiment.	18.4
WD2.5	0.702	0.707	2,500	2,440	2,430	Flowing, after experiment.	18.4
WD2.5	0.702	0.707	2,590	2,510	2,490	Not flowing, immediately after experiment.	18.4
WD2.5	0.702	0.707	2,950	2,890	2,850	Not flowing, 20 minutes after experiment.	18.4
WD2.6	0.857	0.729	1,960	1,940	1,852	Flowing, before experiment.	18.4
WD2.6	0.857	0.729	3,250	3,170	3,090	Not flowing, after experiment.	18.4
WD2.10	1.0	0.741	1,800	1,790	1,728	Flowing, before experiment.	18.4
WD2.10	1.0	0.741	1,750	1,730	1,673	Not flowing, 12 hours after experiment.	18.4

*Measured across center 25 cm of core. Cross-sectional area of core = 25.95 cm^2.
**Material balance.

BIBLIOGRAPHY

Aggarwal, S. K., and Johnston, R. H., "Oil and Water Content Measurement of Sandstone Cores Using Microwaves," SPE 12291, May 1983.

Amott, E., "Observations Relating to the Wettability of Porous Rock," Trans. AIME, *216*, pp. 156-162, 1959.

Anderson, W. G., "Wettability Literature Survey—Part 1: Rock-Oil-Brine Interactions, and the Effects of Core Handling on Wettability," J. Pet. Tech., *38*, pp. 1125-1144, October 1986.

Anderson, W. G., "Wettability Literature Survey—Part 2: Wettability Measurement," J. Pet. Tech., *38*, pp. 1246-1262, November 1986.

Anderson, W. G., "Wettability Literature Survey—Part 3: The Effects of Wettability on the Electrical Properties of Porous Media," J. Pet. Tech., *38*, pp. 1371-1378, December 1986.

Anderson, W. G., "Wettability Literature Survey—Part 4: The Effects of Wettability on Capillary Pressure," SPE 15271, December 1985.

Anderson, W. G., "Wettability Literature Survey—Part 5: The Effects of Wettability on Relative Permeability," SPE 16323, October 1986.

Anderson, W. G., "Wettability Literature Survey—Part 6: The Effects of Wettability on Waterflooding," SPE 16471, February 1987.

Anderson, W. G., and Whitebay, L. E., "Core Analysis Handbook: Part 2," Conoco Research Report, 1987.

Aronofsky, J. S., and Heller, J. P., "A Diffusion Model to Explain Mixing of Flowing Miscible Fluids in Porous Media," Trans. AIME, *210*, pp. 345-349, 1957.

Bailey, N. A.; Rowland, P. R.; and Robinson, D. P., "Nuclear Measurements of Fluid Saturation in EOR Flood Experiments," *Enhanced Oil Recovery*, Proceeding of the Third European Symposium on Enhanced Oil Recovery, held in Bournemouth, U.K., September 21-23, 1981, Edited by F. J. Fayers, Elsevier Scientific Publishing Co., New York City, 1981.

Baker, L. E., "Effects of Dispersion and Dead-End Pore Volume in Miscible Flooding," Soc. Pet. Eng. J., *17(3)*, pp. 219-227, June 1977.

Baker, P. E., "Effect of Pressure and Rate on Steam Zone Development in Steamflooding," Soc. Pet. Eng. J., *13*, pp. 274-284, October 1973.

Baker, P. E., Discussion on "Microwave Attenuation — A New Tool for Monitoring Saturations in Laboratory Flooding Experiments," Soc. Pet. Eng. J., *15*, pp. 309-310, August 1975.

Baldwin, B. A., and Yamanashi, W. S., "Detecting Fluid Movement and Isolation in Reservoir Cores Using Medical NMR Imaging Techniques," SPE/DOE 14884, presented at the SPE/DOE Fifth Symposium on EOR, Tulsa, Oklahoma, April 20-23, 1986.

Bear, J., *Dynamics of Fluids in Porous Media*, American Elsevier Publishing Co., New York, New York, 1972.

Blackwell, R. J., "Laboratory Studies of Microscopic Dispersion Phenomena," Soc. Pet. Eng. J., *2(1)*, pp. 1-8, March 1962.

Boyer, R. L.; Morgan, F.; and Muskat, M., "A New Method for Measurement of Oil Saturation in Cores," Trans. AIME, *170*, pp. 15-33, 1947.

Braun, E. M., and Blackwell, R. J., "A Steady-State Technique for Measuring Oil-Water Relative Permeability Curves at Reservoir Conditions," SPE 10155, presented at the 56th Annual Fall Technical Conference of the SPE, San Antonio, Texas, October 5-7, 1981.

Bretz, R. E.; Specter, R. M.; and Orr, F. M., "Effect of Pore Structure on Miscible Displacements in Laboratory Cores," SPE 15017, presented at the 1986 Permian Basin Oil and Gas Recovery Conference, Midland, Texas, March 13-14, 1986.

Brigham, W. E.; Reed, P. W.; and Dew, J. N., "Experiments on Mixing During Miscible Displacement in Porous Media," Soc. Pet. Eng. J., *1(1)*, pp. 1-8, March 1961.

Brigham, W. E., "Mixing Equations in Short Laboratory Cores," Soc. Pet. Eng. J., *14(1)*, pp. 91-99, February 1974.

Brunner, E., and Mardock, E. S., "A Neutron Method for Measuring Saturations in Laboratory Flow Experiments," Trans. AIME, *165*, pp. 133-143, 1946.

Buckley, S. E., and Leverett, M. C., "Mechanism of Fluid Displacement in Sands," Trans. AIME, *146*, pp. 107-116, 1942.

Caudle, B. H.; Slobod, R. L.; and Brownscombe, E. R., "Further Developments in the Laboratory Determination of Relative Permeability," Trans. AIME, *192*, pp. 145-150, 1951.

Coats, K. H., and Smith, B. D., "Dead-End Pore Volume and Dispersion in Porous Media," Soc. Pet. Eng. J., *4(1)*, pp. 73-84, March 1964.

Craig, F. F., *The Reservoir Engineering Aspects of Waterflooding*, Society of Petroleum Engineers Monograph Series, No. 3, Dallas, Texas, 1971.

Crank, J., *The Mathematics of Diffusion*, Oxford University Press, London, Great Britain, 1956.

Davis, L. A., "VHF Electrical Measurement of Saturations in Laboratory Floods," SPE 8847, presented at the First Joint SPE/DOE Symposium on EOR, Tulsa, Oklahoma, April 20-23, 1980.

Deans, H. A., "Using Chemical Tracers to Measure Fractional Flow and Saturation In-situ," SPE 7076, presented at the Fifth Symposium on Improved Methods for Oil Recovery of the SPE, Tulsa, Oklahoma, April 16-19, 1978.

Delshad, M.; MacAllister, D. J.; Pope, G. A.; and Rouse, B. A., "Multiphase Dispersion and Relative Permeability Experiments," Soc. Pet. Eng. J., *25(4)*, pp. 524-534, August 1985.

Delshad, Mohammad, "Relative Permeability and Dispersion Measurements for a Three-Phase Micellar/ Polymer Mixture," M.S. Thesis, University of Texas at Austin, December 1984.

Delshad, Mojdeh, "Measurement of Relative Permeability and Dispersion for Micellar Fluids in Berea Rock," M.S. Thesis, University of Texas at Austin, 1981.

Delshad, Mojdeh, "A Study of Transport of Micellar Fluids in Porous Media," Ph.D. Thesis, University of Texas at Austin, May 1986.

Donaldson, E. C.; Thomas, R. D.; and Lorenz, P. B., "Wettability Determination and Its Effect on Recovery Efficiency," Soc. Pet. Eng. J., *9(1)*, pp. 13-20, March 1969.

Donaldson, E. C.; Kendall, R. F.; Pavelka, E. A.; and Crocker, M. E., "Equipment and Procedures for Fluid Flow and Wettability Tests of Geological Materials," Bartlesville Energy Technology Center, U.S. Department of Energy, Report DOE/BETC/IC-79/5, May 1980.

Donaldson, E. C., "Oil-Water-Rock Wettability Measurement," Preprints, American Chemical Society. Division of Petroleum Chemistry, *26(1)*, pp. 110-122, March 29-April 3, 1981.

Dreher, K. D., and Sydansk, R. D., "Observation of Oil-Bank Formation During Micellar Flooding," SPE 5838, presented at the Fourth SPE Symposium on Improved Oil Recovery, Tulsa, Oklahoma, March 22-24, 1976.

Fatt, I.; Maleki, M.; and Upadhyay, R. N., "Detection and Estimation of Dead-End Pore Volume in Reservoir Rock by Conventional Laboratory Tests," Soc. Pet. Eng. J., *6*, pp. 206-212, September 1966.

Geffen, T. M.; Owens, W. W.; Parrish, D. R.; and Morse, R. A., "Experimental Investigation of Factors Affecting Laboratory Relative Permeability Measurements," Trans. AIME, *192*, pp. 99-110, 1951.

Geffen, T. M., and Gladfelter, R. E., "A Note on the X-Ray Absorption Method of Determining Fluid Saturation in Cores," Trans. AIME, *195*, pp. 322-323, 1952.

Gladfelter, R. E., and Gupta, S. P., "Effect of Fractional Flow Hysteresis on Recovery of Tertiary Oil," SPE 7577, presented at the 53rd Annual Fall Technical Conference of the SPE, Houston, Texas, October 1-3, 1978.

Graham, J. W., "Reverse-Wetting Logging," Trans. AIME, *213*, pp. 304-309, 1958.

Greenkorn, R. A., "Steady Flow Through Porous Media," A.I.Ch.E. J., *27(4)*, pp. 529-545, July 1981.

Gupta, S. F., "Dispersion and Adsorption in Porous Media," Ph.D. Thesis, Purdue University, 1972.

Hassler, G. L., and Brunner, E., "Measurement of Capillary Pressure in Small Core Samples," Trans. AIME, *160*, pp. 114-123, 1945.

Ionescue, E.; Batycky, J. P.; and Maini, B. B., "Miscible Recovery of Residual Oil — Effect of Wettability on Dispersion in Porous Media," Petroleum Recovery Institute, Report 1984-4, October 1984.

Johnson, E. F.; Bossler, D. P.; and Naumann, V. O., "Calculation of Relative Permeability From Displacement Experiments," Trans. AIME, *216*, pp. 370-372, 1959.

Jones, S. C., and Roszelle, W. O., "Graphical Techniques for Determining Relative Permeability From Displacement Experiments," J. Pet. Tech., *30(5)*, pp. 807-817, May 1978.

Josendal, V. A.; Sandiford, B. B.; and Wilson, J. W., "Improved Multiphase Flow Studies Employing Radioactive Tracers," Trans. AIME, *195*, pp. 65-76, 1952.

Laird, A.D.K., and Putnam, J. A., "Fluid Saturation in Porous Media by X-Ray Technique," Trans. AIME, *192*, pp. 275-284, 1951.

Lake, L. W., and Hirasaki, "Taylor's Dispersion in Stratified Porous Media," Soc. Pet. Eng. J., *21(4)*, pp. 459-468, August 1981.

Leverett, M. C., and Lewis, M. B., "Steady Flow of Gas-Oil-Water Mixtures Through Unconsolidated Sands," Trans. AIME, *142*, pp. 107-116, 1941.

Levine, J. S., "Displacement Experiments in a Consolidated Porous System," Trans. AIME, *201*, pp. 57-66, 1954.

Maini, B. B.; Ionescue, E.; and Batycky, J. P., "Miscible Displacement of Residual Oil — Effect of Wettability on Dispersion in Porous Media," Petroleum Society of CIM Paper No. 85-36-63, presented at the 36th Annual Technical Meeting of the Petroleum Society of CIM, Edmonton, Canada, June 2-5, 1985.

Marle, C. M., *Multiphase Flow in Porous Media*, Gulf Publishing Co., Houston, Texas, 1981.

McCaffery, F. G.; Sigmund, P. M.; and Fosti, J. E., "Pore Space and Displacement Characteristics of Carbonate Reservoir Rocks," Sixth Formation Evaluation Symposium of the Canadian Well Logging Society, pp. B1-B16, Calgary, Alberta, October 24-26, 1977.

Morgan, F.; McDowell, J. M.; and Doty, E. C., "Improvements in the X-Ray Saturation Technique of Studying Fluid Flow," Trans. AIME, *189*, pp. 183-194, 1950.

Naiki, M., "Numerical Simulation of Polymer Flooding Including the Effect of Salinity," Ph.D. Thesis, University of Texas at Austin, 1979.

Nicholls, C. I., and Heaviside, H., "Gamma Ray Absorption Techniques Improve Analysis of Core Displacement Tests," SPE 14421, presented at the 60th Annual Technical Conference of the SPE, Las Vegas, Nevada, September 22-25, 1985.

Nunge, R. J., and Gill, W. N., "Mechanisms Affecting Dispersion and Miscible Displacement," in *Flow Through Porous Media*, Edited by R. J. Nunge, American Chemical Society, Washington, D. C., 1970.

Oak, M. J., and Ehrlich, R., "A New X-Ray Absorption Method for Measurement of Three Phase Relative Permeability," SPE 14220, presented at the 60th Annual Technical Conference of the SPE, Las Vegas, Nevada, September 22-25, 1985.

Orr, F. M., and Taber, J. J., "Displacement of Oil by Carbon Dioxide," U.S. Dept. of Energy, Report DOE/BC/10331-13, March 1984.

Parsons, R. W., "Microwave Attenuation—A New Tool for Monitoring Saturations in Laboratory Flooding Experiments," Soc. Pet. Eng. J., *15*, pp. 302-309, August 1975.

Perkins, T. K., and Johnston, O. C., "A Review of Diffusion and Dispersion in Porous Media," Soc. Pet. Eng. J., *3(1)*, pp. 70-84, March 1963.

Pope, G. A., "The Application of Fractional Flow Theory to Enhanced Oil Recovery," Soc. Pet. Eng. J., *20(3)*, pp. 191-205, June 1980.

Provoust, L. P., "Research Report on Phase Behavior of Micellar Systems," Report No. 84-2, Center for Enhanced Oil and Gas Recovery Research, University of Texas at Austin, May 1984.

Reid, S., "The Flow of Three Immiscible Fluids in Porous Media," Ph.D. Dissertation, Chem. Engr. Dept., U. of Birmingham, 1958, referenced by Saraf and Fatt.

Russel, R. G.; Morgan, F.; and Muskat, M., "Some Experiments on the Mobility of Interstitial Waters," Trans. AIME, *170*, pp. 51-61, 1947.

Salter, S. J., and Mohanty, K. K., "Multiphase Flow in Porous Media: 1. Macroscopic Observations and Modeling," SPE 11017, presented at the 57th Annual Fall Technical Conference of the SPE, New Orleans, Louisiana, September 26-29, 1982.

Saraf, D. N., and Fatt, I., "Three Phase Relative Permeability Measurement Using a Nuclear Magnetic Resonance Technique for Estimating Fluid Saturation," Soc. Pet. Eng. J., *7(5)*, pp. 235-242, September 1967.

Schneider, F. N., and Owens, W. W., "Sandstone and Carbonate Two- and Three-Phase Relative Permeability Characteristics," Soc. Pet. Eng. J., *10*, pp. 75-84, March 1970.

Sharma, M. M., and Wunderlich, R. W., "The Alteration of Rock Properties Due to Interactions With Drilling Fluid Components," SPE 14302, presented at the 60th Annual Technical Conference of the SPE, Las Vegas, Nevada, September 22-25, 1985.

Shuler, P. J., "A Study of the Mechanisms Affecting the Enhanced Recovery of Oil by Surfactant Flooding," Ph.D. Thesis, University of Colorado at Boulder, 1978.

Slobod, R. L.; Chambers, A.; and Prehn, W. L., "Use of Centrifuge for Determining Connate Water, Residual Oil, and Capillary Pressure Curves of Small Sandstone Samples," Trans. AIME, *192*, pp. 127-134, 1951.

Snell, R. W., "Measurement of Gas Phase Saturation in a Porous Media," J. Inst. Pet., *45(428)*, pp. 259-261, August 1959.

Snell, R. W., "Three Phase Relative Permeability in an Unconsolidated Sand," J. Inst. Pet., *48(459)*, pp. 80-88, March 1962.

Spence, A. P., and Watkins, R. W., "The Effect of Microscopic Core Heterogeneity on Miscible Flood Residual Oil Saturation," SPE 9229, presented at the 55th Annual SPE Fall Technical Conference, Dallas, Texas, September 21-24, 1980.

Stalkup, F. I., "Displacement of Oil by Solvent at High Water Saturation," Soc. Pet. Eng. J., *10(9)*, pp. 337-348, December 1970.

Taylor, G. I., "Dispersion of Soluble Matter in Solvent Flowing Slowly Through a Tube," Proc. Royal Soc. London, Series A., *219*, pp. 186-203, 1953.

Walther, H. C., "Saturation From Logs—Laboratory Measurement of Logging Parameters," J. Pet. Tech., *20(3)*, pp. 251-258, March 1968.

Wang, F.H.L., "Effect of Wettability Alteration on Water-Oil Relative Permeability, Dispersion, and Flowable Saturation in Porous Media," SPE 15019, presented at the 1986 SPE Permian Basin Oil and Gas Recovery Conference, Midland, Texas, March 13-14, 1986.

Wang, S. Y.; Ayral, S.; and Gryte, C. C., "Computer-Assisted Tomography for the Observation of Oil Displacement in Porous Media," Soc. Pet. Eng. J., *24(1)*, pp. 53-55, February 1984.

Wang, S. Y.; Ayral, S.; Castellana, F. S.; and Gryte, C. C., "Reconstruction of Oil Saturation Distribution Histories During Immiscible Liquid-Liquid Displacement by Computer Assisted Tomography," A.I.Ch.E. J., *30(4)*, pp. 642-646, July 1984.

Wasan, D. T.; Perl, J. P.; and Milos, F. S., "Microwave Spectroscopic Analysis of Surfactant/Polymer Flooding: Interrelationships Between Chemical Slug Properties, Coalescence Phenomena, and Tertiary Oil Recovery," SPE 8327, presented at the 56th Annual Technical Conference of the SPE, Las Vegas, Nevada, September 23-26, 1979.

Whalen, J. W., "A Magnetic Susceptibility Method for the Determination of Liquid Saturation in Porous Materials," Trans. AIME, *201*, pp. 203-208, 1954.

Welge, H. J., "A Simplified Method for Computing Oil Recovery by Gas or Water Drive," Trans. AIME, *195*, pp. 91-98, 1952.

Wellington, S. L., and Vinegar, H. J., "CT Studies of Surfactant-Induced CO_2 Mobility Control," SPE 14393, presented at the 60th Annual Technical Conference of the SPE, Las Vegas, Nevada, September 22-25, 1985.

Zierfuss, H., and Maltha, A., "Regarding the Relationship Between the Formation Resistivity Index and the Oil Recovery Mechanism During Waterflooding Procedures," Erdöl und Kohle-Erdgas-Petrochemie, *20*, pp. 549-552, 1967. English translation available from the John Crerar Library, Translation No. 68-15700.

VITA

Jeffrey Craig Smith was born in Columbia, Missouri, on January 11, 1962, the son of Charles and Kay Smith. After graduating from Okemos High School, Okemos, Michigan, in 1980, he entered the University of Texas at Austin, Texas. He received a Bachelor of Science degree in Petroleum Engineering in May 1985 and entered the Graduate School of the University of Texas at Austin in June 1985. In September 1985, he moved to Ponca City, Oklahoma, for nine months to do the research for this thesis at Conoco's Production Research and Development laboratories.

Permanent address: 91 Feldspar
Williamston, MI 48895

This thesis was typed by Conoco's word processing group.